ROCK MECHANICS IN JAPAN

VOLUME II

JOINT COMMITTEE ON ROCK MECHANICS

1 9 7 4

E r r a t a

P.97 line 15 q_u , q_u' should read q_u' , q_u

P.97 line 15 $\beta = \tan\left(\frac{\pi}{4}+\frac{\phi}{2}\right)$ should read $\beta' = \tan\left(\frac{\pi}{4}+\frac{\phi'}{2}\right)$

P.97 line 16 $\beta' = \tan\left(\frac{\pi}{4}+\frac{\phi'}{2}\right)$ should read $\beta = \tan\left(\frac{\pi}{4}+\frac{\phi}{2}\right)$

P.97 line 25 and 29 q_u' and β' should read q_u , β

ROCK MECHANICS IN JAPAN

VOLUME II

1974

BY JOINT COMMITTEE ON ROCK MECHANICS
c/o JAPAN SOCIETY OF CIVIL ENGINEERS

CHAIRMAN ; Yoshio HIRAMATSU

SOCIETIES CONCERNING JOINT COMMITTEE

JAPAN SOCIETY OF CIVIL ENGINEERS
Yotsuya 1-chome Shinjuku-ku Tokyo

THE JAPANESE SOCIETY OF SOIL MECHANICS AND FOUNDATION ENGINEERING
Toa-Bekkan 13-5 Nishishinbashi 1-chome Minato-ku Tokyo

THE MINING AND METALLURGICAL INSTITUTE OF JAPAN
5-4 Ginza 8-chome Chuo-ku Tokyo

THE SOCIETY OF MATERIALS SCIENCE, JAPAN
1 Yoshida Izūmidono-cho Sakyo-ku Kyoto

Printed in Japan

PREFACE

This "Rock Mechanics in Japan, Volume II, 1974", published by the Joint Committee on Rock Mechanices, Japan, organized by the four societies given on the preceding page, contains brief comments on the activities on rock mechanics in Japan from 1970 to 1974, in the field of civil engineering, the soil mechanics and foundation engineering, the mining engineering and material science, followed by the summaries of selected papers and by the list of literatures appeared in sixteen journals.

Recently construction works have become more and more large-scale for example the construction of the undersea railway tunnel called Seikan Tunnel, the bridge between Honshu and Shikoku and so on. Also in the mining industry, the situation is similar as that of civil engineering owing to adoption of large-scale trackless machines underground. Furthermore some deep mines are facing with the danger of rock burst or gas outburst.

Success in those modern construction works and safe and efficient performance of mining in those mines will only be accomplished by remarkable development of rock mechanics, both theoretical and experimental. It will be a great pleasure if this publication be of use for investigators and engineers concerning rock mechanics in exchanging informations and in searching for the direction of future investigation.

July 1974

Yoshio Hiramatsu

Yoshio HIRAMATSU
Chairman of Joint Committee
on Rock Mechanics, Japan

CONTENTS

I RECENT ACTIVITIES

ON

ROCK MECHANICS IN JAPAN

RECENT ACTIVITIES ON ROCK MECHANICS IN THE JAPAN SOCIETY OF CIVIL ENGINEERS

Tatsuo MIZUKOSHI, Managing director of Tokyo Electric Power Co., Inc.

OUTLINE OF RECENT ACTIVITIES

The committee for rock mechanics of the Japan Society of civil Engineers (JSCE) has been playing an leading role in investigation and research activities into rock mechanics in the civil engineering world in Japan, ever since its organization in 1962.

The committee has about one hundred members and they are taking active parts in four divisions and one subcommittee. The main activities are as follows:

(a) The first division ----
research and standardization for the geological investigation methods and grauting technics for rock foundations of dams

(b) The second division ----
research for the mechanized excavation of tunnels

(c) The third division ----
standardization of in-situ rock test, and the collection and analysis of the data on rock mass tests in-situ in Japan

(d) The fourth division ----
research for soft rocks

(e) The subsommittee for the revision of publications ----
editorial activities for the revision of "Rock Mechanics for Engineers" published in 1966

(f) Symposium on rock mechanics of JSCE ----
to hold a symposium once a year, 8 times so far

(g) Meeting on rock mechanics ----
to hold a meeting on specific theme three or four times a year attended by members of the committee and concerned of JSCE

ACHIVEMENTS OF THE ACTIVITIES

The results of member's activities are reflected in the publications and printed matters as follows:

(a) Grauting Manual for Foundation of Concrete Dams ---- published in June 1971

(b) Construction Data Book of Grauting for Rock Foundation of Dams ----
published in September 1973, representative 57 dams in Japan contained, about 300 pages

(c) Manual for Geological Investigation of Dams ----
to be published by the end of 1974

(d) Rock Mechanics for Engineers (revised edition) ----
to be published by the end of 1974
This book has been widely read in Japan since its first edition in 1966. But it's become necessary to revise it thoroughly because of the recent remarkable advance in the rock mechanics.

(e) Research reports of the committee
- In-situ mechanical properties of rock masses, Jour. of JSCE, vol. 57, No. 9, 1972
- Standard method of test for load-deformation relationship in-situ tock mass with a plate,1973

(f) And others
- Symposiums on rock mechanics (1970-1973)

The reported papers are published as "Proceedings" by JSCE. The numbers and themes for each symposium are as follows:

Sympo.	year	mechanical properties of rock	mechanical properties of rock mass	construction technics	others	total numbers
6th	1970	1	8	5	3	17
7th	1971	3	8	4	3	18
8th	1972	1	11	2	3	17

PRESENT SUBJECT OF THE RESEARCH

(a) To make a classification table of rock masses for the excavation of tunnels

(b) To investigate the applicability of tunnel boring machine (TBM) and to collect the data for the actual results of using TBM.

(c) To establish the standard for in-situ shearing test method, of rock mass, and others.

(d) To study the mechanical properties of soft rocks and the behaviours of rock mass under the sea.

(e) and others

ACTIVITIES ON ROCK MECHANICS IN THE JAPANESE SOCIETY OF SOIL MECHANICS AND FOUNDATION ENGINEERING

Koichi AKAI, Kyoto University

The Japanese Society of Soil Mechanics and Foundation Engineering has had the committee on rock mechanics since 1966 on the point of view that the Society should coherently take up the problems in the continuous field from soil to rock.

The committee has decided to take the problems of rock mass geotechnically in relation to soil, directly related to small or middle scale structures, and approved the following three basic problems to be concerned: 1) unified engineering classification of rock mass, 2) standardization for rock test and 3) definite explanation on technical terms in the field of rock engineering.

Among these subjects working circumstances on unified classification has been briefly summarized in the previous report. The task on standardization for rock test is being performed under combination with related societies in rock mechanics.

The subject on definite explanation on technical terms in the field of rock engineering has been main theme in the Society between 1970 and 1972. This work is summarized in a booklet with the indices of English, German, French and Italian under the following idea.

A human cultural life is based on various branches of learning and technique which are in harmony with each other like as warp and woof of beautiful textiles. It is desirable that words and letters should be something in common for the human life, since it is necessary for the elevation of the cultural level. This fact results in the fundamental significance to unify technical terms and testing standard, and one can readily realize that scientific and technical terms have deeply to do with the actual human life and other branches of science and engineering.

Especially, in newly born and young science and engineering fields, making words and letters be common without delay is definitely required to establish the interrelation between science, technology and the human life, and contribute their mutual prosperity. Rock mechanics is closely related to such scientific fields as geology, mineralogy, geophysics and material science as well as engineering fields of mining, civil, structural, debris control, resources and disaster prevention. Thus it is important to unify the terminology in rock mechanics as soon as possible.

International Society for Rock Mechanics(I.S.R.M.) has already described the necessity of unifying the terminology as one of essential subjects to be solved in near future. The Rock Mechanics Committee in the Japanese Society of Soil Mechanics and Foundation Engineering had taken up the problem to unify the terminology in connection with that of soil mechanics since 1970 and published the booklet as the results of the Committee in 1972. To appeal to the public as early as possible is the main reason for the publication in such a way with hoping that it may contribute to the progress in rock engineering field as well as the human society. This work will be authorized as a publication by the Society.

The Society has also engaged himself in recent years with publication of an elaborated book titled "Engineering Properties of Rock and Their Application to Design and Execution." This book is the one on rock engineering, however, it covers broader area than the ordinary conception about the engineering. From the beginning, the Committee has recognized the world-wide trend of growth of Geotechnology by unifying rock and soil engineerings, since rocks and soils are nonseparable materials of primary concern which constitute ground.

The contents of the book are shown below.

RECENT ACTIVITIES ON ROCK MECHANICS IN THE MINING AND METALLURGICAL INSTITUTE OF JAPAN

Tomio HORIBE, Tohoku University

There are many practical works dealing with rocks in the mining field such as the drilling, the blasting, the cutting, the mine support and the crushing etc., and concerning these works, the problems involving the fundamental rock properties have been studied in the laboratories of universities and others.

Many researchers have pursued and extended the studies related to the subjects introduced in Vol. 1, Rock Mechanics in Japan, 1970.

Accomplishments of these studies appear in the list of literatures of this issue.

Conspicuous studies of rock mechanics in the mining field may be summarized as followings as a recent tendency.

One subject of them is the application of the computer to the stress analysis related to the rock pressure, the blasting and the stability of structures in rocks. I. ITO and his cooperators[1] have studied on the formation of cracks and a crater caused by a blasting with one free face. The processes of cracks and the crater formation caused by the blasting have been simulated to the results that the dynamic stresses in a material with one free face were analysed applying a numerical technique, which involved the finite-difference approximation, to the momentum equation. Y. HIRAMATSU and his cooperators[2] have made the determination of the ratio of the width of rib pillars to that of openings with the method of the three dimensional analysis of stresses. S. KINOSHITA and his cooperator[3] have made a theoretical analysis of the stress distribution around multiple circular openings under the plane stress condition and computed the stress concentration at the surface of a circular hole. K. SUZUKI and his cooperators[4] have made a theoretical study of the three dimensional analysis of stresses around a borehole and the consideration on the measurement of stresses in a rock by a complete stress relief technique using a borehole deformation method.

A lot of investigations on the observation of microcracks in rocks have been made in connection with the mechanism of rock fracture. T. YANO[5] has found many "divergent" fissures in the coal of the stress zone in danger of outbursts by the microscopic study of fissures in the coal thrown out by outbursts.

I. ITO and his cooperators[6] have made the discussion on the mechanism of the crack propagation caused by the blasting, through the microscopic observation of the surface of the crack produced in a polymethyl methacrylate plate by the attack of a detonator. S. KINOSHITA and his cooperator[7] have investigated the fracture mechanism of rocks by the microscopic observation of the chip formed near the cutting point of rocks.

Several studies of the thermal fractures of rocks have been reported for a few years. Z. HOKAO and his cooperators[8) 9)] have developed a fire jet piercing thermodrill and presented results of the fire jet piercing tests at the underwater depths of 10 to 30 meters. I. ITO and his cooperators[10] have tried to develop an efficient method of rock excavation for hard rocks, using a mechanical rock-cutting device combined with the thermal action by the flame. U. YAMAGUCHI and his cooperator[11] have made the measurement of the change of compressive and tensile strengths of rocks heated to high temperatures, and attempted to find the relationship between the difference of the thermal characteristics of rock-forming minerals and the change of the strengths.

Studies on the velocity of elastic waves in rocks and on the acoustic property of rocks have been done with the attention of interest. M. INOUE and his cooperators[12] have studied on the relationships of the water content to the velocity of elastic waves and to the compressive strength of sedimentary rocks. U. YAMAGUCHI and his cooperators[13] have tried to find stress states or cracks in rocks around mine openings with the measurement of the sound velocity in rocks between the neighbouring boreholes by exploding detonators. T. HORIBE and his cooperator[14] have developed a drummy rock detector of which principle is based on the ratio of areas surrounded by the envelope of the filtered wave form and by that of the original wave form of the impact sound of rocks, and its application tests under the noises in underground have been presented.

Investigations of fundamental mechanical properties of rocks have been made not only with intact rocks, but also with jointed rocks and but also with rocks, each of which has a plane of weakness. Y. SHIMOMURA and his cooperators[15] have investigated on influences of schistocity planes of schistose rocks to the compressive strength, the tensile strength and the sonic velocity in rocks. T. NISHIDA and his cooperators[16] have investigated the relationships between the angle of the joint inclination, and the compressive strength, the cohesion and the angle of the internal friction by the triaxial compression tests on the plaster models containing a single joint. K. SUZUKI and his cooperators[17] have studied on the rheological property of rocks under the pulsating compressive load as a fatigue test. S. TAKAOKA and his cooperators[18] have presented a method for determining the fracture resistance of rocks by strain waves generated in a drill-rod during a percussive fracturing of rocks and discussed the

method to determine the hardness and the viscousness of rocks from thier fracture resistance. In the field of rock crushing, S. YASHIMA and his cooperators[19] have made an experimental study concerning the relationship between the specific fracture energy and the specific surface area of the fractured product in the single particle crushing. R. KOBAYASHI[20] has studied on the shear strength of rocks and proposed an equation to approximately calculate the shear strength from the compressive strength and the tensile strength of a rock.

Further, T. HORIBE and his cooperators[21] have made an experimental study on the borehole deviation in a laboratory. T. ISOBE[22] has made some considerations on the mechanism of rockbursts and outbursts.

Moreover, field measurements have been carried out with activity. S. OGASAWARA and his cooperators[23] have observed rock noises for several months by geophones placed around the working faces. N. NANKO[24] has had the observation of cracks of mine pillars, and had the measurements of the earth pressure and of the movement of rock strata, considering the application to the design and maintainance of mine pillars.

Literatures

1) - 20) were published as full papers in the Journal of the Mining and Metallurgical Institute of Japan and these are appeared in the list of literatures at the end of this issue.

21) T. HORIBE, M. USHIDA, Y.T. SUNG : Paper presented at Symp. in Fall Meeting, Min. Met. Inst. Japan, Oct. 1973, I-2, P. 1-4

22) I. ISOBE : Paper presented at Symp. in Fall Meeting, Min. Met. Inst. Japan, Sep. 1971, H-7, P. 1-3

23) S. OGASAWARA, K. SAKAI, K. ISHIHARA : Paper presented at Symp. in Fall Meeting, Min. Met. Inst. Japan, Oct. 1972, B-9, P. 1-6

24) N. NANKO : Paper presented at Symp. in Fall Meeting, Min. Met. Inst. Japan, Oct. 1973, J-8, P. 1-4

RECENT ACTIVITIES ON POCK MECHANICS IN THE SOCIETY OF MATERIALS SCIENCE, JAPAN

Minoru YOSHIDA, Managing Director
The Kansai Electric Power Co., Inc.

The committee on rock mechanics was organized in 1963 in the Society of Materials Science, Japan. Since then, 52 regular meetings were held till March, 1974. In 1971, a subcommittee specialized in comminutions was newly set up in the committee on rock mechanics and 4 regular meetings were held till March, 1974.

The Committee now consists of about 50 authorized members, who are engaged in such fields as civil engineering, mining engineering, metallurgy, chemical engineering, geology, geophysics and seismology.

Activities by the committee are not confined to regular meetings, but involve public lecture meeting, symposium, short study course, field inspection and publication of special issue on rock mechanics and comminutions.

Those conducted under the auspices of the committee or in cooperation with the other society since 1970[1)] are as follows; two symposiums on rock mechanics, one symposium on comminutions, three field inspections, one release of special issue on rock mechanics for The Journal of The Society of Materials Science, Japan[2)]

The regular meeting on rock mechanics has been carried out bimonthly to deal with the following matters;

(1) Lectures on rock mechanics and discussions thereon.
(2) Selection of subjects on the public lecture, symposium, short study course, etc. related to rock mechanics.
(3) Discussion on managements of the committee.
(4) Introduction among the committee members of information on activities by national and international societies for rock mechanics.
(5) Other related topics.

The title of lectures and discussions at the regular meeting of the committee from May, 1970 to March, 1974 is as follows;

(1) Mechanism of Rock Burst of Pillars in Mines, by T. Saito, Y. Oka and Y. Hiramatsu.
(2) Reviews of the Topics Presented to the 7th International Conference on Soil Mechanics and Foundation Engineering, held at Mexico City, by S. Murayama.

(3) The Effects of the Couple-Stresses on Stress Concentrations, by S. Kobayashi.
(4) Flow of Rocks and Crust, by N. Kumagai and H. Ito.
(5) The Finite Element Analysis Applied to the Cosserat Elastic Body, by S. Sakurai.
(6) Free Discussion on Unusual Behaviors of Rocks, Which are Difficult to be Explained by the Classical Theory of Solids.
(7) Applications of the Finite Element Method to Soils and Rocks, by T. Kawamoto.
(8) Continued Discussion on Unusual Behaviors of Rocks.
(9) Dynamics Stress Analysis by the Tensor Code, by K. Sassa and I. Ito.
(10) Further Discussion on Unusual Behaviors of Rocks.
(11) Some Simulation Analyses for Laboratory Tests, by Y. Niwa and K. Nakagawa.
(12) Seismic Records on a Rock Burst in Ikuno Mine, by Y. Tanaka and R. Nishida.
(13) Discussions on Strength of Pock in Tension and Compression.
(14) Mechanism of Rock Burst and Gas Explosion, by Y. Hiramatsu.
(15) Study on Effects of Earthquake on Fractured Zone of the Earth's Crust, by K. Iida.
(16) Measurements of Initial Stresses or Tectonic Stresses in Rocks, by H. Ito, Y. Oka, S. Kobayashi and T. Saito.
(17) A General Method to Obtain Solutions of Boundary-Value Problems by the Use of Superposition of Fundamental Solutions, by S. Kobayashi.
(18) Some Problems of Stiff Test for Rocks, by Y. Hiramatsu, Y. Mizuta and K. Sugawara.
(19) Measurements of Velocities of Elastic Waves in Rocks under High Temperature and Confining Pressure, by S. Matsushima.
(20) Creep and Fracture of Cement Mortar, by S. Sakurai.
(21) The Finite Element Analysis Applied to Some Problems Containing Stochastic Distributions of Properties of Constituent Materials, by T. Kawamoto.
(22) Spline Function Applied to Stress-Strain Relations, by T. Kawamoto.
(23) Tectonic Stress Field in South-West Japan Determined by the Geological Surveys, by K. Fujita.
(24) Tectonic Stress Field in South-West Japan Determined by the Mechanism of Earthquake, by T. Kishimoto.
(25) Electric Resistance Investigations in Geological Survey for Tunneling, by E. Yoshizumi, T. Kanno and A. Saito.
(26) Topics Presented to the 5th International Conference of Strata Control, held at London, by Y. Oka.
(27) Stresses Around Circular Cavity Excavated in Brittle Materials, by T.Saito
(28) Transient Stresses Around Tunnels by the Passage of Traveling Waves, by S.

Kobayashi.

(29) Strain Analysis of Bottom Surface of Borehole Drilled in Anisotropic Rock Mass, by H. Kiyama.

(30) Thermal Fragmentations of Rocks, by I. Ito, and M. Terada.

(31) Mechanism of Large Earthquake Around Japan, by K. Mikumo.

(32) An Approach to Rock Engineering Based on the Visco-Elast-Plastic Theory, by T. Adachi.

(33) Some Examples of Rock Slide and Collapse of Tunnels, by Y. Kobayashi.

(34) Measurements of Crustal Deformations, by I. Ozawa.

(35) In-Situe Tests of Soft Rocks, by Y. Niwa and S. Kobayashi.

The title of lectures given at the regular meeting of the sub-committee on comminutions is as follows;

(1) Comminution Properties of Brittle Solids, by S. Okuda.

(2) Theory of Comminutions and Some Indices, by K. Matsui.

(3) Comminutions by Impact, by F. Yokoyama.

(4) Pock Mechanics and Comminutions, by Y. Oka.

Recent activities of the Committee on Rock Mechanics in the Society of Materials Science, Japan are known by the papers contained in the special issue, Rock Mechanics No.3[2)], published February, 1971. The list of the original papers is as follows;

(1) A New Element of the Mechanical Model of Rock Substance, by Y. Nishimatsu.

(2) Rheological Equation of Anisotropic Viscoelastic Materials and Its Application to Problems Pertinent to Rock Mechanics, by S. Sakurai.

(3) Failure Criteria of Rocks (Study by a New Triaxial Compression Technique), by K. Mogi.

(4) Viscoplasticity and Direct Shear Test of Rock Type Materials, by T. Adachi and S. Serata.

(5) Variation in the Characteristics of Deformation of Marble and Mortar due to Transition of Stress from Isotropic State to Anisotropic State, by T. Kawamoto and K. Tomita.

(6) Initiation and Propagation of Brittle Fracture in Rock-Like Materials under Compression, by S. Kobayashi.

(7) The Effects of the Mean Stress and of the Stress Amplitude on the Rate Constants of Fatigue Failure of the Rock, by Y. Nishimatsu and R. Heroesewojo.

(8) Deformation of Dunite at Slow Strain Rates under High Temperature and Pressure, by K. Iida, H. Tsukahara, Y. Kobayashi, I. Suzuki, J. Kasahara and M. Kumazawa.

(9) The Experimental Study of Secular Bending of Big Granite Beams for a Period of 13 Years with Correction for Change in Humidity, by N. Kumagai

and H. Ito.

(10) The Flow of the Earth's Crust Considered from the Quaternary Crustal Movements in Southwest Japan, by H. Ito and K. Fujita.

(11) The Stress in and near the Pillars, by Y. Mizuta, Y. Hiramatsu, Y. Oka and Y. Tanahashi.

(12) Mechanism of Rock Breakage under Pressure of Gas Explosion, by I. Ito, K. Sassa and C. Tanimoto.

In addition to these papers, the following review, technical note and technical topic[2] are also included in the issue.

(Rev.) Plastic Theory of Formation Mechanics and its Application to Rock Mechanics, by J. Makiyama.

(Tech. Note) The Failure Surface of Isotropic and Anisotropic Rocks under Multiaxial stresses, by K. Akai.

(Tech. Topic) Applications of the Finite Element Method of Analysis to Problems in Soil and Rock Mechanics, by T. Kawamoto.

The special issue, Rock Mechanics No.4, will be published in May, 1974, which contains two reviews, two technical notes and six original papers covering various problems such as prediction of earthquake, blasting of rocks, in-situ measurements of deformation of underground cavities, stresses and deformations around tunnels, transient stresses around tunnels, properties of soft rocks, processes of rock failures, tectonic stresses and crustal deformations.

References

1) Rock Mechanics in Japan, Vol. 1, 1970, pp 14-16, in which the activities till March 1970 were described.

2) Special Issue on Rock Mechanics No.3, Reprinted from Journal of the Society of Materials Science, Japan, Vol. 20, No.209, February 1971, pp 107-226.

II BRIEF SUMMARY OF RECENT STUDIES

FAILURE CRITERIA OF ROCKS

- Study by a new triaxial compression apparatus -

Kiyoo MOGI, Earthquake Research Institute, University of Tokyo

In the earth's crust and upper mantle, fracture and flow of rocks occur under complex combined stresses. To study this phenomenon a number of laboratory experiments on rock deformation have been made under high confining pressure ($\sigma_1 > \sigma_2 = \sigma_3$). Until recently, however, few investigations of the effect of the more general triaxial stresses ($\sigma_1 > \sigma_2 > \sigma_3$) have been made because of experimental difficulties. Fig. 1 shows our new triaxial apparatus by which σ_1, σ_2 and σ_3 can be applied independently. Fig. 2 shows the stress-strain relation obtained by this new triaxial apparatus. One important result is that the effects of σ_2 and σ_3 on the stress-strain curve are very different. Ductility increases with increasing σ_3, but decreases with increasing σ_2. The yield stress and the coefficient of strain-hardening in the post-yield region increases with increasing σ_2, but are nearly independent of σ_3.

Fig. 3 shows the fracture strength under combined stresses obtained by our new triaxial method. Stress (σ_1) at fracture is shown as a function of σ_2. Different symbols show different σ_3. The curve shows a similar pattern in various kinds of rocks.

Current fracture criteria failed to correlate those observed fracture stresses under various stress states. As a satisfactory fracture criterion, the following new formula was obtained by generalization of the Von Mises criterion.

$$\tau_{oct} = f(\sigma_1 + \sigma_3) \qquad (1)$$

To examine the new formula, τ_{oct} is plotted against $(\sigma_1 + \sigma_3)/2$ in Fig. 4. Circles for different combined stress states form a single curve. That means that this formula is applicable as a fracture criterion.

Frequently, the yield point is not sharply defined; however, it can be uniquely determined in some cases. The yield

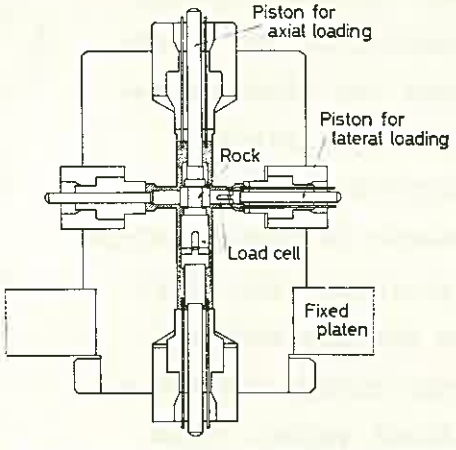

Fig. 1. High pressure cell with axial and lateral pistons for the new triaxial compression apparatus.

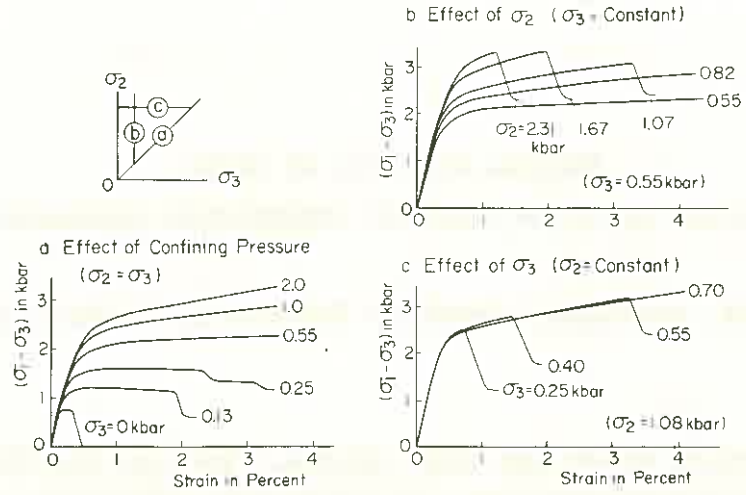

Fig. 2. Stress-strain curves of Yamaguchi Marble under triaxial compression.
a: Curves at various confining pressures.
b: Curves at various values of σ_2 (σ_3 = 0.55 kbar).
c: Curves at various values of σ_3 (σ_2 = 1.08 kbar).

stresses under general combined stresses are correlated well by the following formula which is different from the Fracture Equation (1).

$$\tau_{oct} = f(\sigma_1 + \sigma_2 + \sigma_3) \qquad (2)$$

In Fig. 5, τ_{oct} at yielding is plotted against $(\sigma_1 + \sigma_2 + \sigma_3)/3$. Circles for different combined stresses form a single curve. Thus, this formula is satisfactory as a yield criterion of rocks. This criterion includes the Von Mises criterion as a special case with the curve slope of zero. The formula is that proposed by Nadai (1950) and other investigators without any sufficient experimental examination. (This formula is not inconsistent with the above-mentioned result that the yield stress is not appreciably affected by σ_3.)

Fig. 6 shows a summary of the stress states at fracture and yielding under combined stress, according to the generalized Von Mises criteria. The physical interpretation of the criteria is that fracture or yielding will occur when the distortional strain energy reaches a critical value. This critical energy is not

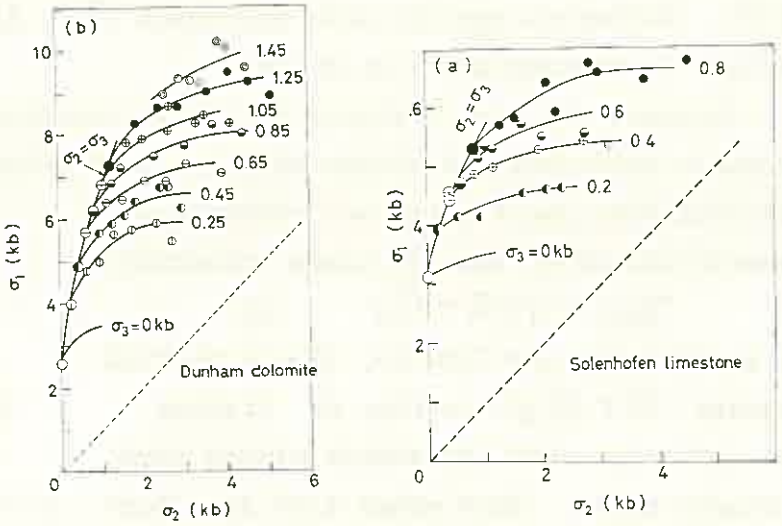

Fig. 3. Stress (σ_1) at fracture as functions of the intermediate principal stress (σ_2). Different symbols show the different minimum principal stress (σ_3), which is indicated by numerals in kb. (a) Solenhofen limestone; (b) Dunham dolomite

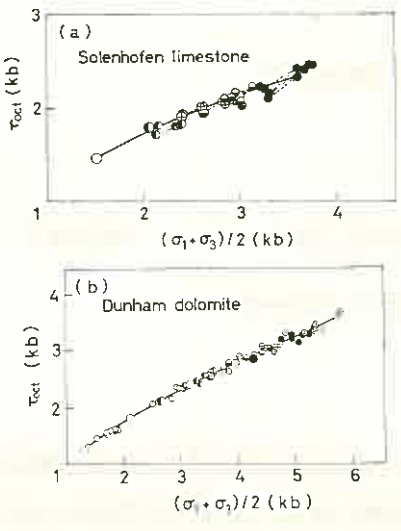

Fig. 4. Octahedral shear stress (τ_{oct}) at fracture versus $(\sigma_1+\sigma_3)/2$. Different symbols show different σ_3. (a) Solenhofen limestone ; (b) Dunham dolomite

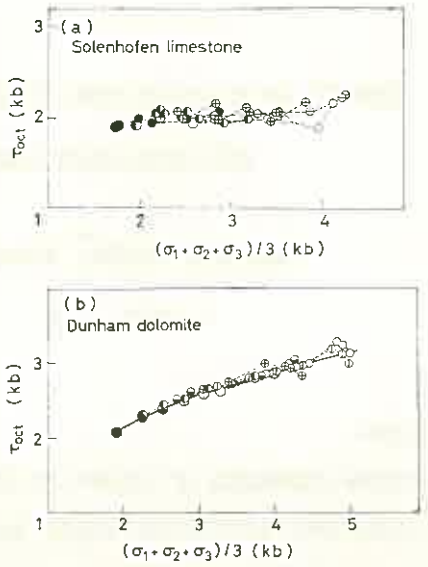

Fig. 5. Octahedral shear stress (τ_{oct}) at yield point versus $(\sigma_1+\sigma_2+\sigma_3)/3$. Different symbols show different σ_3.

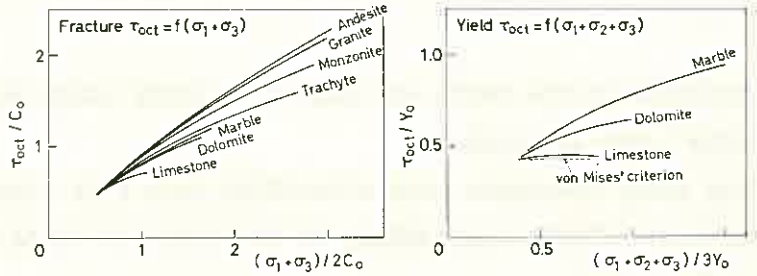

Fig. 6. Summary of stress states at fracture and yielding of tested rocks (Expression by generalized von Mises' criteria). C_0 : uniaxial compressive strength ; Y_0 : yield stress at the ductility 1 percent, obtained for $\sigma_2=\sigma_3$.

constant, but monotonically increases with the effective mean normal stress. In fracture, shear faulting takes place on a plane parallel to the σ_2-direction, and so the effective mean normal stress is $(\sigma_1+\sigma_3)/2$. On the other hand, yielding does not occur on any definite slip plane with a definite direction, so the mean stress is taken as the effective mean normal stress. The slope of these curves characterizes the pressure sensitivity of failure stress of each rock.

REFERENCES

Mogi, K., 1971. Effect of the triaxial stress system on the failue of dolomite and lime-stone. Tectonophysics, 11: 111-127.

Mogi, K., 1971. Fracture and flow of rocks under high triaxial compression. J. Geophys. Res., 76: 1255-1269.

Mogi, K., 1972. Effect of the triaxial stress system on fracture and flow of rocks. Phys. Earth Planet. Interiors, 5: 318-324.

EFFECT OF FLAWS ON THE STRENGTH OF ROCK SPECIMEN AND ROCK-MASS CLASSIFICATION

Kazuhiko IKEDA*, Yoshimasa KOBAYASHI**, and Takashi SAKURAI*

* RTRI, JNR ** DPRI, Kyoto University

1. Introduction

A compressive strength of rocks is often used as a parameter for rock-mass classification. However, in the strength tests rock pieces with minimum flaws are conventionally employed as specimens, without studing much about the effects of them on the strength.

In the present study series of compressive-strength tests of rock specimens which include visible flaws are conducted and the mentioned effect are studied.

2. Rock Specimen

Sample rocks employed in the tests are paleozoic sandy slate and 79 cylindrical specimens are sampled from the rock.

Prior to loading every specimens were classified into four classes A, B, C and D defined as illustrated in Table 1,according to the observed state of weathering, joints, stratification, etc.

3. Mode of Failure

The orientation of flaws in specimens may be considered to be arbitrary, since they were shaped from boring cores obtained at a tunnelling site. In almost all cases for classes A, B and C, which correspond to more or less deteriorated states, failure occured along one of flaws in the specimens. The failure looked like at a glance to have followed the fracture theory by Coulomb, but the angle of failure did not correspond to that of the maximum shear, $\alpha=1/2\cot^{-1}\mu$, because the specimens were not homogeneous nor isotropic. In the above cases the shearing resistance would not have been uniform within the specimens and as a consequence they failed along planes of the minimum shearing resistance,i.e.the planes of the most remarkable flaws.

A large part of class-D specimens also failed along flaws. A few of them, however, failed at different angles, which were smaller than those in the other cases measured from the axes of the specimens. In these cases the exsistance of flaws dose not seem to have influenced the failure angles, but the specimens failed at the plane of the maximum shearing stress.

4. Effect of Flaws on Compressive Strength

The compressive strength when a specimen fails at an angle β is given by

$$\sigma = \frac{P}{a} = \frac{\tau_s}{\sin\beta(\cos\beta - \mu\sin\beta)}$$

where P, a, τ_s and μ are the ultimate axial load, the initial sectional area, cohesion and coefficient of friction along failure plane, respectively. Plots of the test results are shown in Fig.1. Curves of compressive strength versus angle corresponding to assumed values of cohesion and friction calculated with the above relation are also drawn in the figure.

On the other hand the failure angle α in a homogeneous specimen would be given by

$$\alpha = \frac{\pi}{4} - \frac{\phi}{2}$$

where $\phi = \tan^{-1}\mu$. In this case the angle and the load would correspond to the tops of the parabola-like curves in Fig.1.

In general cases specimens do not fail at an angle α, but along flaws at a different angle, in which cases the failures correspond to upper or lower wings of the parabolas, and the strengths become higher than those in failures corresponding to the tops of the curves. In the test results, however, no failure at angles larger than 50 degrees and smaller than 5 degrees could be found. It implies that flaws do not influence the strength when their angles are larger or smaller than the above values.

5. Effect of Flaws on Elastic-Wave Velocity

It is widely believed that the effect of flaws would also be found in the decrease of elastic-wave velocity in rocks.

Velocities determined by seismic exploration in situ are in general lower than those in fresh rock specimens extracted from the same site, and the grade of flaws in rock mass may be estimated from the ratio between the both velocities.

Thus, the coefficient of flaws defined by $(v/V)^2$ may correspond to the state of flaws, where v and V are velocities in situ and in fresh rock specimen, respectively. It must be born in mind that the coefficient includes not only the effect of flaws but weathering or other facters which may decrease the in-situ velocity.

The mean velocities for classes from A to D of paleozoic sandy slate are given in Table 2, where the values exibit a reasonable correlation with the deteriorated grades of every classes of rocks.

6. Quasi Strength of Rock Mass and Strength of Flaw

One of the authers has presented an idea of quasi strength of rock mass which is defined by

$$\sigma_q = (v/V)^2 \cdot \sigma_c$$

where σ_q, σ_c, v, V are quasi strength, strength of core of fresh rock, velocities in situ and in fresh rock, respectively. The coefficient $(v/V)^2=k$ was called coefficient of cracks (or flaws).

On the basis of the test results and V were assumed respectively to be 1300 kg/cm and 5.60 km/s which correspond to the values for class D. The velocities in situ where the rock specimens were taken from are given in Table 3.

On the above assumption of strength and velocity for fresh rock the quasi strengths of rock masses were calculated as given in Table 3. In the table the strengths of rock flaw are also tabulated for comparison with the quasi strengths. The both strengths exhibit a rather good agreement and the quasi strength introduced in the above mentioned paper has got a reason to be considered as a representative of the strength of rock mass in situ.

It must be noted, however, that the existance of flaw dose not influence the strength, if the angle of it exceeds a range, 5 to 50 degrees in the present case, as seen from Fig.1.

Table 1 State of flaws

Class	State of flaws
A	Flaws are open, very distinct, strongly weathered, or large in number.
B	Flaws are distinct, weathered, or in parallel orientation.
C	Flaws are visible but not open, and are not weathered.
D	Flaws are not distinct, or there is no visible flaw.

Table 2 Class of rock and elastic-wave velocity for Palaeozoic sandy slate

Class	Piece number	Mean elastic wave velocity (km/s)
A	30	5.14
B	17	5.38
C	20	5.53
D	12	5.61

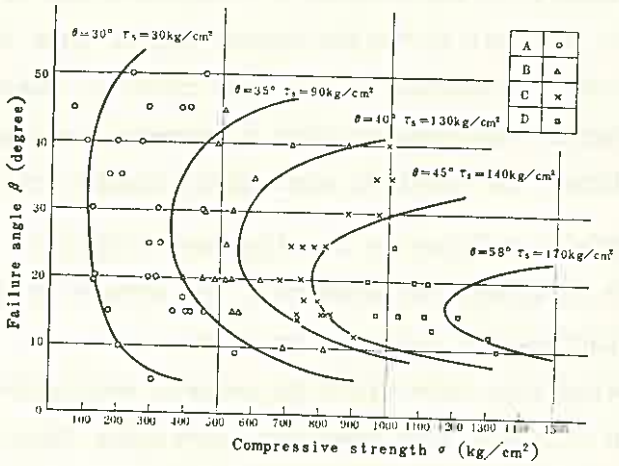

Fig. 1 Failure angle versus compressive strength

Table 3 Quasi strength of rock mass and strength of flaw determined in the test

Class	Velocity in situ v (km/s)	Coefficient of flaw k=(v/V)²	Quasi strength σc=σc×k (kg/cm²)	Strength of flaw σ (kg/cm²)
A	1.4~2.3	0.06~0.17	81~218	100~300
B	3.0~3.6	0.29~0.39	372~507	400~600
C	4.0~4.5	0.51~0.65	660~838	700~900
D	4.8~5.2	0.73~0.86	950~1120	900~1,300

* V was assumed as 5.61 km/s
** σc was assumed as 1,300 kg/cm²

1) Ikeda,K : ibid Vol.11,No.2, 1970, pp 71~74

FAILURE PROPERTIES OF ANISOTROPIC BRITTLE MATERIAL WITH WEAKNESS PLANE

Kazuo YAMAMOTO, Osaka Prefectual Technical College
Masaki ARIOKA, Kumagaigumi Co., Osaka

1. Introduction

There are some types of anisotropy (as foliation, stratification and shistosity, etc.) in some rocks. It is essential to investigate their effects on the mechanical properties of rocks.

Theoretical approaches that expound the failure on anisotropic brittle material have been suggested by Jaeger, Hoek, and Walsh and Brace. These approaches are two-dimensional analyses developed from Mohr-Coulomb and Griffith criteria.

Similarly, such experimental researches on slate have been done by Donath and Hoek. They show the relative correspondence between the experimental results and the previous theoretical analyses. In these researches, however, the failures on cylindrical specimens which are subject to the conventional triaxial compressive stresses are investigated.

In the present research, since some types of anisotropy in real rocks are irregular and complicated, a series of uni-, bi- and triaxial compression tests were performed using the specimens of artificial anisotropic mortar cubes.

From these experiments, we examined the effects of joints on the strength and aspect of failure and referred to the shape of failure surface in principal stress space on the anisotropic specimens.

2. Experiments

(1) Specimen and method of experiment

Specimens are the mortar cubes with the construction joints and are 5.5 cm in a side size. The joints exist parallel with a principal stress σ_3. The inclinations α of joints to a principal stress σ_1 are seven kinds of 0°, 15°, 30°, 45°, 60°, 75° and 90°.

The apparatus used is a large-sized triaxial compression testing machine that can give independently three principal compressive stresses. The rates of loading are about 2 to 4 $kg/cm^2/sec$.

The kinds of experiments are as follows. Firstly, the uni- and triaxial conventional compression tests were carried out to examine the effects of confining pressure on the strength and aspect of failure. Secondly, the triaxial extension test and the compression test under constant mean principal stress were done to examine the shape of failure surface in principal stress space.

(2) Uniaxial and conventional triaxial compression test

Fig.1 shows the correlation between the inclination of joint and the strength and aspect of failure at each stage of confining pressure in triaxial compression test. The uniaxial compressive strength σ_c for generalization is equal to 248 kg/cm^2.

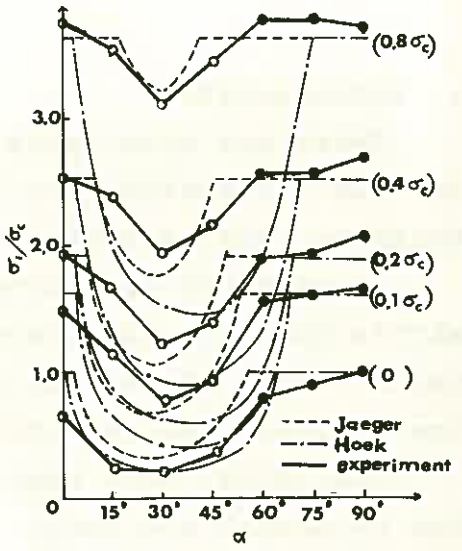

Fig. 1 Relation between inclination of joints and strength, in experiments and criteria
○ full-separated
◐ semi-separated
● no-separated

The effect of joints on strength appears at $\alpha=15^\circ$-45°, especially at $\alpha=30^\circ$. The rate of decrease in strength becomes smaller as confining pressure increases. On 30°-specimen the rate of decrease becomes to 80% and 15% under confining pressure 0 and 200 kg/ cm^2 and respectively.

Next, let us observe the aspect of failure in relation to the separation along joints. The full-separated failure along joints occurs at $\alpha=15^\circ$-45° showing the decrease in strength. The separation is mainly caused at $\alpha=15^\circ$ by cleavage. The aspects of failure on 0°-, 60°-, 75°- and 90°-specimen are similar to that on the isotropic specimen under no influence of joints. These correlations are compatible with the experiment results by Donath.

Moreover, let us consider the comparison of failure criteria with experiment results. Jaeger's and Hoek's criteria are shown together in Fig.1. The material strength constants of joint and mortar itself obtained from experiments (as shearing test, etc.) are used in case of application to these criteria.

Jaeger's criterion is relatively in agreement with experiment results except the regions under lower confining pressure and at $\alpha=45^\circ$-60°. This lower strength at $\alpha=45^\circ$-60° in experiments, we guess, will be due to mixed failure midway between slip along joints and slip in mortar, because Jaeger's criterion represents that the

failure of anisotropic material may take place from slip possible either along joints or in mortar itself. Besides, we guess, it will be due to adding the axial cleavage that the lower strength under lower confining pressure is observed in experiments.

Next, Hoek's criterion is not widely lower strength value than that of experiment. The discrepancy, we guess, will be traced to the assumptions of criterion that the opened long cracks exist in line along joints and that the ultimate strength is defined by initiation of growing cracks. But, the modified criterion that assumes the closed crack is similar to Jaeger's criterion.

(3) Triaxial extension and compression test

It is well known that a failure surface in principal stress space forms column, cone or pyramid. Therefore, in order to determine the failure surface in the region of compressive stress, it is necessary to examine the loci on Π- plane and Rendulic-plane.

The loci on Π-planes for 30°-60° specimen are shown in Fig.2. The broken line drawn in Fig.2 shows the loci for the isotropic specimen.

With respect to 30°-60°-specimen, the decrease in strength on accout of the effect of joints is shown at $\sigma_1>\sigma_3>\sigma_2$. The rates of decrease in terms of τ_{oct} are 12% and 9% at maximum for $\sigma_{oct}=0.8\sigma_c$ and $1.2\sigma_c$ respectively. This tendency is also shown similarly for 45°-specimen.

The locus on Rendulic-plane,without graphical representation in this paper, describes a curve of parabola and straight line under lower and higher mean principal stress respectively.

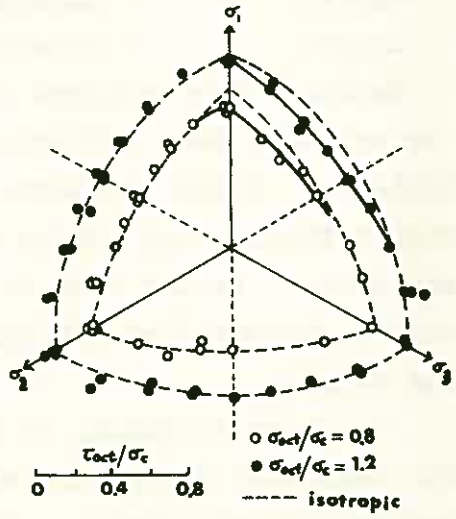

Fig. 2 Loci of failure surface for 30°-60° anisotropic specimen

From the results of these tests and biaxial compression tests, the failure surface in principal stress space is similar to pyramidal surface whose intersectional locus on Π-plane is shown in Fig.2.

Published in Journal of the Society of Materials Science, Japan, Vol.19, No. 197, Feb.1970.

STUDY ON WEATHERING OF IGNEOUS ROCKS

Tokumi SAITO
Mamoru ABE , Tohoku University
Shoichi KUNORI

The relationship between physical and mineralogical properties of weathered igneous rocks were studied to define a quantitative measure of the degree of weathering. The rock specimens used in this study are as follows:

quartz diorite : Mizunuma dam, Ibaragi prefecture
andesite : Atagoyama quarry, Miyagi prefecture
dacite : Sakunami quarry, Miyagi prefecture
basalt : Hirasawayama quarry, Fukushima prefecture.

Based on the research of structure of weathered zones at four places, we proposed some criteria on the degree of weathering as given in Table 1. These specimens were investigated in terms of microscopic observation, X-ray powder diffraction method and differential thermal analysis. In the case of quartz diorite, the altered area in feldspar is also measured as a " measure of altered area " by means of Integrating Stage.

As shown in Fig.1, it is possible for quartz diorite to classify the degree of alteration of feldspar and biotite and the degree of destruction of quartz. The classification of the degree of mineralogical weathering is as follows:

total number of degree of alteration and destruction	degree of mineralogical weathering
3 - 4	1
5 - 6	2
7 - 8	3.

On the other hand, the experimental results in the case of other three kinds of volcanic rocks indicate that the alteration of groundmass is well marked, and that the alteration of main minerals follows the sequence; primary mineral → montmorillonite mineral → halloysite mineral. From these results the degree of mineralogical weathering of volcanic rocks can be divided into the following classes :

secondary minerals during the course of weathering	degree of mineralogical weathering
clay mineral rare	1
montmorillonite mineral	2
montmorillonite mineral and halloysite mineral	3
halloysite mineral	4.

We measured the elastic wave velocities, density, effective porosity, uniaxial compressive strength and rebound value by Schmidt test hammer.

The dependence of elastic wave velocities on water saturation was also investigated. They are clearly seen from Figs.2 and 3 that the elastic wave velocity and density decrease with increasing porosity. The uniaxial compressive strength, which is considerably affected by the alteration of main minerals, decreases as the porosity increases. The relation between longitudinal wave velocity and uniaxial compressive strength is given in Fig.4. Fig.5 may show a linear correlation between rebound value and longitudinal wave velocity in natural dry condition. This suggests that rebound value can be used as a convenient yardstick for estimating longitudinal wave velocity. Fig.6 shows elastic wave velocities as a function of water saturation. Longitudinal wave velocity is influenced by saturation with water, while no effect of water saturation on transversal wave velocity is observed. Variation of longitudinal wave velocity with respect to degree of saturation in quartz diorite is different from the results for other three kinds of volcanic rocks. Wave velocity - water content curve is affected also by the porosity of sample. The experimental results are summarized in Table 2.

References (in Japanese)

1) Kunori, S. , M. Abe, and T. Saito : Study on Weathering of Granitic Rocks (1), BUTSURI-TANKO (Geophysical Exploration), Vol.24, No.1, 6-17, 1971.

2) Saito, T., M. Abe, and S. Kunori : Study on Weathering of Granitic Rocks (2), ditto, Vol.24, No.5,10-15, 1971.

3) Saito, T. and M. Abe : Study on the Physical Properties of Weathred Igneous Rocks by Schmidt Test Hammer, ditto, Vol.26, No.1, 19-31, 1973.

4) Abe, M. and T. Saito : Variation of Elastic Wave Velocity with Saturation in Igneous Rocks (1) : ditto, Vol.26, No.4, 3-13, 1973.

5) Saito, T. , M. Abe and S. Kunori : Study on Weathering of Volcanic Rocks (1),(2),ditto, Vol.27, No.1, 1974.

Table 1. Zones of weathering

Zone of weathering	Weathering profile: Quartz diorite	Weathering profile: Volcanic rocks	Colour of rocks: Quartz diorite	Andesite	Dacite	Basalt	Friability	Features of fissure
5	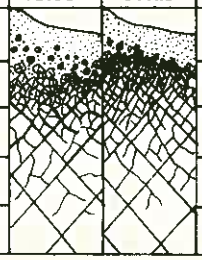		brown	dark brown	reddish brown	light brown	very friable with hand	Rock structure is barely retained.
4			brownish gray	dark brown	reddish brown	light brown	very friable with hammer	Cracks are filled up with debris and clay.
3			brownish gray	brown	brown	light brown	friable with hammer	marked irregular cracks
2			light brownish gray	light brown	light brown	brown~light brown	hardly friable with hammer	irregular cracks
1			gray	bluish gray	greenish gray	dark gray	not friable with hammer	joint only

Table 2. Summarised experimental results.

	Quartz diorite				Andesite, Dacite, Basalt			
Zone of weathering	1	2	3	4	1	2	3	4
Longitudinal wave velocity (Km/s)	>4.50	4.50-3.00	3.00-1.50	1.50-0.60	>4.50	4.50-3.00	3.00-1.50	1.50-0.60
Transversal wave velocity (Km/s)	>2.60	2.60-1.75	1.75-0.75	0.75-0.30	>2.60	2.60-1.75	1.75-0.75	0.75-0.30
Dry density (g/cm^3)	>2.80	2.80-2.70	2.70-2.45	2.45-1.95	>2.45	2.45-2.20	2.20-1.80	1.80-1.20
Effective porosity (%)	<1.5	1.5-3.0	3.0-8.0	8.0-25.0	< 10	10-18	18-30	30-60
Compressive strength (Kg/cm^2)	>1000	1000-300	300 >		>1500	1500-600	600 >	
Rebound value by Schmidt test hammer	> 60	60-45	45-30	30-0	> 55	55-40	40-25	25-0
Longitudinal wave velocity increase with saturation(%)	< 30	30-60	60-140	140-250	0	0-15	15-60	60-150
Degree of mineralogical weathering	1	2	3		1	2	3	
Altered area in feldspar (%)	< 10	10-16	16-22	22 <				

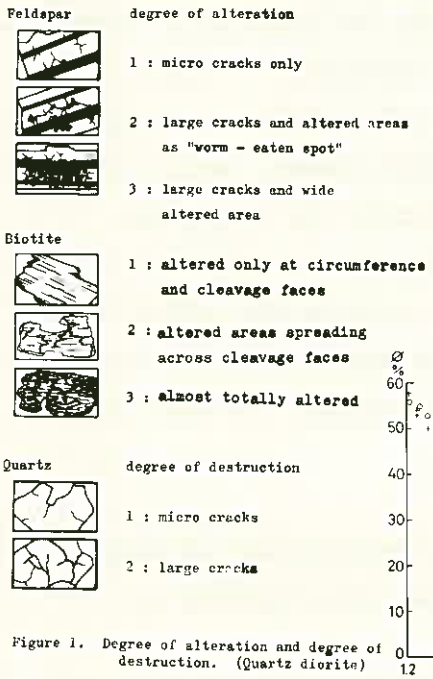

Figure 1. Degree of alteration and degree of destruction. (Quartz diorite)

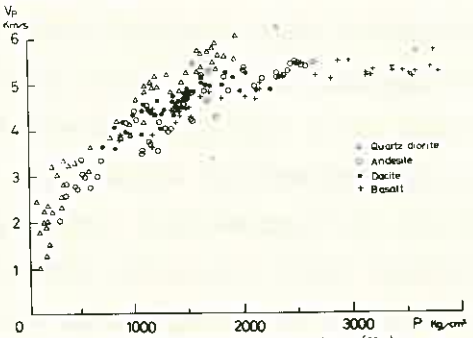

Figure 4. Longitudinal wave velocity (Vp) versus uniaxial compressive strength (P) .

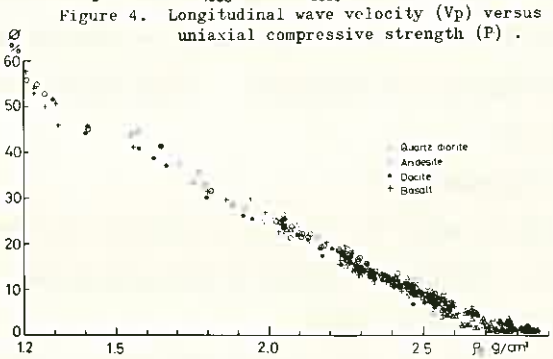

Figure 3. Effective porosity (Ø) versus dry density (ρd) .

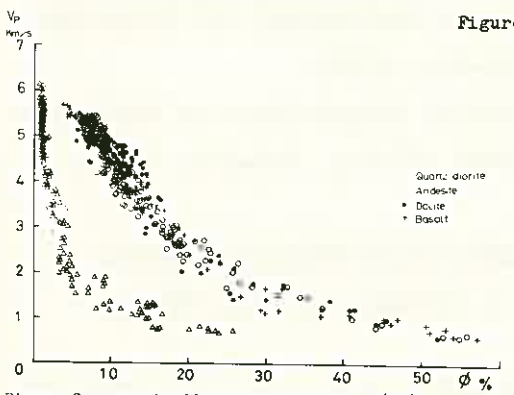

Figure 2. Longitudinal wave velocity (Vp) versus effective porosity (Ø).

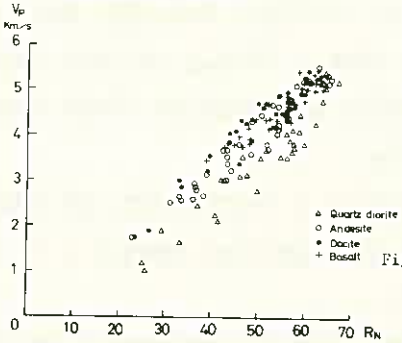

Figure 5. Longitudinal wave velocity (Vp) versus rebound value by Schmidt test hammer (R_N).

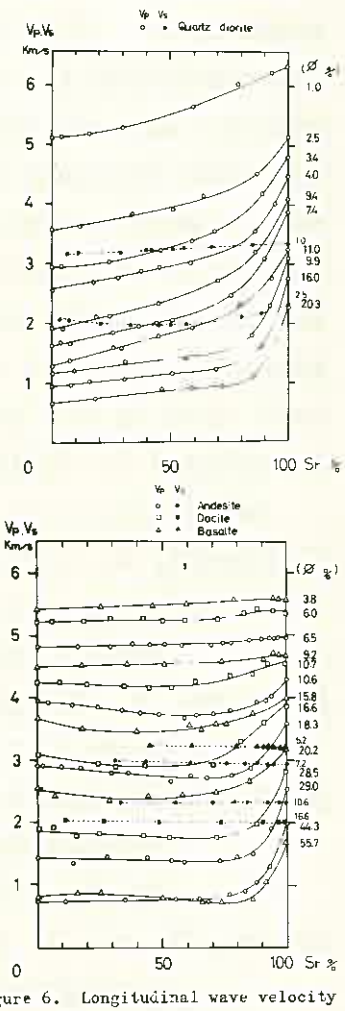

Figure 6. Longitudinal wave velocity (Vp) and tranversal wave velocity (Vs) as a fanction of degree of saturation (Sr).

EFFECT OF WATER SATURATION TO VELOCITIES OF ELASTIC WAVES, ELASTIC CONSTANTS AND COMPRESSIVE STRENGTH OF ROCKS

Michito ŌMI and Masayasu INOUE
Kumamoto University

In order to reserch for the degree of variation of elastic waves, elastic constants and uniaxial compressive strength due to water content of rocks, the authors have carried out an attempt experimentally and theoretically for various kinds of rocks. The samples used in this investigation are sandstone,andesite,granite, tuff and lava collected in Kyushu district.

Velocities of elastic waves were measured by means of an ultrasonic pulse method and a resonant frequency method.But when elastic constants are calculated from pulse velocities, velocity of shear wave is not always reliable at the present in its measurement. In this investigation, then, we have carried out measurement of two velocities-a dilatational wave $V_{p\ell}$ by pulse method and a longitudinal vibration $V_{r\ell}$ by resonance frequency method.

Shear modulus, bulk modulus, Poisson's ratio, density and longitudinal frequency are denoted by μ, K, ν, ρ and f,respectively, then $V_{p\ell}$,$V_{r\ell}$,and ν are approximately expressed by Eq.(1),(2) and (3).

$$V_{p\ell} = \sqrt{\frac{K + (4/3)\mu}{\rho}} \qquad (1)$$

$$V_{r\ell} = 2\ell f = \sqrt{\frac{E}{\rho}} \qquad (2)$$

$$\nu = F\left(V_{p\ell}/V_{r\ell}\right) \qquad (3)$$

In the measurement of the resonant frequency, as the rock specimens were not ideal bar but have some radial dimensions.But the authors have neglected this correction for it because it will be less than 1%.The typical examples of change in $V_{p\ell}$, $V_{r\ell}$ with saturation are shown in fig.1.

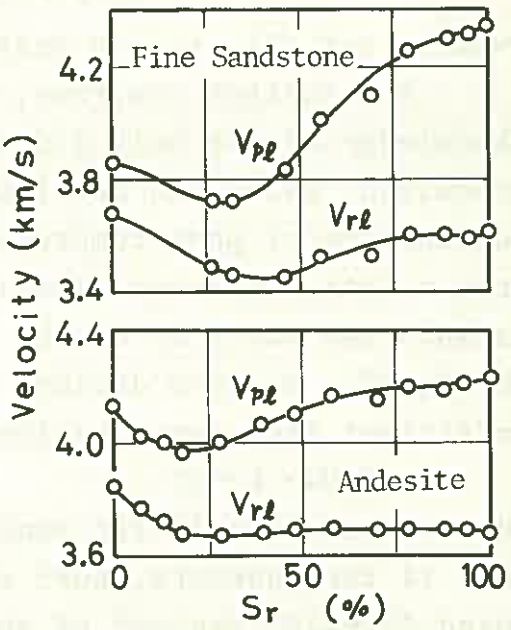

Fig.1 Change of Velocities with Saturation

An interesting result was obtained for weathered rocks. It is that degree of the velocity change with saturation

is different for the same kind of rocks which have various stages of weathering. Results of the measurements of V_{pl} on the various weathered rocks which are coarse sandstones in the Tertiary are shown in fig.2.

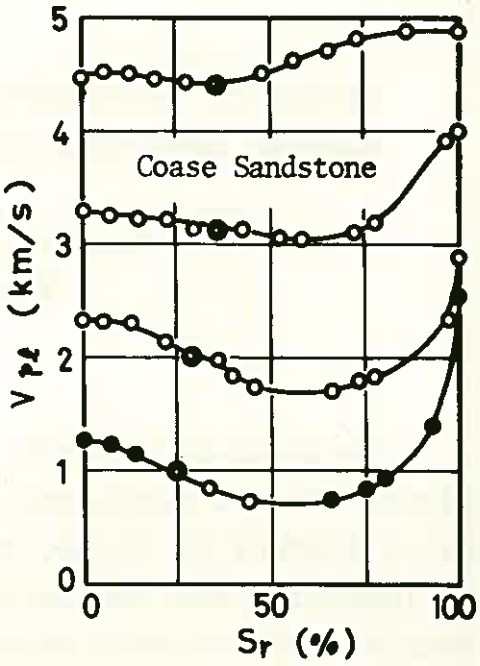

Fig.2 Velocity Change due to Degree of Weathering

We will attempt to apply the theory of porous elastic media which were derived by Biot for our results except the weathered rocks. Velocity of the dilatational wave in porous dry rocks is given by Eq.(4),

$$V_{dry}^2 = \frac{K_b + (4/3)\mu}{(1-\phi)\rho_s} \qquad (4)$$

where, K_b is bulk modulus of the porous dry rock, ϕ is porosity and ρ_s is density of the solid material. At low frequency range, velocity of the dilatational wave in water saturated rocks by taking an average of Poisson's ratio $\nu=0.2$ is expressed as follows,

$$V_{sat\cdot 0}^2 = \left[\frac{(1-K_b/K_s)^2}{\phi/K_f + (1-\phi)/K_s - K_b/K_s^2} + 2K_b \right] \frac{1}{\rho} \qquad (5)$$

where, $\rho=(1-\phi)\rho_s+\phi\rho_f$, K_s, K_f are the bulk modulus of solid material and fluid in pore. At higher frequency range, the velocity is expressed by Eq.(6),

$$V_{sat\cdot\infty}^2 = \left[\frac{\rho\phi/\kappa\rho_f + (1-\beta)(1-\beta-2\phi/\kappa)}{(1-\phi-\beta)/K_s + \phi/K_f} + 2K_b \right] \times \frac{1}{\rho\left(1-\frac{\rho_f}{\rho}\cdot\frac{\phi}{\kappa}\right)} \qquad (6)$$

where, $\beta=K_b/K_s$, κ is a mass coupling factor(=1~3).

For further progress, basic knowledge of the bulk modulus is required. Using van der Knaape's definition of pore compressibility, the relation between elastic constants and porosity can be written by Eq.(7). We have decided this coefficient from our experimental

$$K_s/K_b = 1 + c\phi \qquad (7)$$

data. Those are 50 for sandstones and 14 for andesite, tuff etc. We used 37.9×10^{10} dyn/cm^2 of quartz for K_s in this calculation of c.

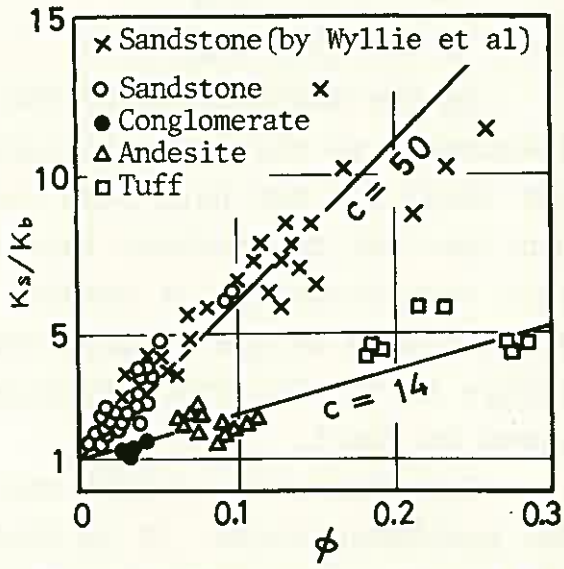

Fig.3 K_s/K_b as a Function of ϕ

A calculated relation between the dilatational wave velocity and porosity is showed in fig.4.

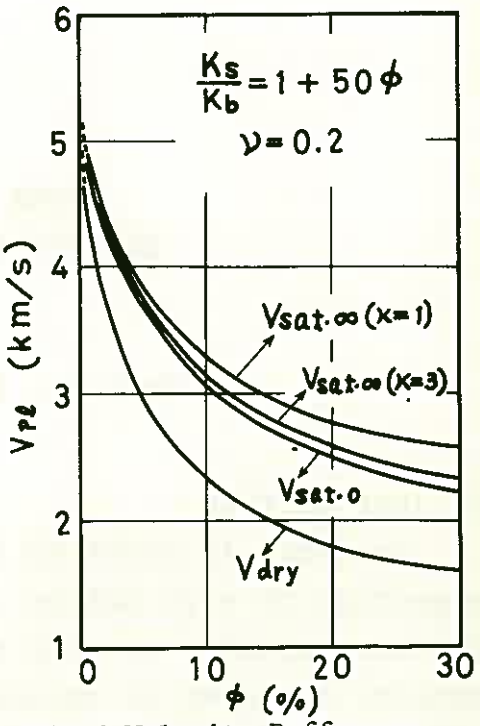

Fig.4 Velocity Defference between Dry and Saturated Rocks

Change of Poisson's ratio due to saturation are showed in fig.5. It is evident from this figure that Poisson's ratio increases with saturation. Change of it for sandstone is the most remarkable of all rocks. Now we will attempt to explain this increment of Poisson's ratio based on the theory of porous media. Stress-strain relations of fluid saturated porous media were as follows,

$$\left.\begin{aligned}\sigma_{ij} &= 2\mu e_{ij} + (Ae+Q\varepsilon)\delta_{ij} \\ -p &= Qe + R\varepsilon\end{aligned}\right\} \qquad (8)$$

where, A,Q and R are the Biot's elastic constants, p is the pressure acts on pore fluid part, σ_{ij}, e_{ij} are the stress and strain tensor of solid part, and the volume change of the solid and fluid part are denoted by e and ε.

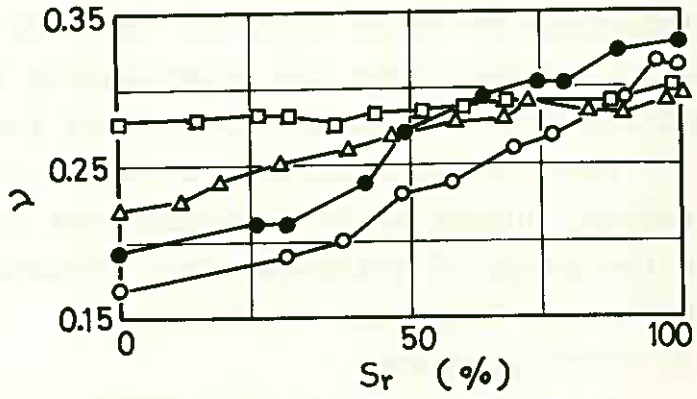

Fig.5 Change of Poisson's Ratio with Saturation

In order to simplify the treatment, it was assumed that plane waves will propagate at low frequency in closed system. The stress-strain relation under this assumption is compared with a classical stress-strain relation, then,Poisson's ratio of fluid saturated porous media is expressed by Eq.(9).

$$\nu = \frac{1}{2}\left[1 - \frac{\mu}{(A+2Q+R)+\mu}\right] \qquad (9)$$

While, strength have a different tendency of change due to water content to that of velocities. The uniaxial compressive strength changes in the form of following exponential relation as a function of the water content of rocks in our experiments,

$$\sigma_c = ae^{-bw} + c \qquad (10)$$

where, σ_c is uniaxial compressive strength (kg/cm^2), w is water content (%) and a, b and c are constants.

SOME CONSIDERATIONS ON ELASTIC WAVE VELOCITY OF ROCKS

Takeshi ŌKUBÔ, OYO Corporation

1. Introduction

Recently in order to investigate and evaluate the engineering properties of rock masses , the measurements of elastic wave velocity have been usually carried out. It is well known that elastic wave velocity of rocks is ralated to its elastic moduli (Young's modulus , rigidity, Poisson's ratio, etc.), which are largely influenced by the states of pore, water content, pressure, temperature and so on. Accordingly, for knowing sufficiently the physical and mechanical properties of rocks from its velocity of elastic wave, it is necessary to make clear the relationship between elastic wave velocity and the above-mentioned factors of rocks.

While there have been a number of experimental studies on this problem, author again examines some interrelations in this paper, on the basis of extensive test results by rock specimens obtained at various locations in Japan.

2. Tests procedure

5cm cube-shaped and cylinder-shaped test pieces which ratio between diameter and length is nearly 1:2, were made use of in the present study. The tests were performed about velocity of longitudinal wave, bulk density, effective porosity and static Young's modulus, by rule of the principle of the Japan Industrial Standards and the Society of Exploration Geophysicists of Japan. Besides, the tests were carried out at the two conditions that are dry state and wet state. These states are defined here as follows.

dry state ; drying the test pieces in the oven at 110°C above 24 hours.

wet state ; immersing the test pieces in water during about 48 hours.

3. Summery of test results

By arranging about a thousand sets of data obtained by the te-

sts, the relationships between velocity of longitudinal wave and other physical properties have been got, in which, as the velocity value, that of dry state was employed.

The relation of velocity of longitudinal wave to bulk density is shown in Fig.1, with those histogram in each kinds of rocks. It is seen from this figures that they have a tendency concentrating at a fixed range for respective rock kinds, as explained so far.

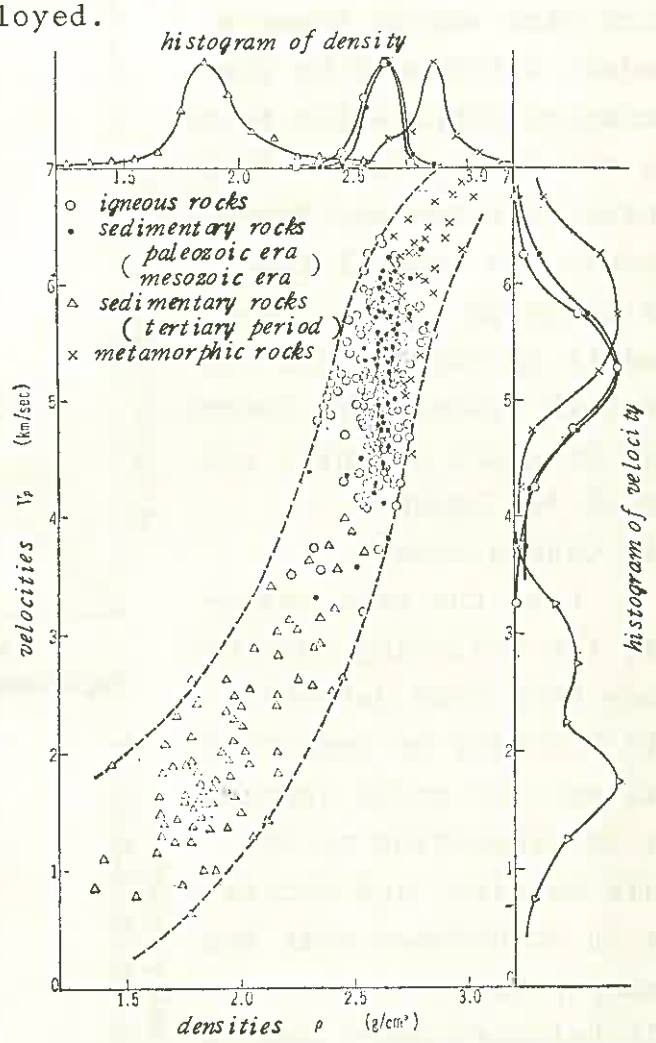

Fig.1 Velocities and densities

Fig.2 represents the interrelation between velocity of longitudinal wave and effective porosity. As shown in Fig.2, velocity decreases remarkably with increase of porosity. This fact indicates that effective porosity will have influence considerably on longitudinal wave velocity when pores are saturated by water. Consequently, for investigating how the saturation of rocks effects on its longitudinal wave velocity, velocities of dry state and those of wet state have been compared and are shown in Fig.3, in which the curved line is calculated one by the theory of Gassmann (1953). It is observed that the test results approximately correspond to Gassmann's curve in where the velocities are more than 3 km/sec, while many of velocities rather fall by containing water at the area of under 3 km/sec of those. The latter fact may be caused by chemical changes or bulk variations of matrix and clayey minerals with water saturation of rocks.

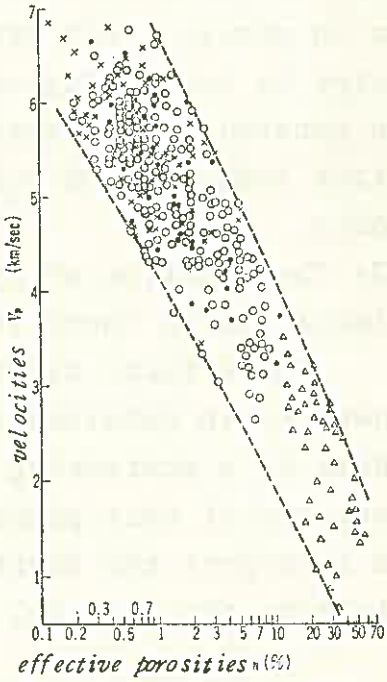

Fig.2 Velocities and effective porosities

In Fig.4, dynamic Young's moduli calculated from the longitudinal wave velocities

by the theory of isotropical elastic body are compared with static Young's moduli determined by the uniaxial compression tests on the same pieces. It is noted that dynamic Young's moduli are several times as large as static Young's moduli in whole data, while both evaluations become nearly equal at their value of 10^6 kg/cm^2.

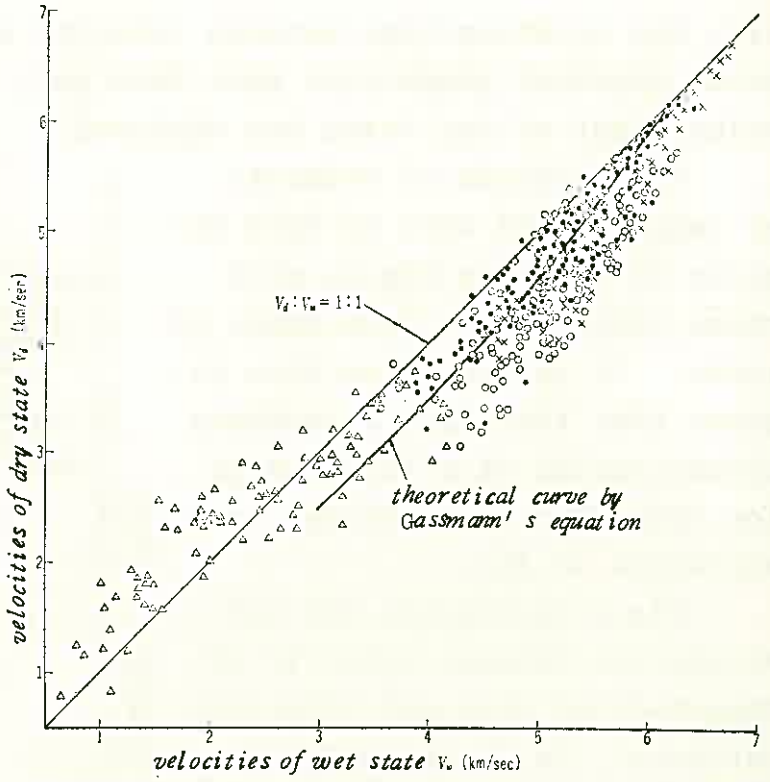

Fig.3 Comparison of velocities between dry state and wet state

4. Conclusions

From the test results, the following conclusions have been derived.

(1) Velocity of longitudinal wave of rocks increases in proportion to its bulk density, and decreases in accordance with becoming porous.

(2) Velocity value varies with the existence of water in pores. That grows large by containing water in general, but reversly, grows less in some soft rocks.

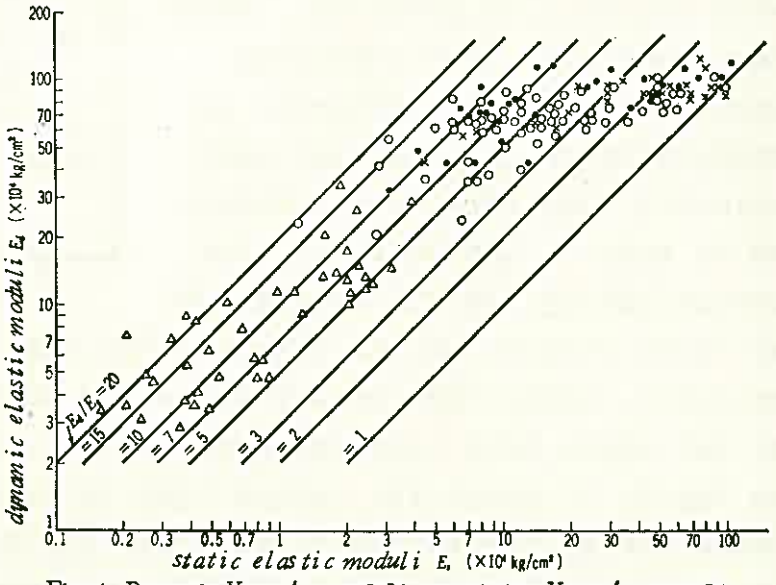

Fig.4 Dynamic Young's moduli and static Young's moduli

(3) The relation of dynamic Young's modulus to static one is non-linear, while there is considerable correlation between the two.

These facts may be admitted as a general trend respectively. However, in detailed observations for each correlation figures, there is a scattering of plotted points, which may suggest a characteristic of rock properties. Therefore, it will be important how to interpret the scattered data in each correlation figures for explaining the physical and mechanical properties of rocks.

INDICATION OF MECHANICAL PROPERTIES OF GRANITE

Ryunoshin YOSHINAKA, Saitama University
Kōzō TAKAHASHI, The Honshu-Shikoku Bridge Authority
Hiroto OCHI, ditto
Kōji ISHIKAWA, Chuo Kaihatsu Corporation

ABSTRUCT

There are several ways to designate mechanical properties of rock masses. The properties used in the indication are called Index Properties. In this report we'll show the relation between indexes and its mechanical properties. Rocks investigated herein are granite which destributed in the Inland-Sea region of Japan.

INDICATION FOR THE DEGREE OF WEATHERING

There are two ways to indicate the degree of weathering, the one is according to chemical compornents, the other is to physical properties. For the fomer, WPI (Weathering potential index) and PI (Potential index) are well known.

WPI from fresh to strongly weathered granite in this region takes about 0∿10 and its PI is around 75, those values are not enough to distingish the degree of weathering. On the other hand the relation between $2Fe_2O_3/(FeO+Fe_2O_3)$ and the ignition loss of biotite at 800°C is linear on the rectangular-coordinate, and $2Fe_2O_3/(FeO+Fe_2O_3)$ takes 1∿77, the ignition loss 0.25∿0.85%. Therefore it seems that both can be weathering indexes.

An example on physical properties is shown in Fig. 1. Porosity is closely related to compressive strength, tensile strength, shore hardness and

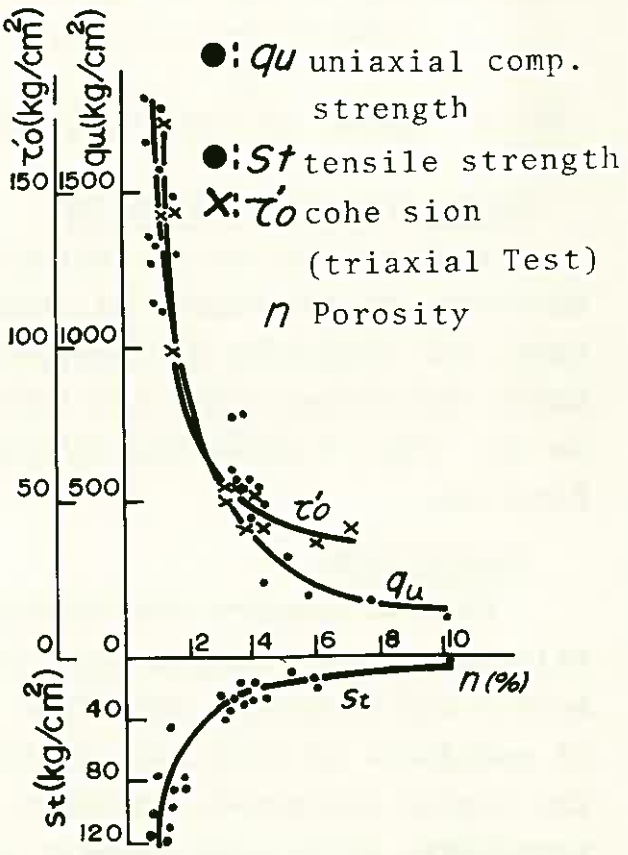

Fig. 1 Porosity and mechanical properties of granite

others. It seems that porosity is a good index for granite.

DESIGNATION OF BORING CORE

Boring cores reflects various conditions of rock mass, the relation between RQD and density of cracks N (per meter), and RQD and deformation modulus with pressiometer (E_b) are shown in Fig. 2 and 3 respectively. It is obvious that RQD and E_b indicate the deferent properties of rock mass.

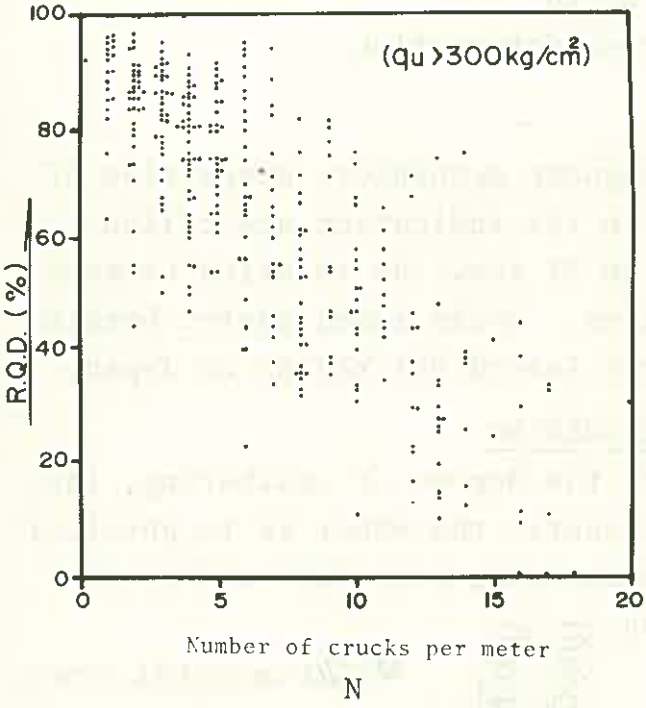

Fig.2 Number of crucks and RQD

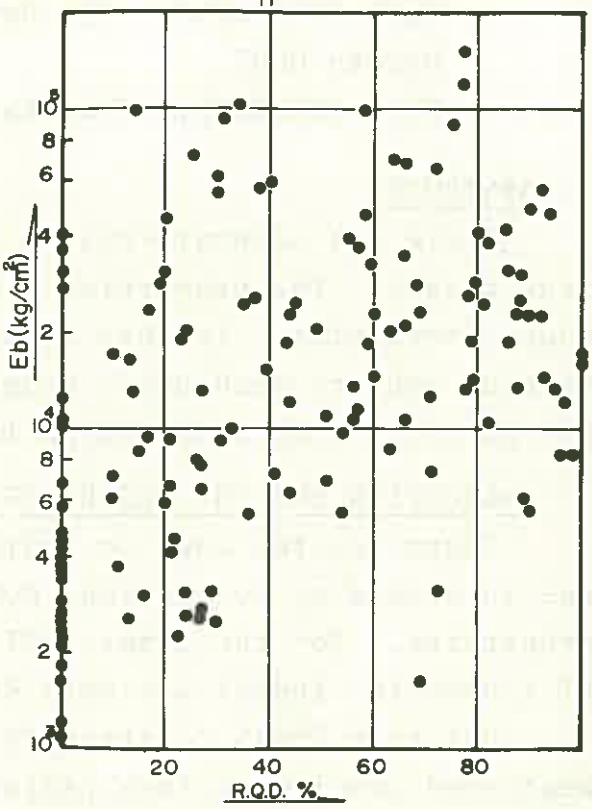

Fig.3 RQD and E_b

GEOLOGICAL CLASSIFICATION

Rock masses can macroscopically be classified into six groups, according to the degree of weathering, the length and shape of core, the condition of fissures. They are A, B, C_H, C_M, C_L and D. Earch classified group has some correlation with RQD, N, E_b and so on. Fig. 4 shows the relation between E_b and geological classification.

VELOCITYLOG

When we compare the velocity with sonic logging (1) to the velocity of core sample (2), (1) is generally smaller than (2) in both P and S waves. Therefore there are attempts to get the index of soundness of rock mass by the ratio of both velocity. But in the region concerned, it can't be applied for the reason of no remarkable difference between both two measured velocities.

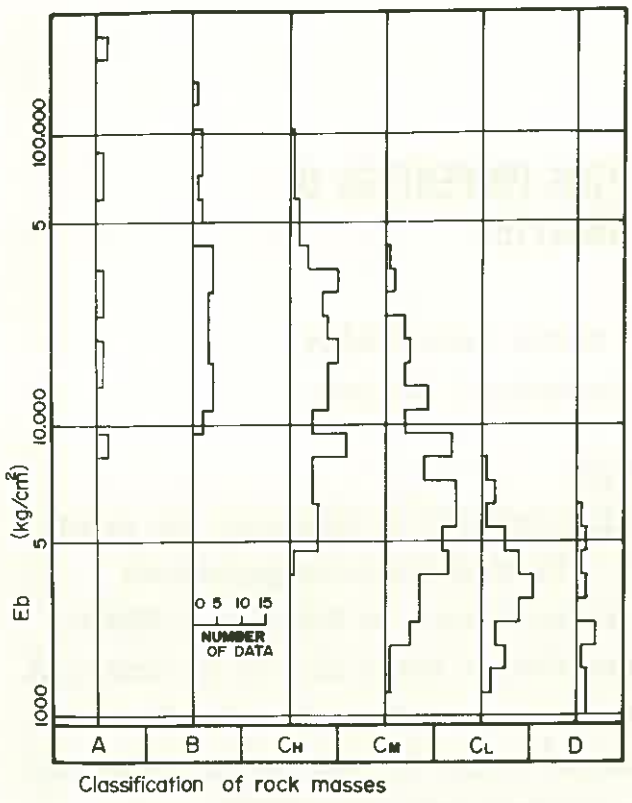

Fig.4 Rock classification and deformation modulus of rock-mass

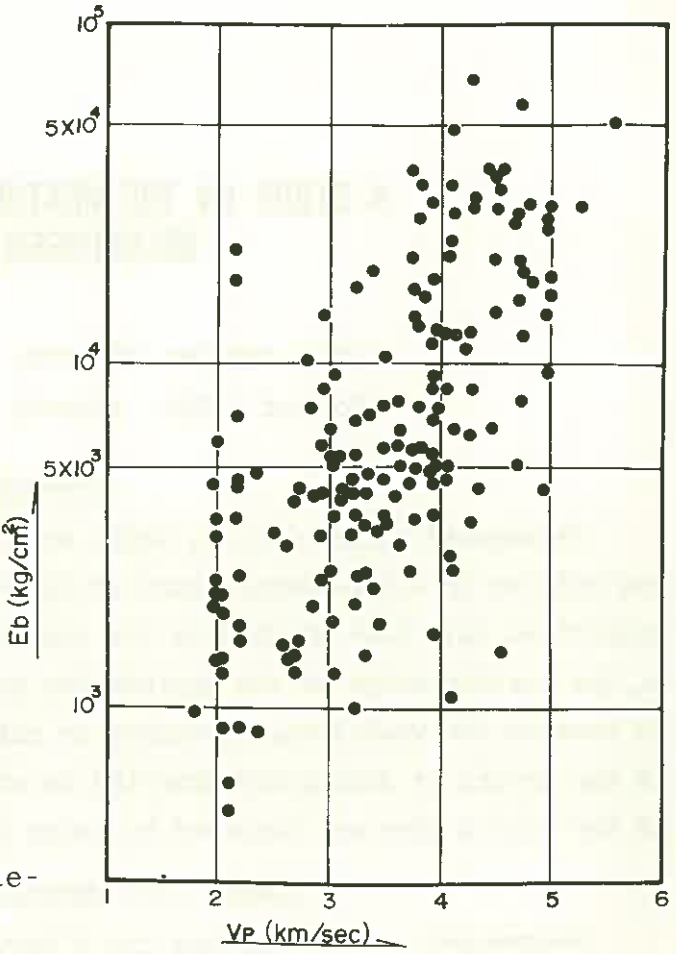

Fig.5 Velocity and E_b

INDICATION WITH PLURAL INDEXES

As mentioned above, it is difficult to indicate the complicated rock condition with single index. So we propose the indication with plural indexes.

The indexes to be used are chosen from the properties closely related with the purpose for classification, and mainly taken from the bore hole investigation. For example, there are indication with RQD and shore hardness to evaluate the shearing strength of rock masses, with E_b and V_p to evaluate the deformability, and so on.

ACKNOWLEDGEMENTS

We express our deep gratitude to Shigeo TAJIMA, Toshiaki TAKEUCHI and Masanobu ODA of members of the committee for foundation engineering of the Honshu-Shikoku Bridge, Japan Society of Soil Mechanics and Foundation Engineering, for the cooperation with our project.

A STUDY ON THE WEATHERING PROPERTIES OF DECOMPOSED GRANITES

Shin-ichiro MATSUO, Kyoto University
Kouhei SAWA, Akashi Technical College

INTRODUCTION

Decomposed granite soils, which are called MASA-DO in Japanese, are widely distributed in south-western part of Japan. Their engineering-geological properties have been studied by the committee to reseach on MASA-DO in JSSMFE. On the consideration of the engineering properties of the soils, it is important to reseach the weathering processes or patterns. In this paper, the alteration of the grains of decomposed granites is studied[1], and the weathering properties of the soil grains are observed by using an electron microscope[2),3)].

SAMPLES AND METHODS OF EXPERIMENTS

Decomposed granite samples are 3 from Mt. Hiei near Kyoto (Hi-A, B, C), and 3 from Mt. Rokko near Kobe (Ro-A, B, C). Both A samples are fresh rocks and C is more weathered. From these samples, 10 × 10 × 30 mm specimens are made, and a simple tension test is carried out by using the equipment such as Fig.1. After the observation of the fracture surfaces, the percentage of the areas of intra-grain fracture (quartz-quartz and feldspar-feldspar) and of inter-grain fracture (quartz-feldspar) are obtained. Hence, as the proportion of mica is generally less than that of quartz and feldspar, and it has the same properties of weathering as feldspar, so the quantity of mica is included in feldspar.

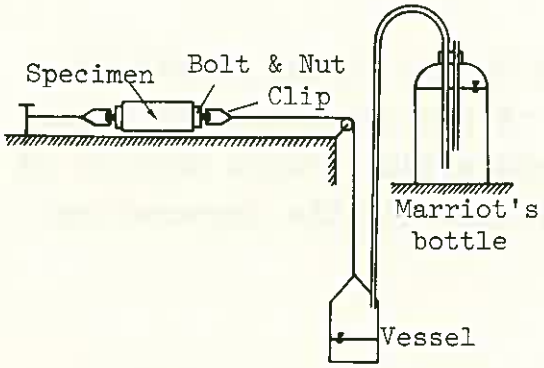

Fig.1 Equipment of simple tension test.

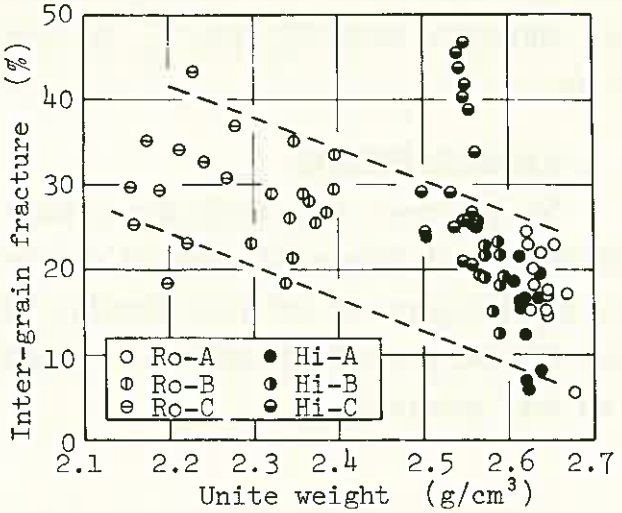

Fig.2 Weathering degree vs. inter-grain fracture.

Fig.2 shows the relation between the weathering degree (shown by an unit weight) and the percentage of the inter-grain fracture. With more weathering, the latter increase. Thus, it appears that cracks occur at the inter-grain between quartz and feldspar at the first stage of weathering, as combinning forces of minerals decrease; and that fracture occurs at the weakened grain-boundary.

Fig.3 shows the relation between the inter-grain fracture and the intra-grain one. As the former grows with weathering, the latter of both quartz and feldspar becomes reduced. The decrease of the intra-grain fracture means that the fracture doesn't penetrate the interior of grains because they are strong, and also that grains aren't yet weakened by weathering. As shown in Fig.3, in Hiei samples the decreasing quantity of intra-grain fracture of feldspar is larger than that of quartz, so it is clear that feldspar doesn't alter with weathering, and that an effect of weathering appears in quartz. On the contrary, in Rokko samples it is evident that feldspar alters and quartz is strong.

Weathering can be classified physical one and chemical one, and these two types of weathering are usually combined. In general, feldspar is altered by chemical actions, while quartz is stable. On the other hand, physical actions work on mainly quartz. Under this hypothesis, it is evident that Hiei samples examined here, takes mainly physical weathering and quartz is crushed into small grains; and that Rokko samples are subjected to chemical weathering and feldspar alters and produces clay minerals. Thus, it is considered that the properties of decomposed granite soils that result from physical weathering is different in texture from those that are produced by chemical one.

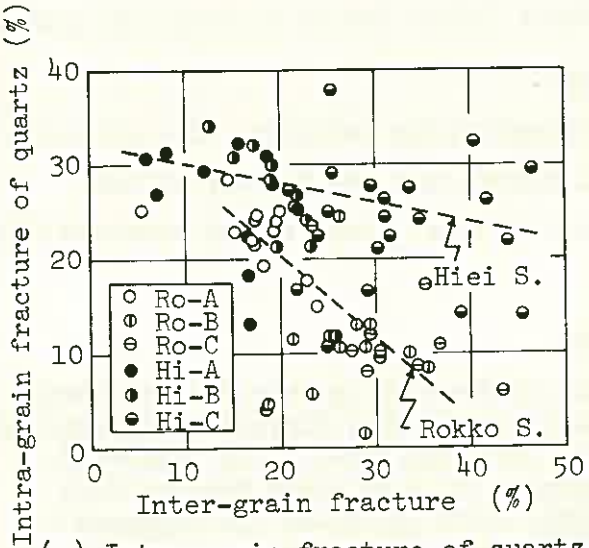

(a) Intra-grain fracture of quartz vs. inter-grain fracture.

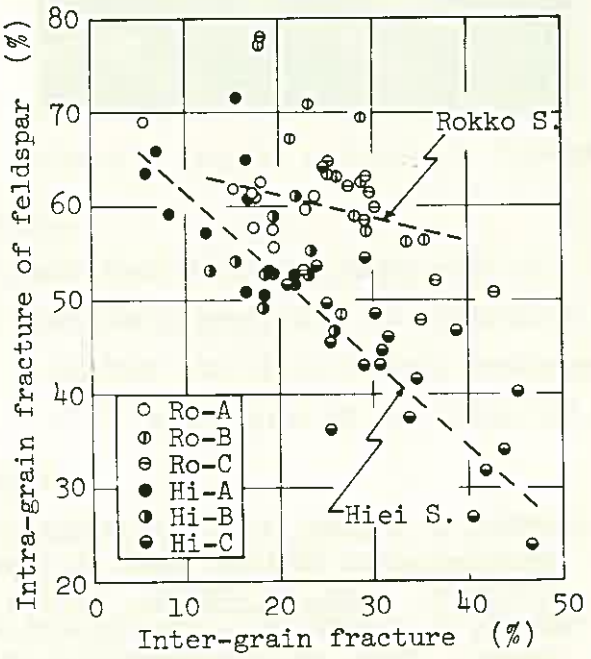

(b) Intra-grain fracture of feldspar vs. inter-grain fracture.

Fig.3 The relation between intra-grain and inter-grain fracture.

MICRO CHARACTERISTICS OF THE SURFACE OF THE SOIL GRAINS

Photo.1 and 2 show the surface of feldspar grains of different weathering degree. Photo.1 shows less-weathered samples, in which the distinct cleavages due to crystal structure of feldspar can be seen and cracks are found along the cleavage. Whereas, in the severely weathered one, the crystal structure of the grain breaks down and clay minerals are produced (see Photo.2). Photo.3 is of the surface of quartz grain. The cracks in quartz develop with micro faults. The characteristics of the cracks of quartz are that they progress in all directions and that they are sharp and clear.

Photo.1 Cleavage of feldspar.

Based on these photographes, it is summarized that the fracture of feldspar develops from fault points at cleavage, and that feldspar turns perfectly into clay particles. The fracture of quartz, however, occurs from the inherent cracks and takes place in the progress of these cracks. Quartz, therefore, cannot crush easily into small grains.

Photo.2 Production of clay minerals.

Photo.3 Micro faults & cracks in quartz

CONCLUSION

In this paper, it is evident that, with weathering patterns, the process of alteration of rock-forming minerals is different and the texture of the decomposed granite soils are various. Based on these results, the crushability of the soils can be considered[2),3)].

REFERENCES

1) MATSUO, S. & SAWA, K. - The Identification of Weathering Patterns and their Representation Methods Based on Observation of Brocken Surface on Decomposed Granites. Jour. of JSSMFE, Vol.12, No.4, 1972, pp.105-112 (in Japanese).
2) MATSUO, S. & SAWA, K. - The Selective Fracture of Decomposed Granite Soil Grains. Proc. of 18th Symposium of JSSMFE, 1973, pp.37-44 (in Japanese).
3) MATSUO, S. & SAWA, K. - Studies on the Weathering Properties and the Crushability of Decomposed Granite Soil Grains. First Australian Conference on Engineering Materials, 1974, pp.18·1-18·15.

STUDY ON SHEAR STRENGTH OF ROCK

Ryoji KOBAYASHI, Tohoku University
Kiyohiko OKUMURA, Tohoku University

In order to find out the methods for measuring the shear strength of rocks, various direct-shear tests have been undertaken by several investigators. The defects of these tests, however, are that both normal and shear stresses develop in the shear plane and that these stresses interfere with the reliable determination of the shear strength. To eliminate unknown normal stress developed in the shear plane, a method of shearing with compression are proposed by I.B.G.[1]. The test-device for measuring the single shear strength with compression is shown in Fig. 1. A cube -, or cylinder-shaped specimen (f) is placed between two beveled dies (b) set up on a testing machine. When the test-device is pressed vertically by the testing machine, both normal and shear stresses develop in a shear plane defined by the beveled dies. The ratio of these stresses is determined by the inclination of the shear plane to the direction of the applied load. For each shear tests, the average normal stress (σ_n) and the average shear stress (τ) are calculated by

$$\sigma_n = \frac{P}{A}\sin\alpha \quad --(1)\ , \quad \tau = \frac{P}{A}\cos\alpha \quad --(2)$$

where P is the compressive force (Kg), A is the shear area (cm^2) and α is the angle of shear plane inclined against the compressive force.

To obtain various ratios between the normal and the shear stresses, the test-device proposed by I.B.G. must be equipped with the accessories of different dies and wedges, however.

A new test-device for measuring the shear strength with compression is made as a trial in this investigation. The test-device, as shown in Fig. 2 and Fig. 3, can be arbitrarily adjusted the inclination angle of the shear plane by setting a pair of rotary-dies (C) and (E) . Then the rock specimens used in this investigation are five kinds of rocks, namely "KIMACHI" sandstone, "IZUMI" sandstone, "AKIYOSHI" marble, "OGINO" tuff and "MURATA" andesite. Each specimen for the single shear with compression is formed into a cube (35 x 35 x 35 mm^3).

Satisfactory results in this test are usually to be obtained with the inclination angles ranging from 15° to 45°. Fig. 4 shows representative rock

specimen after the test of single shear with compression, and this photograph shows that the clear shear planes of these specimens are seen in the direction of shear force.

According to Mohr's theory, the shear strength is approximately shown by an intersection of τ-axis and a common tangent drawing from St-stress circle to Sc-stress circle. The shear strengths in these cases are calculated by following equations :

$$Ss\text{-}1 = \frac{\sqrt{Sc \cdot St}}{2} \quad --(3), \quad Ss\text{-}2 = \frac{\tau d}{2\sqrt{\frac{\tau d}{Sc}\left(1 - \frac{\tau d}{Sc}\right)}} \quad --(4)$$

where Sc is the uniaxial compressive strength, St is the uniaxial tensile strength and τd is the pure shear stress and equal to the uniaxial tensile strength.

We then may consider the stress-circle in tension side of the $\tau - \sigma$ co-ordinates. If Griffith's theory hold, the criterion for brittle fracture is

$$(\sigma_1 - \sigma_3)^2 + 8St(\sigma_1 + \sigma_3) = 0 \quad , \text{ if } \sigma_3 + 3\sigma_1 < 0 \quad --(5)$$

$$\sigma_1 = St \quad , \text{ if } \sigma_3 + 3\sigma_1 > 0 \quad --(6)$$

In these equations, σ_1 and σ_3 are two principal stresses, and σ_1 is algebraically larger than σ_3 . Based on the theory postulated by Griffith, the diameter of a maximum stress circle through St-point, which represents the uniaxial tensile strength on Mohr's diagram, is equal to 4St, as shown Fig. 5. Consequently, the Mohr's envelope is expressed in a common tangent drawing from 4St-stress circle to Sc-stress circle, which represents the uniaxial compressive strength. In this case, the shear strength is approximately obtained from an intersection of τ -axis and a common tangent, and can be calculated by using the following equation :

$$Ss\text{-}3 = \frac{Sc \cdot St}{2\sqrt{St(Sc - 3St)}} \quad , \text{ if } Sc > 3St$$

Griffith's theory is reasonable in the tension fracture but cannot fully explain the compression fracture of rocks. It is considered that the compression fracture of rocks can be explained well by Mohr's theory. For purpose of correcting the weak points of both theories, the failure envelope in this investigation is described by the combination of both theories. The failure envelopes of various rock specimens shown in Fig. 6 are based on above considerations. The experimental points in these figures are obtained by the test of single shear with compression, and represent the relationship between the shear strength and the normal stress developed in the shear plane of rock specimen. The failure zones represented in the shadowed portion of Fig. 6 are formed by

these experimental points. The shear strengths of rocks may be approximately estimated by the failure zone, because the failure zones approach to a failure envelopes in the vicinity of τ-axis, as shown in Fig. 6.

References

1) G. Everling : Bergbau Archiv, 25 (1964), S. 85/91

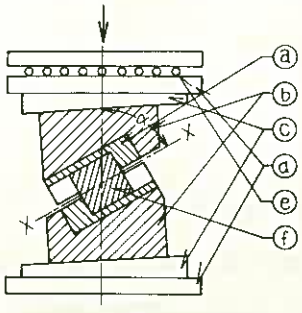

Fig. 1 Schematic diagram of test-device proposed by I.B.G

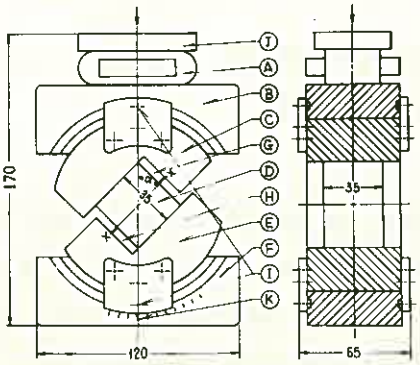

Ⓐ : Roller bearing Ⓑ,Ⓓ : Die bodies
Ⓒ,Ⓔ : Rotary-dies Ⓖ,Ⓗ : Edges
Ⓕ : Specimen Ⓘ : Screws
Ⓙ : Plate
Ⓚ : Scale which shows inclination angle of rotary-dies

Fig. 2 Schematic diagram of test-device of rotary -dies type

Fig. 3 Test-device of rotary -dies type

Fig. 4 Each rock specimen after test of single shear with compression ($\alpha = 20°$)

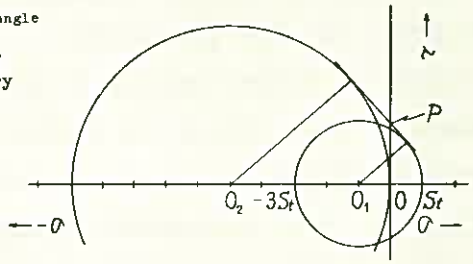

Fig. 5 Mohr's falure diagram

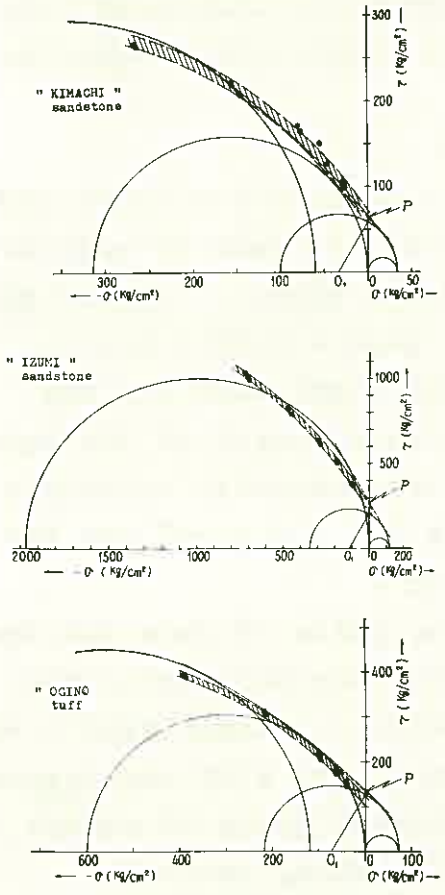

Fig. 6 Failure envelopes of each rock specimen

VARIATION IN THE CHARACTERISTICS OF DEFORMATION OF CEMENT MORTAR AND MARBLE DUE TO TRANSITION OF STRESS STATE

Toshikazu KAWAMOTO, Nagoya University
Kazumasa TOMITA

1. Introduction

It was found in the previous triaxial tests[1] that cement mortar, which seems macroscopically to be homogeneous and isotropic, exhibits the anisotropy of deformability not by the intrinsic property of material, but by the transition of stress state, and that the internal change of texture of material depends upon the degree of its porosity. In this study, the triaxial compression tests by Experiments I and II were performed for cement mortar and marble specimens in order to investigate the relationships between the characteristics of deformation and the stress states in relation to the textural change and the degree of anisotropy. The term of the textural change is used in the sense of the change of deformability of material due to the hydrostatic stress and the term of anisotropy means the change of deformability due to the deviatoric stress.

2. Specimens and Experimental Procedures

The cubic specimens of cement mortar used in the tests had a dimension of 10.8 cm in length of each side and made of ordinary Portland cement and Toyoura standard grained sand. Their mix proportion in weight is water : cement : sand = 0.65 : 1 : 2. The age of specimens at testing was twenty eight days and the specimens had the mean uniaxial compressive strength of 366 kg/cm^2.

The cubic specimens of marble were intrinsically isotropic and homogeneous and had a dimension of 5.5 x 5.5 x 5.5 cm^3 and the uniaxial compressive strength of 797 kg/cm^2.

The testing machine consists of three pairs of jack and the loading capacities of jacks are 100 ton for the horizontal two pairs and 200 ton for the vertical one pair. Experiment I was performed for cement mortar and marble specimens with the loading hysteresis. In Experiment II, the triaxial tests of cement mortar were carried out for many kinds of loading patterns.

3. Experiment I

(a) In order to discuss the change of texture due to hydrostatic stress, the following loading procedures were applied to cement mortar and marble specimens. The specimen was firstly subjected to the hydrostatic load to a prescribed mean (octahedral normal) stress state, and then it was unloaded from this state. Secondly, the specimen subjected to such a loading hysteresis was reloaded uniaxially and the axial deformation of specimen was measured. The stress-strain relationships under uniaxial compression after subjected to historical hydrostatic stress are shown in Fig. 1.

(b) The following loading patterns were applied to the specimen in order to discuss the degree of anisotropy of material after subjected to the deviatoric stress. The specimen was firstly loaded hydrostatically to a mean stress state and then was subjected to the prescribed deviatoric stress state keeping the mean stress constant. Secondly, the specimen was unloaded reversely and was successively loaded uniaxially in each direction in order to measure the anisotropy of deformability. Some stress-strain relationships of the specimens after subjected to historical deviatoric stress are given in Fig. 2. The degree of anisotropy is estimated by the variation of Young's modulus in each direction as shown in Fig. 3.

4. Experiment II

In this experiment, the cement mortar specimens were loaded triaxially under the following loading patterns: loading with constant confining stress

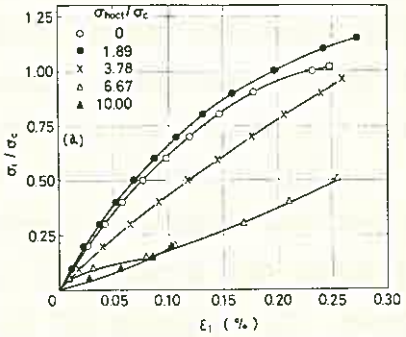

Fig. 1. (a) Stress-strain relationships of mortar specimens after subjected to historical hydrostatic stress.

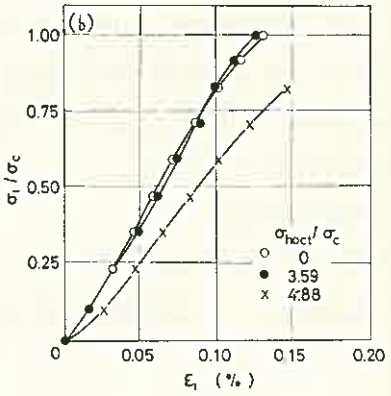

Fig. 1. (b) Stress-strain relationships of marble specimens after subjected to historical hydrostatic stress.

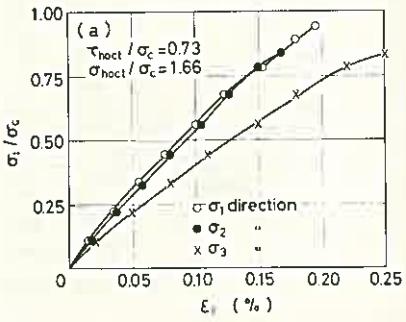

Fig. 2 (a) Stress-strain relationships of mortar specimen after subjected to historical deviatoric stress.

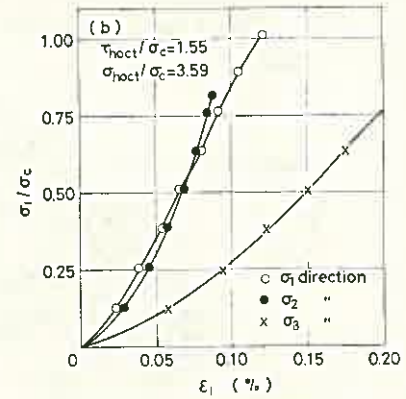

Fig. 2 (b) Stress-strain relationships of marble specimen after subjected to historical deviatoric stress.

(c-1), loading with constant ratio of σ_1/σ_3 (c-2) and loading with constant mean stress (c-3). These stress paths are shown by the relationship between $p = (\sigma_1 + 2\sigma_3)/3$ and $q = (\sigma_1 - \sigma_3)$ with various parameters in Fig. 4.

Fig. 5 shows the comparisons of Young's modulus in the axial direction obtained under different loading paths. In order to confirm the degree of anisotropy procuced with the change of stress state, the values of the ratio of Young's moduli in the σ_1- and σ_3-directions are plotted in the locations indicating the stress state as shown in Fig. 6. This figure suggests that the anisotropy hardly appears due to the deviatoric stress when the confining stress is comparatively low, but the anisotropy appears rapidly with the increase of the deviatoric stress under the high level of confining stress.

Reference

1) T. Kawamoto, et al., Proc. of 2nd Cong. of ISRM, Beograd, 2-2, (1970).

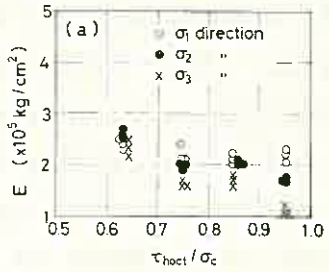

Fig. 3 (a) Variation of Young's modulus of mortar specimen to magnitude of historical deviatoric stress.

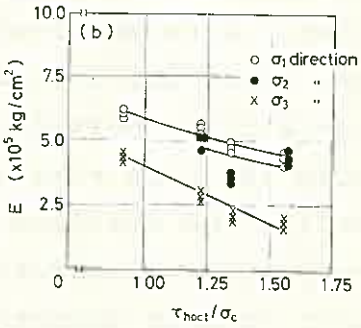

Fig. 3 (b) Variation of Young's modulus of marble specimen to magnitude of historical deviatoric stress.

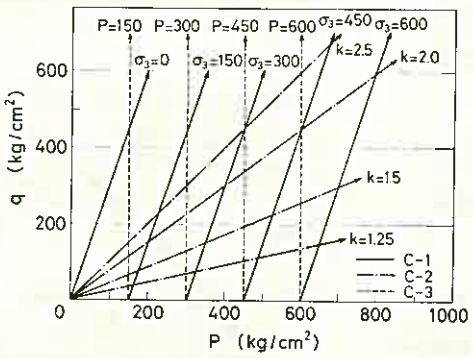

Fig. 4 Loading paths.

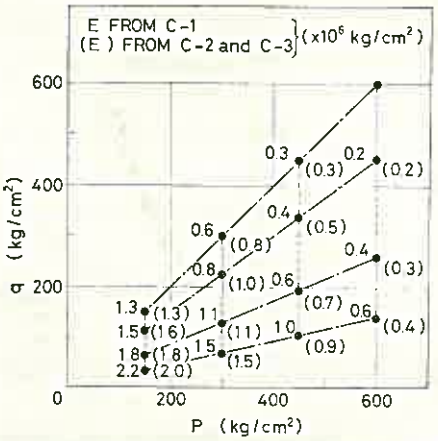

Fig. 5 Comparisons of Young's moduli in the axial direction obtained under different loading paths.

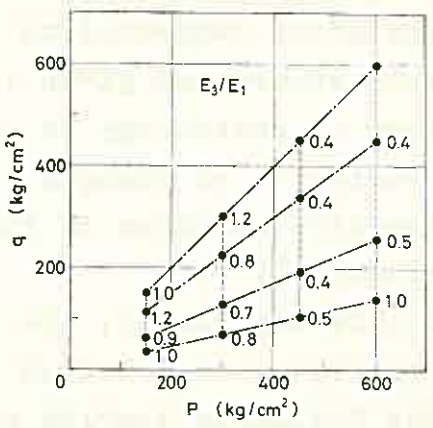

Fig. 6 Ratio of lateral Young's modulus to axial Young's modulus under different loading paths.

A STOCHASTIC ASPECT OF THE FATIGUE FAILURE OF ROCK

Yuichi NISHIMATSU, University of Tokyo

1. Introduction

It is well known that the result of standerd rock strength test shows a fluctuation wider than those of metallic materials. This suggests that the result of fatigue test of rock would show a much wide range of fluctuation and it needs some stochastic approaches to evaluate and discuss the test result.

In this paper the author would give some typical results of fatigue test of rock and discuss on the stochastic distribution of fatigue life related with the failure process of rock.

2. Experiments

2.1. Test apparatus and method

The fatigue test of rock specimen is carried out under the pulsating compressive or tensile load by means of a standerd Losenhausen type fatigue testing machine. Therefore, the applied stress is given by

$$\sigma = \sigma_m + \sigma_a \cdot \sin(2\pi\omega t + \phi) \qquad (1)$$

where σ_m is the mean stress and greater than the stress amplitude σ_a, ω is the freguency of loading which is kept in 5 Hz.

2.2. Preparation of test pieces

The test piece is cored from a block of rock sample and cut with a diamond wheel saw. The both end faces of test piece are ground on the grinding table and furnished to be parrallel with each other within the accuracy of ±25/1000 mm.

The test piece furnished by this procedure for the compression fatigue test is a cylinder of 20 mm in diameter and 40 mm in height. However, the test piece for the tension fatigue test must be a dog-bone shape. In order to prepare such a dog-bone shaped test piece, the rock cylinder of 40 mm in diameter and about 150 mm in length is furnished by the procedure described above. The both end faces of this rock cylinder are glued to the steel end caps by means of the alignment jig which has been developed in

the author's laboratory. After drying out the adhesive, the section of rock cylinder is reduced and aligned over about three quarters of its length by means of the grinding lathe. The dimension of furnished test piece is 30 mm in effective diameter and about 60 mm in effective length. More than 15 test pieces are tested under the same test condition.

3. Stochastic didtribution of fatigue life

The theory of mathematical statistics indicates that the mean frequency P_ν of the νth among n ordered observations is given by

$$P_\nu = \frac{\nu}{n+1} \qquad (2)$$

Hence, the probability that fatigue life is greater than N_ν, i.e. the frequency of survival $P(N_\nu)$ is given by

$$P(N_\nu) = 1 - P_\nu = 1 - \frac{\nu}{n+1} \qquad (3)$$

where N_ν is the fatigue life of the νth among n specimens in increasing order of their fatigue lives.

The test result is plotted on the diagram in which the ordinate is the logarithm of the frequency of survival calculated by Eqs. (2) and (3), and the abscissa is the fatigue life. This diagram is named as the P-N diagram and should be distinguished from the S-N diagram or Wöhler diagram.

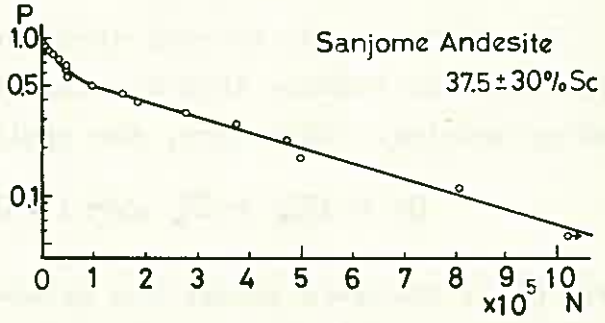

Fig. 1. P-N diagram of the compression fatigue test of a two-pyroxene andesite

Two examples of P-N diagram obtained from the fatigue test of a two-pyroxene andesite are shown in Figs. 1 and 2. All of test results give curves opening upwards on the P-N diagram. These curves are explicitly expressed as

$$P(N) = \xi_1 e^{-\lambda_1 N} + \xi_2 e^{-\lambda_2 N} \qquad (4)$$

where ξ_1 and ξ_2 is called the distribution factor and $\xi_1 + \xi_2 = 1$.

It means that the process of fatigue failure of rock consists of two Poisson processes of the step one, in parrallel and exclusive mutually. The probability of

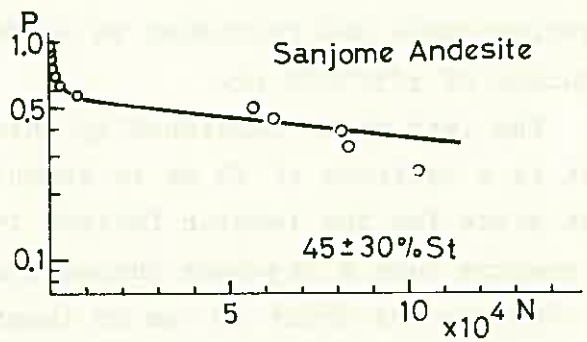

Fig. 2. P-N diagram of the tension fatigue test of a two-pyroxene andesite

the failure with one of these two processes is ξ_1 and the rate constant, i.e. the probability of failure occurrence with this failure process per unit cycle of pulsating loading is λ_1. The suffix 2 means those of the other of these two failure processes.

The test results shows that λ_2 is about 100 times greater than λ_1. Considering the results of petrographical and microfractorgraphical observation, it is suggested that a process with the smaller rate constant corresponds to the intragranular fracture and the other one with the greater rate constant corresponds to the intergranular fracture.

If the probability of survival is given by Eg. (4), then the mean fatigue life is given by

$$\overline{N} = \frac{\xi_1}{\lambda_1} + \frac{\xi_2}{\lambda_2} \qquad (5)$$

4. The effect of stress amplitude and mean stress on the rate constant of fatigue failure

The fatigue test of two-pyroxene andesite specimen is carried out under the appropriate combinations of several levels of stress amplitude and mean stress for both of pulsating compressive and tensile load.

The test result shows that the effect of stress amplitude and mean stress on the rate constants is given by

$$\left.\begin{aligned} \lambda_1 &= 8.13\times10^{5}\left(\frac{\sigma_m}{S_c}\right)^{9.78}\left(\frac{\sigma_a}{S_c}\right)^{14.5} \\ \lambda_2 &= 1.62\times10^{8}\left(\frac{\sigma_m}{S_c}\right)^{13.2}\left(\frac{\sigma_a}{S_c}\right)^{14.0} \end{aligned}\right\} \qquad (6)$$

for the compression fatigue test, and

$$\left.\begin{aligned} \lambda_1 &= 6.97\times10^{9}\left(\frac{\sigma_m}{S_t}\right)^{21.5}\left(\frac{\sigma_a}{S_t}\right)^{15.6} \\ \lambda_2 &= 3.09\times10^{8}\left(\frac{\sigma_m}{S_t}\right)^{14.8}\left(\frac{\sigma_a}{S_t}\right)^{12.5} \end{aligned}\right\} \qquad (7)$$

for the tension fatigue test.

Furthermore, the static strength test of the rock specimen survived after 10^6 cycles of repeated loading shows that the static strength of the survived specimen is not different from the mean strength of virgin specimen.

This fact suggests that the process of fatigue failure of rock is not cumultive and serial one, but a process with a remarkable rate controling step.

CONSIDERATION ON THE FRACTURE MODES AND STRENGTH OF ROCKS UNDER COMPRESSION TEST

Masao SATAKE, Tohoku University
Hisataka TANO, Nihon University

Introduction This paper discribes a consideration on the fracture modes and strength of rocks under uniaxial and biaxial compression tests. It is known that fracture of rock specimen have two typical modes, i.e. one is the cleavage type and the other is the slipping type. In this paper, the difference of these fracture modes is analysed and the idea of fracture mode ratio is presented.

Case of uniaxial compression

Cleavage type fracture The most dangerous inclination of crack is 0° as is shown in Fig.1 from the consideration[1] on stress concentration and propagation of energy. It can be assumed that the uniaxial strengths σ_{ca} and σ_{ta} are given by

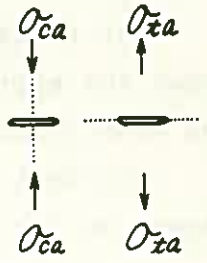

Fig. 1

$$\sigma_{ca} = \alpha \sigma_T \qquad (1)$$

$$\sigma_{ta} = \sigma_T / \beta \qquad (2)$$

where α and β are the modification coefficients in compressive and tensile strengths respectively and σ_T is the ideal (or theoretical) tensile strength.

$$\alpha\beta = \sigma_{ca} / \sigma_{ta} \qquad (3)$$

is usually called the brittleness factor of the materials.

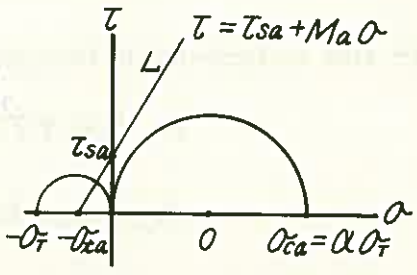

Fig.2

Slipping type fracture For this type of fracture, the concept of Coulomb's criterion may be applied. In the rock like materisls, however, it is necessary to introduce the ratio M_a of τ_{sa} and σ_{ta} which corresponds to the coefficient of internal friction in soil mechanics. Thus we have

$$\tau = \tau_{sa} + M_a \sigma \qquad (4)$$

Fracture mode ratio Fig.2 explains the difference of possibility for the above two fracture modes. Whether the line L becomes to contact the circle O or not determines which type of fracture may occur. That is, if

$$M_a > M_a^* \qquad (5)$$

Table 1

	Compressive Strength	Shear Strength	Tensile Strength	Brittleness Factor	Fracture Mode Ratio		Expected Fracture Mode		Modification Coefficients	
	σ_{ca} (Kg/cm²)	τ_{sa} (Kg/cm²)	σ_{ta} (Kg/cm²)	$\alpha\beta$	M_a	M_a^*			α	β
Jaspilite	6930	395	77.1	90.0	5.1	4.7	C		(1.5	60)
Limestone	1500	93	24.5	60.8	3.8	3.9		S	2.0	30
Sandstone(1)	1040	63	16.1	64.4	3.9	4.0		S	2.0	32
Granite	2470	123	35.0	70.6	3.5	4.2		S	(3.0	24)
Marlstone	1750	119	33.6	52.1	3.5	3.6		S	2.0	26
Chert	2260	203	69.5	32.6	2.9	2.8	C		2.0	16
Salt	154	15	6.0	25.8	2.5	2.5		S	2.0	26
Sandstone(2)	161	27	15.2	10.6	1.8	1.6	C		2.0	5
Concrete	210	39	24.5	8.5	1.6	1.4	C		2.0	4
Shale	365	100	108.0	3.4	0.9	0.8	C		2.0	1.7
Coal	112	14	21.0	5.4	0.7	1.1		S	(6.0	1)

C: Cleavage type fracture S: Slipping type fracture

where $M_a^* = \alpha\beta / 2\sqrt{1+\alpha\beta}$, the cleavage type may occur, and if M_a becomes equal to M_a^* , the slipping type may occur. In this meaning, M_a will be named the fracture mode ratio. Using the experimental results by Wuerker[2], fracture modes for various rocks expected by this theory are listed in Table 1. It is seen that M_a is approximately equal to M_a^* in almost kinds of rocks, and this fact means that the fracture modes of rocks are not simply determined. Putting $\alpha = 2$ from the experimental reports[3], it is found that β varies from about 1 to 60 as is shown in Table 1. (For values with the round bracket, $\alpha = 2$ is not suitable[5].)

Case of biaxial compression

Cleavage type fracture This type of fracture under biaxial compression may be explained by the consideration on the stress condition at the top of branch cracks. Assuming that the supperposition law can be applied, the stress at the top of branch crack is expressed as

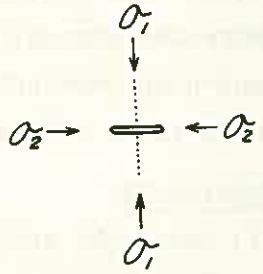

Fig.3

$$\sigma_T = K_1\sigma_1 - K_2\sigma_2 \qquad (6)$$

where K_1 and K_2 are the coefficients for σ_1 and σ_2 respectively in the cases where they are applied independently. Since it is given, from the case of uniaxial compression, that $K_1 = 1/\alpha$ and $K_2 = \beta$, Eq.(6) becomes

$$\sigma_1 = \alpha\beta\sigma_2 + \alpha\sigma_T \qquad (7)$$

As is seen in Eq.(7), as σ_2 increases, the biaxial compressive strength σ_1 increases. In such case, however, the circle O shown in Fig.2 may become larger and will contact the line L, and from this reason the fracture mode may change from the cleavage type to the slipping one.

Slipping type fracture If the shear strength τ_{sa} of rocks is smaller

than the tensile strength σ_{ta} comparatively, slips occur on the maximum shear plane ($\theta = 45^\circ$), before the growth of preexisted microcracks. Such slips may be distributed irregularly in practice, but the regular case as is shown in Fig.4 will be considered. When the concentrated tensile stress σ_t which occurs at the point with distance r from the ends of a slip becomes equal to σ_T, the crack with length r occurs as is shown in Fig.4, and the slipping type fracture may occur along the line OP with inclination ψ in this case. σ_t is given by the following equation[4]:

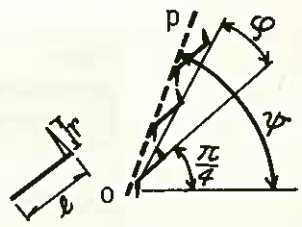

Fig.4

$$\sigma_t = \frac{2}{\sqrt{3}} \left(\frac{l}{r}\right)^{1/2} \tau \qquad (8)$$

Thus the condition of slipping type fracture under the biaxial compression is expressed as

$$\Sigma = \frac{\sqrt{3}}{2} \frac{(2\sigma_T + \sigma_1 + \sigma_2)}{(\sigma_1 - \sigma_2)} \qquad (9)$$

where $\Sigma = \sqrt{\frac{l}{r}} = \sqrt{\cot\varphi}$ ($\psi = \pi/2$ and $\pi/4$ for $\Sigma = 1$ and ∞ respectively)[5]. Generally Σ is shown by a curved surface Σ in Fig.5. This figure suggests that (1) when confining pressure σ_2 increases, the inclination ψ of slip line decreases gradually and approaches to $\frac{\pi}{4}$, (2) under the same value of the confining pressure, rocks which have the large value of ψ get also the large value of biaxial compressive strength σ_1.

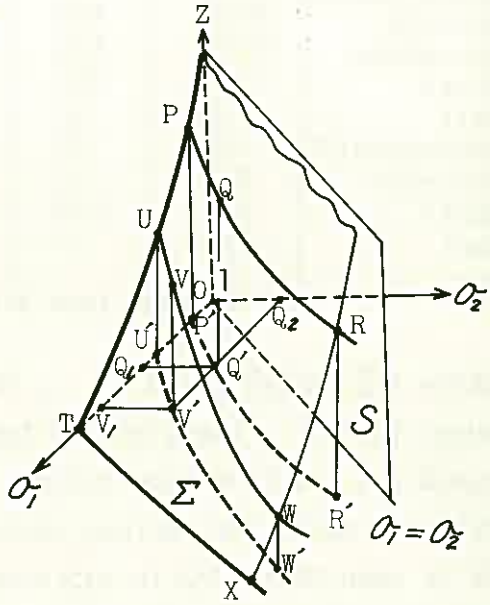

Fig.5 [5]

References

1) Satake,M. and Tano,H. : A Consideration on the Final Strength of Brittle Materials with Single Slit, Proc. 7th Symp. Rock Mech. JSCE, 46-49 (1972).

2) Wuerker, R. G. : The shear Strength of Rocks, Min. Eng., 10, 1022-1026 (1959).

3) Mae, I. and Nakao, K. : Characteristics in the Generation of Micro-Vibration Noises in Rocks under Uniaxial Compressive Fracture Test, J.Soc. Mat. Sci., 17, 181, 908-913 (1968).

4) Stroh, A.N. : The Formation of Cracks as a Result of Plastic Flow, Proc. Roy. Soc. A223, 404-414 (1954).

5) Satake, M. and Tano, H. : Consideration on the Fracture Modes and Strength of Rocks under Compression Test, Proc. 4th Nat. Symp. Rock Mech., 49-54 (1973).

A CONSIDERATION ON THE MECHANICAL BEHAVIOR OF SCHISTOSE ROCKS

Takakoto SHIMOTANI, Umetaro YAMAGUCHI, Yataro SHIMOMURA,
University of Tokyo

1. Introduction

It is well known that the structure of rocks has important influences on its mechanical properties. An investigation was made to study the influence of schistosity planes of green schist of Bessi Mine, Ehime prefecture.

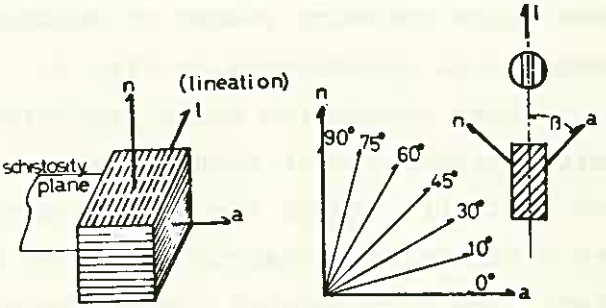

FIG.1

2. Experimental procedure

Uni-axial compression test and radial compression test were carried out on the cylinder and disc samples, of which axes were as illustrated in Fig. 1.

In the case of uni-axial compression test, more than 10 samples were tested with respect to each direction. For radial compression test, more than 10 samples were prepared with respect to each direction, and about the halves of them were loaded parallel to the schistosity plane (A type), and the others were loaded perpendicular to that direction (B type). (See Fig. 3)

3. Results

(1) Uni-axial compressive strength varied with the direction of loading, taking the minimum value at 30～45° as shown in Fig. 2. Schematic fracture surfaces were also shown in the figure.

(2) In Fig. 3, results of radial compression test were shown with schematic fracture surfaces.

(3) Stress-strain curves under uni-axial compression were shown in Fig. 4 with the angles of loading directions. And, in Fig. 5, the curve under repeated uni-axial compression in the case of 75° loading direction was shown.

(4) Tangent Young's moduli at each stress level were shown in Fig. 6.

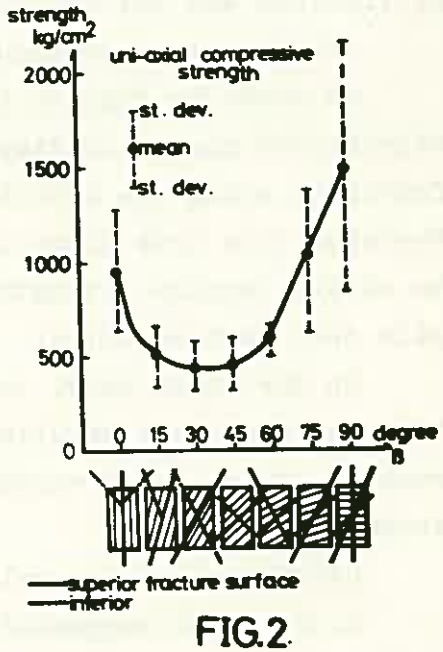

FIG.2

4. Discussion

(1) Uni-axial compressive strength

Adopting Coulomb's criterion of failure, and assuming, that i) the angle of internal friction is independent on directions, and ii) the shear strength S on the plane which makes angle ω to the weakest plane is given as $S = So - S_1 \cos 2\omega$ (where So, S_1 are constants), J. C. Jaeger suggested that uni-axial compressive strength of rock which contains planes of weakness of weakness varied parabolical as Fig. 2.

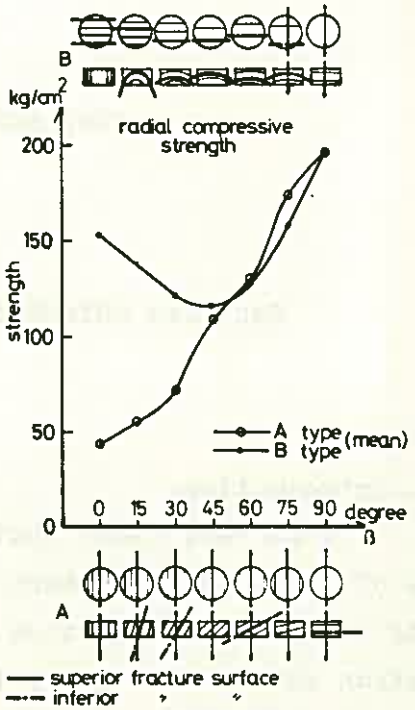

FIG.3

Above discussion means implicitly that mechanical properties of these rocks are homogenious and isotropic except the shear strength. And if the shear stress attained specified value on a plane, fracture occured simultaneously on this plane, and in the case that secondary fracture (i. e. 'granulation' on this created surface) did not occure, this plane turned into the fracture plane.

As shown in Fig. 2, about the 0° direction, eminent fracture surface was parallel to the loading direction. On the plane parallel to the loading direction, shear stress is 0, then by above discussion these surfaces must be made by the secondary fracture, Therefor, experimental results sustained the discussion phenomenally, but its mechanical interpretation of fracture was not satisfied.

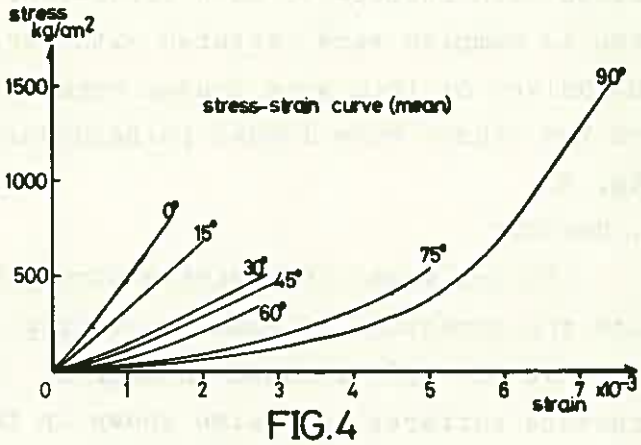

FIG.4

(2) Radial compression

As shown in Fig. 3, in B type, significant number of samples were fractured along the schistosity plane. Therefor this test migth be unlikly to obtain tensile strength, and the direct tensile test must be tried.

On the other hand, in A type, eminent fracture surfaces were parallel to the loading direction, then, these values would give tensile strengths.

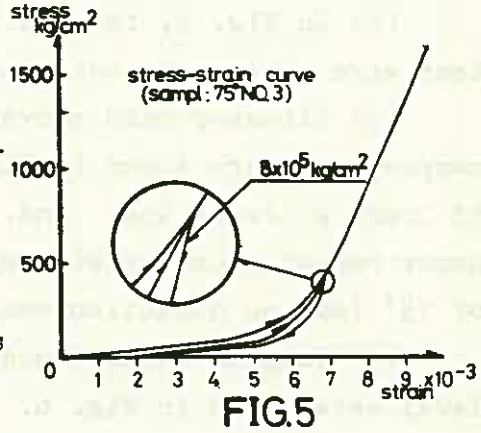

FIG.5

(3) Stress-strain relation, Young's modulus

J. B. Walsh suggested that downword convex

stress-strain curve indicated the process of the closure of cracks existing in rock under compressive stress, and showed that effective Young's modulus Eef of continuum including a crack was in plane stress condition for open crack; $1/Eef = (1 + 4\pi c^3 \sin^2\beta / v)/E$, for closed crack; $1/Eef = \{1 + 4\pi c^3 \sin^2\beta \cos\beta(\cos\beta - \mu\sin\beta)/v\}/E$, ---(1) where, E; Young's modulus of continuum, c; crack length, v; volume of continuum, μ; coefficient of friction on the crack surface, β; the angle between loading direction and the major axis of the crack. And he also showed that the slope of the tangent of the stress-strain curve immediately after unloading gave the value of E.

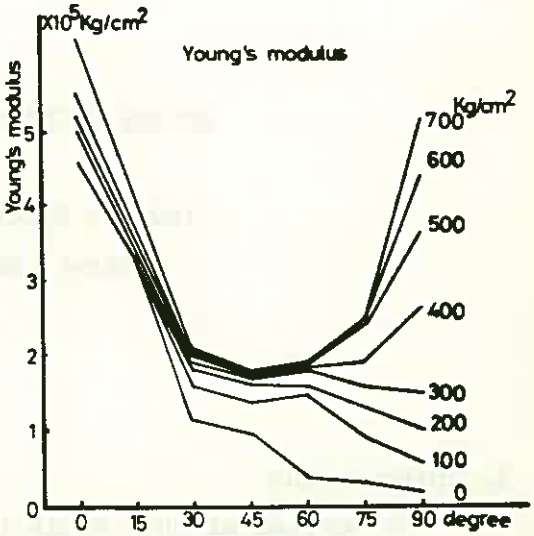

FIG.6

In the case of schist cracks may extend on the schistosity plane. Then, the greater the angle between the direction of compressive stress and the major axes of cracks, the easier the closure of cracks may be. The relation of stress and strain in Fig. 4 can be interpreted as above.

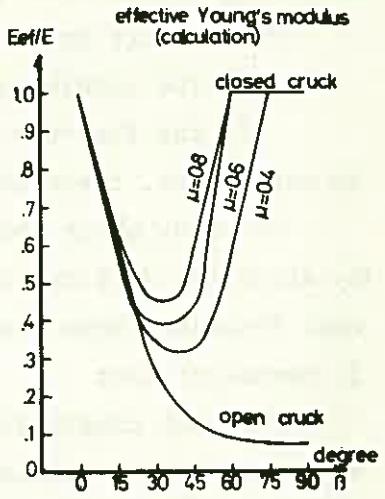

FIG.7

Substituting $c^3/v = 1$, and $\mu = 0.4$, 0.6, 0.8 to equation (1), the curves in Fig. 7 are obtained. Comparison of these curves to Fig. 6 reveals some relationship which corresponds the low stress level in Fig. 6 to the curve of open crack, and the high stress level in Fig. 6 to the curves of closed crack, respectively. The increase of stress make the curves U-shaped in Fig. 7. This is due to the crack closure.

5. Conclusion

The results obtained were as follows.

(1) The uni-axial strength was represented against the angle of sample axes by a parabolic curve having a minimum value at 30°.

(2) Radial compression test gave tensile strength, when loaded parallel to schistosity plane, but when loaded perpendicular to this direction, samples were fractured along the schistosity plane.

(3) The mechanical behavior could be interpreted based on the theory of Walsh, and assuming the presence of cracks elongating along the schistosity plane.

ON THE SLIDING OF JOINTED ROCK MASSES

Tadashi NISHIDA, Kyushu University
Kazuo AOKI, Kyushu University

1. Introduction

The purpose of this study is to know the mechanical behavior of jointed rock masses. So, we carried out a series of triaxial compression tests on mortar specimens with a pre-formed joint.

The failure modes of jointed rock masses may be considered as follows:

1. the sliding along the joint
2. the fracture except the sliding

In many cases, there will be a combination of above two failure modes.

We study about the variation of properties of jointed rock masses, especially about the differential stress, apparent cohesion, and apparent angle of internal friction, when the sliding occures along the joint.

2. Method of test

Triaxial compression tests were carried out on mortar specimens with joint or intact mortar specimens. The size of specimens is 6-cm diameter, and 12-cm length. For four different confining pressures, 0, 50, 100, and 200 kg/cm², the axial load is increased at constant rate of about 5 kg/cm²/sec. until the fracture occures. The inclination of joint is from 0° to 90° at 10° intervals in Fig. 1. The joint is bonded by synthetic adhesives. Five or six specimens were tested for each inclination of joint, each confining pressure.

Then, the properties of intact mortar specimens used at tests are as follows:

Uniaxial compressive strength σ_c 380 kg/cm²

Cohesion c_o 80 kg/cm²

Angle of internal friction ϕ_o 42°

And, the properties of joint itself are as follows:

Cohesion c_f 16.5 kg/cm²

Angle of internal friction ϕ_f 11°

3. Results and discussions

The curves of differential stress ($\sigma_1 - \sigma_3$) at fracture for four confining pressures versus inclination of joint are shown in Fig.1. They are all concave

upward and roughly parabolic in form. Increasing the confining pressure, the differential stress increases. The differential stress for 50°-specimens is the least, and that for 0°-specimens is the largest. The each failure mode of 0°-, 10°, 80°-, and 90°-specimens is nearly same as that of intact mortar specimens, but that of 20°-, 30°-, 40°-, 50°-, 60°-, and 70°-specimens is the sliding the joint. It is understood that the differential stress of jointed rock masses which the sliding occures along the joint very decreases as compare with that of the fracture except the sliding the joint.

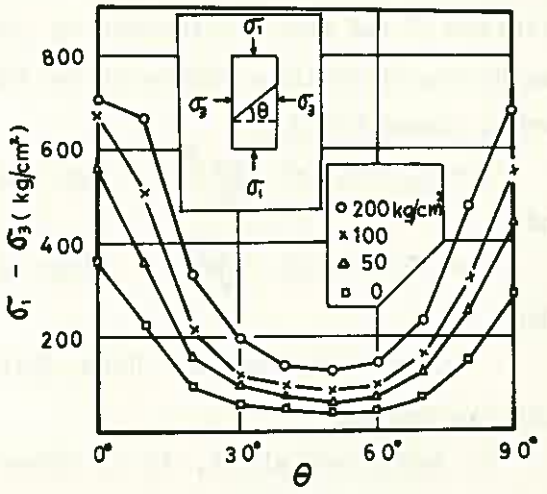

Fig.1 Variation of differential stress (σ_1-σ_3) With inclination of joint θ

Fig.2 (a),(b),(c), and (d), show Mohr circle diagrams of 0°-, 30°-, 60°-, and 90°-specimens. In the case of sliding fracture along the joint, Mohr envelopes become so straight as in Fig.2 (b),(c). In other words, if Mohr envelopes are straight, we can understand that the jointed rock masses may be fractured by the sliding along the joint.

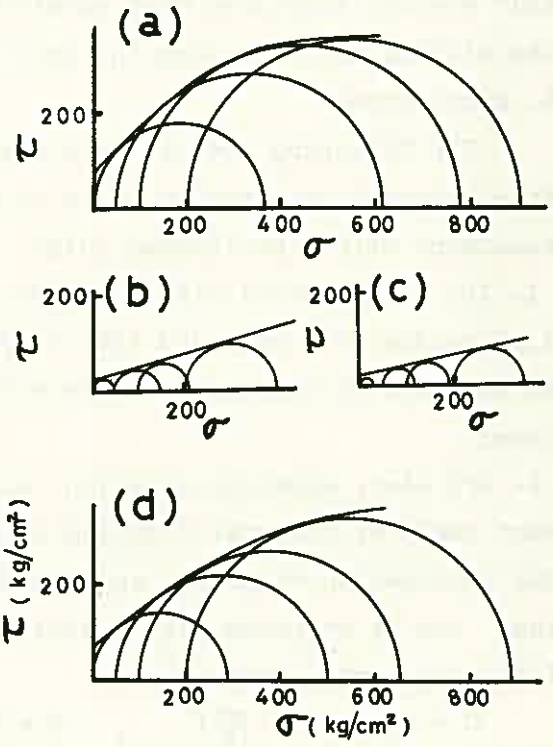

Fig.2 Mohr circles diagrams

Apparent cohesion C and apparent angle of internal friction ϕ can be obtained from Mohr envelopes. The each curve of apparent cohesion C and apparent angle of internal friction ϕ versus the inclination of joint θ is shown in Fig.3 and Fig.4. These are so concave upward and nearly parabolic in form as the differential stress. In these Fig., C_o and ϕ_o are cohesion and angle of internal friction of intact mortar specimen, C_f and ϕ_f are cohesion and angle of internal friction of joint itself, respectively: i.e. apparent cohesion of jointed rock masses exsists between the cohesion of intact rock mass and the cohesion of joint itself, and also, apparent angle of internal friction of jointed rock mass exsists between that of intact rock mass and that of joint itself. The relations between apparent cohesion C and the inclination of joint

θ, and between apparent angle of internal friction ϕ and the inclination of joint θ can be approximately indicated by following forms, respectively.

$$C = C_f + a\left(\theta - \frac{5\pi}{18}\right)^2 \qquad [\theta: \text{radian}]$$

and

$$\phi = \phi_f + b\left(\theta - \frac{5\pi}{18}\right)^2 \qquad [\phi, \phi_f: \text{radian}]$$

where

a, b : constants Here, 83.3 and 0.71 are given.

As described above, it is schon understood that Mohr envelopes which the sliding occure along the joint become straight. So, Colomb's assumption, $\tau = C + \sigma \tan\phi$, can be applied, when the sliding occures along the joint. That is,

$$\tau = C_f + a\left(\theta - \frac{5\pi}{18}\right)^2 + \sigma \tan\left\{\phi_f + b\left(\theta - \frac{5\pi}{18}\right)^2\right\}$$

This eqation indicates Mohr envelopes which the sliding occures along the joint.

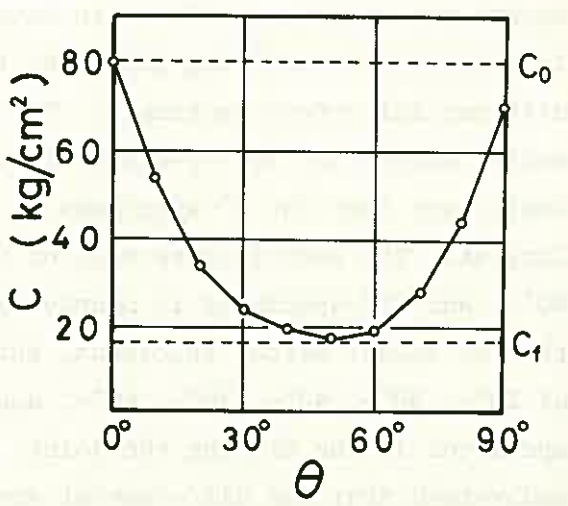

Fig.3 Variation of apparent cohesion C with the inclination of joint θ

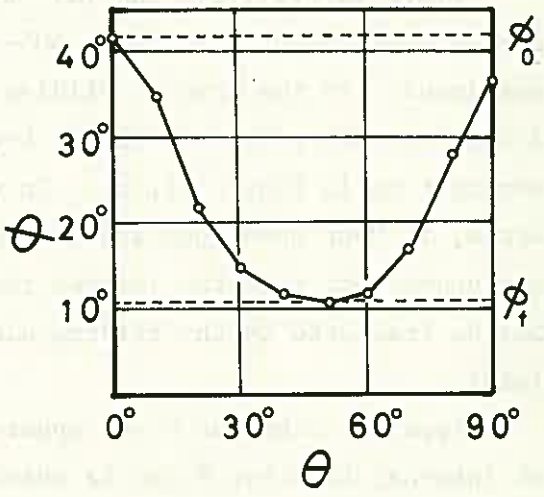

Fig.4 Variation of apparent angle of internal friction ϕ with the inclination of joint θ

4. Conclusions

The following results were obtained from triaxial compression tests on mortar specimens with a pre-formed joint:

1. The differential stress varies with the inclination of joint, and that very decreases in the case of sliding fracture along the joint.

2. And also, apparent cohesion, and apparent angle of internal friction vary with the inclination of joint, and those relations can be approximately indicated by following forms, respectively.

$$C = C_f + a\left(\theta - \frac{5\pi}{18}\right)^2 \quad , \quad \phi = \phi_f + b\left(\theta - \frac{5\pi}{18}\right)^2 \qquad [\theta: \text{radian}]$$

where

a, b : constants

STRESS-DILATANCY RELATION OF GRANULAR MATERIAL

Masanobu ODA, Saitama University

Rock and rock mass with high crack density, rock fill material and so on are considered as granular materials composed of irregular blocks or irregular particles. Sands and random mass of photoelastic circular rods were tested to simulate mechanical response of granular materials under the conditions of triaxial compression stresses and of simple shear stresses. The experimental results and theoretical analyses (see references 1) to 7)) are summarized as follows:

1) As a first approximation, granular materials are considered to be plastic anisotropically strain-hardening materials composed of rigid, cohesionless particles. In order to get a reliable stress-dilatancy relation of granular materials, it is useful to assume that elastic strain and plastic strain due to grain shatterings are negligible as compared with plastic strain due to frictional slidings at some critical contacts.

2) Spatial arrangement of solid particles and associated voids (fabrics) of granular material are characterized by three-dimensional distribution of normals (N_i) to tangential planes at contacts (Fig. 1) and by void ratio. The gradual concentration of N_i toward the major principal stress direction plays an essential role in strain-hardening of material during both of triaxial compression test and simple shear test. The mobilized principal stress ratio $(\frac{\sigma_1}{\sigma_3})$ has close bearing on the fabric index $(\frac{S_z}{S_x})$ of granular mass which depends only on the three-dimensional probability density of N_i (i.e., $E(\alpha, \beta)$), as follows;

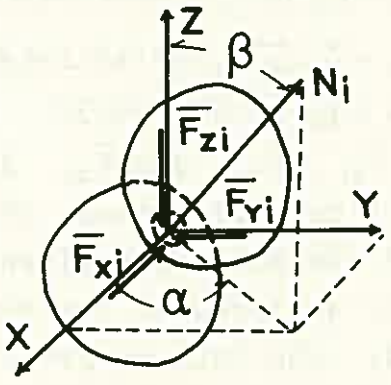

Fig. 1 Normal (N_i) and contact forces

$$\frac{\sigma_1}{\sigma_3} = \frac{S_z}{S_x} \cdot \tan^2\left(\frac{\pi}{4} + \frac{\phi_\mu}{2}\right) \quad \cdots (1)$$

where

$$\frac{S_z}{S_x} = \frac{\int_0^{\pi/2}\int_0^{2\pi} E(\alpha,\beta)\sin 2\beta \, d\alpha \, d\beta}{\int_0^{\pi}\int_{-\pi/2}^{\pi/2} 2E(\alpha,\beta)\cos\alpha \cdot \sin^2\beta \, d\alpha \, d\beta}$$

and ϕ_μ = interparticle friction angle. Experimental relation between $\frac{\sigma_1}{\sigma_3}$ and $\frac{S_z}{S_x}$ is well in accordance with the theoretical equation (1) throughout an early stage of deformation to failure, irrespective of initial void ratio and initial fabrics (Fig. 2). The dilatancy rate ($1 - \frac{dv}{d\varepsilon_1}$) of granular material has also close relation to the fabric index $\frac{S_z}{S_x}$.

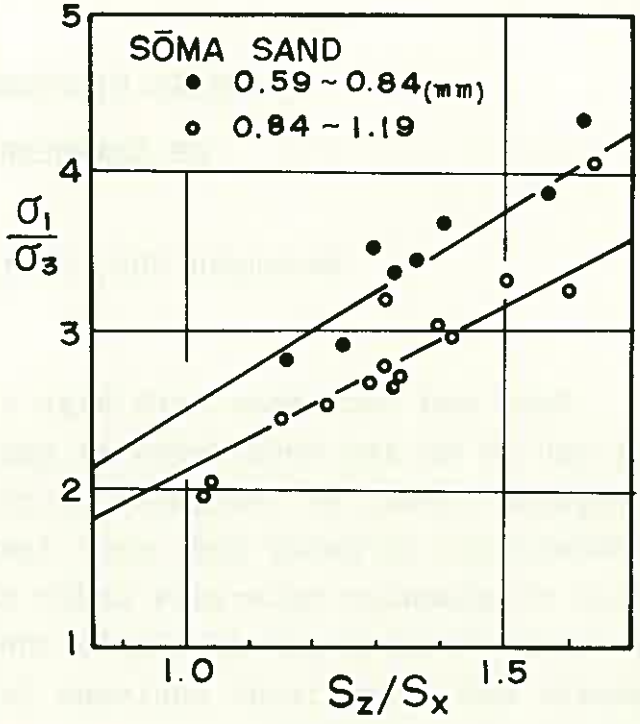

Fig. 2 Relation between σ_1/σ_3 and S_z/S_x for Soma sand

$$\left(1 - \frac{dv}{d\varepsilon_1}\right) = \frac{4}{\pi \tan\left(\frac{\pi}{4} + \frac{1}{2}\phi_\mu\right)} \cdot \frac{S_z}{S_x} \quad \cdots (2)$$

Stress-dilatancy is easily derived from Eqs. (1) and (2).

3) Interparticle contact force at a contact whose normal (N_i) inclines to Z at β can be estimated with sufficient accuracy by the following equation (distribution law of contact force):

$$\left.\begin{aligned} \bar{F}_{xi} &= k_x \bar{\Delta S} \sigma_3 \, |\cos\alpha \sin\beta| \\ \bar{F}_{yi} &= k_y \bar{\Delta S} \sigma_3 \, |\sin\alpha \sin\beta| \\ \bar{F}_{zi} &= k_z \bar{\Delta S} \sigma_1 \, |\cos\beta| \end{aligned}\right\} \quad \cdots (3)$$

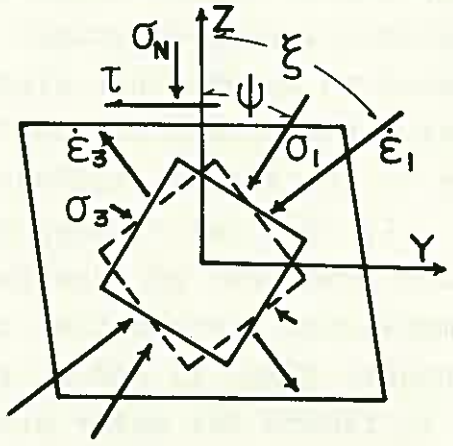

Fig. 3 Principal axes of stress and of strain increment in simple shear test

where $\bar{F}_{xi}$, $\bar{F}_{yi}$ and $\bar{F}_{zi}$ are contact forces resolved in the principal stress directions (Fig. 1), and $\frac{k_x}{k_z} = \frac{S_z}{S_x}$. The distribution law of contact force given by Eq. (3) was supported by the photoelastic analyses on two-dimensional model.

4) The both of principal axes of stress and of strain increment rotate gradually during simple shear test of granular mass. The direction of principal stress is estimated from the following relation between stress ratio ($\frac{\tau}{\sigma_N}$) acting on horizontal shear

plane and inclination angle (ψ) of principal stress axis to vertical direction (Z) (Fig. 3):

$$\frac{\tau}{\sigma_N} = \kappa \cdot \tan\psi \qquad \cdots (4)$$

where κ is a material constant for a given granular mass. Using Eq. (4), the stress-dilatancy relation can be determined by taking into consideration about discrepancy between principal axes of stress and of strain increment as follows:

$$\frac{t}{s} = \frac{\cos 2(\xi-\psi)\left\{\tan^3\left(\frac{\pi}{4}+\frac{1}{2}\phi_u\right)-1\right\} - \frac{\dot{v}}{\dot{\gamma}}\left\{\tan^3\left(\frac{\pi}{4}+\frac{1}{2}\phi_u\right)+1\right\}}{\cos 2(\xi-\psi)\left\{\tan^3\left(\frac{\pi}{4}+\frac{1}{2}\phi_u\right)+1\right\} - \frac{\dot{v}}{\dot{\gamma}}\left\{\tan^3\left(\frac{\pi}{4}+\frac{1}{2}\phi_u\right)-1\right\}} \qquad \cdots (5)$$

where $t = \frac{\sigma_1-\sigma_3}{2}$, $s = \frac{\sigma_1+\sigma_3}{2}$, $\dot{\gamma} = \dot{\varepsilon}_1 - \dot{\varepsilon}_3$, $\dot{v} = \dot{\varepsilon}_1 + \dot{\varepsilon}_3$

References

1) Oda, M. (1972): "Initial fabrics and their relations to mechanical properties of granular material", Soils and Foundations, Vol. 12, No. 1.
2) Oda, M. (1972): "The mechanism of fabric changes during compressional deformation of sand", Soils and Foundations, Vol. 12, No. 2.
3) Oda, M. (1972): "Deformation mechanism of sand in triaxial compression tests", Soils and Foundations, Vol. 12, No. 4.
4) Oda, M., Onodera, T. and Konishi, J. (1973): "An approach from granular mechanics to rock mechanics on strength and deformation behaviour of clastic materials", Proc. 4th Interior Meeting on Rock Mechanics (in Japanese).
5) Oda, M. (1974): "A mechanical and statistical model of granular material", Soils and Foundations, Vol. 14, No. 1.
6) Oda, M. and Konishi, J. (in press): "Microscopic fabrics of granular material subjected to shear stress and their relations to granular mechanics", Soils and Foundations.
7) Oda, M. and Konishi, J. (in preparation): "Principal stress axes and their relations to stress ratio mobilized in simple shear test of granular material," Soils and Foundations.

FILL-TYPE DAM AND SOFT ROCKS

Takayasu YAMANO, Toyama College of Technology

For the civil engineering use, only a little attention has been paid to mudstone, sandstone and tuff, generally named "soft rocks", because their properties are inferior from the view point of rock mechanics. Recently, selection standard for fill-up materials for fill-type dam has been changed and the soft rocks has come to be used for rock materials. For instance, Azuma Dam in Hokkaido constructed in 1971 is a central core fill-type dam, which is 38.2m in bank height and 542,000m³ in bank volume. There, since suitable materials were not avairable, soft rocks (mudstone and sandstone), base rocks in the area, were used in the permeable zones at upper and lower courses.

The amount of the rocks were slightly over 70% of the bank volume. The rocks were quarried by blasting, carried to the bank and then tamped. In the case of Azuma Dam, while durability of the soft rocks was lower than reqirement for concrete aggregate and the possiblity of weathering of the rocks was not neglisible, the rocks are toohard to crush to the enough small chips. The soft rocks behave as rock materials at the fill-up stage and still retain the function as permeable zone after tamping. However, it is possible that according as the bank will be exposed to dam water and rain over long time, small fragment will gradually exfoliate from the rock surface and will be carried away with seeping water. Calculation of the stability of the fill-type dam, which consists of such zones in large proportion, has to be done with the following two conditions; (a) the condition immediately after the fill-up is completed and (b) the condition after weathering will proceed some years hence. In order to do so, development of method to assume the degree of weathering is required. Here, we report our research on the subject.

The degree of weathering expressed in the " Weathering Degree " is defined as follows;

$$\text{Weathering degree} = \frac{\text{dry weight of fragments, which have exfoliated up to the time and smaller than 4.76mm meshes}}{\text{initial dry weight of the rock sample}} \quad \ldots\ldots(1)$$

This new concept is to make relative evalution of weathering of soft rocks placed inside of bank compararing with condition of rocks at the initial

fill-up stage. In this definition, weathering of the soft rocks is considered in the terms of physical change, that is break down and surface exfoliation of the rock.

The rock inside of the bank is forced to follow the air temperature change throughout of the year, and further is repeatedly subjected to dry and wet condition due to the change of dam water level and due to rain. Regarding to these aspects, several preliminary experiments were undertaken, to investigate the correlation among the disintegration of soft rocks, temperature of water, humidity andrepetitionof wet and dry condition. From the results of experiments, it is concluded that for evaluation of durability of soft rocks against weathering, tests carried out under mild condition on the basis of temperature and humidity variation are desirable.

Tne standardized tests of weathering were performed with 27 samples were collected at eight dam sites including Azuma Dam in 1966 and 1967, in a chamber equipped with conditioner controled by a program. The experimental procedure was as follows;

(1) during the preparation of the specimen, the sample was handled carefully to minimanize the change of a moisture content. The specimen was usually prepared into a cube with 5cm in side. The rock easily susceptible to disintegration was submitted without preparation.

(2) The specimen was immersed in water for a few days, and then a portion of the specimen was submitted to measurments of specific gravity, water absorption and compression strength.

(3) The specimen saturated was allowed to stand untill its surface became dry and then it was weighed and placed in a beaker in the chamber.

(4) The weathering was accelerated by programmed condition as shown below,

highest temperature.....80°C

humidity at the temperature.....20%

lowest temperature.....0°C

humidity at the temperature.....66%

number of repetition.....8 cycle/day

(5) When the weathering was observed to some extent, exfoliated fragments were collected, sieved through 4.76 meshes and weighed. The fragments remaing on the sieve were returned to the beaker. This procedure was repeated at approximatery regular intervals.

(6) Weathering degree was calculated, and the relationship between weathering degree and number of cycle was examined.

Since it was assumed that temperature of in side of dams varies within non-frost range, the conditioning program was set as described in (4).

The results of some tests are shown in the Fig. 1 and 2 and Table 1.

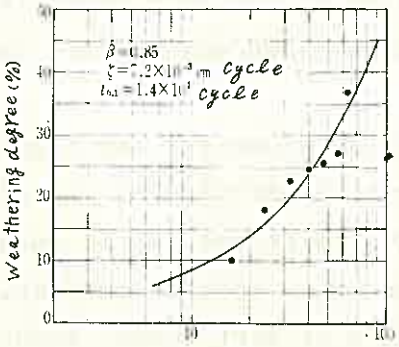

Fig.-1 Nokanan

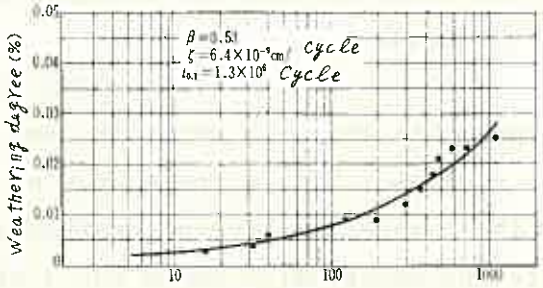

Fig.-2 Füren

item \ dam site	Nokanan	Füren
kind of rock	siltmudstone	alterated agglomerate
water absorption (%)	6.0	1.1
specific gravity, G_S	2.35	2.70
compression strength (kg/cm²)	108	393

Table 1.

From these data, it was found that the next equation held for relationship between number of the cycle and the weathering degree.

$$I = 1-\left\{1-\left(\frac{\zeta t}{L}\right)^{\beta}\right\}^{3} \quad \cdots\cdots\cdots\cdots\cdots\cdots (2)$$

I : weathering degree

t : number of cycle

L : initial side length of specimen $\quad L=\left(\frac{W_S}{G_S \gamma_\omega}\right)^{\frac{1}{3}}$

W_S : initial dry weight

G_S : specific gravity under dry condition

γ_ω : weight of water of unit volume

ζ, β : experimental constants

In the Fig. 1 and 2, $t_{0.1}$ were calculated by the equation (2), where I =0.1, L =5.0cm. From the results, durability of rocks of different places to weathering can be evaluated and compared.

When correlation between the " number of cycle " and weathering period is established by progress in the method to estimate weathering factors, the weathering degree of rocks at a time will be able to be calculated depending on their size. Also approximate grading of the rocks would be estimated. Thus the stability of rock zone depending on long time would be calculated on the basis of reasonable fundamental values.

MEASUREMENT OF THE INITIAL IN SITU STRESSES IN THE UNDERGROUND AT THE SHIN-TAKASEGAWA UNDERGROUND POWERSTATION

Tatsuo MIZUKOSHI, Dr. Eng., Managing Director
Youichi MIMAKI, Tokyo Electric Power Co., Inc.

1. Introduction

According to recent reports on initial in situ stresses at various places, horizontal stress near the surface is unexpectedly large. This means that in situ stresses are determined not only by the weight of overlying rock, but also by topographical and geological structures, diastrophism, orogenic movements etc. This problem requires special attention for designing large scaled underground structures.

The underground power plant which is under construction at Takase river for Tokyo Electric Power Co., Inc. consists of a machine hall (27.0 m wide, 54.5 m high, 163.0 m long) and the adjoining transformer hall. (20.0 m wide, 35.3 m high, 107.8 m long, 41.5 m apart from the machine hall)

The results of the initial rock stresses measurement conducted for the cavity opening revealed horizontally predominant stress. These results are extremely interesting in connection with the topography and faults.

2. Measurement Method and Result

The measurement method using overcoring in this site consists of simultaneous measuring three components of the radial direction and one component of the axial direction (total of four components).

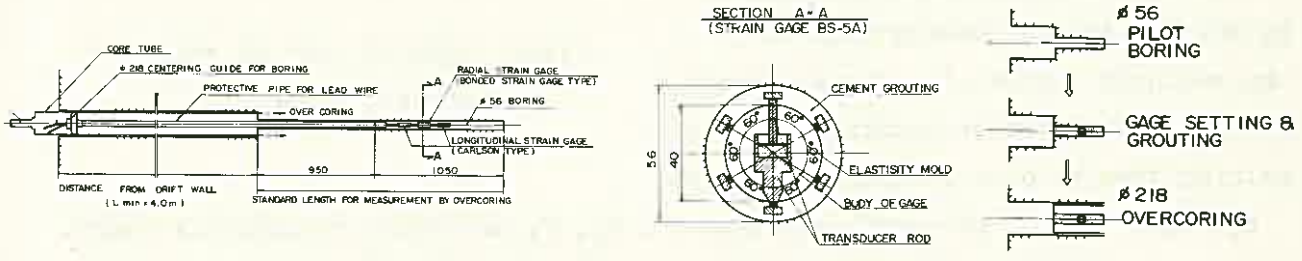

Fig.1 Overcoring procedure

The stress of the radial direction and the normal stress of the longitudinal direction can be obtained for each measurement point in the bore hole. Six independent relieved strains are necessary for obtaining three dimensional stresses.

They can be obtained by taking measurement at least two bore holes in different directions and by combining relieved strains. For the present project, the most probable value was obtained and the error was estimated by combining many relieved strains.

The results of the initial rock stresses measurement conducted here revealed horizontally predominant stress. These are extremely interesting in connection with the topography and faults.

Rocks properties (Young'smodulus, Poisson's ratio) that are necessary for obtaining initial rock stresses by using relieved strain were obtained by triaxial test in laboratory, using **over cored rock** specimen (ø 218 mm) still burying gauges.

The responses of the setting gauges were also checked at the same time. The maximum loading was large enough to compensate for 120% of relieved strain that is induced by overcoring.

The results of the triaxial test showed that the responses of setting gauges were regular and that the elastic modulus was $20\times10^4 \sim 35\times10^4$ kg/cm^2. These modulus were slightly smaller than the results of the unicompression test using ø46mm core specimen with the same rocks.

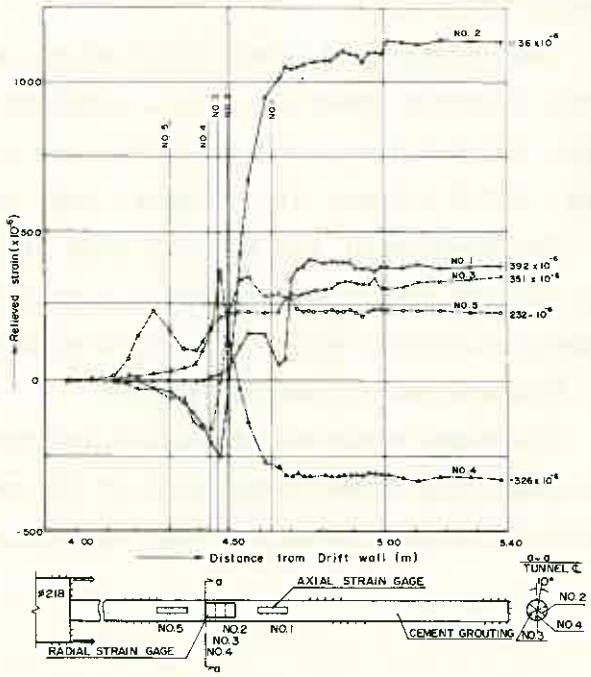

Fig.2 Typical plot of relieved strain change

3. Analytic results of in situ principal stress

In situ stresses were determined by making various combinations of the measured values of a radial strain, by making observation equations and by solving them to obtain in situ stresses σ_X, σ_Y ···· τ_{XY}, principal stresses P_1, P_2, P_3 and their reliability range.

$$\begin{pmatrix} \alpha_{11} & \alpha_{12} & \cdots & \alpha_{16} \\ \alpha_{21} & \alpha_{22} & \cdots & \alpha_{26} \\ \vdots & \vdots & & \vdots \\ \alpha_{m1} & \alpha_{m2} & \cdots & \alpha_{m6} \end{pmatrix} \begin{pmatrix} \sigma_X \\ \sigma_Y \\ \vdots \\ \tau_{XY} \end{pmatrix} = \begin{pmatrix} \beta_1 \\ \beta_2 \\ \vdots \\ \beta_m \end{pmatrix}$$

In the above equations, αij ($1 \leqq j \leqq 6$) is an observation matrix and βji ($1 \leqq i \leqq m$) is a measured strain.

The number of combinations of measured relieved strains are four hundred and eighty eight. Some scattering was found with the results of calculation. Unstable data of relieved strain and the data near the side walls were excluded. Figure-3 show the results of stress analysis.

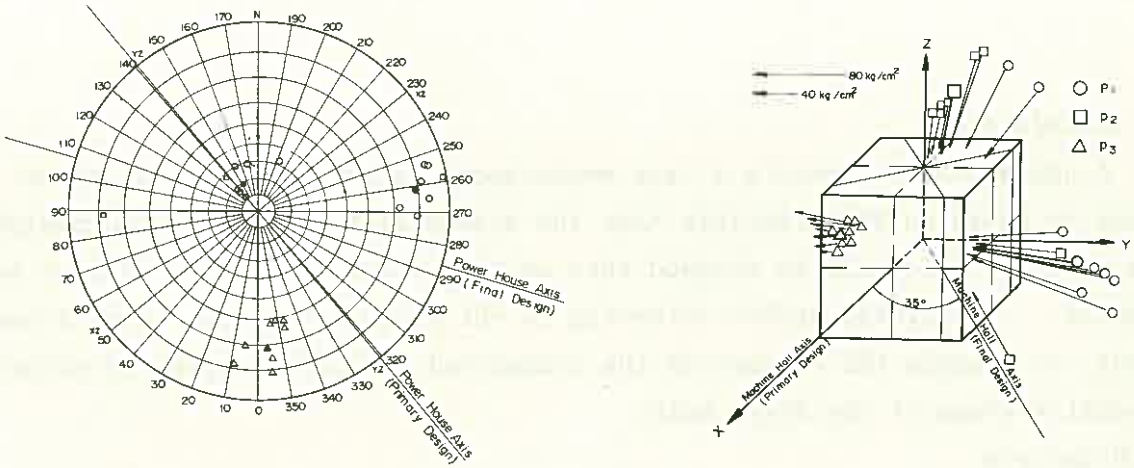

Fig.3 Results of initial rock stresses analysis

In situ principal stresses at the position of the machine hall were estimated to be as given below.

	Values for Design
P_1 = 80~110kg/cm²	(110kg/cm², 260/80)
P_2 = 35~ 75kg/cm²	(65kg/cm², 155/20)
P_3 = 0~-45kg/cm²	(0kg/cm², 355/70)

4. Conclusion

The results of measurements have shown that the horizontal stress is larger than the vertical stress and the ratio K of horizontal to vertical stress is nearly equal to 1.8.

The main cavity, of the original plan was situated to meet at right angles with the direction of conduit, then K values were nearly equal to 1.3 and the required excavation was to be 32.5 m wide. By analyzing the cavity stability on that conditions, we knew that the cavity stability for opening would be unfavourable, so the cavity axis was rotated to the direction of the in situ principal stress.

We can obtain K values nearly equal tc 0.3, and by making the cavity meet with the pressure tunnel system obliquely, we can make the size of the cavity reduce. As the result, the cavity stability could be improved.

Measurement of Ground Stress by Multiple Circular Holes Method

Y. TOMINAGA, S. KINOSHITA

1. Introduction

A new method of in-situ stress measurement is proposed in this paper. This method is based on the principle that the stress distribution at the periphery of a circular hole will be changed when another circular hole is drilled adjacently. Therefore, stress releasing is not necessary in this method but it is only to measure the changes of the tangential strains at selected points on the wall surface of the first hole.

2. Principle

Suppose that a bore hole is drilled into a linear elastic homogeneous rock mass which is in a stress condition of σ_{Gx} , σ_{Gy} , τ_{Gxy} at the perpendicular plane to the hole axis (Z). If we consider the part of bore hole at a large distance from the mouth and bottom of the hole, the tangential stress at an arbitrary point in the wall surface of the part can be given by the general form as

$$\sigma_\theta = X_\theta \cdot \sigma_{Gx} + Y_\theta \cdot \sigma_{Gy} + T_\theta \cdot \tau_{Gxy} \qquad (1)$$

where X_θ , Y_θ and T_θ are the stress concentration factors for the independent stress field of $\sigma_{Gx}, \sigma_{Gy}, \tau_{Gxy}$ and their values are the functions of central angle θ .

If another hole is drilled in the vicinity of the first hole the tangential stress will be changed by an amount $\Delta\sigma_\theta$ which will be given:

$$\Delta\sigma_\theta = \Delta X_\theta \cdot \sigma_{Gx} + \Delta Y_\theta \cdot \sigma_{Gy} + \Delta T_\theta \cdot \tau_{Gxy} \qquad (2)$$

where ΔX_θ , ΔY_θ and ΔT_θ are the difference of the stress concentration factors between the two cases respectively.

Providing that the third and fourth hole are drilled in addition, the stress concentration factors of the first hole will vary moreover. Thus we can obtain two more simillar equations with respect to the tangential stress change. Accordingly by solving the three or more first order simultaneous equations the three unknown stresses σ_{Gx} , σ_{Gy} , τ_{Gxy} can be determined.

3. Ditermination of stress concentration factors for multiple circular holes applied stress field (σ_{Gx} , σ_{Gy} , τ_{Gxy}).

The stress distribution around multiple holes in an infinitely wide plate

was generally analysed by using the complex stress functions of complex variables Z_k. The complex stress functions assumed to consist of three functions, i. e. the first concerns field stress, the second is log Z_k and the third is algebrical sum of infinite series which are made up of a minus power of Z_k whose origin is the center of each hole.

The unknown coefficients of the complex stress functions are determined so as to satisfy the boundary condition at every point of the all openings.

By using these complex stress functions, stress distributions or stress concentration factors at the boundary of a hole can be computed for various cases of a single hole or multiple holes existing in an arbituary arrangement.

4. Procedure of in-situ stress measurement

(1) One strain gage method (Fig.1)

Assume that the tangential strain is measured at the point A of the circle O_1. When another hole O_2 is drilled as shown in Fig.1, the strain will be changed. The magnitude of the strain variation ($\Delta\varepsilon_\theta$) can be read from the strain measurement and be represented theoretically as the difference ($\varepsilon_\theta^{II}-\varepsilon_\theta^{I}$).

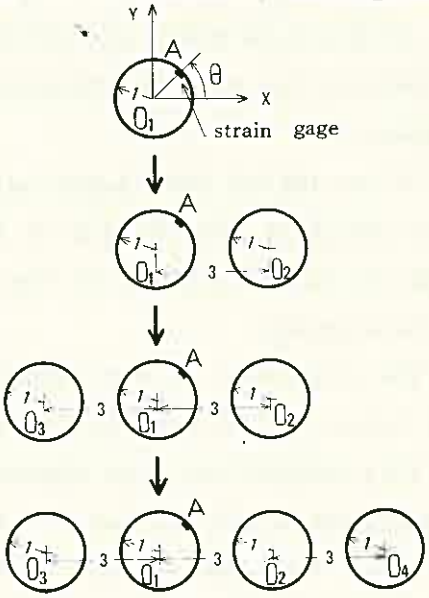

Fig. 1

ε_θ^{I} is the tangential strain in case of a single hole and ε_θ^{II} is the tangential strain in case of two holes. Both of the tangential strains are given by the following equations:

$$\varepsilon_\theta^{I}=\frac{1-\nu^2}{E}\cdot\sigma_\theta^{I}-\nu\varepsilon_c \quad , \quad \varepsilon_\theta^{II}=\frac{1-\nu^2}{E}\cdot\sigma_\theta^{II}-\nu\varepsilon_c \qquad (3)$$

where ν = poison's ratio, E = Young's modulus

σ_θ^{I} = tangential stress at the point A for a single hole

σ_θ^{II} = tangential stress at the point A for two holes

ε_c = normal strain in axial direction of bore hole which is reckoned to be constant for plane strain condition

Then the strain variation ($\Delta\varepsilon_\theta$) can be written by the equation:

$$\Delta\varepsilon_\theta=\frac{1-\nu^2}{E}(\sigma_\theta^{II}-\sigma_\theta^{I})=\frac{1-\nu^2}{E}\Delta\sigma_\theta \qquad (4)$$

If $\Delta\varepsilon_\theta$ is known we can obtain the stress variation ($\Delta\sigma_\theta$) from Eq.(4).

By performing simillar procedure, we can get the stress variations when bore hole is increased in number from two to three and from three to four respectively.

Since the stress variation ($\Delta\sigma_\theta$) and the stress concentration factor variation (ΔX_θ, ΔY_θ , ΔT_θ) are known it is easy to determined the unknown ground stresses by solving the three pair of Eq.(2).

(2) Modification of the method

The number of additional hole can be decreased if the points measuring strains are increased. For example if we measure strains at three different points of a circle in the first hole, it is enough to drill only one hole in addition for the determination of the field stresses.

Instead of increasing number of bore holes the enlargement of the adjacent hole can be employed because the stress concentration factors vary depending on the change in the diameter of the adjacent hole.

It is easily understand that the bore holes are not necessary to be arranged in a row as shown in Fig.1 and that any arrangement of bore hole are valid as far as holes are drilled in parallel.

If the bore holes are drilled more than the minimum number of necessity, the extra holes will be effective to get more precise measurements of ground stresses.

If we employ four gages method to measure field stresses it is also possible to estimate the changes of the field stresses by only keeping the observation on the variations of the strain at the measuring points.

5. Conclusion

The principle of new method of in-situ stress measurement by multiple circular holes method was illustrated in this paper.

This method has been demonstrated in laboratory test which was carried out using gypsum model but has never been demonstrated in field test.

There are some difficulties for the method to be applied in practice, for example it may not be easy to attach strain gages on the periphery at large depth of the bore hole and it is also difficult to attach strain gages in weak rocks. Authors are now tring to apply this method to the inclusion mould gage method.

If internal pressure is applied to an adjacent hole by oil or water and the change of strain is measured we can get stress-strain conversion factor in Eq.(4) of the in-site rock mass in the field.

Reference

1) Y.TOMINAGA, S.KINOSHITA: A Theoretical Analysis of the Stress Distribution around Multiple Holes in an Elastic Infinite Plate, Journal of the mining and metallurgical institute of JAPAN, Vol.87, No.1004 (1971)
2) Y.TOMINAGA, S.KINOSHITA: Stress Concentration around the Multiple Circular Openings in the Elastic Rock, Journal of the mining and metallurgical institute of JAPAN, Vol.88, No.1017 (1972)
3) Y.TOMINAGA, S.KINOSHITA: Measurement of Ground Stress by Multiple Circular Holes Method, Journal of the mining and metallurgical institute of JAPAN, Vol.89, No.1025 (1973)

THEORETICAL CONSIDERATION ON THE MEASUREMENT OF STRESS IN ROCK USING A BOREHOLE CONTAINED WITH A METER OF THE TYPE OF A CYLINDRICAL INCLUSION

Yoji ISHIJIMA, Hokkaido University
Hitoshi KOIDE, Geological Survey of Japan
Ko SUZUKI, Taisei Construction Co.

1. Introduction

The aim of this paper is to deduce the calibrating equations for the meters of the cylindrical inclusion type to measure the stress in rock. Cylindrical mould gauge such as NCB type or Kajima Construction Co. type (1) belongs to this category. Borehole deformation gauge and Leeman's multi-component borehole strain cell of which rigidities are 0 also belong to the same category. As the calibrating equations, the elastic solution of a cylindrical inclusion in an infinite body should be applicable under the assumption that the rock is linearly elastic, homogeneous and isotropic and the meter of cylindrical type is glued perfectly to the wall of a borehole.

The solution has been deduced here based on the Edwards' analysis on the spheroidal inclusion problem (2). Brief discussion is made referring to the measurement of the absolute stress using a meter of this type and the overcoring technique.

2. Three dimensional solution of a cylindrical inclusion

A cylinder is a spheroid of which slender ratio $\bar{q}/q$ is very small. So by appropriate operation, that is by neglecting infinitly small higher order terms than $(\bar{q}/q)^2$ and then by taking the limit $\bar{q}/q \to 0$, Edwards' original solution can be modified to the one of a cylindrical inclusion. Because of the destrictions on length for an article it is impossible to represent detailed computations, so will present only a final form.

The stress $\{\sigma'\}$ in the inclusion is uniform and is expressed in terms of rock stress at infinity $\{\sigma\}$ in the matrix form as,

$$\begin{Bmatrix} \sigma'_x \\ \sigma'_y \\ \sigma'_z \\ \tau'_{xy} \\ \tau'_{yz} \\ \tau'_{zx} \end{Bmatrix} = \begin{vmatrix} c_1 & c_2 & b_4 & 0 & 0 & 0 \\ c_2 & c_1 & b_4 & 0 & 0 & 0 \\ c_3 & c_3 & b_5 & 0 & 0 & 0 \\ 0 & 0 & 0 & b_3 & 0 & 0 \\ 0 & 0 & 0 & 0 & b_6 & 0 \\ 0 & 0 & 0 & 0 & 0 & b_6 \end{vmatrix} \cdot \begin{Bmatrix} \sigma_x \\ \sigma_y \\ \sigma_z \\ \tau_{xy} \\ \tau_{yz} \\ \tau_{zx} \end{Bmatrix} \qquad (1)$$

where $c_1 = -\nu' b_1 - \frac{3}{4} b_2 + \frac{1}{2} b_3$

$c_2 = -[\ \nu' b_1 + \frac{3}{4} b_2 + \frac{1}{2} b_3\ ]$

$c_3 = (\nu' - 1) b_1 + \frac{3}{2} b_2$

$b_1 = -\dfrac{(1+H)(-\nu\nu' H - 2\nu\nu' + 2\nu')}{\nu'(1+\nu)(H+2-2\nu')}$

$b_2 = -\dfrac{4}{3}\dfrac{(1+H)(\nu\nu' H + 1 + \nu\nu' - 2\nu')}{(1+\nu)(H+2-2\nu')}$

$b_3 = \dfrac{4(1-\nu)(1+H)}{(3-4\nu)H + 4(1-\nu)}$

$b_4 = -\dfrac{(1+H)(\nu-\nu')}{(1+\nu)(H+2-2\nu')}$

$b_5 = \dfrac{(1+H)[H(1+\nu') + 2(1-\nu\nu')]}{(1+\nu)(H+2-2\nu')}$

$b_6 = 2\,\dfrac{1+H}{2+H}$

$H = \dfrac{G'}{G} - 1$

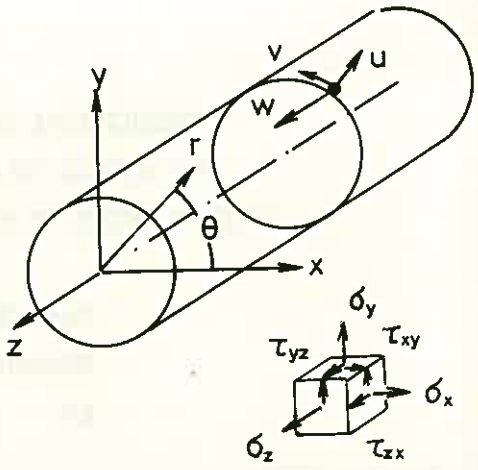

Fig.1 Borehole contained with an inclusion

and ν is Poisson's ratio of the rock, ν' is Poisson's ratio of the inclusion, G is rigidity of the rock, G' is rigidity of the inclusion.

In case where G' is 0, the inclusion is replaced by the cavity, the solution of which is easily derived in a similar way as that of the inclusion. The meaningful quantities for the measurement are the displacement (u,v,w) and strains (e_{ij}) on the borehole surface. They are expressed as,

$$u = \frac{d}{2E}[\ \sigma_x + \sigma_y - \nu\sigma_z + 2(1-\nu^2)(\sigma_x - \sigma_y)\cos 2\theta + 4(1-\nu^2)\tau_{xy}\sin 2\theta\ ]$$
$$v = \frac{d}{2E}[\ -2(1-\nu^2)(\sigma_x - \sigma_y)\sin 2\theta + 4(1-\nu^2)\tau_{xy}\cos 2\theta\ ] \qquad (2)$$
$$w = \frac{3d}{4G}[\ \tau_{yz}\sin\theta + \tau_{zx}\cos\theta\ ]$$

and

$$e_{rr} = -\frac{\nu}{E}(\sigma_x + \sigma_y) + \frac{\nu}{G}(\sigma_x - \sigma_y)\cos 2\theta - \frac{\nu}{E}\sigma_z + \frac{2\nu}{G}\tau_{xy}\cos 2\theta$$
$$e_{\theta\theta} = \frac{1}{E}[\ \sigma_x + \sigma_y - \nu\sigma_z - 2(1-\nu^2)(\sigma_x - \sigma_y)\cos 2\theta - 4(1-\nu^2)\tau_{xy}\sin 2\theta\ ] \qquad (3)$$
$$e_{zz} = \frac{1}{E}[\ \sigma_z - \nu(\sigma_x + \sigma_y)\ ]$$
$$e_{\theta z} = \frac{2}{G}(\tau_{yz}\cos\theta - \tau_{zx}\sin\theta)$$
$$e_{rz} = e_{r\theta} = 0$$

where d is a diameter of a borehole and E is Young's modulus of the rock (Fig.1).

These results are identical to those obtained by the previous studies except an estimation for w (component of displacement in a borehole axis). Hiramatsu and Oka (3) gave an estimation as,

$$w = \frac{d}{G}(\tau_{yz}\sin\theta + \tau_{zx}\cos\theta) \qquad (4)$$

How this happens or what is different will be clarified if we discuss the mode of the deformation. The results calculated are illustrated in Fig.2. Here δ and ω are the rotation and the component of rotation about the axis of a borehole respectively.

The mode A of Fig.2 corresponds to pure shear. On the other hand the mode B corresponds to simple shear. Note that the deformation along the borehole is same between the two and is represented by Eq. 4. Of course Eq. 4 should be used as the calibrating equation for the borehole deformation method.

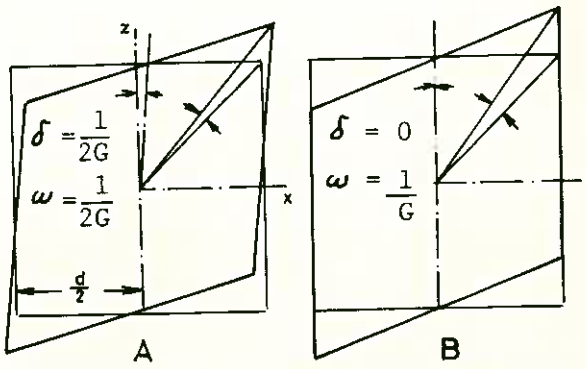

Fig.2 Borehole deformation induced by the stress $\tau_{zx}=1$: A corresponds to Edwards, B to Hiramatsu et.al.

3. Measurement of absolute stress

The equations derived in the previous section give the rigorous evaluation when used to measure the stress change in rock. However these give only the approximate one generally when applied to the measurement of the absolute stress with a combination of the overcoring technique.

Two dimensional analysis leads that the limit of the ratio of the stiffness G'/G is 0.4% which distingwishes the soft type of a meter from the stiff one; For the former the theory of the cavity can be applicable as the calibrating equation. In this case the diameter and the eccentricity of the overcoring have no effect on the measured value (4).

On the other hand, for the latter these advantageous properties do not hold and the theory of the inclusion must be used with the ristriction for the diameter of the overcoring. It is estimated from the two dimensional analysis that the limit of the ratio of the diameter between the overcoring and the inclusion is 5.5 which can apply the theory of the inclusion in an infinite body within a error of 5 % when the ratio of the stiffness G'/G is 5.

4. References

(1) Research group for rock mechanics; Study on rock quality in design and construction of underground powerhouse (part 1): Annual Rep. Kajima Inst. Const. Tech., vol. 21 pp. 104-110

(2) Edwards; Stress concentrations around spheroidal inclusions and cavities: J. Appl. Mech., Mar. 1951 pp. 19-30

(3) Hiramatsu and Oka; Determination of the stress in rock unaffected by boreholes and drifts, from measured strains or deformations: Int. J. Rock Mech. Min. Sci., vol. 5 pp. 337-354

(4) Suzuki and Ishijima; Theoretical consideration on some fundamental problems concering in situ measurements of stresses in rock by relief technique: J. Mining Metall. Inst. Japan, vol. 86 pp. 153-156

C. DEFORMATION AND FAILURE IN ROCK MASSES

THEORETICAL STUDY ON THE NONELASTIC BEHAVIORS OF JOINTED ROCKMASSES

Ryuichi IIDA, Shigetoshi KOBAYASHI
Public Works Research Institute, Ministry of Construction

There exist many joints and cracks in rockmasses, then the rockmasses behave in different manners than the elastic bodies. In this study, based on the assumption that nonelastic behaviors of rockmasses are due to the slidings on the discontinuous planes and that the slidings on the discontinuous planes can be treated by the theory of plasticity, a mechanical model provided suitable for the mechanical characteristics of jointed rockmasses and analytical method are proposed.

It is indicated by von Mises that the variation of the increment of plastic strain energy by stresses has the stational value near thereal solution,

$$\delta\sigma\, dW^p = d\varepsilon_x^p \delta\sigma_x + d\varepsilon_y^p \delta\sigma_y + d\varepsilon_z^p \delta\sigma_z + d\gamma_{yz}^p \delta\tau_{yz} + d\gamma_{zx}^p \delta\tau_{zx} + d\gamma_{xy}^p \delta\tau_{xy}$$

If the criterions of yielding for groups of discontinuous planes are represented as follows

$$f_\nu(\sigma_{\tau j}) = k_\nu$$

the following equation be induced by the method of Lagrange's multiplyer

$$d\varepsilon_{ij}^p = \sum_\nu \frac{\partial f_\nu}{\partial \sigma_{ij}} d\lambda_\nu$$

Based on this equation, first let us consider the characteristics of the sliding on the discontinuous planes on which the slidings can be occurred only in y direction smoothly, (Fig. 1)

$$du^p = dw^p = 0, \quad dv^p \neq 0,$$

$$\frac{\partial}{\partial y} dv^p = \frac{\partial}{\partial z} dv^p = 0, \quad \frac{\partial}{\partial x} dv^p \neq 0$$

Then, the increments of plastic strain can be represented as follows

$$d\varepsilon_x^p = d\varepsilon_y^p = d\varepsilon_z^p = d\gamma_{yz}^p = d\gamma_{zx}^p = 0$$

$$d\gamma_{xy}^p \neq 0$$

$$\frac{\partial f}{\partial \sigma_x} = \frac{\partial f}{\partial \sigma_y} = \frac{\partial f}{\partial \sigma_z} = \frac{\partial f}{\partial \tau_{yz}} = \frac{\partial f}{\partial \tau_{zx}} = 0$$

$$\frac{\partial f}{\partial \tau_{xy}} \neq 0$$

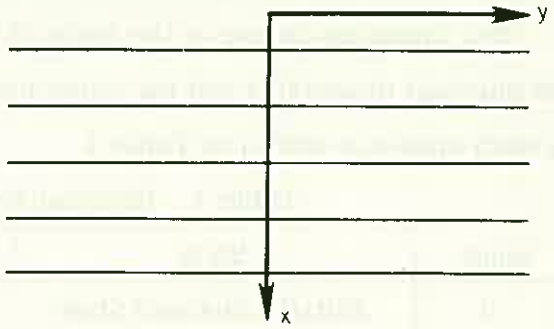

Fig. 1

Then, in this case the criterion of yielding becomes the function of τ_{xy} only and coincides with the Tresca's criterion.

Next, let us consider the characteristics of the sliding on the discontinuous planes on which the criterion of yielding obey to the Coulomb's internal friction theory. In this case the criterion is represented as follows,

$$f(\sigma_{ij}) = |\tau_{xy}| - (C + \sigma_x \tan\phi) = 0$$

Then, the increments of plastic strains are

$$d\varepsilon_x^p = -\tan\phi\, d\lambda, \quad d\gamma_{xy}^p = \pm d\lambda$$

$$d\varepsilon_x^p / d\gamma_{xy}^p = \mp \tan\phi$$

If it is assumed that no plastic deformations are occurred outside the discontinuous planes and uniform slidings are occurred on the discontinuous planes, then

$$d\varepsilon_x^p / d\gamma_{xy}^p = d(du^p) / d(dv^p) = \mp \tan\phi$$

From these considerations, it can be interpreted that when the criterion of yielding is represented in the form of the internal friction theory, there exist undulations in these discontinuous planes, and the angle between the undulated planes and discontinuous plane is equal to ϕ.

Based on this interpretation, a mechanical model for the discontinuous plane are deviced as shown in Fig. 2, and it is assumed that a rockmass is initially in the loosened state, that when a load are applied, these loosenesses are compacted and the rockmass changes its state to the compacted state and that when the load becomes further larger, the rockmass changes its state to the later loosened state and finally to the fracture.

The changing course of the state of the rockmass, the physical properties and the criterions of yielding in each state are shown in Table 1.

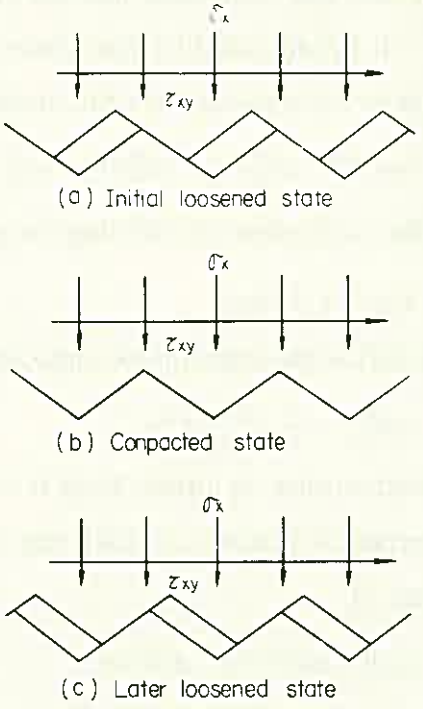

Fig. 2. Model of Discontinuous Plane

Table 1. Physical Prop. and Criterion of Yielding

Stage	State	Physical Prop.	Criterion of Yielding
I	Initial Loosened State	Elastic	
II		Elasto-plastic	$\lvert\tau_{xy}\rvert = C - \sigma_x \tan\phi$
III	Compacted State	Elastic	
IV	Later Loosened State	Elasto-plastic	$\lvert\tau_{xy}\rvert = C + \sigma_x \tan\phi$
	Fracture		

Based on the abovementioned assumptions, the analytical methods for stratiformed rockmass and block-formed rockmass are presented.

Fig. 3 shows the load-displacement curve in the shearing test for a stratiformed rockmass and Fig. 4 shows the distribution of the principal stresses in the shearing test under the load a little smaller than upheaval load.

Fig. 5 shows the distributions of the surface displacements in the deformation test for a block-formed rockmass.

By these analyses the following phenomena can be explained theoretically

1) In the deformation test, a rockmass will small looseness behaves comparatively elastically, but a rockmass with large looseness behaves nonelastically even under small load and the deformations outside the loaded area are very smaller than that inside the loaded area.

2) Upheaval phenomena observed in the shearing test.

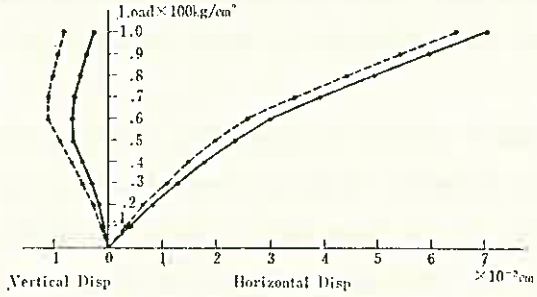

Fig. 3. Load-Deformation Curve in Shearing Test.

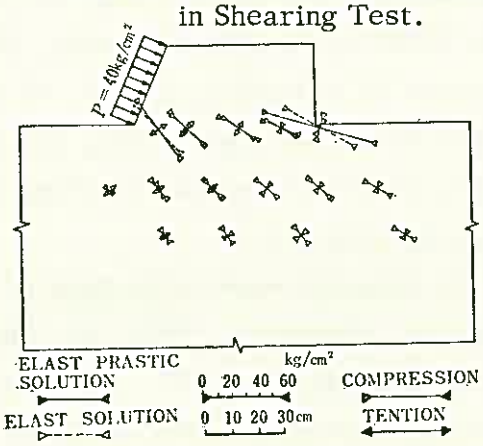

Fig. 4. Distribution of Principal Stresses in Shearing Test.

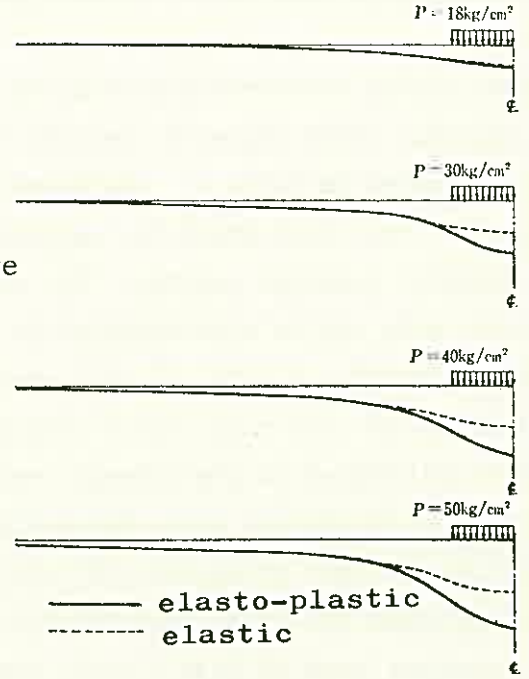

Fig. 5. Distributions of the Surface Displacements.

Reference

R. Iida, and S. Kobayashi; "Theoretical study on the nonelastic behaviors of jointed rockmasses" Journal of Public Works Research Institute, Vol. 144 No. 2 1972.

DYNAMIC DEFORMABILITY AND VISCOSITY OF ROCK MASS AND ROCK FILL MATERIAL UNDER REPEATED LOADING IN SITU AND TRI-AXIAL TEST

Masao HAYASHI, Yoshihiro KITAHARA,
Yoshikazu FUZIWARA and Hiroya KOMADA

Central Research Institute of Electric Power Industry

Dynamic repeated loading test was carried out on the foundation in test adit under the planning nuclear power stations. (Fig. 1) This test was tried to obtain some knowledges on the dynamic repeated deformability and viscosity in large deformation of foundation rock during design earthquake.

Conventional velocity test of elastic wave was limited to the information of deformability in micro strain level and was insufficient on the one in large strain level such case as in contact zone of building to rock foundation earthquake.

Then static deformability modulus under repeated load Es, dynamic deformability modulus under repeated load Ed and dynamic modulus from the elastic wave Ev were compared in Table 1. Furthermore, it is desired to know the dynamic viscosity of rock mass which is important to evaluate so called viscous damping of the dynamic response system. The stress-strain hysterisis loop of the experimental data can be approximated by the VOIGT visco-elastic model, (Fig. 2) and Young's modulus E (Fig. 3) and coefficient of viscosity η (Fig. 4) of several kinds of rock mass can be determined from the loop. Then, the properties were introduced to the dynamic response analysis between building and visco-elastic foundation with three-dimension. (Fig. 5)

Similar dynamic properties of rock fill material were experimented by means of dynamic tri-axial compressive test in laboratory. (Fig. 6) Void ratio decreases more or less during repeated loading. (Fig. 7) Hysterisis loop inclines and becomes smaller as longer becomes loading period. (Fig. 8) And, coefficient of viscosity η is shown in Fig. 9 and Fig. 10 which were applied in three-dimensional earthquake response analysis of rock fill dams. Then, the damping constant h was compared between observed result and calculated result in actual rock fill dam as shown in Table 2.

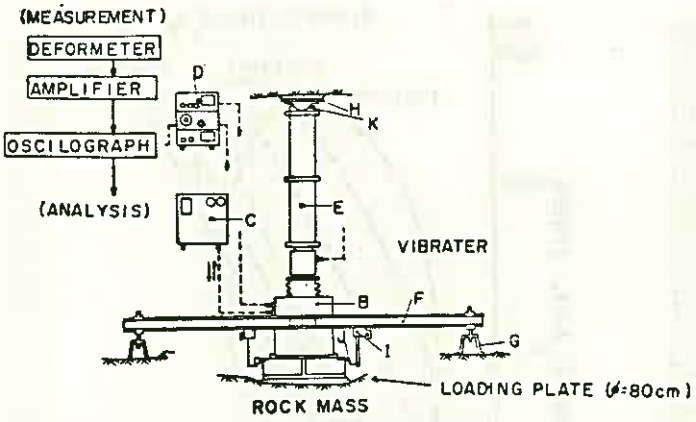

FIG 1 DYNAMIC REPEATED LOADING ON ROCK MASSES AND MEASURING SYSTEM

TABLE-1 SEVERAL KINDS OF DEFORMATION MODULUI (ROCK MASS)

ROCK MASS	static repeated Es (kg/cm²)	dynamic repeated Ed (kg/cm²)	elastic wave Ev (kg/cm²)	Ed/Es	Ev/Es	Ev/Ed
CONGLOMERATE	36 700 ~ 43 900	65 400 ~ 81 500	320 300	1.6 ~ 2.0	7 ~ 9	3.9 ~ 4.9
SHALE	4 200 ~ 5 800	3 700 ~ 4 800	66 700	0.6 ~ 1.0	12 ~ 16	14 ~ 18
SAND STONE	5 000 ~ 16 500	11 000 ~ 23 000	130 000 ~ 160 000	2 ~ 4	8 ~ 10	6 ~ 12
GRANITE	3 000 ~ 10 000	13 500 ~ 30 300	93 000 ~ 174 000	1.3 ~ 4	9 ~ 17	6 ~ 13
		11 500 ~ 25 600	109 000 ~ 204 000	1.3 ~ 4	10 ~ 20	8 ~ 18
MUD STONE	8 300 ~ 8 550	8 200 ~ 49 200	49 200	1 ~ 6	5.8 ~ 6	1 ~ 6
	13 000 ~ 17 500	17 800 ~ 77 200	61 300	1 ~ 6	3.5 ~ 4.7	0.8 ~ 3.4
	12 400 ~ 19 900	20 000 ~ 89 900	71 400	1.6 ~ 4	3.5 ~ 5.8	0.8 ~ 3.6
GABBRO	11 000	20 400 ~ 22 500	——	1.9 ~ 2.0	——	——
DIABASE	19 900	16 500 ~ 22 000	560 000	0.8 ~ 1.1	28	2.5 ~ 3.4
DIORITE	18 000	33 600 ~ 35 000	434 000	1.9	24	1.2 ~ 1.3
TUFF	100 000 ~ 160 000	230 000 ~ 250 000	430 000	1.9	2.7 ~ 4.3	1.8
	100 000	120 000 ~ 130 000	445 000	1.3	4.5	3.6
	30 000 ~ 35 000	50 000 ~ 60 000	415 000	1.7	12 ~ 14	7.7
	180 000 ~ 240 000	270 000 ~ 290 000	305 000	1.3	1.3 ~ 1.7	1.1
SLATE	150 000 ~ 250 000	220 000 ~ 250 000	385 000	1.5	1.5 ~ 2.5	1.6
	90 000	110 000 ~ 125 000	445 000	1.3	5	3.9
DIORITE	18 400	22 000 ~ 24 000	——	1.3	——	——
	12 900	17 000 ~ 21 000	——	1.3 ~ 1.6	——	——

note : dynamic stress amplitude 20 ~ 30 kg/cm²
load frequency 1 ~ 3 Hz

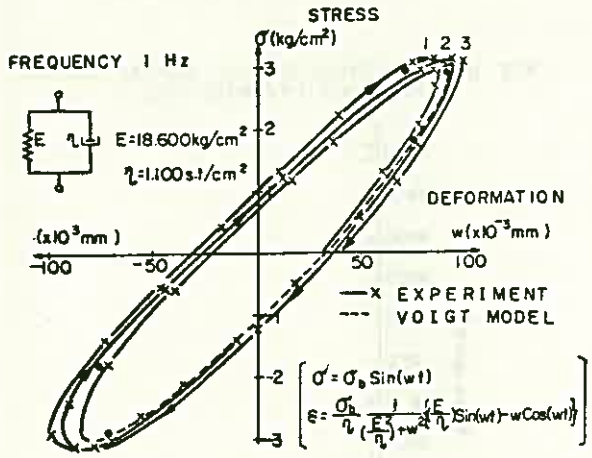

FIG 2. VOIGT MODEL AND EXPERIMENTAL CURVE OF DYNAMIC DEFRMATION

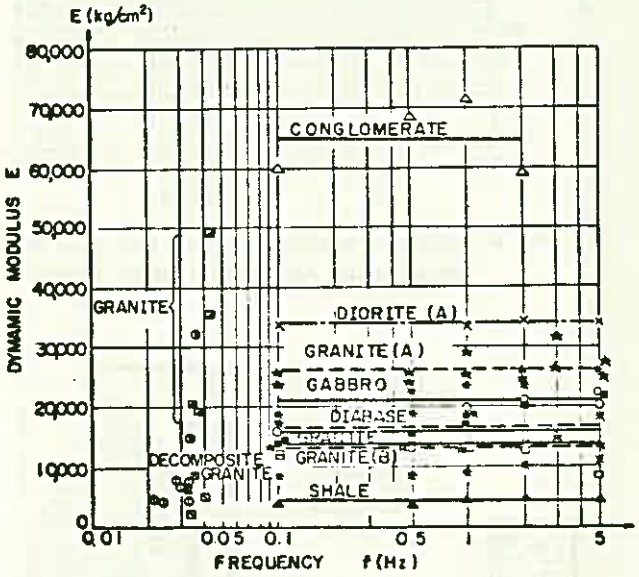

FIG 3 DYNAMIC MODULUS E OF VOIGT MODEL VERSUS LOAD FREQUENCY f (ROCK MASSES)

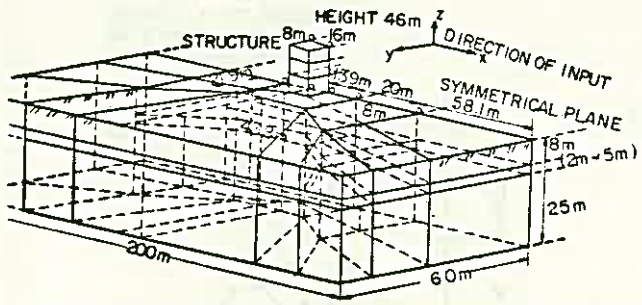

FIG 5 THREE DIMENSIONAL FINITE ELEMENT MODEL FOR ANALYZING STRUCTURE-GROUND ROCK INTERACTION DURING EARTHQUAKE

{ TETRAHEDRONS 396
HEXAHEDRONS 66
MOVABLE POINTS 66
TOTAL POINTS 140

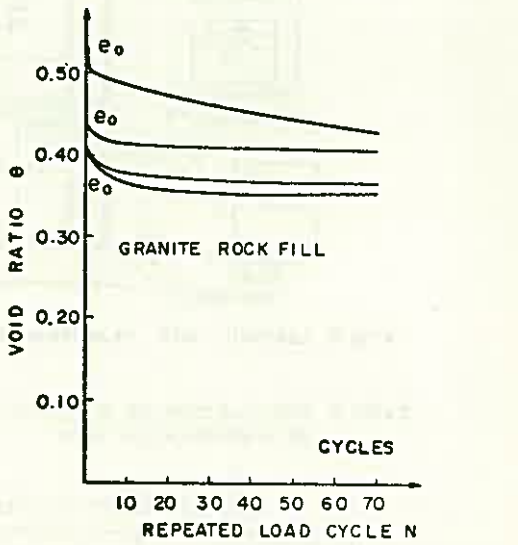

FIG. 7 CHANGE OF VOID RATIO e DURING REPEATED LOADING CYCLES N (GRANITE ROCK FILL MATERIAL)

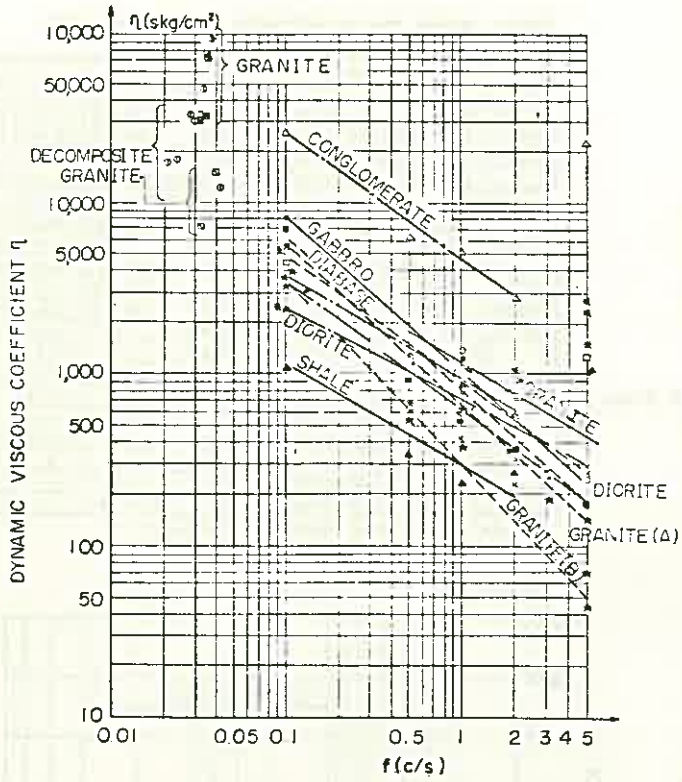

FIG 4 DYNAMIC VISCOUS COEFFICIENT η OF VOIGT MODEL VERSUS LOAD FREQUENCY f (ROCK MASSES)

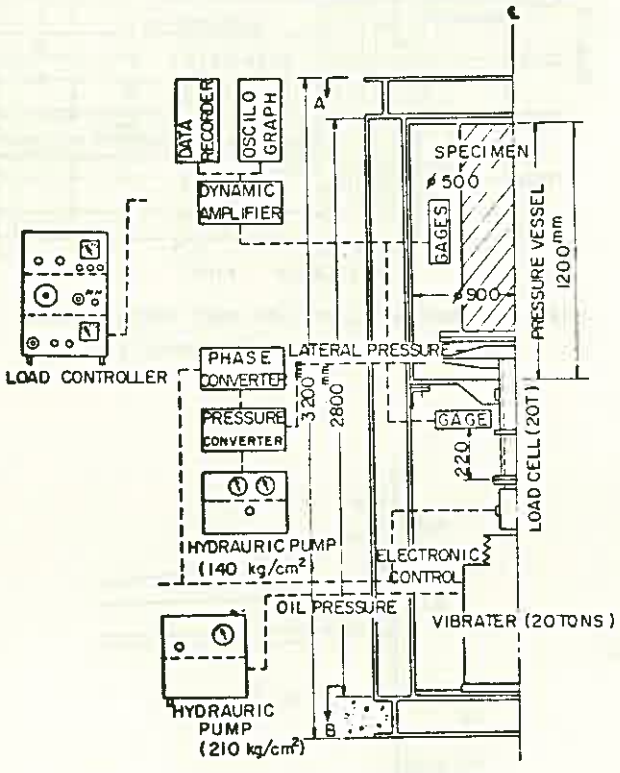

FIG 6 LOADING AND MEASUREMENT

Table 2 COMPARISON OF DAMPING CONSTANTS OF A ROCK FILL DAM

DAMPING IN FIRST MODE OF DAM	
Observed h	Calculated h
0.105	0.125

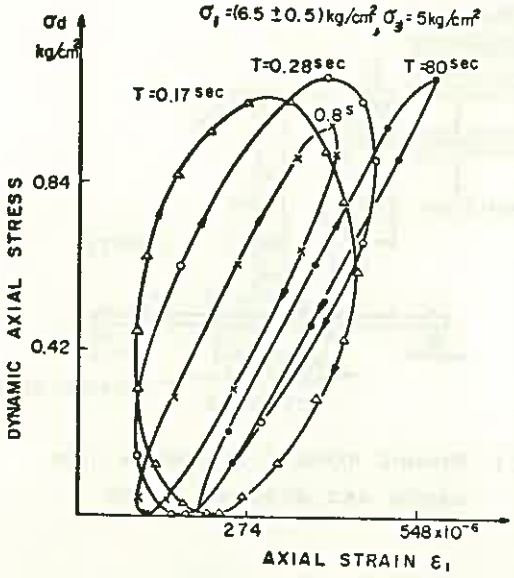

FIG 8 HYSTERISIS LOOPS IN SEVERAL LOADING PERIODS (TUFF ROCK FILL)

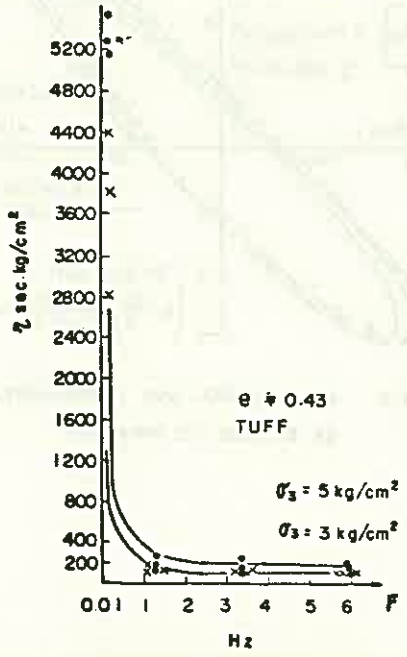

FIG. 9 VISCOSITY η VERSUS LOAD FREQUENCY F OF ROCK FILL MATERIAL

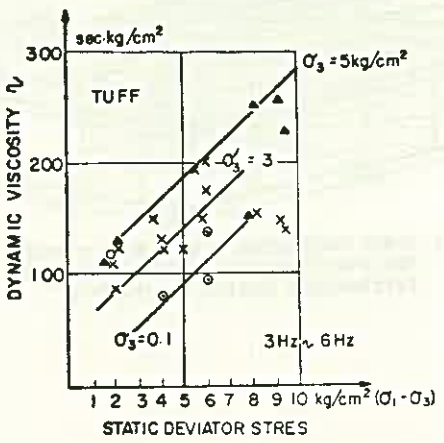

FIG. 10 DYNAMIC COEFFICIENT OF VISCOSITY η AGAINST STATIC DEVIATOR STRESS (ROCK FILL MATERIAL)

STRESSES AND DEFORMATIONS AROUND A TUNNEL WITH A CIRCULAR CROSS SECTION IN ANISOTROPIC ELASTIC BODY UNDER A THREE-DIMENSIONAL STRESS STATE

Yoshiji NIWA, Kyoto University
Shoichi KOBAYASHI, Kyoto University
Ken-ichi HIRASHIMA, Yamanashi University

In order to understand the earth pressure phenomena, it is of importance to analyze the distribution of stresses and deformations around underground tunnels taking into account the fact that the undisturbed ground is generally in a three dimensional stress state. It is not easy to clarify the distribution of stresses and deformations under every conditions, since it is affected by the initial stress conditions of ground, shapes of tunnel, mechanical properties of rock and so on. The authors have attempted to analyze theoretically the distribution of stresses and deformations around a tunnel with an elliptical cross section under a three-dimensional stress state. In the present paper, we set the assumptions that (a) the rock is homogeneous and anisotropic elastic body, (b) the stresses in the undisturbed ground do not vary along the generator of a tunnel, that is, the three-dimensional stress state is uniform over the wide region as compared with the diameter of a tunnel, and (c) body force is absent. Assumptions (b) is a reasonable one when a tunnel is excavated in considerable depth far from the ground surface.

The tunnel is considered to be an opening of an elliptical cross section with its axis coincided with the z-axis of a cartesian coordinate system (x,y,z). In this case, principal elastic axes of the body assumed that the surrounding material is homogeneous and anisotropic body, incline to arbitrary directions against this coordinate system. The principal stresses σ_1°, σ_2° and σ_3° in the undisturbed ground applied at infinity from arbitrary orthogonal directions inclined independently with not only the directions of principal elastic axes but also the axis of a tunnel, can be devided into six components of stress along the axial directions of coordinates (x,y,z) as shown in Fig. 1.

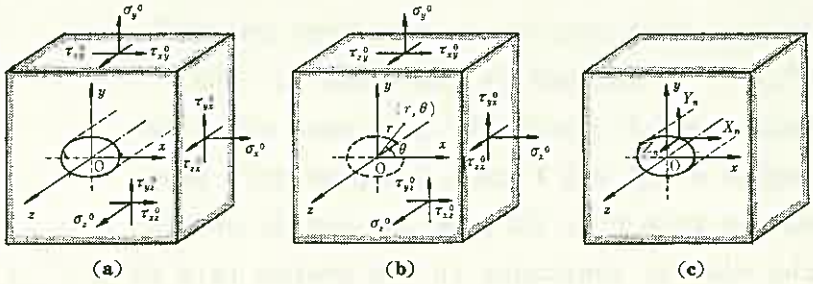

Fig. 1

In order to obtain the stresses and deformations in an anisotropic body, let us introduce the complex variables

$$z_k = x + \mu_k y \equiv \omega_k(\zeta_k) = \frac{1}{2}\left\{(a - i\mu_k b)\zeta_k + (a + i\mu_k b)\zeta_k^{-1}\right\}, \quad (k = 1, 2, 3) \cdots\cdots (1)$$

μ_1, μ_2 and μ_3 are the roots of characteristic equation for the anisotropic body under consideration. The stress components in the coordinates (x,y,z) are expressed in terms of three complex analytic functions $\phi_k(z_k)$ as follows.[1)]

$$\left.\begin{aligned} \sigma_x &= 2\,Re\left[\mu_1^2\phi_1'(z_1) + \mu_2^2\phi_2'(z_2) + \mu_3^2\lambda_3\phi_3'(z_3)\right], \\ \sigma_y &= 2\,Re\left[\phi_1'(z_1) + \phi_2'(z_2) + \lambda_3\phi_3'(z_3)\right], \\ &\cdots\cdots\cdots\cdots\cdots\cdots\cdots\cdots\cdots\cdots \end{aligned}\right\} \cdots\cdots\cdots\cdots\cdots\cdots (2)$$

Where λ_k (k=1,2,3) are complex constants related to the roots μ_k and the elastic constants a_{ij}. We can seek the expressions for the functions $\phi_k(z_k)$ in the forms

$$\phi_1(z_1) = \frac{1}{\mu_1 - \mu_2}(\mu_2\bar{a}_1 - \bar{b}_1)\zeta_1^{-1}, \quad \phi_2(z_2) = \frac{1}{\mu_1 - \mu_2}(\bar{b}_1 - \mu_2\bar{a}_1)\zeta_2, \quad \phi_3(z_3) = \bar{c}_1\zeta_3^{-1} \cdots\cdots (3)$$

In which $\bar{a}_1$, $\bar{b}_1$ and $\bar{c}_1$ are the complex constants to be determined by external stresses on the contour of a hole and the shape of the hole. When the stress components equal and oposite sign σ_x^0, σ_y^0, τ_{xy}^0, τ_{xz}^0 and τ_{yz}^0 applied at infinity act on the contour of the elliptical hole with semi-axes of a and b, these constants take the values:[3)]

$$\bar{a}_1 = \frac{1}{2}(\sigma_y^0 a - i\tau_{xy}^0 b), \quad \bar{b}_1 = \frac{1}{2}(\tau_{xy}^0 a - i\sigma_x^0 b), \quad \bar{c}_1 = \frac{1}{2}(\tau_{yz}^0 a - i\tau_{xz}^0 b) \cdots\cdots (4)$$

Then we can solve the problem under consideration by superimposing the stress components $\sigma_x, \sigma_y, \ldots, \tau_{yz}$ by eq.(2) to the components $\sigma_x^0, \sigma_y^0, \ldots, \tau_{yz}^0$ applied at infinity. The deformations u, v and w may be also obtained as the same manners.

Table 1 Relations between the rectangular cartesian coordinates (x, y, z) and (x''', y''', z''').

	x	y	z
x'''	$\cos\beta\cos\gamma$	$-\cos\beta\sin\gamma$	$\sin\beta$
y'''	$\sin\alpha\sin\beta\cos\gamma + \cos\alpha\sin\gamma$	$\cos\alpha\cos\gamma - \sin\alpha\sin\beta\sin\gamma$	$-\sin\alpha\cos\beta$
z'''	$-\cos\alpha\sin\beta\cos\gamma + \sin\alpha\sin\gamma$	$\sin\alpha\cos\gamma + \cos\alpha\sin\beta\sin\gamma$	$\cos\alpha\cos\beta$

Let the elastic constants for the system (x‴,y‴,z‴) be known and consider the anisotropic body being inclined to the axis of the tunnel (Fig. 2). In this case, the position of the new coordinate system (x,y,z) with respect to the first one (x‴, y‴,z‴), is defined by the Table 1. The rotations of coordinate axes such that the angles α, β and γ take independently any values from 0 to 2π, we can easily obtain the elastic constants in the system (x,y,z) for all inclinations of axes of elastic moduli[1)].

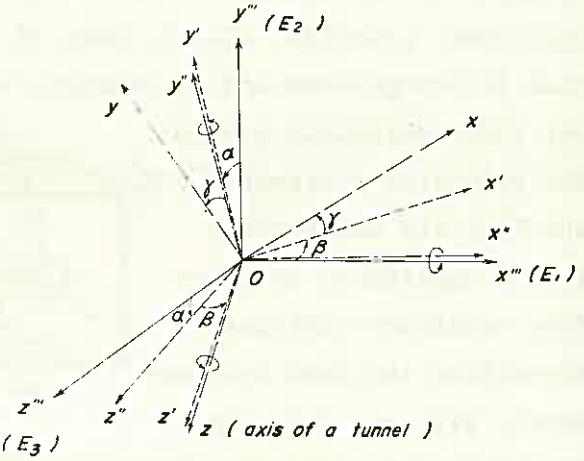

Fig. 2

For the sake of simplicity, let us consider the cross-anisotropic elastic body such that the elastic moduli and Poisson's ratios are given respectively by $E_1 = E_2 = 3E_3 = 6.0\times10^4\ kg/cm^2$, $\nu_{23} = \nu_{31} = 0.15$, and the moduli of rigidity are defined as $\nu_{12} = 0.25$

$$1/G_{ij} = 1/E_i + 1/E_j + 2\nu_{ij}/E_i, \quad (i, j = 1, 2, 3)$$

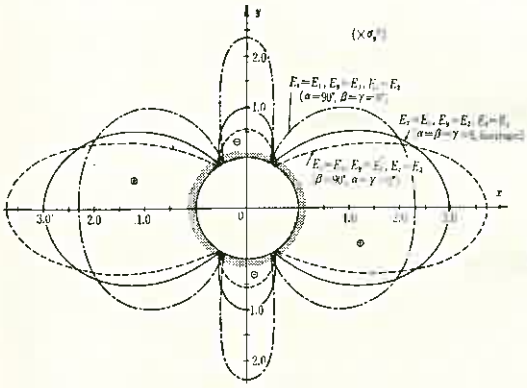

Fig. 3

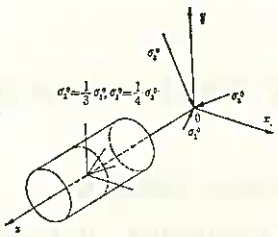

	σ_1^0	σ_2^0	σ_3^0
x	64°14′	32°43′	71°15′
y	119°37′	94°20′	30°00′
z	41°09′	122°22′	67°27′

$$\sigma_2^0=\frac{1}{3}\sigma_3^0,\quad \sigma_1^0=\frac{1}{4}\sigma_3^0$$

$$\sigma_x^0=0.387\,\sigma_3^0,\quad \sigma_y^0=0.813\,\sigma_3^0,\quad \sigma_z^0=0.384\,\sigma_3^0$$
$$\tau_{xy}^0=0.203\,\sigma_3^0,\quad \tau_{xz}=0.055\,\sigma_3^0,\quad \tau_{yz}=0.253\,\sigma_3^0$$

Fig. 4 An example of state of stress in the undisturbed ground (After Hiramatsu and Oka[2]).

These assumptions do not lose in generality for our problem as an anisotropic elastic body.

Let us show some numerical examples. Fig. 3 shows the stress distributions around the circular opening when the stress $\sigma_y^0=1$ acts at infinity. Now assuming that the principal stresses σ_1^0, σ_2^0 and σ_3^0 in the undisturbed ground with prescribed elastic constants are as shown in Fig. 4,[2] the distributions of stresses and deformations on the wall of the tunnel with a circular cross section are illustrated in Figs. 5 and 6. In these figures, normal stress σ_z along the axial direction of the tunnel was calculated from the assumption of plane strain of the z-direction. Fig. 5 indicates the distributions of stresses and deformations for the isotropic elastic body (Poisson's ratio ν =0.25).

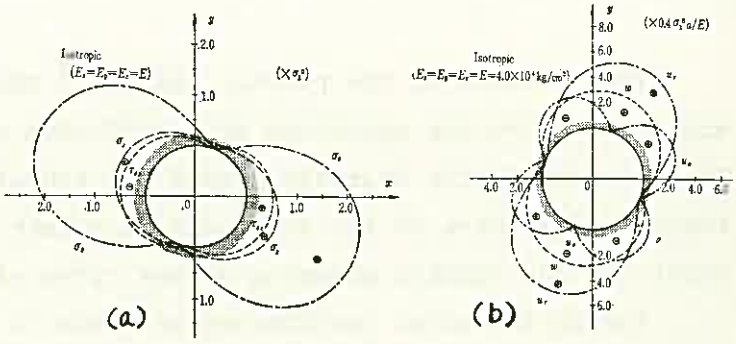

Fig. 5

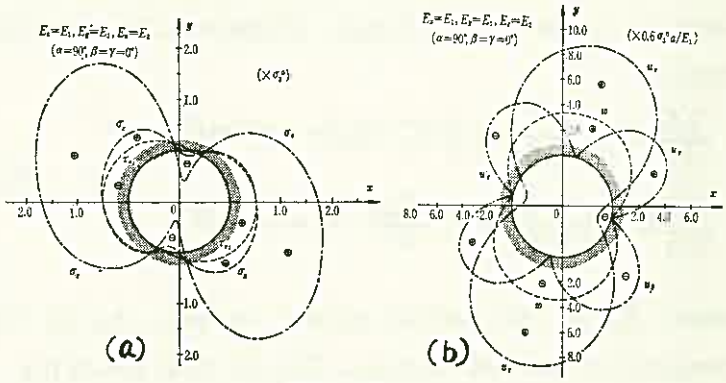

Fig. 6

REFERENCES:

1) S. G. Lekhnitskii:"Theory of Elasticity of an Anisotropic Elastic Body", Holden-Day Inc., (1963), pp.1-174

2) Y. Hiramatsu and Y. Oka: Stress Around a Shaft or Level Excavated in Ground with a Three-Dimensional Stress State, Mem. Fac. Eng., Kyoto Univ., Vol.24 Pt.1 (1962), pp.56-76

3) Y. Niwa, S. Kobayashi and K. Hirashima: Stresses and Deformations Around a Tunnel with a Circular Cross Section in Anisotropic Elastic Body, Trans. Japan Soc. Civil Eng., No.178 (1970), pp.7-17 (in Japanese)

STRESS ANALYSIS OF THE PLASTIC REGION AROUND A TUNNEL

Eiichi ODA and Takuo YAMAGAMI
Faculty of Engineering, Tokushima University

The stresses in the plastic region of the ground around a circular tunnel are analysed by the equations of equilibrium of stresses and yield condition. The plastic-elastic boundary around the tunnel is approximately determined by the plotting curve of the intersecting points of the plastic shearing stress curve and the elastic shearing stress curve along the slip lines.

Taking the polar coordinates as shown in Fig. 1, we have the equations of equilibrium of stresses in a two-dimensional element with gravity force.

$$\left.\begin{aligned} \frac{\partial \sigma_r}{\partial r} + \frac{1}{r}\frac{\partial \tau_{r\theta}}{\partial \theta} + \frac{1}{r}(\sigma_r - \sigma_\theta) &= -w\cos\theta \\ \frac{\partial \tau_{r\theta}}{\partial r} + \frac{1}{r}\frac{\partial \sigma_\theta}{\partial \theta} + 2\frac{\tau_{r\theta}}{r} &= w\sin\theta \end{aligned}\right\} \cdots (1)$$

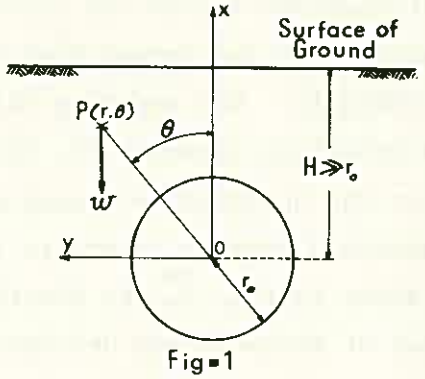

Fig.1

where σ_r is the radial normal stress, σ_θ is the tangential normal stress, $\tau_{r\theta}$ is the shearing stress, and w is the unit weight of the ground. Postulating that the plastic ground has cohesion without frictional resistance, we have the yield condition:

$$\left.\begin{aligned} \sigma_r &= \sigma + k\cos 2\varphi \\ \sigma_\theta &= \sigma - k\cos 2\varphi \\ \tau_{r\theta} &= k\sin 2\varphi \end{aligned}\right\} \cdots\cdots (2)$$

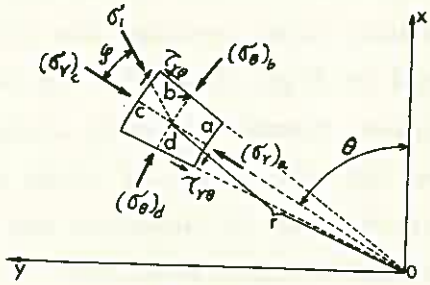

Fig.2

where as shown in Fig.2 and Fig.3, σ_1 is the maximum principal stress, σ_2 is the minimum principal stress, φ is the angle between the radial direction and that of σ_1, and

$$\sigma = \frac{\sigma_1 + \sigma_2}{2} = \frac{\sigma_r + \sigma_\theta}{2} \qquad \cdots\cdots (3)$$

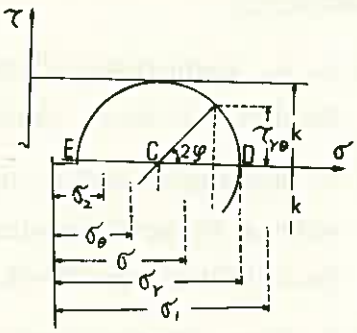

Fig.3

Substituting eq. (2) into eq. (1), we have the following equations:

$$\left.\begin{aligned}&\frac{\partial\sigma}{\partial r}-2k\sin 2\varphi\frac{\partial\varphi}{\partial r}+\frac{2}{r}k\cos 2\varphi\frac{\partial\varphi}{\partial\theta}+\frac{2}{r}k\cos 2\varphi+w\cos\theta=0\\&\frac{1}{r}\frac{\partial\sigma}{\partial\theta}+2k\cos 2\varphi\frac{\partial\varphi}{\partial r}+\frac{2}{r}k\sin 2\varphi\frac{\partial\varphi}{\partial\theta}+\frac{2}{r}k\sin 2\varphi-w\sin\theta=0\end{aligned}\right\}\cdots\cdots(4)$$

The theory of partial differential equations shows that the characteristic equations for the simultaneous partial differential equations (4) are given by

$$C_+:\quad \frac{\partial\theta}{\partial\alpha}=\frac{1}{r}\tan\left(\frac{\pi}{4}+\varphi\right)\frac{\partial r}{\partial\alpha}\qquad\cdots\cdots\cdots(5)$$

$$C_-:\quad \frac{\partial\theta}{\partial\beta}=\frac{1}{r}\tan\left(-\frac{\pi}{4}+\varphi\right)\frac{\partial r}{\partial\beta}\qquad\cdots\cdots\cdots(6)$$

on the physical r, θ plane, while the characteristic equations are given by

$$\Gamma_+:\ \frac{\partial\sigma}{\partial\alpha}+2k\frac{\partial\varphi}{\partial\alpha}+\left(2k\sin 2\varphi-wr\sin\theta\right)\frac{\partial\theta}{\partial\alpha}+\left(\frac{2}{r}k\cos 2\varphi+w\cos\theta\right)\frac{\partial r}{\partial\alpha}=0\qquad\cdots\cdots(7)$$

$$\Gamma_-:\ \frac{\partial\sigma}{\partial\beta}-2k\frac{\partial\varphi}{\partial\beta}+\left(2k\sin 2\varphi-wr\sin\theta\right)\frac{\partial\theta}{\partial\beta}+\left(\frac{2}{r}k\cos 2\varphi+w\cos\theta\right)\frac{\partial r}{\partial\beta}=0\qquad\cdots\cdots(8)$$

on the σ, φ-i.e. stress plane, where α and β are the parameters of the characteristics. We can discuss the state of stresses by solving eqs. (5),(6),(7) and (8) instead of grappling with eqs. (1) and (2). There exists one-to-one correspondence between a point in the physical plane and a point in the stress plane.

It is shown by eqs.(5) and (6) that C_+-curve and C_--curve are slip lines, and r and θ of the intersecting point of C_+-curve and C_--curve are represented by the partial differential equations of the hyperbolic type about α and β. Because of the hyperbolic character of the differential equations of plastic flow, the stresses in plastic zone near the boundary i.e. the periphery of a tunnel depend only on the shape of the boundary and the stresses on the boundary. They are independent of the loading i.e. elastic stresses at large distance from the plastic zone considered. But the loading and the conditions on the other boundary surfaces affect the shape and size of the plastic zone.

We suppose that $\sigma_r=0$, $\tau_{r\theta}=0$ and $\varphi=\pi/2$ on the periphery of the circular tunnel with radius r_o, and hence

$$(\sigma_\theta)_{r=r_o}=2k,\qquad (\sigma)_{r=r_o}=\frac{\sigma_\theta}{2}=k$$

As shown in Fig.4, assuming that the plastic flow takes place on AB of the circular periphery of the tunnel, we can consider that C_+ and C_--curves are the curvilinear coordinate axes α and β which are AC and BC curves respectively, and the boundary AB intersects α and β lines at the points A and B respectively. The stresses and

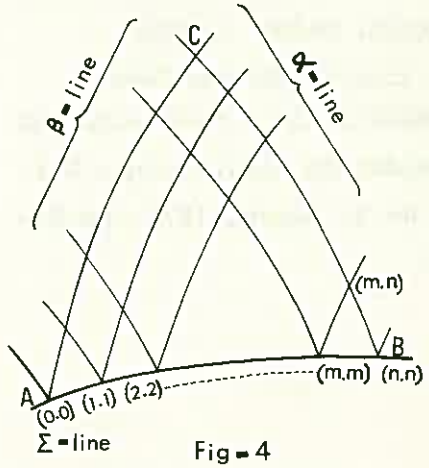

Fig-4

the coordinates of the nodal point in a network of the slip lines depend on the boundary conditions of the arc AB. The solutions of eqs.(5),(6),(7) and (8) are obtained by an approximate step-by-step procedure.

Assuming that the ground is elastic solid and the depth of the center of the circular tunnel is H, we can calculate the stresses around the tunnel by the theory of elasticity proposed by H. Schmidt.[1]

We shall investigate the shape and the position of the elastic-plastic boundary by the following approximate method proposed hypothetically. We determine the point on the elastic-plastic boundary around the tunnel to be the intersecting point of the distribution-curve of shearing stress of the plastic theory and the distribution-curve of shearing stress of the elastic theory along the slip line.

Assuming that H=50m, r_o=3m, w=2.0 t/m^3, k=3.0 kg/cm^2, poisson's number μ=2.33 or 3.00, we calculate the network of slip lines and the elastic-plastic boundary which are shown in Fig.5. Fig.6 shows the distributions of stresses around the tunnel.[2]

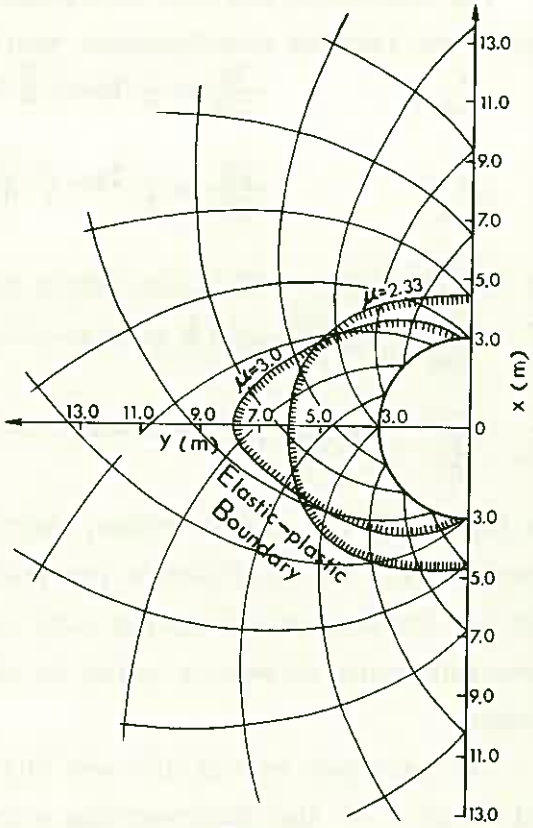

Fig-5

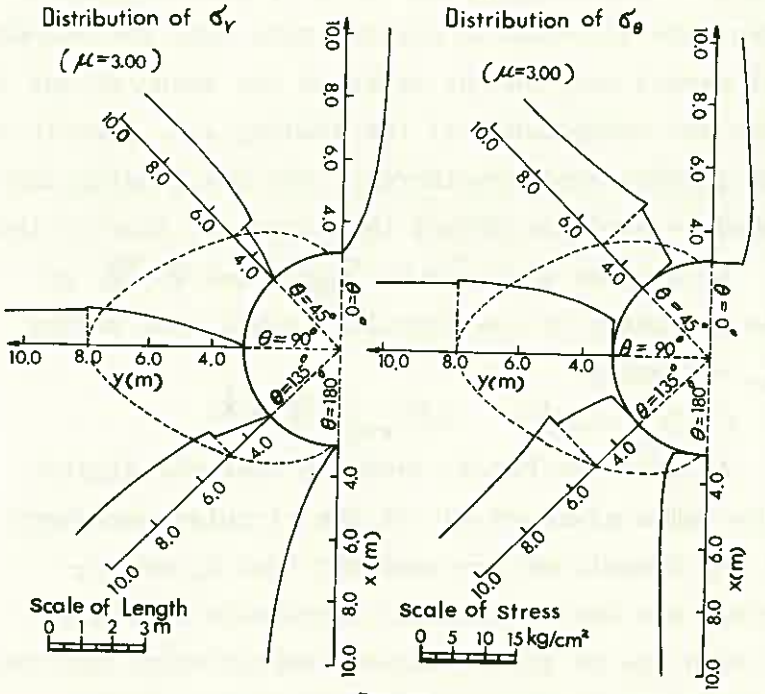

Fig-6

Reference

1) H. Schmidt: "Statishe Probleme des Tunnel und Druckstollenbaues und ihre gegenseitigen Beziehungen" Verlag von Julius Springer, Berlin 16/26 (1926).

2) Eiichi ODA and Takuo YAMAGAMI: Soil Mechanics and Foundation Engineering, Vol. 19 No.3, March, 1971, pp.39-46.

AN ANALYTICAL METHOD FOR DETERMINATION OF EARTH PRESSURE ACTING ON TUNNEL LINING IN VISCOELASTIC MEDIUM

Shunsuke SAKURAI, Kobe University

1. Introduction

One of the most difficult problems in the design of a tunnel lining is how to estimate the pressure acting on it. The pressure depends not only on the initial stresses in the underground medium but on the rigidity of the lining, and usually increases with time, so that in a theoretical analysis a time factor must be considered. For the purpose of designing the lining, however, the maximum pressure especially is of more importance than a transient pressure change.

The author proposes herein a new analytical technique for the determination of the maximum pressure distribution acting on the lining, constructed at a large depth underneath the ground surface. The proposed method does not require a time-dependent analysis, but follows exactly the same technique as the one in the theory of elasticity. It can be extensively applied for the case of an orthotropic viscoelastic ground as well as for an isotropic medium, and the Finite Element Method can be easily adopted for the case with complex boundary conditions.

2. Procedure of analysis

The creep function expressing the relation between the shearing stress and shearing strain in an isotropic medium is assumed as follows ;

$$\psi(t) = \frac{1}{G} + \frac{1}{G^*}\{1 - \exp(-t/\tau_0)\} \qquad (1)$$

where G and G^* are the shear modulus and retarded shear modulus, respectively. τ_0 denotes the retardation time. It is also assumed that Poisson's ratio does not change with time.

The calculation procedure whose mathematical verification has been given in the reference [1], is as follows ;

First, the displacement $u_g^{(1)}$ at internal surface of an unlined tunnel due to the initially existing stresses before tunnelling, as shown in Fig. 1 (a), is calculated by introducing the apparent shear modulus $G^*\exp(t_0/\tau_0)$, where t_0 denotes construction time of lining after excavation.

It should be noted here that in the calculation of $u_g^{(1)}$, only its variation

due to tunnelling must be considered. It is interesting to know that the apparent rigidity of the underground medium increases with the delay of the construction of the lining. Second, the displacement $u_g^{(2)}$ of the tunnel surface due to the confining pressure R caused by the lining, as shown in Fig. 1 (b), is determined as a function of the pressure, where the apparent shear modulus is taken as GG*/(G+G*). Third, the displacement u_ℓ of the outer surface of the lining which consists of an elastic material, as shown in Fig. 1 (c), is also expressed as a function of the pressure R.

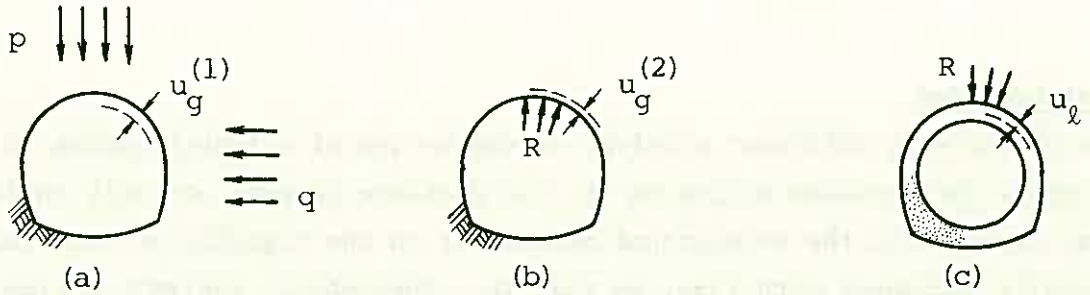

Fig.1 Schematic diagram for explanation of calculation procedure.

Finally, the above obtained displacements are substituted into the following compatibility equation which must be satisfied at the contact plane of the lining and the surrounding medium.

$$u_\ell = u_g^{(1)} + u_g^{(2)} \qquad (2)$$

By solving Eq. (2), the unknown function R which gives the maximum earth pressure acting on lining can be determined.

The proposed method can also be applied for the case of an orthotropic underground medium. If one principal axis of orthtropy coincides with the tunnel axis, the stress-strain relation-ship under the plane condition is expressed as follows ;

$$\begin{Bmatrix} \varepsilon_x \\ \varepsilon_y \\ \gamma_{xy} \end{Bmatrix} = \begin{bmatrix} a_{11} & a_{12} & 0 \\ a_{21} & a_{22} & 0 \\ 0 & 0 & a_{33} \end{bmatrix} \begin{Bmatrix} \sigma_x \\ \sigma_y \\ \tau_{xy} \end{Bmatrix} \qquad (3)$$

where

$$a_{11} = (1 - \nu_{13}\,\nu_{31}) \int_0^t \phi_1(t-\tau)\,\frac{\partial}{\partial\tau}\,d\tau, \quad a_{12} = a_{21} = -(\nu_1 + \nu_{23}\,\nu_{32}) \int_0^t \phi_1(t-\tau) \times \frac{\partial}{\partial\tau}\,d\tau\,, \quad a_{22} = (1 - \nu_{23}\,\nu_{32}) \int_0^t \phi_2(t-\tau)\,\frac{\partial}{\partial\tau}\,d\tau\,, \quad a_{33} = \int_0^t \phi_3(t-\tau)\,\frac{\partial}{\partial\tau}\,d\tau\,.$$

If the following creep functions are given,

$$\begin{aligned} \phi_1(t) &= \{1 - \exp(-t/\tau_0)\}/E_1^* \\ \phi_2(t) &= \{1 - \exp(-t/\tau_0)\}/E_2^* \\ \phi_3(t) &= (1 + 2\nu_1)\,\phi_1 + \phi_2 \end{aligned} \qquad (4)$$

then Eq. (3) can be expressed by only one creep function, say $\phi_1(t)$.

Therefore, the above mentioned calculation procedure for an isotropic case can be extended for this problem, as follows ;

First, the displacement $u_g^{(1)}$ can be determined by putting the material constants as follows ;

$$\begin{aligned} a_{11} &= (1 - \nu_{13}\,\nu_{31})\exp(-t_0/\tau_0)/E_1^* \\ a_{12} &= -(\nu_1 + \nu_{23}\,\nu_{32})\exp(-t_0/\tau_0)/E_1^* \\ a_{22} &= (1 - \nu_{23}\,\nu_{32})\exp(-t_0/\tau_0)/E_2^* \\ a_{33} &= (1 + E_1^*/E_2^* + 2\nu_1)\exp(-t_0/\tau_0)/E_1^* \end{aligned} \qquad (5)$$

Second, in the calculation of $u_g^{(2)}$ the following material constans must be used.

$$\begin{aligned} a_{11} &= (1 - \nu_{13}\,\nu_{31})/E_1^* \\ a_{12} &= -(\nu_1 + \nu_{23}\,\nu_{32})/E_1^* \\ a_{22} &= (1 - \nu_{23}\,\nu_{32})/E_2^* \\ a_{33} &= (1 + E_1^*/E_2^* + 2\nu_1)/E_1^* \end{aligned} \qquad (6)$$

Third, u_ℓ is easily calculated, as it can be assumed that the lining generally consists of an isotropic elastic material.

Finally, these displacements are substituted into Eq. (2) to determine the pressure distribution on the lining.

3. Conclusion

A new technique to estimate the earth pressure acting on the tunnel lining constructed in an isotropic or orthotropic viscoelastic underground medium is proposed here. The pressure can be calculated without consideration of a time factor, even though the underground medium is assumed to be viscoelastic.

Reference

[1] Sakurai, S. and Y. Yoshimura, " A METHOD OF CALCULATION OF PRESSURE ACTING ON UNDERGROUND STRUCTURE IN VISCOELASTIC MEDIUM "(in Japanese) Proc. Japan Society of Civil Engineers, No. 218, 1973, pp. 75 - 85.

ON THE MECHANISM OF SQUEEZING-SWELLING ROCK PRESSURE OF MUDSTONE ON TUNNEL SUPPORT IN RELATION WITH THE CASE HISTORY OF NOSHIRO TUNNEL

Ryoki NAKANO, National Research Institute of Agricultural Engineering

1. Swelling characteristics of clayey rock (mudstone or shale) and tunnel load.

As the author pointed out in his previous paper[1], almost all natural clayey rocks such as mudstone or shale show very little swelling cahracteristics when immersed in water at their natural water content, but there are some mudstones or shales (especially those of Neogene Tertiary) which show conspicuous swelling characteristics in water when they are once disturbed and remolded, resulting in much reduction of their strength. These characteristics are especially conspicuous to such mudstones or shales, that contain expanding clay mineral Montmorillonite, which are the bed-rock of the so-called landslide areas. The author once proposed new terms such as "Artificial Mudstone", "Remolded Mudstone" or "Disturbed Mudstone" to mean the rock artificially made (but without simulating the process of diagenesis) by just compressing the powder of natural mudstone with its natural water content to its original density. (He took the remolded or artificial mudstone compressed by the vertical stress of 100 kg/cm^2 as a standard specimen to compare the swelling potential of various remolded mudstone.)

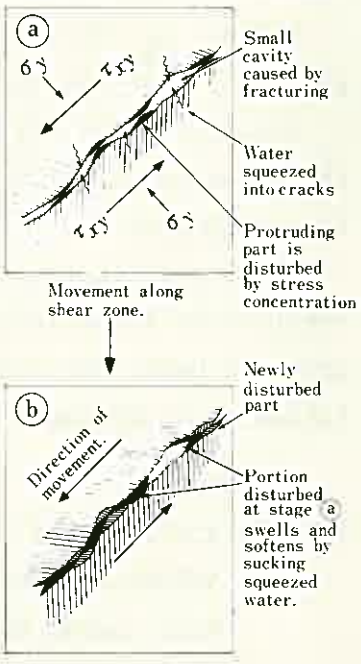

Fig. 1 Illustration of the mechanism of softening and swelling

In the plastic zone around a tunnel, the rock is sheared or cracked, and along the sheared or fractured zone, a disturbed zone is formed.

The water originally held loosely in pores in a rock or loosely absorbed by clay minerals adjacent to this sheared zone is squeezed by the concentrated stress to this zone and is sucked up or absorbed by the expanding clay minerals in the disturbed shear zone (Fig.1), resulting in the remarkable reduction of the strength of rock mass as a whole. Moreover, as the rock mass in the plastic zone dilates as a result of breakage (Fig. 2) and is squeezed into the excavated space of the tunnel, stress relief is to take place and the concentrated stress is transferred gradually from the rock adjacent to the tunnel surface to the rock remote from the wall.

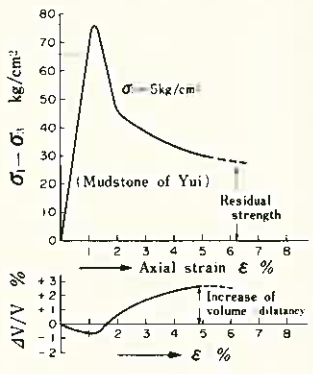

Fig.2 An example of stress-strain curve of mudstone and volume change

Hence a condition favourable for the movement of water squeezed from the stress concentrated elastic zone to the plastic zone is also established and the water accelerates the swelling or softening of the rock mass of sheared and disturbed mudstone. These conditions all contribute to the reduction of cohesion and internal angle of friction of the mass of broken rocks.

2. Mechanism of the squeezing-swelling rock pressure.

Supposing that the radius of a circular tunnel is R_1, and that the hydrostatic stress at a great distance is σ_0, the relationship between the radial stress σ_i at $r=R_1$ and the radius R_a of the boundary surface between the plastic region and the elastic region (ref. Fig. 3) can be expressed as,

$$\sigma_i = \frac{(2\sigma_0 - q_u')(1-\beta^2) - q_u(1+\beta'^2)}{(1+\beta'^2)(1-\beta^2)(R_a/R_1)^{\beta^2-1}} + \frac{q_u}{1-\beta^2} \quad \cdots\cdots(1)$$

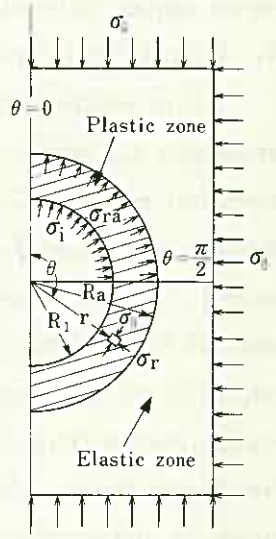

Fig.3 Plastic zone around a circuler hole in an isotropic homogeneous material

Here, both the solid rock in the elastic region and the broken rock in the plastic region are assumed to behave as Coulomb materials.

q_u, q_u' are unconfined compressive strengths and $\beta = \tan(\frac{\pi}{4}+\frac{\phi}{2})$, $\beta' = \tan(\frac{\pi}{4}+\frac{\phi'}{2})$ for solid rock and the mass of broken rocks respectively. As is evident from $E_q.(1)$, the larger the ratio R_a/R_1, namely the more the rock is loosened and the inward movement is allowed, the smaller the radial stress σ_i becomes, so long as the parameters ϕ, ϕ', q_u, q_u' are kept constant. However, if the inward movement is allowed excessively beyond some limited range, strain-softening takes place and the strength of rock in the plastic zone is brought beyond its peak value down to the smaller values and its strength parameters are decreased ultimately to those of residual strength C_r, ϕ_r, resulting in the decrease of q_u' and β and the increase of internal pressure σ_i (R_a must be kept within an allowable value to maintain the required sectional area of the tunnel). This is clear from $E_q.(1)$.

If the disturbed mudstone or shale has a high swelling capacity, water content along a sheared zone increases and q_u' and β are to become very small and a troublesome high rock pressure will ensue.

3. A case history of a typical squeezing-swelling rock pressure.

Three of the tunnels of the main irrigation water line for Noshiro Irrigation and Reclamation Project in Akita Prefecture provide the data for this example (ref. Fig.4).

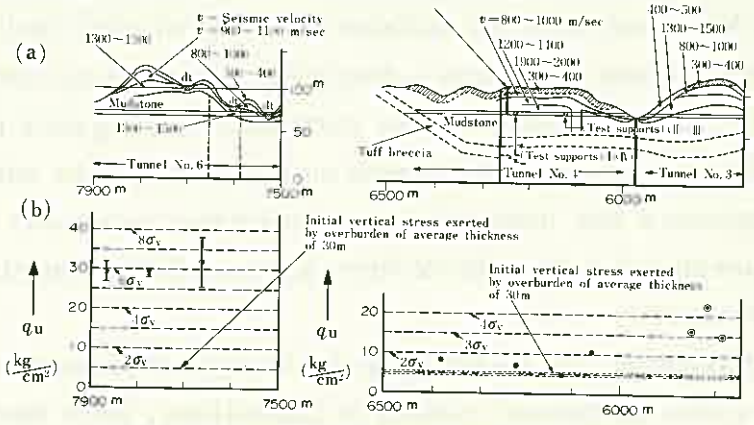

Fig.4 Geologic profile of Noshiro Tunnels No. 3, 4, 6 and unconfined compressive strength of mudstone.
σ_v: Initial vertical stress exerting on the tunnel formation before tunneling by overburden pressure.

Three tunnels, No.3, No.4 and No.6, were all constructed in a massive, occasionally faulted Tertiary mudstone bed named as Fujikotogawa Formation. The phenomena encountered during the construction of Tunnel No.4 were very different from those of the tunnels No.3 and No.6.

In the case of Tunnel No.4, the heavy rock pressure caused an excessive deformation of the first placed light steel supports resulting in the necessity to change to the heavier supports with invert struts.

In contrast with Tunnel No.4, the rock pressure experienced in tunnels No.5 and 6 was considerably smaller in spite of the fact that the mudstone of these tunnels were apparently similar to that of Tunnel No.4.

4. Considerations on the mechanism of heavy rock pressure of Noshiro Tunnel No.4

As is evident from Fig.4, the ratio of the compressive strength q_u of the mudstone of tunnel No.4 to the initital vertical stress $\sigma_v = \gamma_t \cdot h$ (h is the thickness of the overburden rock and γ_t is the rock density), i.e. q_u/σ_v was only 1.5 - 2, whereas that of Tunnel No.3 was 3–4 and that of Tunnel No.6 was around 6. Besides, the swelling capacity of the remolded mudstone of Tunnel No.4 was conspicuous (Fig.5) and much higher than that of Tunnel No.3 and No.6. Although all the mudstones contained more or less expanding clay mineral Montmorillonite, their swelling capacity at remolded or disturbed conditions was very different.

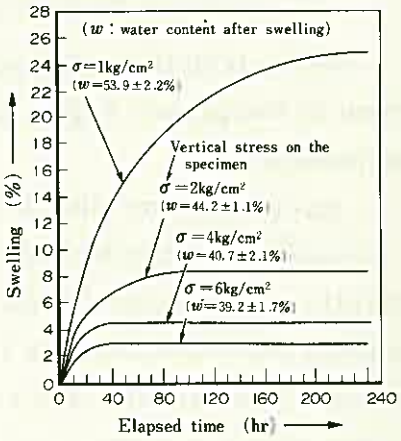

Fig.5 Swelling under various vertical pressures of artificial (or remolded) mudstone sampled from Noshiro Tunnel-No.4

Based on these facts and considering the reasons previously mentioned in section 1, 2 it may be concluded that the rock in Tunnel No.4 was broken by concentrated stress and plastic zone of failure was formed concentric with the tunnel axis and softening due to swelling along the sheared zone (Fig.1) took place, resulting in the rapid decrease of its strength (Fig.6) and the increase of Squeezing-Swelling Rock Pressure, whereas both in Tunnel No.3 and No.6 the mudstone underwent very little breakage and very little softening of mudstone accompanying it, if any, hence a small vertical loosening rock pressure was encountered. Based on these facts, the author proposed a new method for predicting the possibility of Squeezing-Swelling Rock Pressure and for classifying rocks for tunneling purposes.

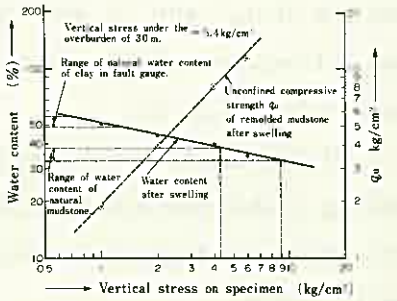

Fig.6. Relationship between the swelling pressure, the water content and unconfined compressive strength qu at the end of swelling (mudstone sampled from Tunnel No.4)

Reference:

1) Nakano R: On weathering and change of properties of Tertiary Sedimentary rocks (mudstone) related to Landslides, Rock Mechanics in Japan Vol. 1. p71-73 (1970)

STRESSES AND DEFORMATIONS AROUND TWO OPENINGS IN ELASTIC BODY UNDER IN-PLANE AND OUT-OF-PLANE LOADS

Ken-ichi HIRASHIMA, Yamanashi University
Yoshiji NIWA, Kyoto University

In the present paper, the following problems are treated: (1) stresses and deformations around two or more openings with arbitrary cross sections in an isotropic body, and (2) stresses and deformations around two or more openings with circular or elliptical cross sections in an anisotropic body under in-plane loads σ_x° , σ_y° , τ_{xy}° and out-of-plane loads τ_{xz}° , τ_{yz}° at infinity.
The method of analysis was used the successive approximation to be obtained by the point matching technique based on the exact solution of an isotropic or an anisotropic elastic body containing an opening.

Let us consider an infinite body to the coordinate system (x , y , z) where the origin lies in the cross section of an opening (see Fig. 1). And we consider the body with an opening, the contour of which is given by the following expression.

$$\left.\begin{aligned} x_0 &= \alpha_0 \cos\theta + \sum_{m=1}^{\nu} (\alpha_m \cos m\theta + \beta_m \sin m\theta) \\ y_0 &= \alpha_0 \sin\theta - \sum_{m=1}^{\nu} (\alpha_m \sin m\theta - \beta_m \cos m\theta) \end{aligned}\right\} \cdots\cdots (1)$$

For the case of an anisotropic body, the present paper treats only the problems containing a circular or an elliptical hole (corresponding to $\nu = 1$) at which the complex stress functions $\phi_k(\zeta_k)$ are single-valued throughout the region.

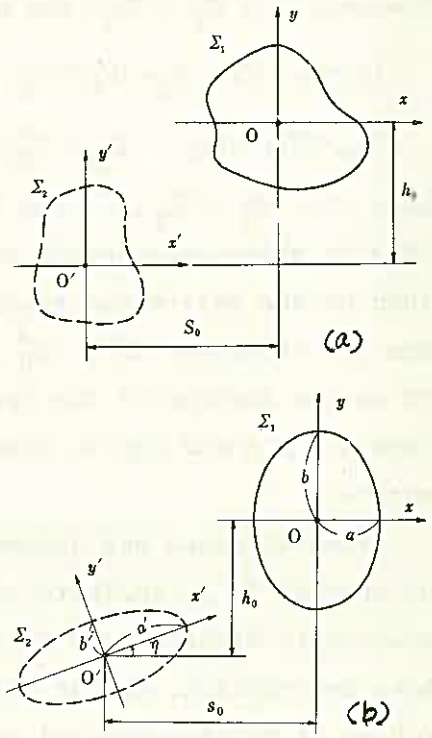

Fig. 1

When an infinite body under consideration is applied by the uniformly distributed loads σ_x° , σ_y° , τ_{xy}° , τ_{xz}° and τ_{yz}° at infinity, stresses and deformations in the body can be calculated by the complex analytic functions as follows[2,3]

$$\varphi(\zeta) = \sum_{m=1}^{\infty} A_m \zeta^{-m}, \quad \psi(\zeta) = -\bar{\varphi}(1/\zeta) - \frac{\bar{\omega}(1/\zeta)}{\omega'(\zeta)} \varphi'(\zeta), \quad \phi(\zeta) = \sum_{m=1}^{\infty} \bar{C}_m \zeta^{-m} \cdots\cdots (2)$$

$$\phi_1(\zeta_1) = \frac{1}{\mu_2 - \mu_1} \sum_{m=1}^{\infty} (\mu_2 \bar{a}_m - \bar{b}_m) \zeta_1^{-m}, \quad \phi_2(\zeta_2) = \frac{1}{\mu_2 - \mu_1} \sum_{m=1}^{\infty} (\bar{b}_m - \mu_1 \bar{a}_m) \zeta_2^{-m}, \quad \phi_3(\zeta_3) = \sum_{m=1}^{\infty} \bar{C}_m \zeta_3^{-m} \cdots\cdots (3)$$

Eq.(2) corresponds to the case of an isotropic body, and eq.(3) to the case of

a plane anisotropic body.

When the stress components equal and opposite signs to σ_x°, σ_y°, τ_{xy}°, τ_{xz}° and τ_{yz}° applied at infinity act on the contour of the opening defined by eq.(1), the complex constants A_p, $\bar{a}_p$, $\bar{b}_p$ and $\bar{C}_p$ take the values[3]

$$A_p = (\bar{a}_p + i\bar{b}_p) + h_{1,\nu-2}^{p} \sum_{\bar{j}=1}^{\nu-p-1} \bar{j}\, \bar{A}_{\bar{j}}\, \gamma_{\bar{j}+p+1}^{*}, \quad \gamma_p^{*} = \frac{1}{\alpha_0}\left\{(\alpha_p + i\beta_p) + h_{1,\nu-2}^{p} \sum_{\bar{j}=1}^{\nu-p-1} \bar{j}\,(\alpha_{\bar{j}} - i\beta_{\bar{j}})\,\gamma_{\bar{j}+p+1}^{*}\right\} \cdots (4)$$

$$\left.\begin{aligned}
\bar{a}_p &= -\frac{1}{2} h_{1,\nu}^{p}\left\{\delta_1^p \alpha_0 (\sigma_y^\circ - i\tau_{xy}^\circ) + \alpha_p(\sigma_y^\circ + i\tau_{xy}^\circ) - \beta_p(\tau_{xy}^\circ - i\sigma_y^\circ)\right\} \\
\bar{b}_p &= \frac{1}{2} h_{1,\nu}^{p}\left\{\delta_1^p \alpha_0 (\tau_{xy}^\circ - i\sigma_x^\circ) + \alpha_p(\tau_{xy}^\circ + i\sigma_x^\circ) - \beta_p(\sigma_x^\circ - i\tau_{xy}^\circ)\right\} \\
\bar{C}_p &= \frac{1}{2} h_{1,\nu}^{p}\left\{\delta_1^p \alpha_0 (\tau_{yz}^\circ - i\tau_{xz}^\circ) + \alpha_p(\tau_{yz}^\circ + i\tau_{xz}^\circ) - \beta_p(\tau_{xz}^\circ - i\tau_{yz}^\circ)\right\}
\end{aligned}\right\} \cdots\cdots (5)$$

In which the symbols δ_1^p and $h_{j,k}^{p}$ in eqs.(4) and (5) are defined respectively

$$\delta_{\bar{j}}^{p} = \begin{cases} 0 & \text{for } p \neq \bar{j} \\ 1 & \text{for } p = \bar{j} \end{cases} \qquad h_{\bar{j},k}^{p} = \begin{cases} 0 & \text{for } p < \bar{j},\ k < p \text{ or } \bar{j} > k \\ 1 & \text{for } \bar{j} \leqq p \leqq k \end{cases}$$

In our cases when the surface of the opening is not loaded and the stresses σ_x°, σ_y°, τ_{xy}°, τ_{xz}° and τ_{yz}° are applied at infinity, the components of resultant stresses σ_x, σ_y, τ_{xy}, τ_{xz} and τ_{yz} can be determined by the expressions:

$$\left.\begin{aligned}
&\sigma_x = \sigma_x^\circ + \sigma_x',\ \sigma_y = \sigma_y^\circ + \sigma_y',\ \tau_{xy} = \tau_{xy}^\circ + \tau_{xy}' \\
&\tau_{xz} = \tau_{xz}^\circ + \tau_{xz}',\ \tau_{yz} = \tau_{yz}^\circ + \tau_{yz}'
\end{aligned}\right\} \cdots (6)$$

where σ_x', σ_y', τ_{xy}', τ_{xz} and τ_{yz}' of the right-hand sides in above expressions are the stresses determined by the well-known equations[2,3] for the case when the stresses $-\sigma_x^\circ$, $-\sigma_y^\circ$, $-\tau_{xy}^\circ$, $-\tau_{xz}^\circ$ and $-\tau_{yz}^\circ$ act on the contour of the opening. The deformations u, v and w may be also obtained as the same manners.

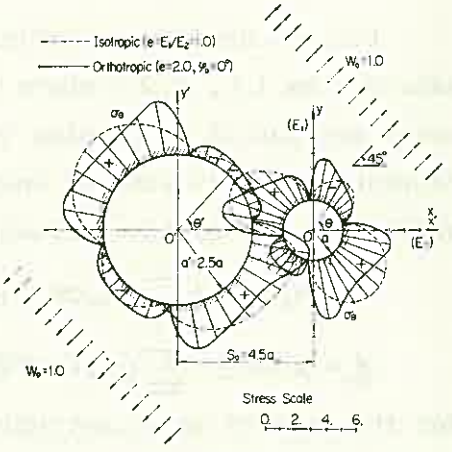

Fig. 2(a)

From stresses and deformations around or near the opening in an infinite isotropic or anisotropic elastic body obtained in above description, we can solve the problem of multi-connected region such as an infinite body with several holes utilizing the point matching technique. The method of analysis due to the point matching approach is repeating operations such that the boundary conditions with free surfaces of two or more openings are satisfied by the finite number of the boundary points of the openings.

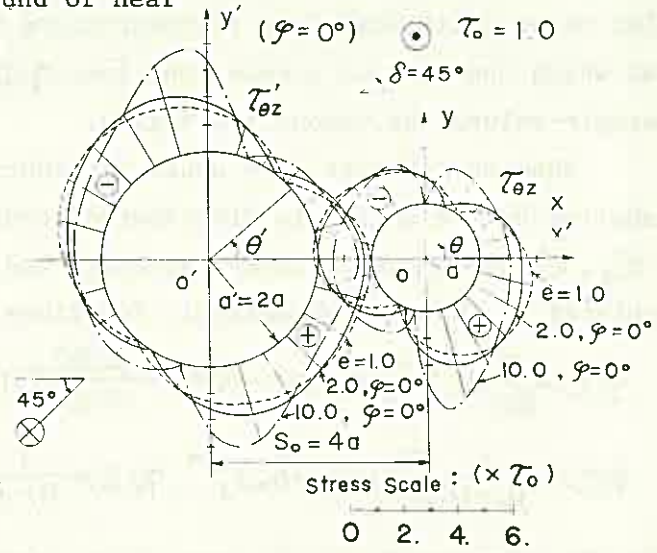

Fig. 2(b)

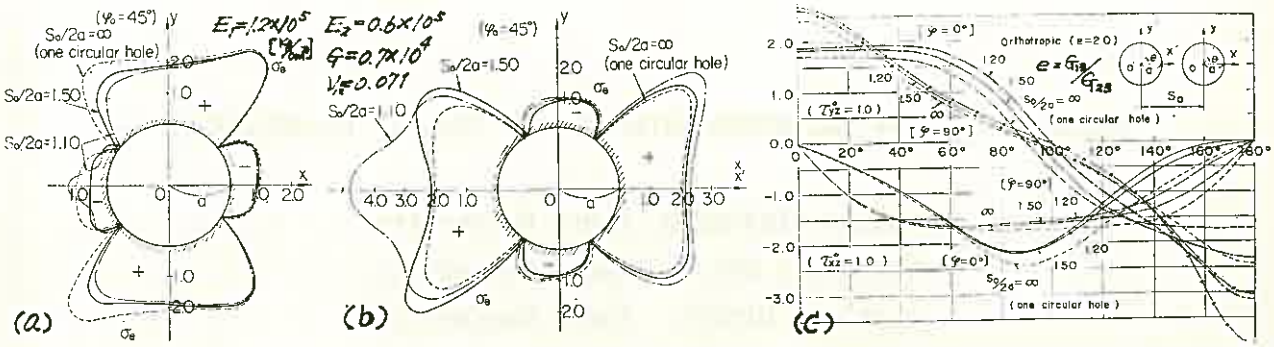

Fig. 3 φ: angle between the direction of E_1 (G_{13}) and the direction of the x-axis.

Obtaining stresses and deformations in the multi-connected body under consideration, the similar functions such as the ones defined by eqs.(2) and (3) were used in these operations. The literatures [1,2] are to be refered for further details relating to this problem.

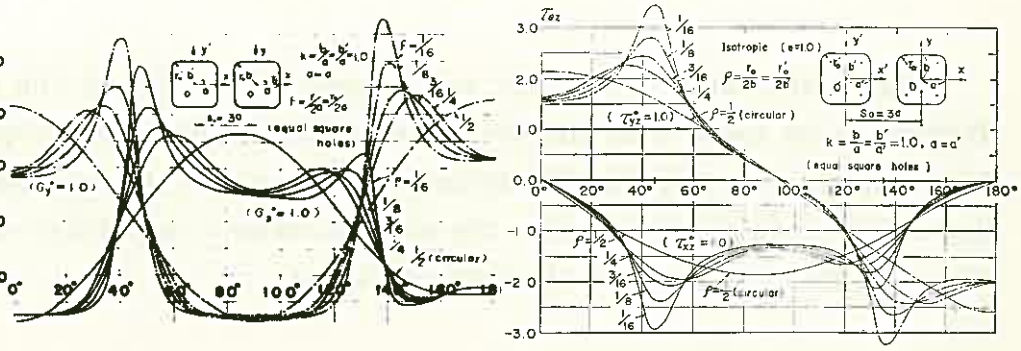

Fig. 4

Let us show some typical examples for the circumfential stresses and deformations at the contours of the openings subjected to uniformly distributed loads at infinity. Fig. 3 shows the stress distributions around the right-side opening Σ_1 (two equal circular holes) with parameters of $s_o/2a$ and the angle φ. Fig. 2 is the case for two unequal circular openings.

Figs. 4 and 5 are the cases for the two equal square openings in an isotropic body when the in-plane and out-of-plane loads apply at infinity.

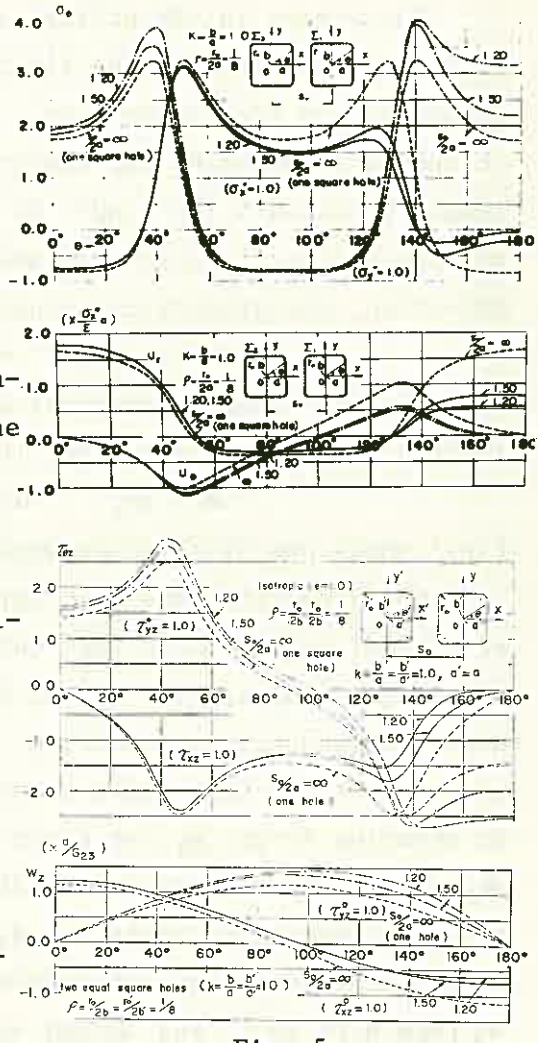

Fig. 5

REFERENCES:

1) Y. Niwa and K. Hirashima: Mem. Fac. Eng., Kyoto Univ., Vol.33(1971), pp.101-117

2) K. Hirashima: Proc. Japan Soc. Civil Eng., No.220 (1973), pp.131-141 (in English)

3) K. Hirashima: Proc. of the 22th Japan National Congress for Applied Mechanics,(1973), pp.211-220

DETERMINATION OF THE WIDTH RATIO OF RIB PILLARS TO OPENINGS

Yoshio HIRAMATSU, Kyoto University
Yukitoshi OKA, Kyoto University
Yoshiaki MIZUTA, Kyoto University

The width ratio of rib pillars to openings is one of the most important factors to be taken into consideration on designing large stopes. The authors have, therefore, investigated theoretically as well as experimentally how to determine it on the basis that the maximum stress in pillars should not exceed the allowable compressive strength of pillars.

Stress Analysis by the Theory of Elasticity

The stress in rib pillars standing side by side regularly in an elastic ground was analyzed by the finite element method on models of both two-dimension and three-dimension. Denote the widths of pillars and openings by t and a, the hight and number of pillars by h and n, and the horizontal length of pillars (openings) by b. In the two-dimensional analysis, where pillars and openings were assumed to be infinitely long in the horizontal-direction, the geometrical conditions of models were as follows:

$$n = 1 \sim 5 \text{ and } \infty, \qquad a/t = 1 \sim 3, \qquad h/t = 0.5 \sim 6,$$

while in the three-dimensional analysis, where pillars and openings had a limited horizontal extention, the geometrical conditions were as follows:

$$n = \infty, \qquad a/t = 2 \sim 5, \qquad h/t = 1.5 \sim 6.$$

Fig.1 shows one of three-dimensional models divided into gross elements.

We assume that the mean normal stress appearing in an optional pillar of a model subjected to vertical pressure, p_v, be given by $k_v k_b p_v (a+t)/t$, where k_v and k_b are the stress distribution factors for the pillar depending upon the geometrical condition, k_b being unity when $b = \infty$. Similarly we assume that the mean shear stress in an optional pillar of a model subjected to shearing force, p_s, be given by $k_s k_b' p_s (a+t)/t$ and $k_b' = 1$ when $b = \infty$, where k_s and k_b' are also the stress distribution factors for the pillar. From analysis the coefficients k_v, k_s, k_b and k_b' were determined. Within the geometrical conditions of models analyzed, k_v ranges from 0.51 to 1, whereas k_s from 0.03 to 1, and k_b and k_b' are as shown in Fig.2. It is seen that k_b' is approximately 0.5 k_b.

The maximum normal stress, σ_{max}, that appears at the upper and lower ends of a pillar in a model subjected to both p_v and p_s will be given, by a little calculation, by

$$\sigma_{max} = \alpha k_v k_b \frac{a+t}{t} p_v + 3\frac{h}{t} k_s k_b' \frac{a+t}{t} p_s$$

where α is the stress concentration factor.

Model Experiments

To investigate under what condition a pillar would collapse, model experiments were carried out. Firstly, models made of so-called Oginotuff, 20cm × 30cm × 2cm in size, as shown in Fig.3, were subjected to vertical loading with the results that fracture of pillars occurred when the mean normal stress reached the compressive strength of specimens with the same width-height ratio as the pillar. It follows that the stress concentration factor α may be regarded as approximately unity at the moment the pillar is fractured.

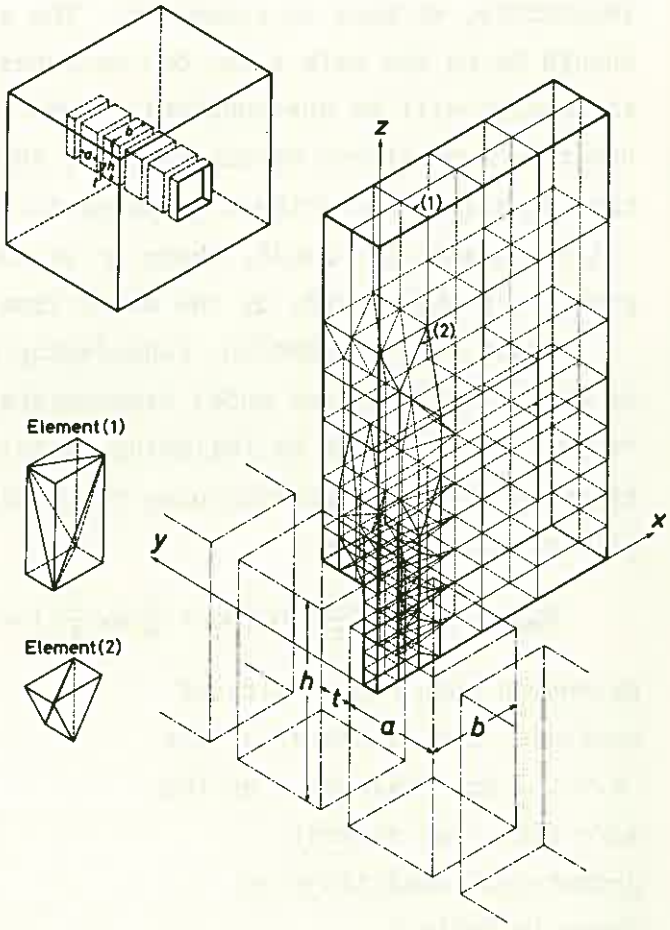

Fig.1

Secondly, shear tests of model pillars under axial compression were carried out. The models were made of marble, h/t being 2. Both shearing force and axial force were applied to models by a stiff loading apparatus elaborated by the authors as shown in Fig.4. A high normal stress appeared near the ends of each pillar by bending. From these tests it was found that the maximum normal stress at the ends of a pillar when compressive fracture took place was considerably lower than the theoretical value, say a half of it.

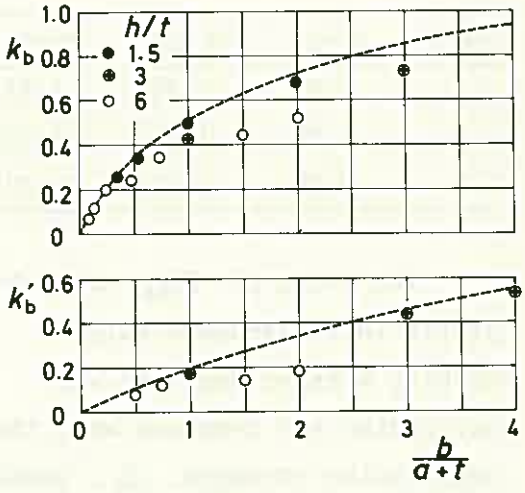

Fig.2

Designing Width Ratio

It is desirable, if possible, to determine the original stress state by measurement. But when it is impossible, we have to assume it. The assumption should be on the safe side, but an excessively safe assumption will be uneconomical. From long experience of stress measurement and theoretical consideration, the authors proposed to take $p_V = \gamma z_0$, $p_H = \gamma z_0$ and $p_S = \gamma z_0/3$, where γ is the specific gravity of the ground, z_0 the depth from the surface.

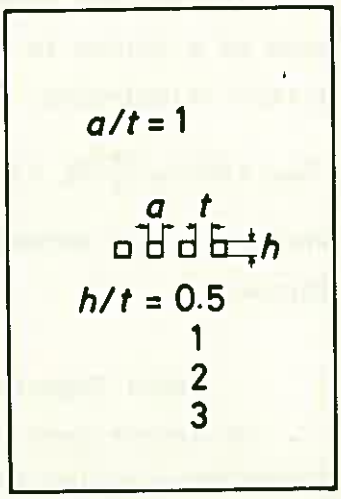

Fig.3

Under this assumption, considering the results of stress analysis and model experiments, the maximum stress, $\bar{\sigma}_{max}$, given by following equation may be taken as the basis on designing the width ratio of pillars and openings:

$$\bar{\sigma}_{max} = \gamma z_0 \frac{a+t}{t} k_b \left(k_v + \frac{1}{4} k_s \frac{h}{t} \right) = \gamma z_0 k_b K \frac{a+t}{t}$$

Depending upon the results of analysis, the values of K for $h/t \geqq 2$ are evaluated, on the safe side, for several geometrical conditions as shown in Table 1.

Table 1

a/t	n =1	n =3	n =5
1	1.07	1.14	1.41
2	1.00	1.19	1.36
3	0.98	1.11	1.27

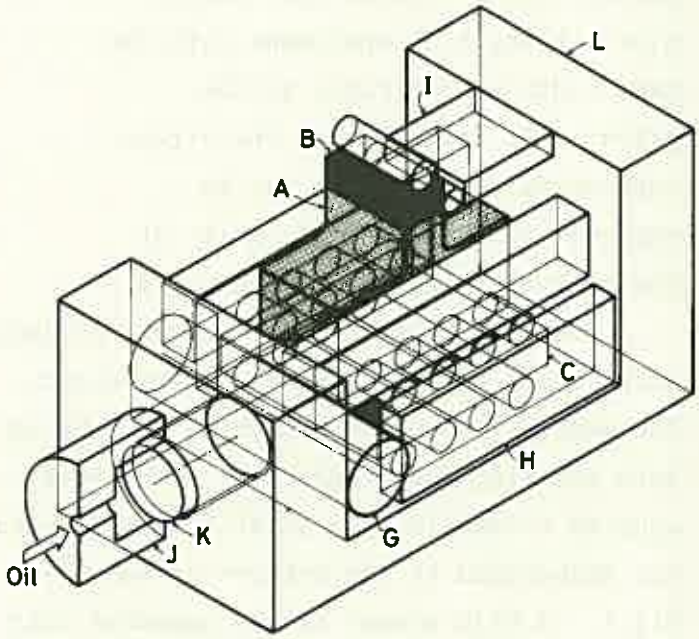

Fig.4

The value of $\bar{\sigma}_{max}$ of each pillar in 11 Japanese mines working massive deposits was calculated and compared with the compressive strength, S_c, tested on specimens taken from the pillar. Even if we estimated the strength of the pillars, S_p, at 50% of S_c, it was found that the safety factors, $S_p/\bar{\sigma}_{max}$, of sound pillars ranged from 3 to 15. Thus it is considerd that we can take the safety factor based on $\bar{\sigma}_{max}$ as small as 3 provided that the mined space is filled with waste when mining is finished.

SEVERAL OBSERVATIONS ON CAUSES AND PREVENTIVE MEASURES ABOUT ROCKBURST

Toshiro ISOBE, Hokkaido University

1. The state of the affair

May the 12th 1968, a violent rockburst broke out at the pit of Bibai colliery in Hokkaido, and 19 persons were killed and injured. This rockburst occurred in the coal seam called Noborikawa. In this pit face was laid 650-750m below the serface. A dip of it was about 40-50°, and it had a length of about 60m and had advanced about 300m from the start line of it. The workable thickness was about 1.7m. Its goaf was treated by full packing, and coal production was 700-750tons daily. The 4th level where the accident happened was drifted among the coal pillar whose width was about 50m. Therefore the both side of this gallery had 25m wide coal pillars respectively. All of the rock arround the seam had high strength as well as coal seam was hard. The state of rockburst is shown in Table 1. Each time a rockburst came about there was a small earthquake, and the epicenter was estimated in the vicinity of Bibai city.

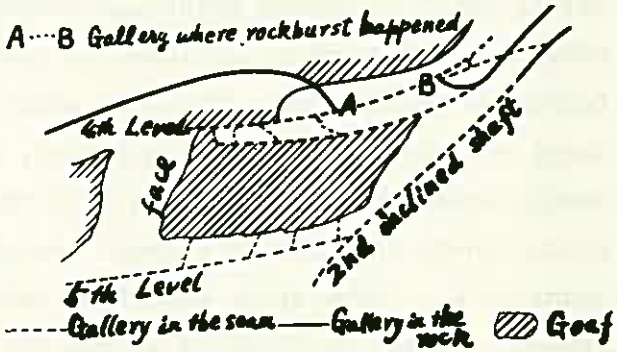

Fig.1. A skech of underground

Table 1. The state of affairs.

date (1968)	Depth from the surface (m)	Damages				Number of victims		2nd Damage
		floor upheaval (m³)	destructed coal (t)	gas emission max. (m³/min)	gas emission total (m³)	killed	injured	
2/27	650-660	740	555	75.6	9700	1	3	none
4/22	660-670	163	89	12.1	450	0	0	none
5/12	610-670	unknown	unknown	86.6	unknown	13	6	fire in the gallery

2. An interpretation about the occurrance mechanism of rockburst

Generally speaking, a rockburst will be occurred when a rock stores strain energy exceeding its storing capacity. This energy strikes rock body accompanied sudden rock destruction. An elastic energy content δA of δV-volume rock body, not being excavated, is expressed next equation.

$$\delta A = \left(\frac{1}{2E}\right)\left\{\left(\sigma_I^2 + \sigma_{II}^2 + \sigma_{III}^2\right) - \left(\frac{2}{m}\right)\left(\sigma_{II}\sigma_{III} + \sigma_{III}\sigma_I + \sigma_I\sigma_{II}\right)\right\} \quad \cdots\cdots (1)$$

where, $\sigma_I, \sigma_{II}, \sigma_{III}$: principal stresses, E , m : Young's modulus and Poisson's number.

Three principal stresses can be determined as follows.

$$\sigma_{III} = \gamma h \quad , \quad \sigma_I = \sigma_{II} = \frac{\gamma h}{m-1} \qquad \cdots\cdots\cdots (2)$$

When being made galleries and face's underground, the strain·energy will be transmitted without decreasing from the part where it is caved to a boundary rock. The reason will be recognized by following simulation. At Fig.2 there are many n-pieces of spring are supporting a weight W. Here, assuming each spring has a same physical property, supported load by each spring is W/n. Then elastic energy of each spring is calculated as $(k/2)(W/n)^2$, (k = const.). So total energy content of this system is expressed $A_0 = (k/2)(W^2/n)$. Next, if eliminating m-pieces of spring from the system, there remains (m-n)-pieces of it yet. Then total energy content must be varied $A_1 = (k/2)(W^2/(n-m))$. Therefore $\Delta A = A_1 - A_0$ can be considered as an increasing quantity of energy by eliminating m-pieces of spring. So

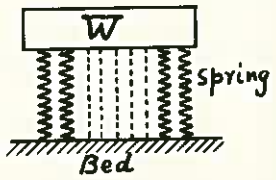

Fig. 2. Simulation

$$\Delta A = (kW^2/2)\left(\frac{1}{n-m} - \frac{1}{n}\right) = \left(kW^2/2\right)\frac{m}{n(n-m)} \fallingdotseq (k/2)\left(\frac{W}{n}\right)^2 \times m$$

can be obtained by assuming $n \gg m$. From the result, it may be understood ΔA is nearly equal to energy which was contained in m-pieces of spring before eliminating ones. Streching the idea, it could be obtained following explanation. Fig.3(1) shows comparatively large rock body, not being excavated, contains strain energy $A_0 + A_1$. And Fig.3(2) shows disturbed state, where the cave is formed, contains its energy quantity A_2. From above described calculations, $A_2 - A_1 = \Delta A = A_0$ is to be assumed. Here, observation should get into the subject. When a rockburst occurs, there is a small earthquake simultaneously. To compare the intensity of seismic motion, it must be taken up "Magnitude". From magnitude M, it is able to get approximate energy of earthquake A_e by Gutenberg-Richer's formula.

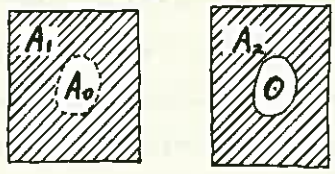

(1) (2)
Fig.3. Energy quantity

$$\log_{10} A_e = 1.5M + 11.8 \qquad \cdots\cdots (4)$$

Here, the author asserts

$$A_e = A_0 \qquad \cdots\cdots\cdots (5)$$

3. Certifications by several calculated conclusions

(a) Estimation of Young's modulus of coal seam

From eq. (1) and (2) V-volume of rock body's strain energy will be obtained as

$$A = \left[\{(m+1)(m-2)\}/\{2Em(m-1)\}\right]\gamma^2 h^2 V \qquad \cdots (6)$$

Taking E and m as coal seam's ones, h as the depth from the surface and γ as a mean specific weight of rock, these values can be settled in this case. i.e. $m = 5$, $h = 650\text{m} = 6.5 \times 10^4\text{cm}$, $\gamma = 2.6\text{g/cm}^3$, $V = L \cdot H \cdot S = (6 \times 10^3\text{cm})(1.7 \times 10^2\text{cm})(3 \times 10^4\text{cm}) = 3.56 \times 10^{10}\text{cm}^3$. Here, L, H, and S are face length, coal seam thickness, and advanced distance from the start line of the face, respectively. Thus $A_0 = 4.38 \times 10^{26}/E_c$ (ergs), (E_c = Young's modulus of coal) will be obtained. On the

other hand, each magnitude relating to each rockburst was calculated as 2.2, 1.9 and 2.7 respectively. Then total energy A_e is 8.56×10^{15} ergs.

Therefore E_c is estimated as 1.15×10^{10} dyne/cm^2 = 5.24×10^4 kg/cm^2. This E_c is approximately coincides with the value of $5 \sim 6 \times 10^4$ kg/cm^2 measured by Prof. Hiramatsu.

(b) comparison with floor upheaval, destructied coal volume and gas emission

Putting each A_e^i as an energy of i-th rockburst, they are $A_e^1 = 1.26 \times 10^{15}$ ergs, $A_e^2 = 0.22 \times 10^{15}$ ergs and $A_e^3 = 7.08 \times 10^{15}$ ergs.

In the case of 1st and 2nd rockburst $A_e^1 / A_e^2 = 1.26/0.22 = 5.7$

The floor upheaval, destructive coal volume of each side of gallery and gas emission volume are guessed from Table 1. So next ratios are got.

upheaval : 740/163 = 4.5, destructed coal : 550/89 = 6.3, gas : 75.6/12.1 = 6.3

Considering each value, it is able to be supposed that these values are proportional to energy quantity.

(4) Estimation on breaking stress from A_e^1

From Table 1. in the case of 1st rockburst, destructed coal volume and floor upheaval are 5.6×10^8 g and 740m^3 respectively. The floor upheaval is also consist of coal. Then total volume including upheaval and destruction is 11.4×10^8 cm^3, where $\gamma_c = 1.4$ g/cm^3. And as A_e^1 is 1.26×10^{15} ergs = 1.29×10^9 kgcm, energy consumption per 1cm^3 is

$$A_e^1 / (\text{Total destructed coal volume}) = (1.29 \times 10^9)/(11.4 \times 10^8) = 1.13 \ \text{kgcm/cm}^3$$

By using Mohr's circle and experimental research on coal seam strength, following formula is concluded. Where σ_1 and σ_2 are principal compressive stresses.

$$\sigma_1 = 1.88\,\sigma_2 + 220 \ (\text{Kg/cm}^2), \ (\sigma_3 : \text{neglected}) \quad \cdots\cdots (7)$$

Putting δA as energy consumption per 1cm^3 and using fomulae (1), (7) and $\delta A = 1.13$ kgcm/cm^3, σ_1 and σ_2 are obtained as follows.

$$\delta A = 0.13 \times 10^{-4}\sigma_1^2 - 8.65 \times 10^{-4}\sigma_1 + 0.15, \quad \sigma_1 = 275 \ \text{Kg/cm}^2, \quad \sigma_2 = 30 \ \text{Kg/cm}^2$$

These stresses measured by Prof. Hiramatsu are reported as $\sigma_1 = 350$ kg/cm^2 and $\sigma_2 = 40$ kg/cm^2. Then the values calculated here are not so different.

4. Some preventive Measures

Conclusions and preventive measures are itemized as follows.

(1) A rockburst will happen when strain energy quantity exceeds boundary rock storing capacity.

(2) The boundary rock must not be a storage of strain energy. Therefore such a storage should be pushed into rock body as far as possible.

(3) The galleries in the coal seam are sometimes dangerous for rockburst, because coal seam stores a great deal of energy owing to its small Young's modulus.

(4) To decrease the capacity of energy content, relief boring will be effective.

(5) To prevent stress concentration in the neibourhood of a goaf, it is better to build strong packs or to practice a caving method.

D. DRILLING, BLASTING AND FRAGMENTATION OF ROCK

BLASTING RESEARCHES

Kunihisa KATSUYAMA, Kyoto University
Koichi SASSA, Kyoto University
Ichiro ITO, Kyoto University

1. Blasting in a infinite material

It is well known that when an explosive detonates in a material, the radial cracks are produced around an explosion by the hoop stress in the spherical stress wave. But, there are many unknown points which must be clarified in the growth mechanism and the properties of these radial cracks. In this study, the behaviour of the crack propagation has been discussed through the microscopic observation of the surface of the crack produced in a polymethyl methacrylate plate by a detonator's attack.

The polymethyl methacrylate plate used in this experiment is 1.8 cm x 30 cm x 30 cm. The propagation velocity of the longitudinal wave is about 3000 m/s, Poisson's ratio is 0.4 and specific gravity is 1.2. When a No. 1 detonator is detonated in a borehole of which diameter is 0.7 cm, the stress wave of which wave length is about 15 cm is projected into the plate and produces the radial cracks of which lengths are about 3 cm.

The main results obtained are as follows:

1) The radial crack caused by an explosion does not grow continuously from the surface of the charge hole, that is, the intense stress wave which is projected into the material by an explosion creates at first many nuclei of the crack, and then the cracks which develop from the respective nucleus interlink with each other and finally produce a long continuous radial crack.

2) The relation between the number of the nucleus per unit area (N) and the distance from the inner surface of the borehole (r) changes with blasting condition. In the case that the decoupling coefficient is 2.0, N decreases gradually with the increase of r, and the values of N at the inner surface of the borehole and the point at r=1.0 cm are about 5×10^3 pieces/cm^2 and 2.5×10^3 pieces/cm^2 respectively. But when the decoupling coefficient is 1.1, the largest value of N which is about 2.5×10^3 pieces

/cm^2 appears at r=1.0 cm other than at the surface of the borehole. It may be considered that one of the reason why this phenomenon appeared is the increase of the ductility of the material caused by the temperature rise in the material due to the adiabatic compression accompanied with the propagation of an intense stress wave.

2. Formation of crack and crater caused by a blasting with one free face

The dynamic stresses in a material caused by a blasting with one free face have been analyzed with the aid of a numerical technique which involves the finite-difference approximation to the momentum equations, and then, the processes of the development of the cracks and crater formation caused by the blasting have been simulated.

At first, experimental studies have been conducted by using a polymethyl methacrylate plate. The diameter of a borehole drilled in the plate is 0.7 cm, and the length of the burden (W) is 2 cm. A No. 1 detonator has been utilized to break the specimen.

The size of the model for the numerical simulation of this experiment is 40 cm x 25 cm. The size of a square element is 0.42 cm x 0.42 cm, and the number of element is about 6000.

The main results obtained are as follows:

1) The maximum values of the tensile stress at the points near the free face (about 0.2 cm from the free face) and near the line of least resistance increase about twice as large as those in the case where there is no free face.

2) The results of the numerical simulation of crack and crater formation agree fairly well with those of the experimental studies. The process of the crater formation deduced from the simulation is as follows. At first, a crack is produced along the line of least resistance, and then, a few of the radial cracks reach to the free face in the range of $x < W$, and lastly the crack perpendicular to the direction of the line of least resistance is produced, where x is the distance from the line of least resistance.

3. Smooth blasting

The dynamic stresses in a material caused by a smooth blast-

ing have been analyzed and then the process of the development of the cracks has been discussed. The size of the model for the numerical analysis is similar to that used for the analysis of the blasting with one free face. Two empty holes are located both sides of a charge hole to simulate the drilling pattern of the smooth blasting.

The main results obtained are as follows:

1) In order to get a good smooth wall by the blasting, the spacing (L)/burden (W) ratio must be kept less than 1.6, and also the explosives in each hole must be initiated simultaneously.

2) When the value of L is 1.6W, the maximum value of the tensile stress at the surface of the empty hole is 1.83 times larger than that of the tensile stress at the other point having same distance from the explosion.

3) Because of the stress concentration at the two points on the adjacent empty hole which are closest to and farthest from the explosion, the separate cracks are initiated at these two points and develop along the projected plane of breakage before the radial cracks from the explosion reach to the empty hole.

4. Effect of the pre-split on the blasting adjacent to it

The dynamic stresses in a material caused by a blasting adjacent to the pre-split have been analyzed. And then, its effects on both the vibration and the breakage caused by a main blasting which is done adjacent to the pre-split have been discussed quantitatively.

The main results obtained are as follows:

1) The pre-split has a greater effect on the control of the cracks caused by the main blasting even if it has a smaller effect on the reduction of the vibration.

2) Existence of many discontinuities makes the greater change in the wave form of the stress wave which propagates through the discontinuities.

THE FRACTURE PHENOMENA OF ROCK IN CUTTING

Iwao NAKAJIMA And Shigenori KINOSHITA
Department of Resources Development Engineering
Hokkaido University

1. Introduction

In the present study, we made microscopic observations on chip formations in rock near and beyond the point of cutting.

The bit was stopped cutting and taken off the cutting plane carefully, then the cutting plane was cemented over the wide range by Canada Balsam. This agglutinated rock sample was sliced to thin slab in parallel with cutting direction and polished to make a thin section for a microscopic observation. The thin section was successful for us to observe the mode of rock fracture occuring in a vertical section of the cutting plane.

Main results of observations for samples of marble, tuff and sandstone are described in the preceeding sections with some disscussions about the fracture mechanism of rock in cutting.

2. Method of cutting

In this study, rock cutting was performed by a wheel cutter using an apparatus as shown in Fig. 1. A thin rectangular parallelepiped rock specimen settled in a holder is fixed on the octagonal ring dynamometer and the unit is placed on the table of milling machine.

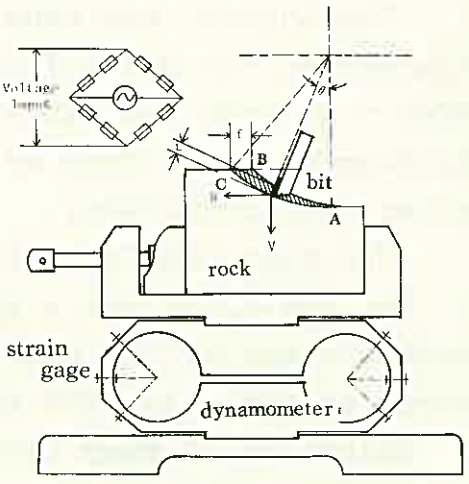

Fig. 1, cutting apparatus.

Prior to the actual test, the specimen is cut to make arciform cutting face like AB in the figure, then the specimen is moved forward horizontally by a small distance (f) so that the bit can scrape the rock along the line AC. The depth of cut (t) is defined as the thickness of triangle ABC measured in the radial direction of the wheel at the point of cut. Therefore it can be estimated by the equation $t = f \sin\theta$ where θ is the rotating angle of bit from the horizontal.

3. Photographic observations on cutting actions of a bit

Twelve photographs are presented here in order to illustrate the characteristic modes of rock fracture in cutting. The first four photographs are the

examples of photographic view of chip formation and others are the photographs obtained by microscopic observations on the fracture plane of cutting.

By reference to the photographs the following concepts were obtained with regard to rock fracturing in cutting.

(1) There should be the two different forms of failure as Goodrich has already postulated. The first is a crushing phase in which the bit reduces the rock to a fine powder and dust. The second is the cutting phase in which the large chips are fractured from the rock.

(2) The first phase occurs in a very small range of cutting depth within about 150μ. The photographic views of the chip formation in this phase are shown in photo.1 and photo.2. It can be seen that the chips are produced continuously in the vicinity of the cutting point, being discharged in curled form into the air. The boundary between the crushing zone and the unbroken rock is observed to be inclined at an angle of about 45 to 50 degrees to the cutting direction.

(3) If the cutting depth is increased beyond the critical value of the first stage, the second phase of fracture will take place succeeding to the first process, At this stage rock would break along a fracture plane at an angle of 25 to 30 degrees to the direction of travel. Since the two processes occur alternately the chip formation becoms discontinuous as seen in photo.3 and 4 at a larger cutting depth.

(4) In the present paper the fracture of the crushing zone in the first phase is called the faulting because it is a shear fracture due to high confining pressure in the crushing zone, and the fracture in the second phase is called the extension fracture because it seems to occur owing to crack propagation.

(5) Photo.5 shows the aspect of the chip formation in the first phase when the cutting depth is very small. It is noticed that the large crystalline particles of the rock are crushed into small pieces by faulting of the compressed zone. This faulting plane could be revealed obviously by photo.6, which was observed on the fracture plane after the cuttings have been removed from the cutting plane.

Photo.7 represents the state of crack formations in the neighborhood of the cutting point at the end of the first stage and how the cracks propagate and develop to the extension fracture are shown in photo. 8.

(6) A model as illustrated in Fig.2(a) may be derived from the photographs mentioned above, with regard to the cutting action of a bit. The model is the same as that of Goodrich. The model characterizes the fracture mechanism as that the two processes, faulting and extension fracture, occur alternatively and that the volume of the faulting zone is approximately equal to the volume of the extension fracture zone. However the model seems to be valid in relatively small cutting depth.

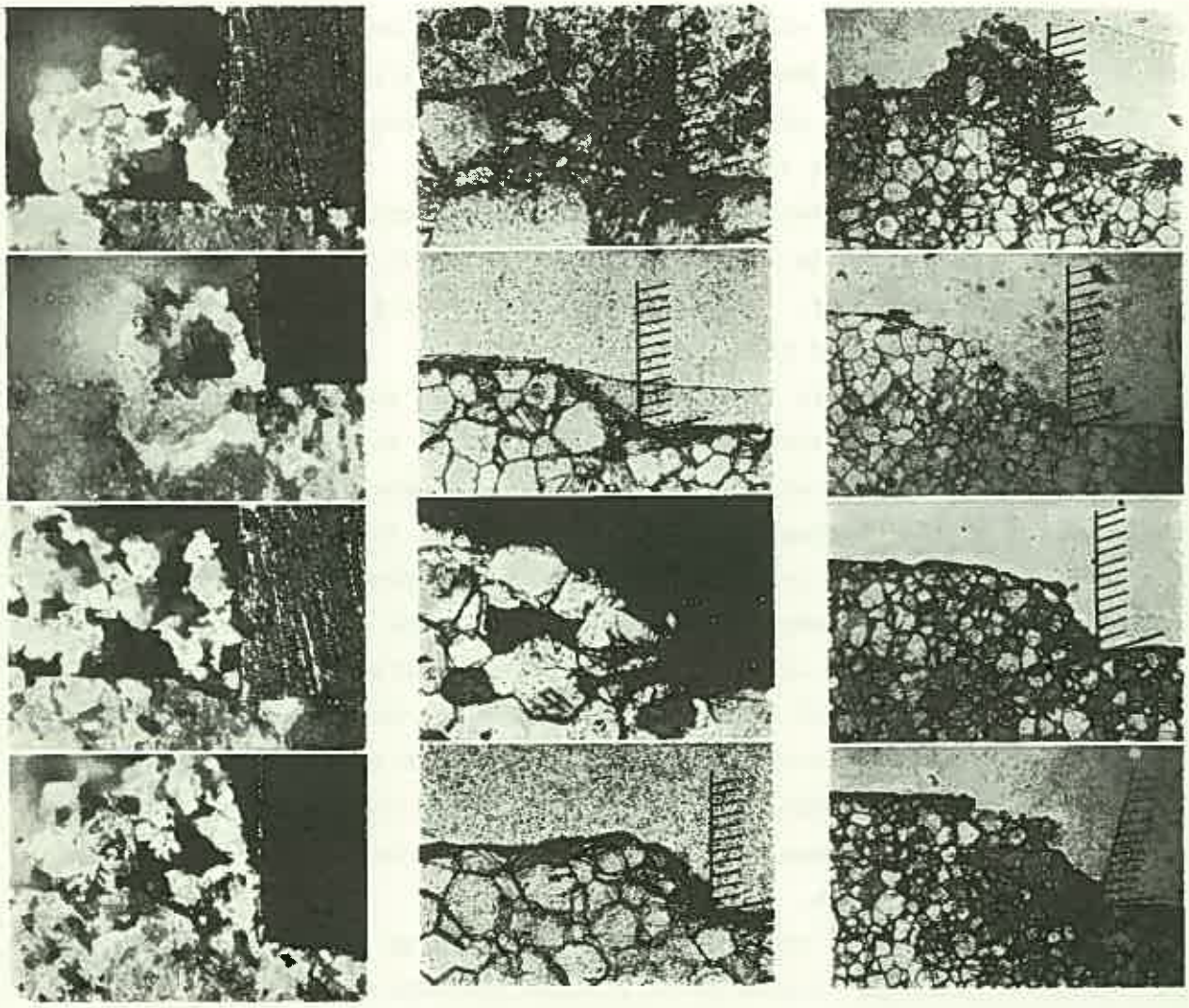

IZU Sandstone
photo. 1 t=30
photo. 2 t=100
photo. 3 t=200
photo. 4 t=500
t = cutting depth

AKIYOSHI Marble
photo. 5 t=50, x=240
photo. 6 t=100, x=80
photo. 7 t=200, x=120
photo. 8 t=100, x=80
t = cutting depth
x = magnification

AKIYOSHI Marble
photo. 9 t=400, x=24
photo.10 t=650, x=24
photo.11 t=500, x=24
photo.12 t=650, x=24
t = cutting depth
x = magnification

(7) When the cutting depth becomes larger than the depth a model like Fig.2(b) should be assumed.

The failure mechanism in this model is not essentially different from the model of Fig.2(a) except that the faulting zone reduces in relation to the increasing of the cutting depth. The evidence of the assumption is found in a series of photographs from photo.9 to 12.

The rock failure by faulting can be observed in photo.9 and the fracture plane thus produced is revealed clearly in photo.10. The extension fracture plane taken place in succession will be seen in photo. 11.

The two fracture planes are recognized more distinctly in photo.12 which is for the case where the rock is cut by a bit with a rake angle of 20 degrees. In the photograph, BD and CB represents the previous extension fracture plane and a newly developed extension fracture plane respectively. The faulting

plane is represented by CD. It is easily known that the faulting plane is taking place across the extension fracture plane.

(8) It was difficult to get clear microscopic observations on the fracture plane for sandstone and tuff because of difficulties of making thin sections. However, it was supposed that similar processes would occur in the cases of those rocks.

4. Conclusions

As the result of microscopic observations on the fracture planes of AKIYOSHI Marble, where it is cut by a bit with a varied cutting depth, it was ascertained that there were two processes in rock failure. The first process is a shear fracture caused directly in the crushing zone by the penetration of the bit. The second process is an extension fracture due to the propagation of the cracks which are brought about by the development of the crushing zone of high confining pressure. It was also demonstrated that the first process occurs alone with a small cutting depth and that when the cutting depth becomes larger the two processes occur alternately. The fracture plane is inclined at the constant angle of 45 to 50 degrees in the first process and at the constant angle of 20 to 25 degrees in the second process to the direction of travel for all kinds of rocks tested in this study.

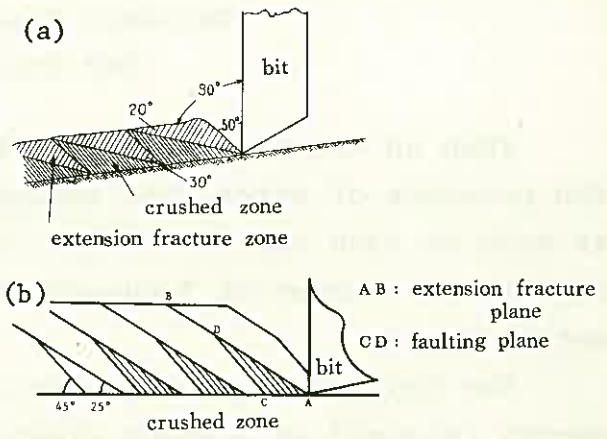

Fig.2, chip formation in rock cutting

Acknowledgements

The authors wish to express their thanks to Instructor J. Sato, Faculty Engineering, Hokkaido University for his advice in taking microscopic photograph and also to Mr. M. Watanabe for his assistance in making the thin sections.

References

(1) R.H.Goodrich : High Pressure Rotary Drilling, Bullutin of Missouri School of Mine and Metallurgy, 1957, No.94, pp. 25

(2) I.F.Jackson and H.L.Hartman : An Investigation of Hard-Metal Inserts for Cutting Slate, A I M E Transactions, 1962, Vol.223, p. 255

SOME EXPERIMENTS OF ROCK FRACTURING BY ELECTRIC SPARK DISCHARGE

Akira TAKATA & Yosihiro OGATA,
National Research Institute
for Pollution and Resources

When an electric spark discharge of large power occurs under the presence of water, the energy level of this stress wave reaches as high as rock can be broken. This idea was born during the study of seismic sources of "geo-sonar" and electrohydraulic forming of metal sheets.

The testing apparatus uses a burst of high voltage electric charge released at a spark electrode in water. The electrode has a coaxial section, and the both poles are connected at the tip by a fine copper wire (Fig. 1). A shock wave is generated by vaporization of the fine wire and surrounding water.

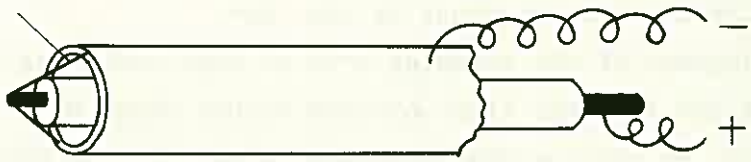

Fig. 1 Spark electrode

In this test, the voltage was kept under 500V to examine the details of electric current in the whole system. Its performance changes at random by fine changes of circumference condition. Only a little part of 1200joules, which can be charged in the capacitor seems to be consumed at the spark electrode.

Plate specimens of some kinds of rocks and cement mortar, 6 to 10cm thick, were broken by this method. The electrode were inserted into 6mm dia. boreholes, 2 to 5cm away from side wall. Water is poured in just before the electric discharge.

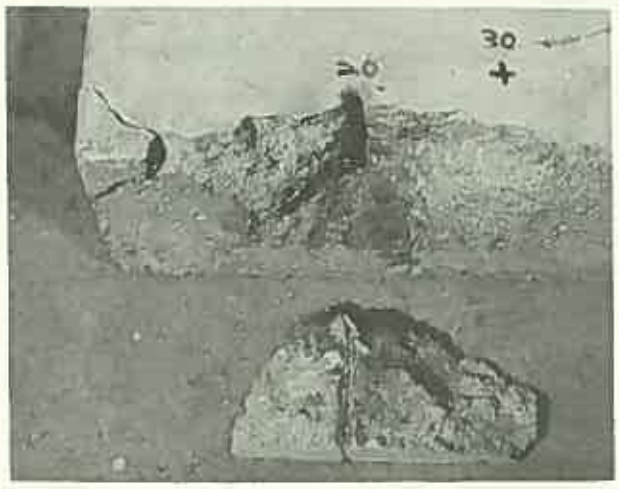

Fig. 2(a) A shape of crater (1)

Tensile cracks formed

Fig.2(b) A shape of crater(2)

Fig.3(a) Effect of another hole

Fig.3(b) Effect of another plane

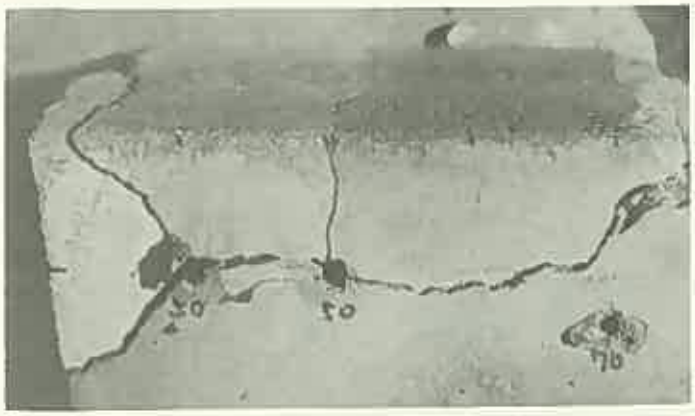

Fig.4 Simultaneous explosion of plural holes

wide-spread craters toward a free face of side wall(Fig.2). Growths of cracks were liable to be affected by another free faces or hollow holes, as shown in smooth blasting(Fig.3). Simultaneous explosion of several holes caused well-controlled breakage line through each holes(Fig.4).

Peak pressures of shock wave in water reached 1.3 to 1.5kg/cm^2 at the point of 13m from the electrode(Fig.5). This means that the pulse pressure reaches more than 20kg/cm^2 in the neighborhood of electrode. Bubble sphere (about 20cm dia.) could be observed, when the spark occurred near the water surface(Fig.6).

If the charging voltage is raised more than 10kV, as we are planning, the electrode will not need fine wire connection, and repeating discharges will show effective breaking power, especially in sea water.

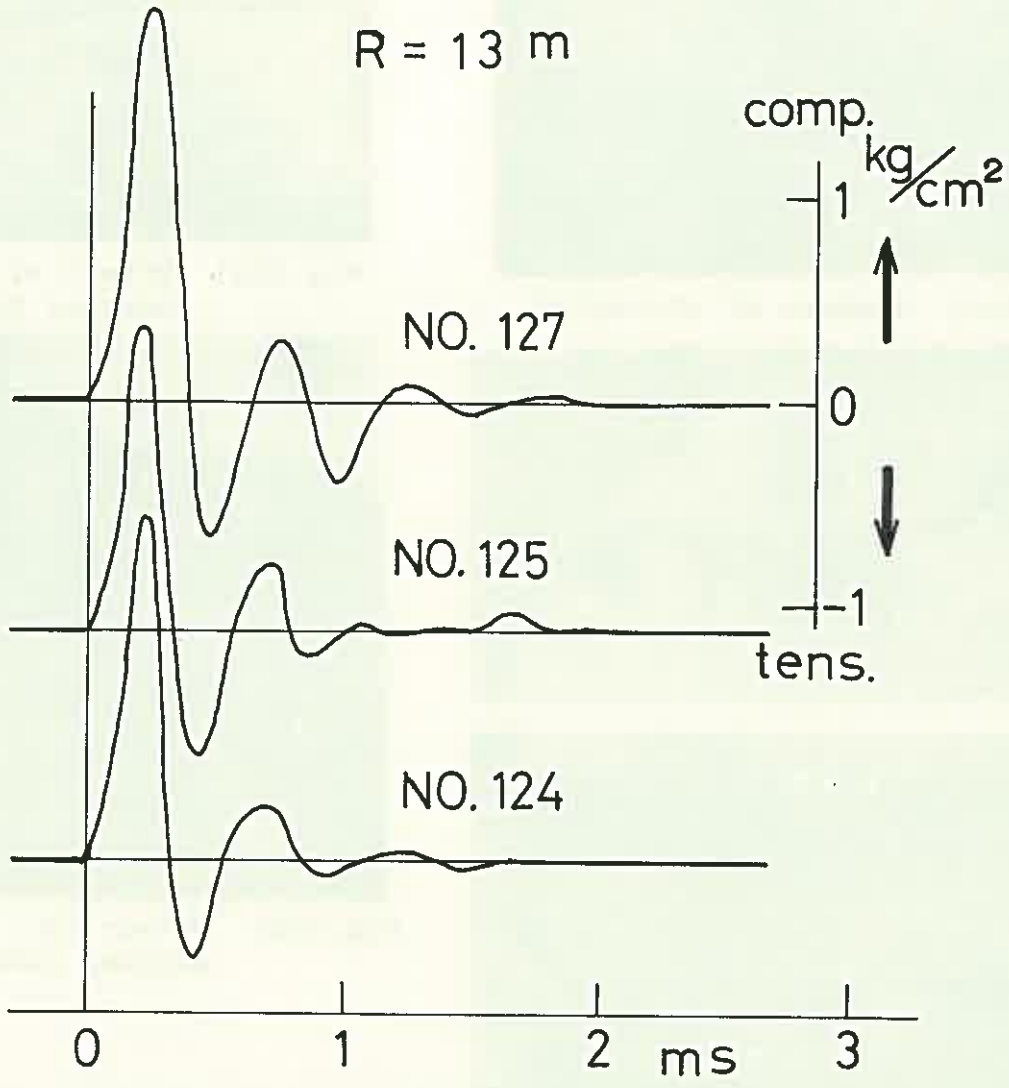

Fig.5 Pressure wave measured in water

Fig.6 Bubble spheres formed near water-surface

THE FRACTURE RESISTANCE OF ROCK DURING PERCUSSIVE DRILLING

Hirohide HAYAMIZU, National Research Institute for Pollution and Resources
Shigeo MISAWA, "
Saburo TAKAOKA, "

Drilling rate for percussive drilling has been studied so far and especially the emphasis was placed on the relationships between the drilling rate and mechanical properties of rock. But these relationships have not been clarified enough.

The following experiment was carried out as the first step to clarify the relationships. The resistance of rock during fracturing by percussive drilling was discussed here.

It is obvious that the fracture of rock by percussive drilling was caused by the strain wave through the drilling rod. Assuming that the behavior of the drilling rod is expressed by one dimensional equation of motion, the strain ε which is generated at a cross section of the drilling rod is given by

$$\varepsilon(x,t) = \varepsilon_1(t-\frac{x}{a}) + \varepsilon_2(t+\frac{x}{a}) \qquad (1)$$

where x is the coordinate along the axis of rod, t is the time and a is the propagation velocity of the strain wave. $\varepsilon_1(t-x/a)$ is the strain wave which propagates through rod from shank end to bit end and $\varepsilon_2(t+x/a)$ is the strain wave which propagates in the opposite direction to that of ε_1.

If the strain wave ε_1 and ε_2 can be separated each other from the results of the measured strain ε , the external force applied to the bit end, the fracture resistance of rock, can be determined by the strain wave ε_1 and ε_2.

Fig.1 shows the one example of the strain which is measured at the middle point of the rod during the fracture of rock. As is clear from this figure, ε_1 and ε_2 were separated each other because ε_1 falls in the range of L/2a to 3L/2a and ε_2 falls between 3L/2a and 5L/2a. L is the length of the drilling rod.

The fracture resistance of rock derived from the measured values are shown by solid lines in Fig.2. In this figure, ordinate is the dimensionless fracture resistance F/(EAv$_c$ /a), where F is

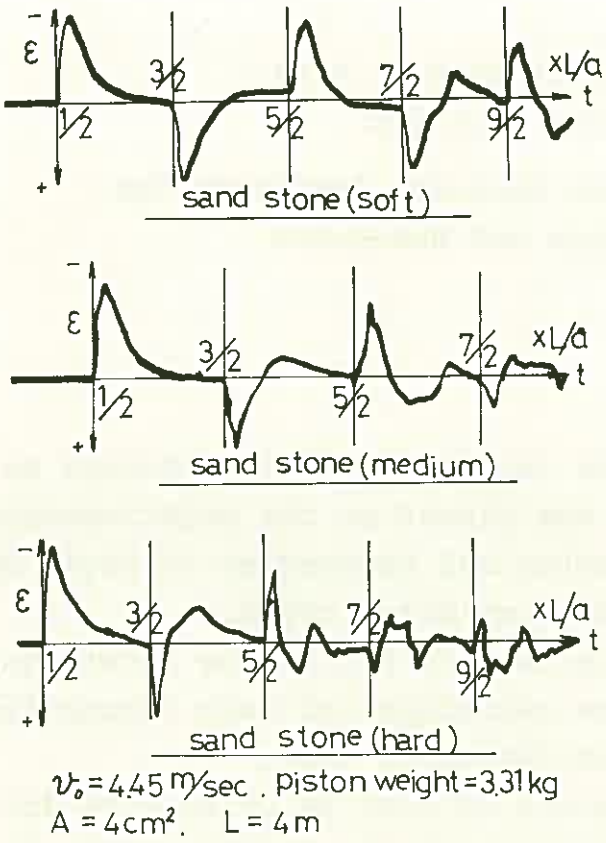

Fig.1 Typical strain wave

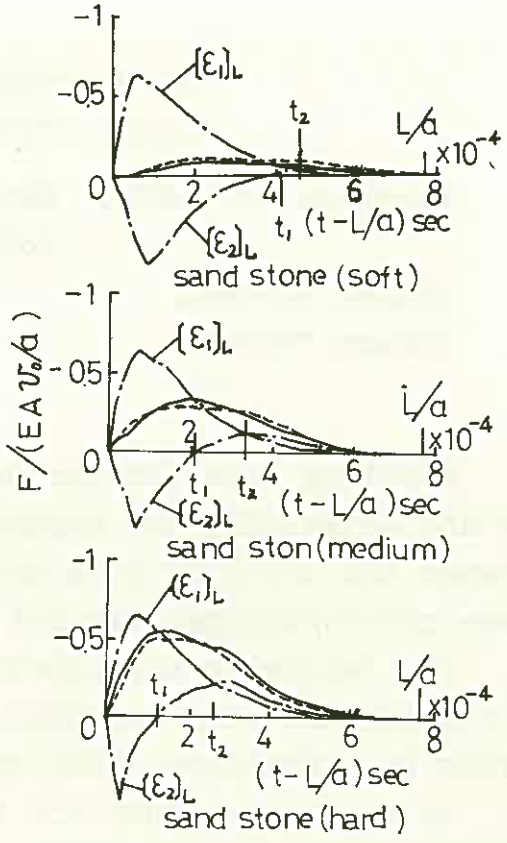

Fig.2 Fracture resistance

the fracture resistance, A is cross-sectional area of rod, E is Young's modulus of rod and v_c is the percussion velocity of the piston of drill.

Following equation is assumed to relate the fracture resistance with the mechanical properties of rock.

$$F = Ru + \eta\, \partial u/\partial t \qquad (2)$$

where u and $\partial u/\partial t$ are the penetration depth and penetration rate respectively, R is the hardness of rock and η is mechanical impedance of rock. Mechanical properties above mentioned are related to the shape and gage of bit.

The strain wave ε, shown in Fig.1 is theoretically approximated with following equation.

$$\varepsilon_1 = -\frac{v_c}{a}\left[\exp\left\{-\lambda_1\left(t-\frac{x}{a}\right)\right\} - \exp\left\{-\lambda_2\left(t-\frac{x}{a}\right)\right\}\right] H\left(t-\frac{x}{a}\right) \qquad (3)$$

where H is unit step function and λ_1 and λ_2 are constants.

Fracture resistance F is derived theoretically as the function of the time from equation (2) and (3).

$$F = -2EA\frac{v_0}{a}\left[\frac{\eta'-R'/\lambda_1}{1-R'/\lambda_1}\left\{\exp\left(-\lambda_1\left(t-\frac{L}{a}\right)\right) - \exp\left(-R'\left(t-\frac{L}{a}\right)\right)\right\}\right.$$
$$\left. - \frac{\eta'-R'/\lambda_2}{1-R'/\lambda_2}\left\{\exp\left(-\lambda_2\left(t-\frac{L}{a}\right)\right) - \exp\left(-R'\left(t-\frac{L}{a}\right)\right)\right\}\right] H\left(t-\frac{L}{a}\right) \qquad (4)$$

where

$$R' = \frac{R}{\left(\frac{EA}{a} + \eta\right)}$$

$$\eta' = \frac{\eta}{\left(\frac{EA}{a} + \eta\right)} \qquad (5)$$

The dotted lines are the dimensionless fracture resistance derived from equation (4). Fig.2 tells us that the theoretical results agree well with experimental values and as a result the fracture resistance can be defined by equation (2).

The experimental results which are derived from the rock fracturing in a certain condition is necessary to determine the hardness and mechanical impedance of rock. By drawing a figure in the same way as that of Fig.2, t_1 , the time when the strain wave ε_2 changes from tensile wave to compressed wave, and t_2 , the time when the strain wave ε_1 and ε_2 coincide each other, can be determined.

Fig.3 shows the theoretically derived relationship between t_2 and R' and Fig.4 shows that of between t_1 and η' . Therefore, R' and η' are determined by t_1 and t_2 which are experimentally obtained and then R and η are determined by equation (5).

In conclusion, if the shape and size of bit does not vary, the fracture resistance of rock in any values of v_0 , A, λ_1 , λ_2 , etc. can be derived from the equation (4) using the values R and η obtained above. And the penetration depth of bit into rock u_m can be approximately given by following equation.

$$u_m = 2\frac{EA}{aR} v_0 \left[\exp(-\lambda_1 t_2) - \exp(-\lambda_2 t_2)\right] \qquad (6)$$

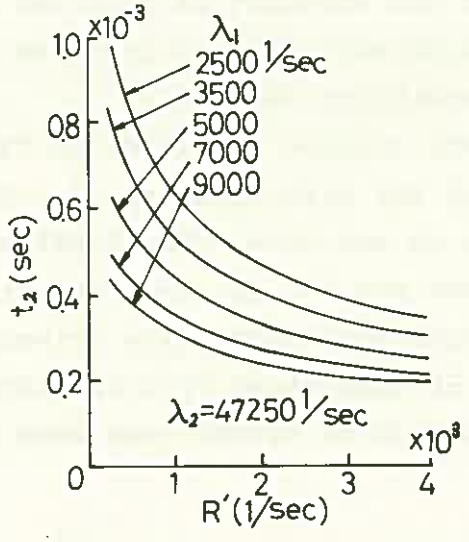

Fig.3

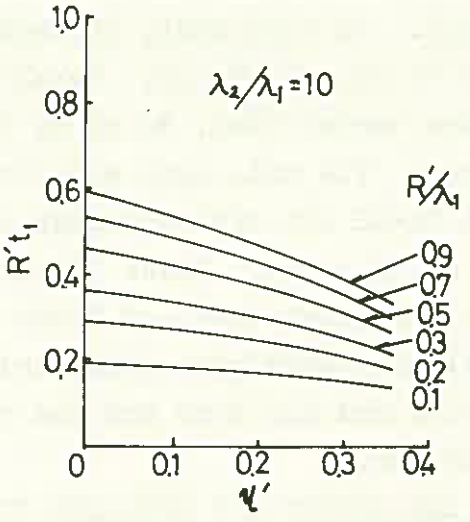

Fig.4

EXPERIMENTAL STUDY ON RELATIONSHIP BETWEEN ENGINEERING PROPERTIES OF ROCK AND MECHANICAL DRILLING CHARACTERISTICS

Takeshi MITANI and Takeo KAWAI

Japan Construction Method and Machinery Reserch Institute

In recent years, Tunnel boring machines and large diameter shaft borers have been used in view of various considerations at construction sites. In the present investigation, drilling experiments were coducted for rock samples listed in table 1.

Table 1 Engineering properties of rocks tested

Test No.	Rock	Location	Specific gravity	Compressive strength	Tensile strength	Brittleness	Shore hardness
1	Granite	Enzan	2.66	1809 kg/cm²	109 kg/cm²	17	89
	Andesite(hard)	Funabara	2.56	1397	102	14	69
	Andesite(soft)	Sanjome	2.21	771	45	17	55
	Sandstone	Kawazu	2.08	251	37	7	20
2	Granite	Inada	2.68	1927	68	28	88
	Andesite	Funabara	2.43	1000	75	13	71
	Marble	Akiyoshi	2.68	638	44	15	46

Main specifications of the drilling test machine are as follows: Thrust exerted on cutter; maximum 16 tons, Rotary speed of cutter head; 0 to 100 rpm, Torque; maximum 1440 kg-m.

In the first test, 20 cm by 20 cm rock samples as listed in Table 1 were used. The bits used were Model 3S, Model 3M, and Model 3H tooth type tri-cone bits with diameter of 6 in. and thrust applied were varied from 0.3 tons to 10 tons depending upon the strength of rock and the type of bit. In each test, the rotary speeds were changed in three steps from 9 to 14 and 19 rpm. Total test conditions were 141.

In the second test, 30 cm by 30 cm rock samples as listed in Table 1 were used. The bits used were Model 3H-8 bit with diameter of 8.62 cm, Model 3H-12 bit with diameter of 12.14 cm and Model 3VH-12 bit with diameter of 12.14 cm. Model 3VH-12 bit used was W-C tip inserted tri-cone bit, and Model 3H-8 and Model 3H-12 bits were tooth type tri-cone bit. Drilling tests were conducted under 65 conditions with the thrusts between 0.72 and 8.0 tons and the rotary speeds of cutter head were 19 rpm and 45 rpm.

1. BIT THRUST AND DRILLING TORQUE

We obtained nearly linear relation between the bit load and drilli-

ng torque from NO.1 test(Fig. 1).

According to the results of NO.2 test, there are some data indicating that the torque is in proportion to 1.2 to 1.7 power of the load applied to bit.

2. W/D and R/N

W/D is the thrust per bit diameter in kg/cm and R/N is the drilling length per bit rotation in cm/rev. In each case of Fig. 2, the characteristic curve has a linear portion(as referred to "performance line"). For relatively soft rocks, there is a tendency for the drilling efficiency to reduce downwards in the region of high thrust (as referred to "transport line"). Such a reduction of drilling efficiency is mainly due to the decrease in the removal of cuttings caused by the increase in drilling speed. Particularly, in case of soft rocks it is considered that the drilling efficiency will be reduced further owing to a sticking action of cuttings on to the teeth of the bit with the increase in drilling speed(or the depth of penetration of teeth). From Fig.2, it is concluded that with respect to the effctive region of drilling thrust there is an upper limit for soft rocks and a lower limit for hard rocks.

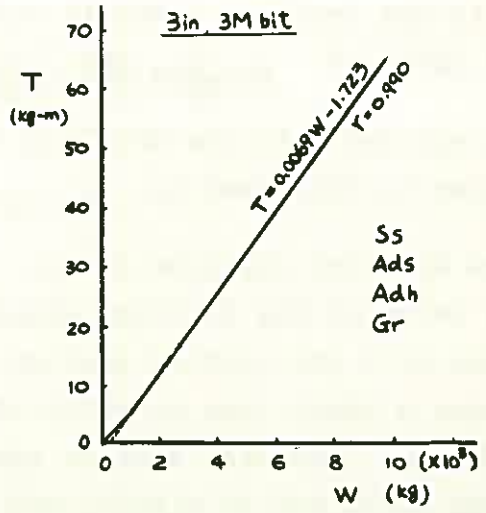

Fig. 1 Variation of torque with increase in thrust

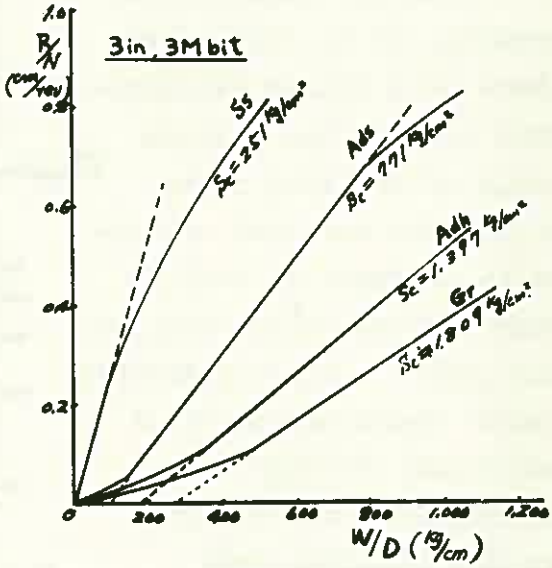

Fig.2 Drilling performance

3. DRILLING INDEX

The drilling index K is expressed in terms of the volume of the rock excavated per minute per rotary horsepower in cm^3/min·ps.

$$K = \frac{A \cdot R}{P}$$

where A is the cross -sectional area excavated in cm^3 and

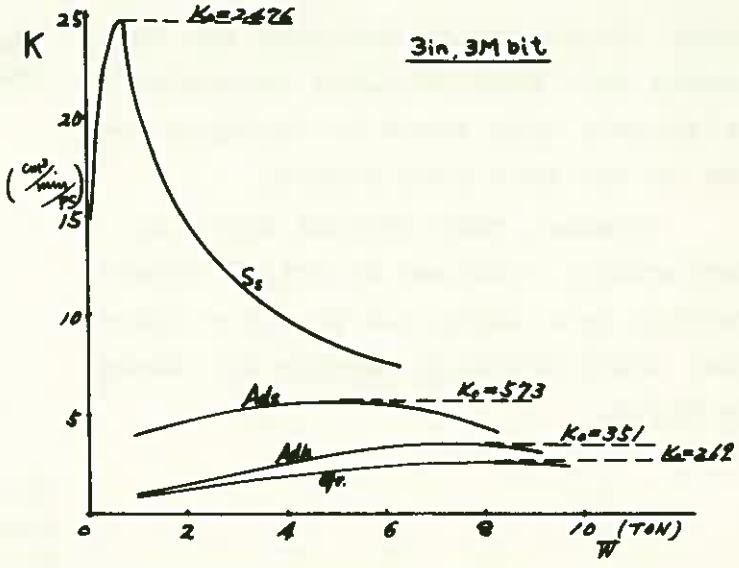

Fig.3 Relation between thrust and K

R is the drilling speed in cm/min. And the drilling horsepower P in ps is given as $P=\frac{1}{75}T\frac{2\pi N}{60}=\frac{N\cdot T}{716.2}$ where N is the rotary speed of bit in rpm and T is the drilling torque in kg-m. Consequentry, the drilling index is expressed as $K = A\cdot R\frac{716.2}{N\cdot T}=\frac{716.2\pi}{4}D^2\cdot(\frac{R}{N})\frac{1}{T}$ where D is the drilling diameter in cm. Thus, the drilling index can be expressed in terms of the drilling diameter, R/N and the drilling torque. The values of K are plotted against those of the bit thrust as shown in Fig.3, where a sharp peak in value of K is recognized in case of soft rock (sandstone), and also similar peaks are occurred in case of hard rocks, even thogh not so significant as compared with soft rocks.

4. DRILLING INDEX AND STRENGTH OF ROCK

From the experimental results, it is shown that there is a linear relationship between the muximum value of drilling index Ko and the uniaxial compressive strength of rock Sc when plotted on a log-log scale graph. Fig.4 indicates linear characteristics of individual straight lines, but distinct correlations are not obtained among these straight lines.

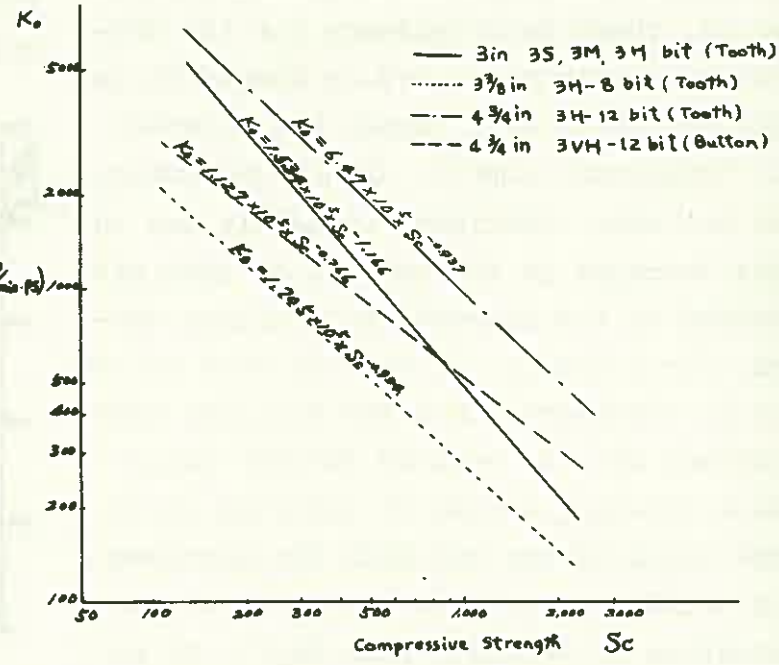

Fig.4 Relationship between Ko and Sc

However, it is found from Fig.4 that Model 3VH-12 cutter designed for extremely hard rock drilling maintains relatively high value of drilling index in the hard rock region.

Finally, some typical drilling performance obtained at actual construction site using 1.0 to 3.6 m diameter shaft drilling machine are shown in Fig.5.

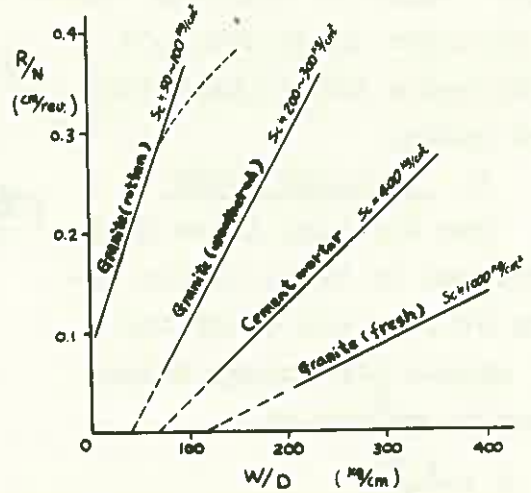

Fig.5 Drilling performance obtained at actual construction site in Japan

THERMAL FRACTURING OF ROCKS BY THERMODRILL

Zenjiro HOKAO, Tokyo University.

Two kinds of thermodrills or jet pircing machines were developed by author. One kind of thermodrill based on a principle of liquid propellant rocket engine and the other a principle of jet engine. The rocket engine principle thermodrill is applied for under water boring and the jet engine principle thermodrill for cutting and boring of rocks on the surface.

In Seto Inland Sea of Japan, under water boring experiments were carried out at the depth of maximum 30 meters and very good results were obtained for granite. The drilling rate at the depth of 10 meters was 42 cm/min. in average, while at the depth of 30 meters it decreased to about 29 cm/min. The diameter of hole was about 100 mm. (Fig.1) (Fig.2). The rock removal rate at the depth of 10 meters was about 3100 cm^3/min. in average, while at the depth of 30 meters about 2000 cm^3/min. In these case, the combustion chamber total pressure was 20 kg/cm^2 and the quantity of kerosene fed to the thermodrill 0.7 ℓ/min., oxygen gas 1.6 Nm^3/min. The diameter of combustion chamber is 18 mm and the total length of thermodrill about 3 meters. The temperature in combustion chamber is about 3400 °K and the velocity of jet about 2000 m/sec. Two divers held the thermodrill and were engaged in boring under water. Fig.3 shows the bore holes drilled into a granite block at the depth of 10 meters

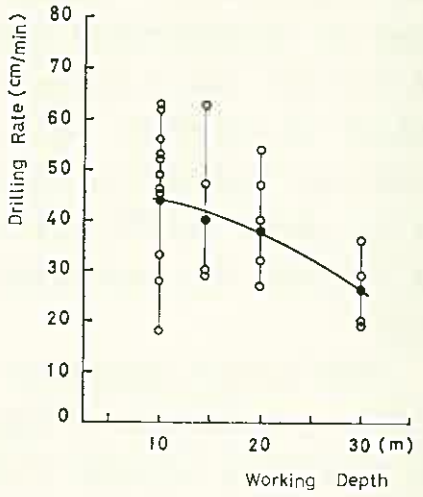

Fig.1 Relation between drilling rate and working depth.

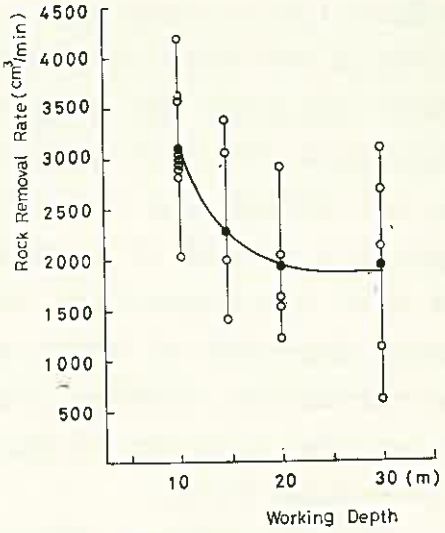

Fig.2 Relation between rock removal rate and working depth.

under water.

Several types of thermodrills using compressed air and kerosene or gasoline were also developed. These thermodrills are based on a principle of jet engine, but the each has a little different designs and technical characteristics. The thermodrill using air and kerosene requires oxygen gas when it is ignited, while the others using gasoline do not have a same requirement. Today two types of thermodrills using air and gasoline are used practically, and the one has a spray injection type injector and a cylindrical combustion chamber, while the other a premixing type injector and a conical combustion chamber. The temperature in combustion chamber is about 2400°K and the velocity of jet about 1200 m/sec. Fig.4 shows the supersonic fire jet stream of air-gasoline thermodrill.

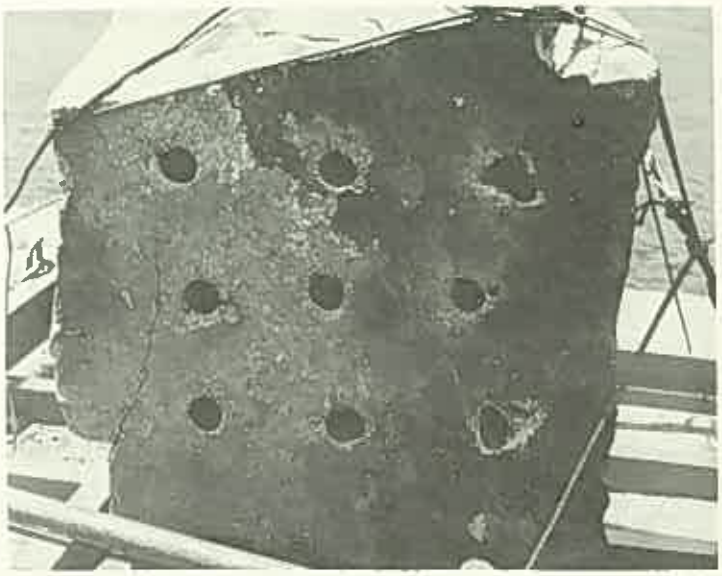

Fig.3 Bore holes drilled in a granite block at the depth of 10 meters.

The author measured the temperature and pressure distributions of free jet stream of oxygen gas-kerosene thermodrill, and examined the relations between these parameters and propellant weight flow rate, distance from a nozzle exit, drilling rate etc.

Thermal characteristics of jet stream impinged to the rock surface differ from that of free jet stream, for the supersonic stream gives rise to shock wave in front of the surface. Then the author measured the temperature distributions of jet impinged vertically upon the rock surface, and a heat transfer coefficient between the jet stream and the rock surface experimentally. The author applied a method of Першин А. П., and used a air-gasoline thermodrill, throat diameter of which was 11 mm, the combustion chamber diameter 40 mm and the quantity of gasoline fed 0.12 ~ 0.18 ℓ/min.

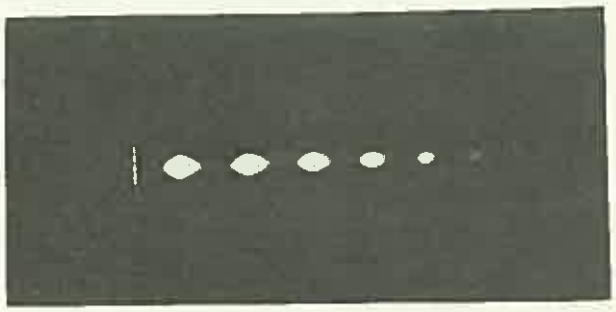

Fig.4 Fire jet stream.

In this method, the flame jet was impinged upon the surface of

one side of cylindrical heat transmitter made of cupper. The heat transmitter has three holes, in which thermocupples are inserted, and the bottom and peripherical surface of which are coverd with insulator.

The heat transfer coefficient was calculated with data of temperature distributions in the heat transmitters. Fig.5 shows a relation between the heat transfer coefficient (h) and the distance of impinged surface from nozzle exit (ℓ). Fig.6 shows the distributions of heat transfer coefficient in cross section in case of ℓ = 10 cm. By the examination of experimental results, the following equation was obtained in general form:

$$\frac{Nu}{Re^{3/4}\,Pr^{1/3}} = 0.05 \sim 0.06$$

when Nu - local Nusselt number
Re - local Reynolds number
Pr - Prandtl number

This equation will be useful for examination of thermal fracturing of rocks by the fire jet stream.

Heat transfer into impinged jets is different from that of jets over flat plates. In case of the latter $Nu/Re^{3/4}Pr^{1/3}$ = 0.0296 and smaller than that for the impinged jets. This must be considered in calculations of thermal stresses induced in rocks in case of thermal fracturing by jets.

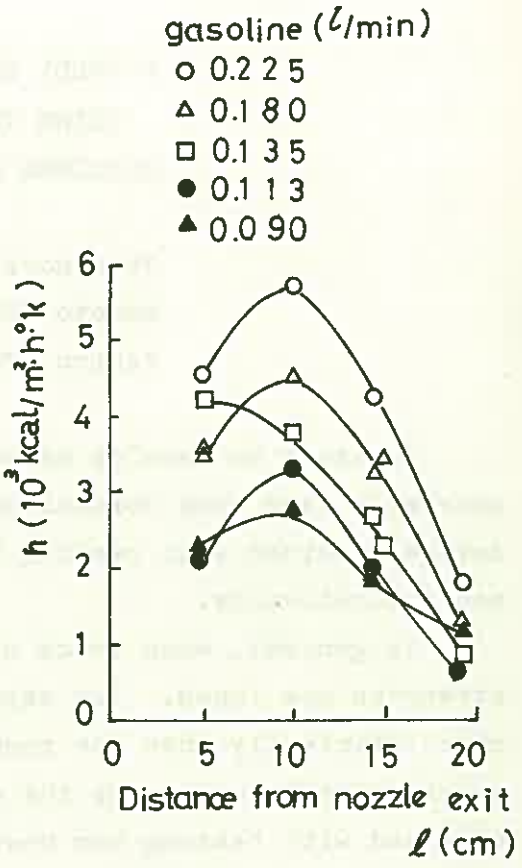

Fig.5 Relation between heat transfer coefficient and distance from nozzle exit.

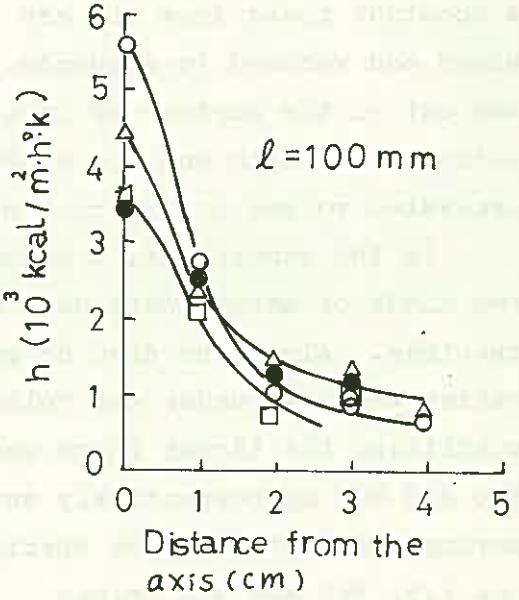

Fig.6 Heat transfer coefficient distributions in cross section.

A STUDY ON THE EXCAVATION METHOD USING THE MECHANICAL CUTTING COMBINED WITH HEATING BY A FLAME

Yoshinori INADA, Hyogo Prefectural Office
Makoto TERADA, Kyoto University
Ichiro ITO, Kyoto University

In order to develop an effectual excavation method for hard or extremely hard rock formations, a method using the mechanical cutting device combined with heating by a flame has been studied experimentally and theoretically.

In general, when rocks are heated, they are degraded and their strengths are losed. The degraded rock may be mechanically excavated more efficiently than the rock which has never been degraded. Therefore, an experiment to examine the efficiency of mechanical rock cutting method combined with heating has been carried out in the laboratory.

The apparatus used in this experiment is illustrated in Fig. 1. The flame nozzle for heating, the atomized water nozzle for cooling, the roller cutter, the air blowing nozzle and the dust collector for rock cuttings are arranged in a row.

When the rock specimen fixed on the rack with wheels was moved at a constant speed from one end to another end, it was heated, cooled, cut, blown and vacumed in sequence. This process was repeated and a trench was cut on the surface of rock specimen. Every ten times of the repetition, the depth and the width of the cut trench were measured and the excavated volume of the rock was calculated.

In the experiment, a granite and two kinds of marble were used as the specimen. Also, the disc or gear cutter was used under the following condition: the thrust force was 400, 500 and 600 kg respectively and the moving speed of the rock specimen was 1.5, 3.0 and 4.0 cm/sec respectively.

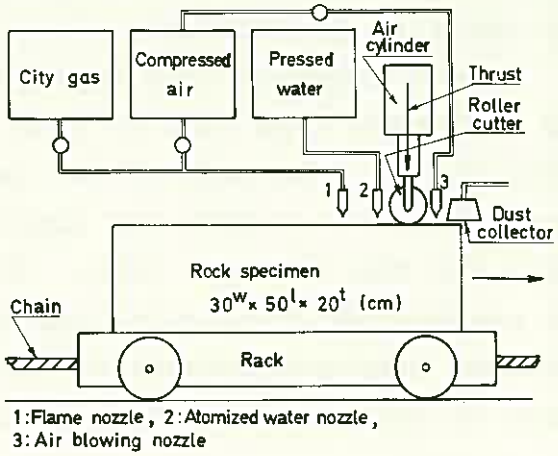

Fig. 1 Experimental arrangement

Examples of the experimental results obtained in granite specimens are shown in Figs. 2 and 3.

Every curve drawn by dotted lines in these figures shows experimental results under the condition of no heating effect.
From these results, it was found that the efficiency of mechanical cutting in granite specimens increased by the effect of heating by a flame and the increasing tendency found in disc cutter experiment was higher than that found in gear cutter experiment. Also, in either case, the bigger the thrust force was, the higher the efficiency became.

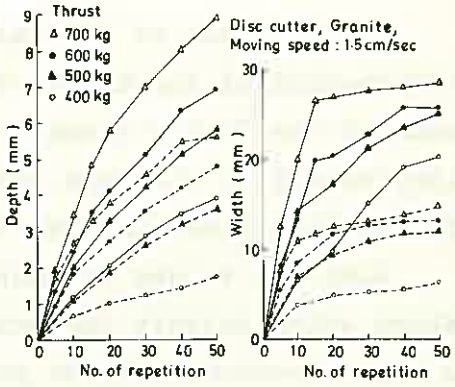

Fig. 2 Depth and width of the trench with cutting repetition

In the experimental results obtained in marble specimens using disc cutter, it was found that the effect of heating by a flame was not always good; on the contrary, it was sometimes bad. In the case of marble specimens using gear cutter, however, the effect of heating by a flame was recognized as well as in the case of granite specimens.

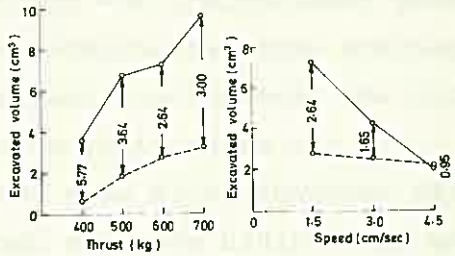

Fig. 3 Correlation between excavated volume, thrust force and moving speed of the rock specimen

Considering the reason, the marble is apt to be chemically disintegrated by the effect of heating and consequently the product forms a pulverized layer on the surface of the heated rock. This layer seems to prevent the effectual excavation by the disc cutter. Therefore, for marbles, it is deduced that the drag type of cutter is desirable rather than the roller type of cutter in order to utilize the effect of heating by a flame in the mechanical cutting.

In order to consider the effect of heating by a flame, firstly, the thermal conduction in the rock specimen was studied. The rock specimen was regarded as a semi-infinite solid and the three dimensional distribution of temperature in the rock specimen was calculated. With regard to the expression used for the calculation, see the reference in detail.

An example of temperature distribution in the rock specimen is shown in Fig. 4. In this calculation, the rectangular coordinates system is used, in which the x and y axes are on the surface of the rock specimen and the z axis is perpendicular to the surface and faces to the interior of the rock specimen. The origin of the coordinates is always at the center of the heat source and it moves toward the negative direction along the x axis.

On the basis of the calculated temperature distribution, secondly, distribution of thermal stresses in the rock specimen was calculated by means of the finite element method. For example, the state of stress distribution in the rock specimen corresponding to the temperature distribution shown in Fig. 4-B is shown in Fig. 5.

When the values of thermal stresses induced in rock reach the values which satisfy the criterion of failure, the local failure such as a micro-crack would be generated and consequently the thermal degradation would be produced. If the heating effect would be further provided with the passage of the heat source, the degraded zone in rock should be expanded toward the interior of the rock. Considering the above postulation, the distribution of thermal stresses in the rock specimen were recalculated and the transition of the degraded zone with time was presumed as shown in Fig. 6.

On the other hand, according to the microscopic observation of the thin sections which were cut from the rock specimen heated by a flame, it was ascertained that the degraded zone thus presumed analytically coincided fairly well with the zone of local failure generated by the effect of heating.

REFERENCE

1) Y. Inada, M. Terada and I. Ito: Jour. of the Mining and Metallurgical Institute of Japan, 88, 1008 (1972)

2) Y. Inada, M. Terada and I. Ito: Jour. of the Mining and Metallurgical Institute of Japan, 88, 1013 (1972)

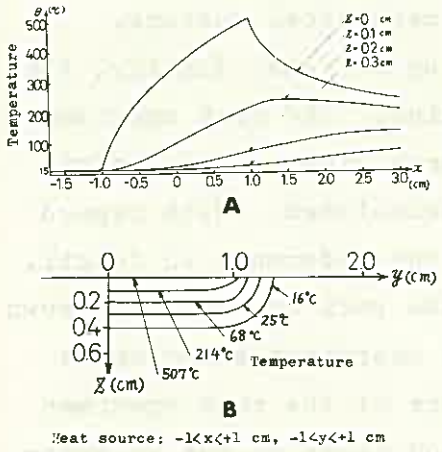

Fig. 4 An example of temperature distribution

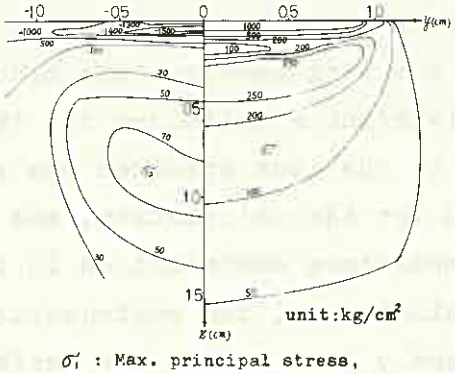

Fig. 5 An example of thermal stress distribution

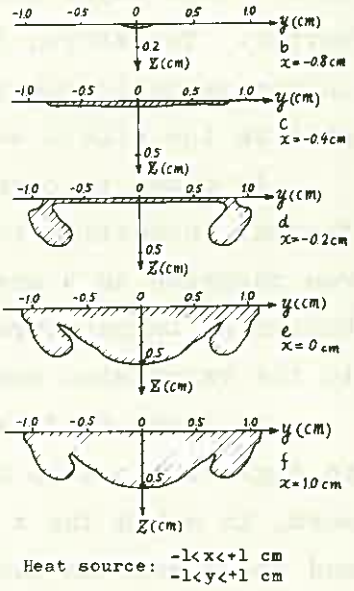

Fig. 6 Transition of degraded zone (hatched)

SIZE DISTRIBUTIONS OF FRACTURED PRODUCTS AND FRACTURE SURFACE ENERGY IN SINGLE PARTICLE CRUSHING

Saburō YASHIMA, Tōhoku University
Yoshiteru KANDA, Yamagata University
Fumio SAITŌ, Tōhoku University

During the course of an investigation on the single particle crushing in this laboratory since 1964, the authors have reported the results; i) Single particle crushing under slow rate of loading.[1] ii) Observation of fracture surface of crushed particle by scanning electron microscope.[2] iii) On the relation of work index and mechanical properties of brittle materials.[3] iv) Size effect of single particle crushing.[4,5] v) Mechanical properties of brittle materials and their single fracture under dynamic loading.[6]

The present paper reports the experimental results of size distributions of fractured products and fracture surface energy in single particle crushing under various loading rate. The samples used in the experiment were sphere of 2.0 cm diameter made of two kinds of glassy materials and six kinds of minerals. The number of specimen was 200~300 in every experimental condition. The universal compression testing machine and the drop hammer testing machine were used in the compression test.

A summary of experimental results was as follows.

1. Size distribution of fractured products

The sizing analysis of fractured products was carried out by the Tyler standard screen. The Gaudin-Meloy-Harris (G-M-H) size distribution applied to the experimental

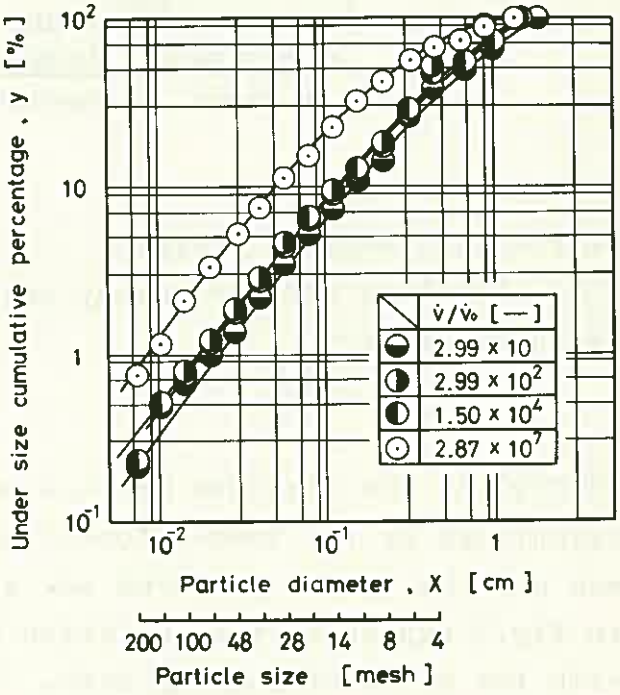

Fig.1 Size distributions of fractured sphere of borosilica glass

results for borosilica glass was shown in Fig.1. Where $\dot{v}_o$($\dot{v}_o$=1.67 x10^{-2}Kg/sec) is the minimum loading rate in this experiment and ($\dot{v}/\dot{v}_o$) is the ratio of loading rate.

It was found that the three parameter (maximum particle size x_o, distribution parameter m, size ratio n) in the G-M-H size distribution function given by Eq.1 could be represented as function of the ratio of loading rate. These functions for silica glass, borosilica glass, quartz, feldspar were presented in Table 1.

$$y = 1 - [\,1 - (x/x_o)^m\,]^n \qquad (1)$$

Table 1 Gaudin-Meloy-Harris distribution of fractured product

Kinds of sample	$y = 1 - [1 - (X/X_o)^m]^n$ * X_o [cm] m [—] n [—]	Range of loading rate $\dot{v}$ [Kg/sec]	Number of specimen**
Silica glass	$X_o = 2.12(\dot{v}/\dot{v}_o)^{-0.0205} \pm 0.100$ $m = 1.29(\dot{v}/\dot{v}_o)^{-0.0146} \pm 0.00729$ (2) $n = 0.895(\dot{v}/\dot{v}_o)^{0.0640} \pm 0.0915$	$3.33\times10^{-1} \sim 5.1\times10^{5}$	200
Borosilica glass	$X_o = 1.91(\dot{v}/\dot{v}_o)^{-0.0217} \pm 0.0535$ $m = 1.21(\dot{v}/\dot{v}_o)^{-0.00220} \pm 0.0323$ (3) $n = 1.69(\dot{v}/\dot{v}_o)^{0.0459} \pm 0.237$	$5.00\times10^{-1} \sim 4.8\times10^{5}$	200
Quartz	$X_o = 1.91(\dot{v}/\dot{v}_o)^{-0.0120} \pm 0.0497$ $m = 0.894(\dot{v}/\dot{v}_o)^{0.00224} \pm 0.00423$ (4) $n = 0.0566(\dot{v}/\dot{v}_o)^{0.165} \pm 0.0175$	$1.67\times10^{-1} \sim 1.12\times10^{5}$	296
Feldspar	$X_o = 1.75(\dot{v}/\dot{v}_o)^{-0.00228} \pm 0.0320$ $m = 0.756(\dot{v}/\dot{v}_o)^{0.00712} \pm 0.00263$ (5) $n = 0.0323(\dot{v}/\dot{v}_o)^{0.129} \pm 0.00607$	$1.00\times10^{-1} \sim 1.12\times10^{5}$	299

* $\dot{v}_o = 1.67\times10^{-2}$ Kg/sec, ** Nominal diameter of specimen is 2.0 cm

2. Fracture surface energy

Fracture surface energy required to enlarge the surface area is shown by Eq.6.

$$\gamma_e = \frac{E/M}{\Delta Sw} \qquad (6)$$

Where γ_e is the fracture surface energy, E is the fracture energy calculated by the load-deformation curve, M is the mass of specimen and ΔSw is the produced new specific surface area. The curves in Fig.2 expressed the variation of the fracture surface energy with the ratio of loading rate. The values of the fracture surface energy in the region of higher loading rate ($\dot{v}/\dot{v}_o \geqq 10^4$ [-]) tended to decrease with the ratio of loading rate and they took the order of 10^4 ergs/cm^2. The values were similar to the one of the

surface energy ($1.67\pm3.10 \times 10^4$ ergs/cm^2) calculated by Jimbo[7] for quartz from thermal balance in the experiment of a vibration ball mill.

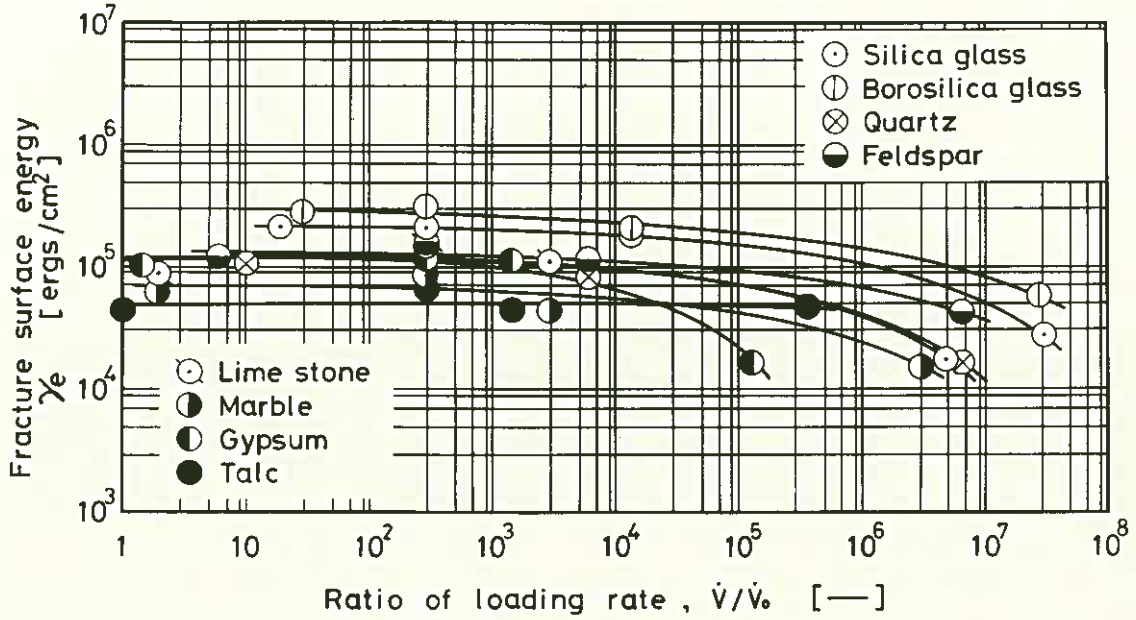

Fig.2 Variation of fracture surface energy with ratio of loading rate

In this study, the relationships between the fracture surface energy and the ratio of loading rate for quartz was given by Eq.7.

$$\gamma_e = 2.02\times10^7(\dot{v}/\dot{v}_o)^{0.0153} / e^{4.58(\dot{v}/\dot{v}_o)^{0.0271}} \pm 1.68\times10^4 \quad [\text{ergs/cm}^2] \quad (7)$$

$$1.67\times10^1 \leqq (\dot{v}/\dot{v}_o) \leqq 1.12\times10^5$$

Literature cited

1) Saburō Yashima, et al.: Kagaku Kōgaku, 34, 210~219 (1970)
2) Saburō Yashima, et al.: Kagaku Kōgaku, 34, 1006 (1970)
3) Saburō Yashima, et al.: Kagaku Kōgaku, 34, 1199~1205 (1970)
4) Saburō Yashima, et al.: Kagaku Kōgaku, 36, 1017~1023 (1972)
5) Saburō Yashima, et al.: Kagaku Kōgaku, 37, 630~632 (1973)
6) Saburō Yashima, et al.: Kagaku Kōgaku, 37, 1218~1226 (1973)
7) Genji Jimbo: J.Chem.Soc.of Japan, Ind.Chem.Section, 71, 1309~1314 (1968)

E. PROTECTION AND IMPROVEMENT OF ROCK

ANCHOR MECHANISM OF ROCK BOLT ENLIGHTENED

Seisuke MISAWA , Akinori TAKAHASHI
Japanese National Railways

1. Preface

For the purpose of the most advantageous rock bolts to be used practically in public eliminating the operators uneasiness for such anchor mechanism, the two species of the expansion type and bonding type have now fully been enlightened with the various test results, and according to an approval of the safety factor for such rock bolting, here have firstly been used about 100,000 rock bolts in the tunnelling works of the New Sanyo Trunk Line by the Japanese National Railways, and then the demand has been increased for various construction fields including highway and waterway tunnels and underground power stations.

2. Test

2-1 Materials for test

The tested rock bolts were expansion type called as "TH type" in style and size as shown Fig.-1, and bonding liquid mainly of the polyester resin called as "CELFIX" manufactured by the Celtite in France, as shown Fig.-2.

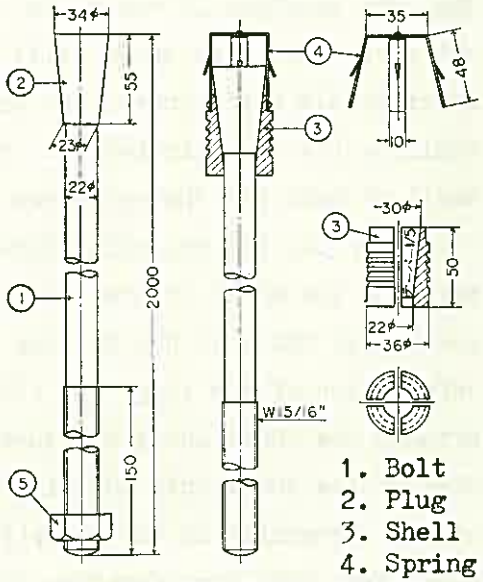

Fig.-1 TH Type

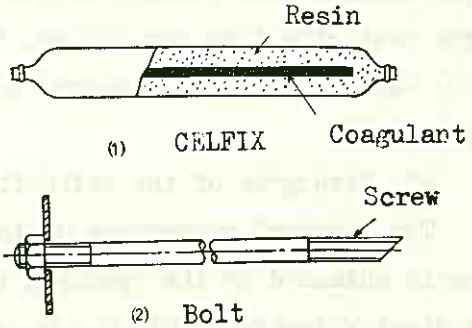

Fig.-2 Bonding Type

2-2 Tests in the field

The field tests were conducted at the actually excavatig spots utilized in the Aioi tunnel of the New Sanyo Trunk Line with the rock bolts installed in the downward holes of 28 to 40 mm. dia. and 1.5 to 2.0 m. long, and the bolts were pulled by a hydraulic jack until the bolts broken off or slipped away from the hole walls, and the relationship between load and displacement was recorded by reading dial gauge for elongation and slipping of the bolts on various load levels. Tested in various ways with different lengths and diameters of the bolts, different amounts of Celfix and different times of mixing as well as waiting times.

2-3 Basic tests in the laboratory

The basic tests were conducted in the laboratory for the following items which could not be known at the field tests.

1) Physical properties of the solidified resin.
2) Anchoring strength of TH type for the different rocks.
3) Adhesive strength of Celfix.
4) Test of Celfix in steel pipes.

3. Test results and considerations

3-1 Relationship between pull-out load and displacement.

Pull-out test results in the field are as shown in Fig.3 & 4, and the real lines show the measured values including slipping and elongation in the field, and the dotted lines show the calculated elongation of the bolts themselves. When compared Fig.-3 with 4, the total amount of displacements with pull-out load 10 tons is about 15 mm. on the TH type and is about 2 to 4 mm. on the Celfix, so that the Celfix is more suitable in the rock bolting anchor mechanism by reason of the less displacement with the more advantages for the rock bolting.

3-2 Anchor mechanism of TH type

Whilst the real lines and dotted lines in the above graph would show the same position if there is no slipping, the graph shows still considerable differences. The causes would be (1) the slip between the shell of bolt and the wall-face of drilled hole, (2) the slip between the plug and shell at the conic portion of the bolt due to the deformation of the plug, and (3) the slip between the shell and plug caused by intrusion of the shell into the side of the drilled hole. Generally in the past,(1) had so far been taken into consideration but as far as the basical test results concerned, (3) was the most affective and (2) was the next, and (1) has never been recognized in such phenomenon.

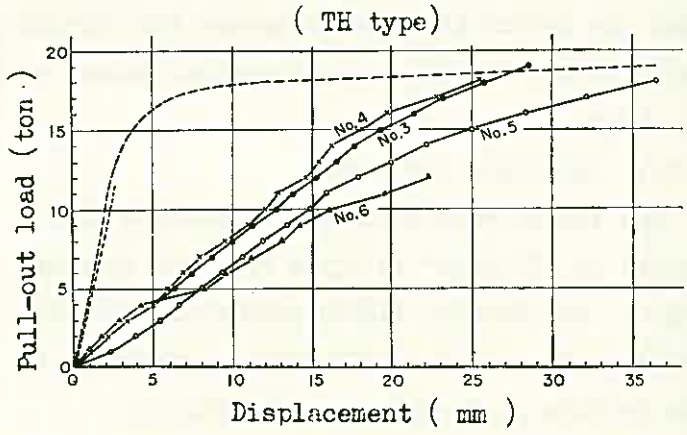

Fig.-3 Curve of Pull-out load and Displacement

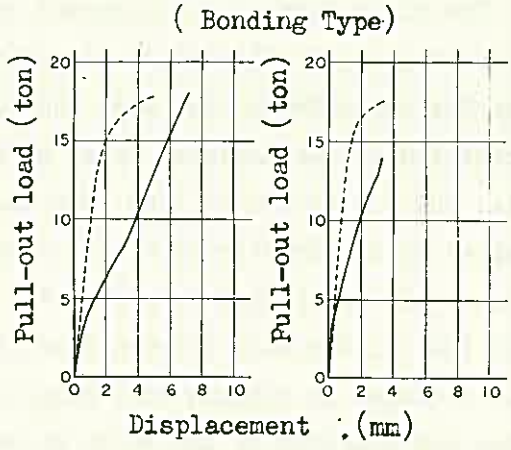

Fig.-4 Curve of Pull-out load and Displacement

3-3 Strengths of the solidified resin

The physical properties of the solidified resin obtained by the specimen test pieces were the specific gravity : 1.77, longitudinal velosity : 2970 M / S, compressive strength :552 Kg /cm^2, tensile strength : 88.7 Kg /cm^2, shear strength : 154 Kg /cm^2, Young's modulus : 38600 Kg /cm^2.

On the other hand, the varieties of the adhesive strength to the surface and different shear strengths according to the object materials, hole boring methods, etc. obtained from the pull-out test results are in such amounts as shown Table-1.

3-4 Adhesive mechanism of Celfix.

If suppose the bolt falling down whilst it was sticked to the rock by the solidified resin, the following three accasions would be considered as (1) slipping between the hole wall and the resin, (2) slipping between the bolt and resin, and (3) break of the resin itself. When the sticking face was smoothly flat, the resin would likely come off as (1) and (2), and to the contrary, when the sticking face was rough, the resin would likely be broken as (3). Therefore these shall differently be valued according to the natural properties of the object materials and to the roughness of their facing points. That is, when the hole wall surface is smoothly finished by drilling with such as a diamond core bit, the resin is likely to come off from the hole wall, and when the hole wall surface is roughly finished by drilling with such as a fish tail bit the resin shall completely be filled through even in the concaved portions of the hole wall face as well as of the bolt threads, so that the resin is likely to cause shear breaking in this portion.

4 Concluding Remarks

By the way, here at present (March 1974) about 30,000 rock bolts are monthly used for various minings and tunnellings in Japan, and now various problems are being studied closely at many research institutes, for such as how to prevent any loosening of the tightened bolts caused due to vibrations by the excavations operated in the vicinity, the photo elastic tests of the fully embeded resin, analysis by the Finite Element Method and examinations by the block models.

Table - 1 Adhesive strengths and shear strengths of solidified resin

Materials	Adhesive strength (Kg / cm^2)	Shear strength (Kg / cm^2)	Remark
Steel pipe	52	114	Drilling by diamond core bit
Rhyolite	32	—	
Andesite	39	—	
Marble	42	—	
Tuff	18	—	
Concrete	100	120	Drilling by fish tail bit
Andesite	114	<133	
Marble	67	86	
Tuff	49	—	

STUDY ON FAULT TREATMENT OF DAM FOUNDATION BY THE COMBINED USE OF FAULT REPLACEMENT WITH CONCRETE, GROUTING OF SURROUNDING ROCK, AND PRESTRESSING OF FOUNDATION BY HIGH-TENSION STEEL MEMBERS

Toshio FUJII

Dept. of Construction, the Tokyo Electric Power Co., Inc.

I. INTRODUCTION

In recent years, the need for development of new water resources has increased, and economical construction of dam is a very strong demand. Sites of dam construction with relatively good geologic conditions have been developed, and the remaining dam sites have, in general, some difficulties in their geologic conditions. Thus, research on the treatment of dam foundation is the most important part of the dam engineering.

There are several methods being used at present for the treatment of dam foundation, i. e. replacement of weak zones with concrete, transmission of the forces from the dam to sound rock beyond fault through the concrete plate in foundation, prestressing of foundation by high-tension steel members, restriction of displacement of foundation by concrete struts, consolidation of weak zones by grouting and so on. These methods are used depending on the special situation at each dam site, and the details of the treatment are quite different in each case. It is therefore difficult to give a general description of the practice of these methods, and at present, accumulation of many examples of dam foundation treatment would lead the technical development and would be beneficial to the engineers concerned.

For this reason, it is significant to introduce the foundation treatment of Nagawado Dam, an arch dam of 155m high, in which bed rock was composed mostly of granite with well developed joints and wide ranges of fault zones.

II. FAULT REPLACEMENT WITH CONCRETE

Foundations of dam should have sufficient strength and rigidity to withstand forces from dam, and also they have to be impervious to avoid leakage from reservoir. Thus, in case the foundation rock has fault zones, it is generally believed that the fault replacement with concrete is the most reliable method. However, in case fault zones are located close together, loosening of surrounding rock as the result of excavating fault zones would become a problem, and the conventional excavation by smooth blasting method would induce such loosening. In such case, the hydraulic excavation using high pressure water jet is very effective, both technically and economically.

In case of Nagawado Dam, there were ten large fault zones to be treated to get good stability of dam foundation, and study on the fault treatment was carried out by calculation and experiment taking account of the required mechanical properties of dam foundation, i. e. strength, deformability, and impermeability. In consequence, it was decided to replace the fault zones with concrete within 30m from the abutment face by making use of high pressure water jet in fault excavation. This method of excavation by high pressure water jet was modified from the one that is being used in coal mines and applied here to the fault excavation for the first time. According to the preliminary test in site, it was decided to use the pressure of 100kg/cm^2 and the nozzle diameter of 17 - 19mm, and to excavate the fault zones of 1 - 2m wide by dividing them into blocks each 10 x 10m. The volume of fault excavation was about 13,000m^3 in

total.

It is important in the excavation by high pressure water jet to investigate the geologic conditions of fault zones. Especially, frequence and direction of joints and cracks, which are often observed between soft fault materials and sound rock around them, would determine the efficiency of the excavation, while the width and gradient of the fault zones would determine the safety and easiness of this process. Thus, it is very important to investigate these subjects at the planning stage, and to make a plan for the excavation process which is based upon the results of the preliminary investigation and test in site. After the process has started, it is important to pay special attention to the training of monitor operators and strutting crew, for the ability of the monitor operators determines the overall efficiency, while skilled workers of strutting can get rid of an accident of rock fall which often takes place immediately after water jetting.

In addition, it is essential for the construction supervisor to observe loosening of surrounding rock during the operation. This observation should be done by not only direct measurement of actual displacement, but also some others which are easy to make a number of measuring points and able to be translated into displacement and should contribute to the accurate judgement of actual displacement. For especially in case the rock contains many well developed joints and cracks, direct measurement of displacement would sometimes indicate the unusual local movement only, and consequently, in order to observe the entire displacement, it is necessary to have a considerable number of measuring points; however, in case this is not possible, the other methods by which numbers of measuring points are easily chosen, such as the measurements of rock noise, permeability, etc., should be attempted.

At Nagawado Dam, the measurements of rock noise and permeability in addition to the actual displacement of the rock was within a few mm, which demonstrated the effectiveness of this excavating technique by high pressure water jet.

III. GROUTING OF SURROUNDING ROCK

This fault replacement technique with the use of effective excavating method by water jet may restrict the damage and loosening of surrounding rock, however, rock around the holes made by excavation is easy to loosen due to ground pressure, and in some cases, an application of cement grouting to the surrounding rock is helpful which would seal cracks that are the causes of loosening after filling the reservoir. In order to perform grouting effectively, it is necessary to determine the area of grouting, and this should be done by careful observation of the behavior of the surrounding rock during fault excavation. The permeability test of surrounding rock before and after the fault excavation is quite essential for this determination. The other important factor is the proportion of grout mix which would determine the effectiveness of grouting. For especially dense and highly viscous grout mix, a detailed regulation must be followed.

At Nagawado Dam, based upon the measurement of displacement in the surrounding rock during the fault excavation, the area of grouting was determined and grouting was performed after the filling of concrete at the fault zones. The total length of grouting holes was about 13km, weighing 59kg/m of cement grouting. This result would make proof of effectiveness not only of the excavating method by water jet to restrict the loosening of surrounding rock, but also of the grouting method to fill the cracks with grout according to the geologic conditions.

IV. PRESTRESSING OF FOUNDATION BY HIGH-TENSION STEEL MEMBERS

The grouting of surrounding rock used together with fault replacement by concrete is a powerful method to restrict loosening of rock, and prestressing of foundation rock by high-tension steel members would further increase the effectiveness of the treatment of dam foundation. However, in case the scale of

prestressing works is big, and consequently, the drilled holes for inserting steel members would become long, actual application of this method tends to encounter with some difficulties. In large scale operations, it is almost inevitable to have deviations of drilled holes from the right locations, troubles in inserting steel members due to chipping-off of hole surfaces, leakage of mortar from the packers around the end of hole, and creep of rock during prestressing works. Thus, it is important to give enough considerations beforehand, and to perform preliminary tests in site to make up a detailed plan, and once the process has started, it is necessary to prepare a flexible measures to deal quickly with eventual changes.

At Nagawado Dam, taking account of geologic conditions and stress distribution in the foundation rock, the scale of prestressing system was determined. The drilled holes were 150mm in diameter, and six high-tension steel bars with 27mm diameter were inserted into each hole, and the tension applied to the bars was 240t/hole which totals 40,000t for the entire area, and on the average 10t/m^2. The total hole length was about 12km, and the total weight of steel bars used was 330t. Tensionings of the bars were done three times before filling the reservoir, and grouting of cement to the holes and surrounding rocks was done after observing that the relaxation of the steel bars and the creep of the rocks were practically finished.

V. OBSERVATION ON STRUCTURAL BEHAVIOUR OF DAM FOUNDATION

The structural behavior of treated portions of dam foundation after filling the reservoir would make clear the effectiveness of entire treatment process, and observation on this behavior is important not only for the maintenance of structure, but also for the development of research on the engineering for foundation treatment. This behavior is best grasped by observing the displacement of foundation at each treated portion. In addition, the observation on its dinamic behavior during an earthquake is of enourmous value.

At Nagawado Dam, this behavior after filling the reservoir has been observed by measuring the displacement of foundation, uplift pressure, acceleration response during earthquakes. The results show that the restriction of loosening of rock around the treated faults has been maintained quite well, and it is concluded that the replaced concrete and surrounding rocks have been behaving as a monolith, and the uplift pressure working on the dam foundation has been properly controlled, and the leakage through the treated area has been minimal, and all in all, the actual construction has fully satisfied the design conditions.

VI. CONCLUSION

The method of fault treatment introduced above was actually used at Nagawado Dam, and the entire construction went quite successfully. The actual measurement indicated that the structural behaviors of the surrounding rocks during excavation of the fault and after filling the reservoir were quite close to the one which had been expected at the designing stage.

According to this fact, it is verified that for the treatment of dam foundation having many fault zones, the combined use of the fault replacement with concrete, grouting of surrounding rock, and prestressing of foundation by high-tension steel members is a very effective and proper method from both technical and economical view points.

REFERENCES

1) T. Fujii, "Fault Treatment at Nagawado Dam", Q.37-R.9, Vol.II, Trans. of the 10th Cong. on Large Dams, 1970.

2) T. Fujii, "Foundation Grouting at Nagawado Dam", C.15, Vol.VI, Trans. of the 10th Cong. on Large Dams, 1970.

GROUTING INTO CRACKED VOLCANIC ROCKS

Isao SHIBATA, Public Works Research Institute, Ministry of Construction

Most remaining dam-sites are frequently consisted of defective foundations in Japan, as a great number of dams have already been built on the sound rock foundations. Such being the case, in order to eliminate seepage, it is the proper treatment to grout into defective foundations when a high dam is built on it. Standing on this point of view, "Technical Standard on Foundation Grouting" was established by Commitee on Rock Mechanics J.S.C.E.. Important contents of it are as followings;

1)permeability of the foundation should be explored by means of "Lugeon Test",

2)it is desirable that the depth of curtain grout holes are extended to more than 0.5H, wher H is the height of dam, as shown in figure 1.

3)primary material of grout should be limited to standard or modified Portland cement,

4)grouting should be carried out by means of "Split Spacing Method",

5)grouting program should be checked by both reduction of Lugeon number and grout take of the respective series of holes, and permeability of finished grout curtain beneath the dam should be less than 2-Lugeon for concrete dams or 5-Lugeon for rock-fill dams.***[1)]

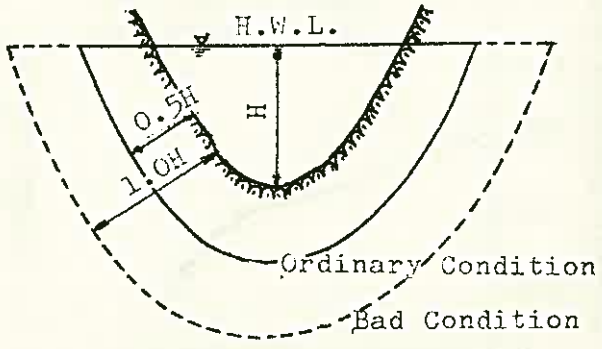

Fig.1 Extent of Grout Curtain

Now when a dam is planned to build on the volcanic rock foundation which is frequently full of open cracks, the dam engineers have to design grouting method carefully as it is very difficult to restrict seepage by the ordinary treatments. In such a case, it is desirable to decide details of grouting method due to the results of preliminary grout tests. And dam engineers in Japan have abundant experiences on these treatments.

In spite of the fact that preliminary grout test at Yata dam site, which was consisted of welded tuff, indicated very different curves on

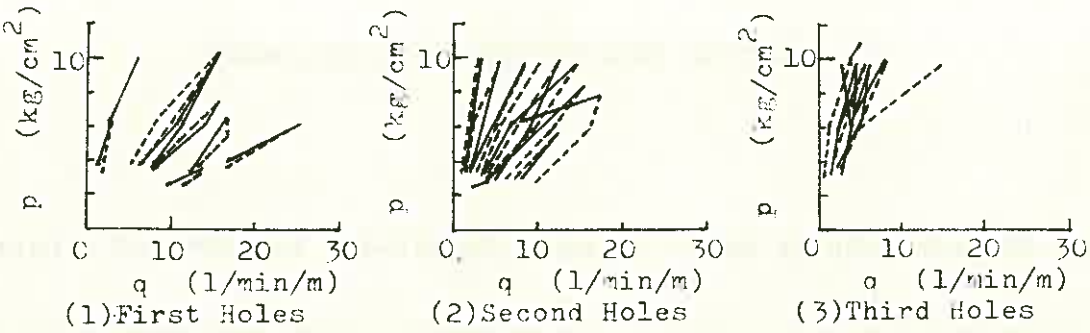

Fig.2 Relations Between Pumping Pressure And Grout Take At Yata Dam

pumping pressure and grout take of the first series of holes, the curves of the third series of holes converged very well as shown in figure 2 by the effect of injection.***[2)]

In a thin ridge at Nidorikawa dam, of which geology was welded tuff and full of open cracks with a width of from 0.5-cm to 10-cm, so large leakage through it was estimated that preliminary grout tests were carried out and details of curtain grouting were decided due to the results of it. Permeability of the ridge of 25-Lugeon before grouting

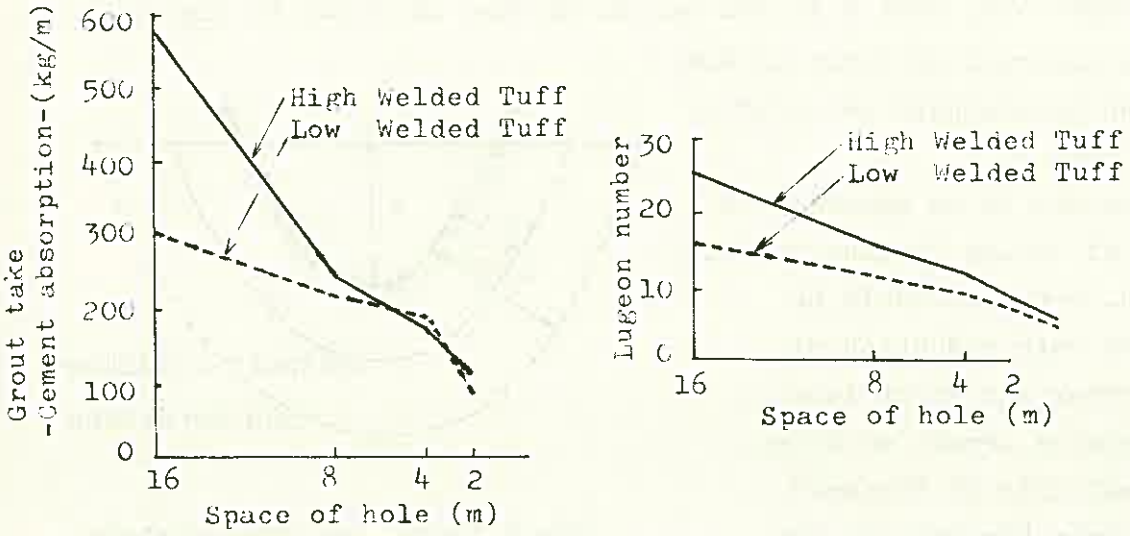

Fig.3 Reduction Of Lugeon Number And Grout Take At Nidorikawa Dam

was reduced to 6-Lugeon after grouting as shown in figure 3, and grout take was decreased to 100-kg/m. Leakage through the thin ridge with a length of 2,000-m amounted to 2.6-m^3/min, but there was no change in the quantity for several experiences of full reservoir.***[3)]

So far as we know, it is possible to reduce the permeability of cracked volcanic rock foundations to about 6-Lugeon by means of careful grouting method, but it is still very difficult to reduce it less than 5-Lugeon. As a large quantity of leakage through it may consequently be estimated, the amount of leakage and water level of reservoir have to

be measured at all times. Due to these measurements we can find out a hazard, because the amount of leakage may increase when the grout curtain is washed out by seepage.***[4])

Reference

1)Commitee on Rock Mechanics J.S.C.E.; Technical Standard on Foundation Grouting

2)I.SHIBATA, M.TAHARA,and S.MIURA, Proceedings of the 8th Symposium on Rock Mechanics, J.S.C.E.; Test Grouting for Layers of Pumice Flow and Scoria in Aso Lava

3)Construction Office of Midorikawa dam, Ministry of Construction; Technical Memorandum on Foundation Treatment at Midorikawa Dam

4)I.SHIBATA, Annual Report of Public Works Research Institute, Ministry of Construction; Foundation Treatment on Easily Permeable Rocks

CORE ZONE WORKS MANAGEMENT METHOD FOR ROCK-FILL DAMS

Tsuguo HARADA, The Kansai Electric Power Co., Inc.

Ideal works management method for core zone of the rock-fill dam is to conduct the works by obtaining the information on coefficient of permeability of embanked-up materials so that the core materials can function in full as water-tight zone. The most critical problem in this case is the speed by which the works are to be managed and conducted. Commonly employed works management methods adopt field permeability tests at dam site where the core materials are embanked up or adopt indoor permeability tests with undisturbed test materials as picked up at the site. However, all these methods cause time delays of two or three days at least, and judging from the embanking-up speed, it is hardly possible to obtain the test results in advance of the related embanking-up work for which the test results would have been truly required and such tests cannot be conducted so frequently or all the time. In many cases, therefore, indirect works management methods are employed by which to assume the permeability coefficient of the soil on a basis of the data on water content in percent of total weight or density at time of the compaction which are deemed to have close relation with the permeability coefficient of soil. However, these indirect methods tend to neglect almost all the time the variances of the material quality and fail to define the permeability coefficient for design with the core material of high content rate of coarse grained soils (usually with particle diameter of 4.76 mm or more), or result in unnecessary repetition of rolling with the core materials of high content rate of fine grained soils.

Higher rock-fill dams requires larger quantity of core materials, which could hardly be even or uniform in quality, such quality of core materials depends largely upon topographic and geologic structure of borrow-pit and, its local weather conditions, and upon works management factors such as picking methods, the spread by the dumping cars and rolling. The variances of the quality must be admitted or taken for granted to some extent. This paper deals with a new works management method which aims to make use of the core materials characteristics and the permeability coefficient data for conducting works management in more directly and without causing any delays in embanking-up speed. One approach is to assume the permeability coefficient by the results of soil tests

and the other is to calculate the permeability coefficient by simple permeability tests with the in-situ pit.

2. Procedures of Works Management

Procedures of the works management are as shown in Flow Charts (1), (2) and (3), respectively. Tests consist of those to be conducted both at borrow-pit and embanked site.

2-1 One-point compacting test to define optimum water content in percent of total weight (W opt) and maximum dry density (γ_d max)

One-point compacting test is conducted with a large mold of 30cm x 31cm with natural water content in percent of total weight and with particle diameter of 50 mm or less. And then the values of W opt and γ_d max will be obtained from the test results and the compacting curve prepared in advance as in Fig. 1 where $1/\gamma_d$ max = 0.01056 W opt + 0.3935, based on the following expressions:

$$w_{-50} = w_{-15}(1 - P_{+15}) + w_{+15} \cdot P_{+15} ,$$

$$\gamma_{d-50} = \gamma_{t-50} / (1 + w_{-50}) ,$$

$$P_{+15} = \frac{W_{+15}/(1+w_{+15})}{(W_{-50} - W_{+15})/(1+w_{-15}) + W_{+15}/(1+w_{+15})}$$

$$\gamma_{t-50} = W_{-50}/21.902$$

2-2 Weight with particle diameter of 0.074 mm or less

Simple sedimentation tests are conducted to define the weight of grain soils of particle diameter of 0.074 mm or less which is deemed to have close relations with the permeability coefficient. Test procedures are given in Flow Chart (3) and the equations used are:

$$P_{-15} = \frac{(W_{-50} - W_{+15})/(1+w_{-15})}{(W_{-50} - W_{+15})/(1+w_{-15}) + W_{+15}/w_{+15}}$$

$$LP_{-0.074} = P_{-15} \cdot SP_{-0.074}$$

2-3 Tests to define γ_d after rolling

Water substitution method is employed with the excavated pit at embanked-up site in order to define the value of γ_d. Same excavated pit is utilized for simple permeability tests to obtain the permeability coefficient by applying the following expressions:

$$\gamma_{d-50} = \frac{(W_{-15} + W_{+15})/V - V_{+50}}{1 + w_{-50}}$$

$$k = \frac{r_c^2}{(t_1 - t_2)} \left[\left(\frac{1}{h_1} \sinh^{-1} \frac{h_1}{2r_c} - \frac{1}{h_2} \sinh^{-1} \frac{h_2}{2r_c} \right) + \frac{1}{(2r_c)^2} \left(\sinh^{-1} \frac{2r_c}{h_1} - \sinh^{-1} \frac{2r_c}{h_2} \right) \right]$$

3. Judgement of test results

After completing the tests as mentioned in the preceding paragraphs, the water content during works in percent of total weight could be defined by W opt, and the degree of compaction by the value of γ_d max. As and when the values are given for Weight with particle diameter of 0.074 mm or less, water content during works in percent of total weight and d-50, the permeability coefficient is obtained by the management chart in Fig. 2. The measured value of the permeability coefficient can be arrived at by Fig. 3.

Thus, the judgement on the permeability coefficient will be made in comparison with the coefficient of permeability for design (for an example 1.0×10^{-5} cm/sec). If the permeability coefficient fails to satisfy the design value, additional rolling will be considered in proportion to rolling energy ratio before repeating another set of procedures as mentioned above.

4. Designations

For the purpose of this paper, the following designations mean respective expressions as assigned thereto:

W-50: bulk weight of grain soils with particle diameter of 50 mm or less

w-15: water content of grain soils with particle diameter of 15 mm or less

w-50: water content of grain soils with particle diameter of 50 mm or less

W+15: surface dry weight of grain soils with particle diameter of 15 mm up to 50 mm

w+15: absorption of grain soils with particle diameter of 15 mm up to 50 mm

P+15: weight of grain soils with particle diameter of 15 mm up to 50 mm

γ_t-50: bulk density of grain soils with particle diameter of 50 mm or less

γ_d-50: dry density of grain soils with particle diameter of 50 mm or less

P-15: weight of grain soils with particle diameter of 15 mm or less

LP-0.014: weight of grain soils with particle diameter of 0.074 mm or less, as in test soil materials with particle diameter of 50 mm or less.

SP-0.074: weight of grain soils with particle diameter of 0.074 mm or less, as in test soil materials with particle diameter of 15 mm or less

V: volume of sands or water

V+50: volume of grain soils with particle diameter of 50 mm or more.

FLOW CHART - (1)

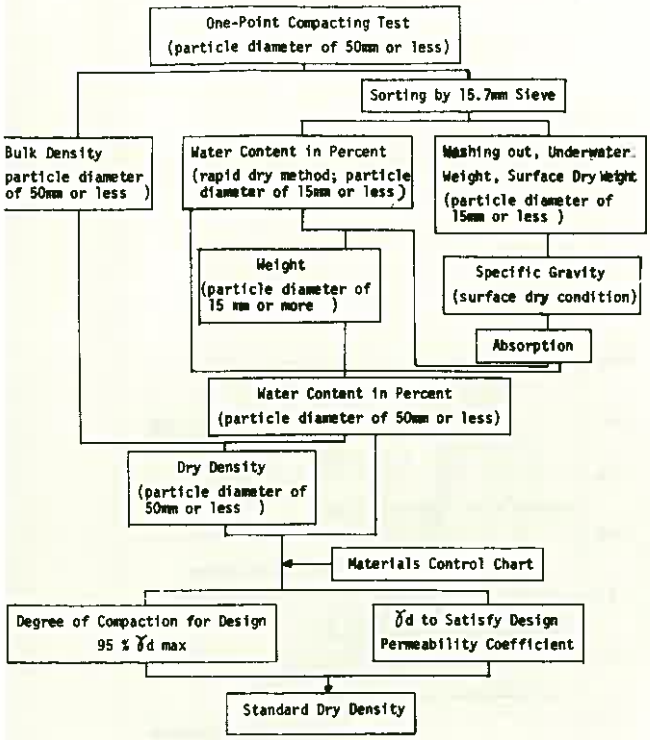

FROW CHART - (2)

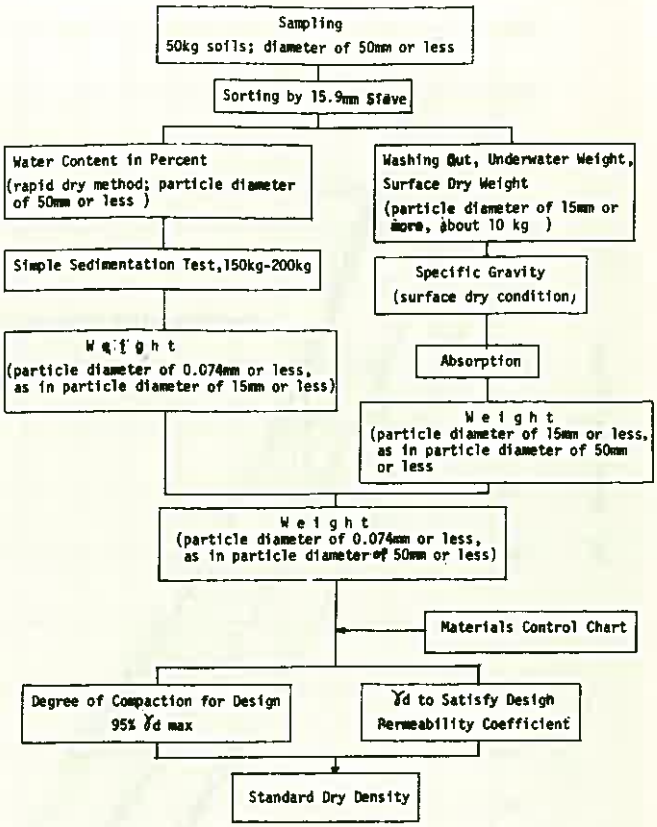

FLOW CHART - (3)

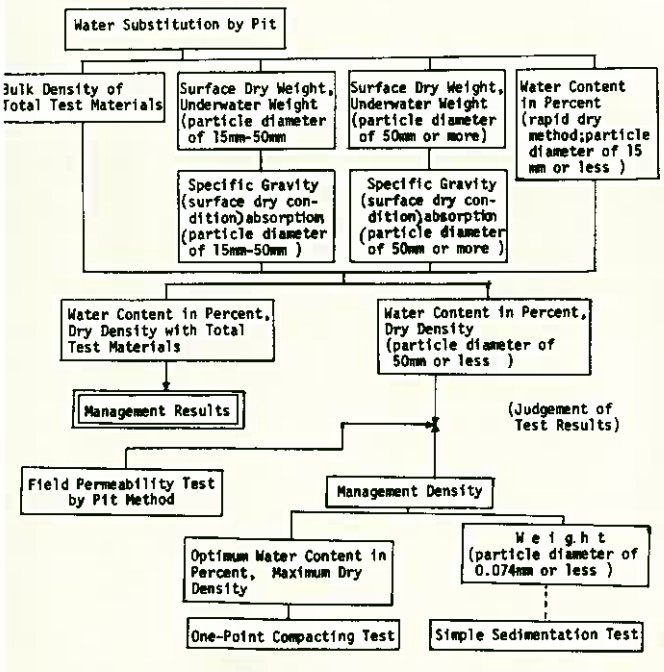

Flow Chart (1)

Flow Chart (2)

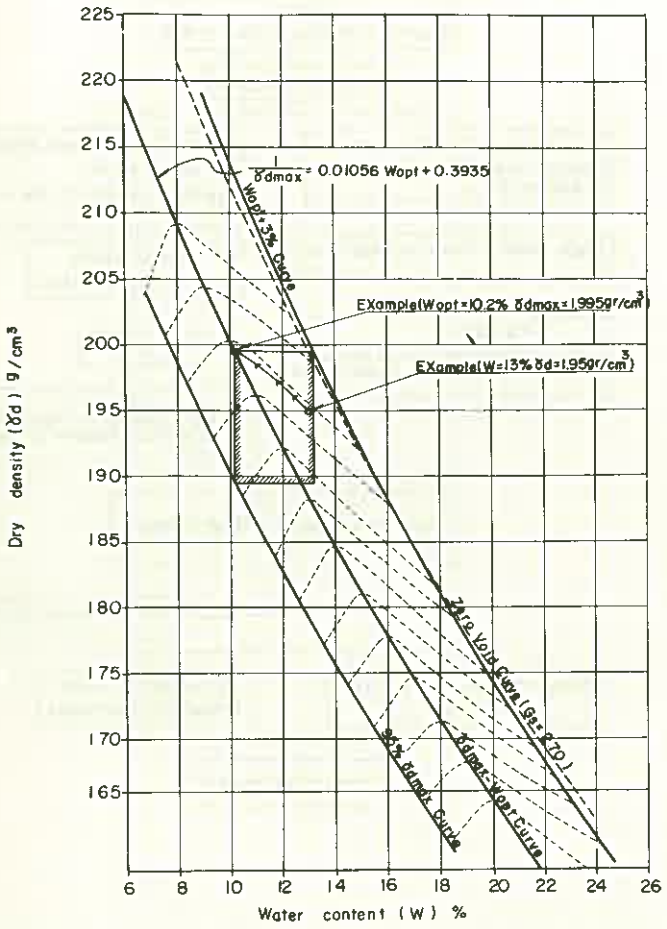

Fig-1 Water content - density curves used for determination of wopt.

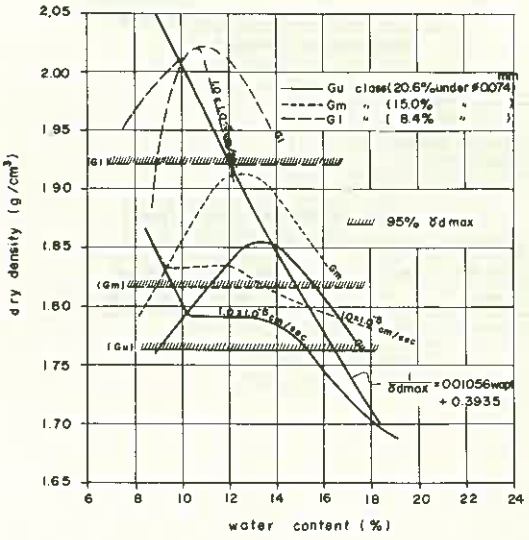

Fig-2 Water content, dry density and design impermeability curves

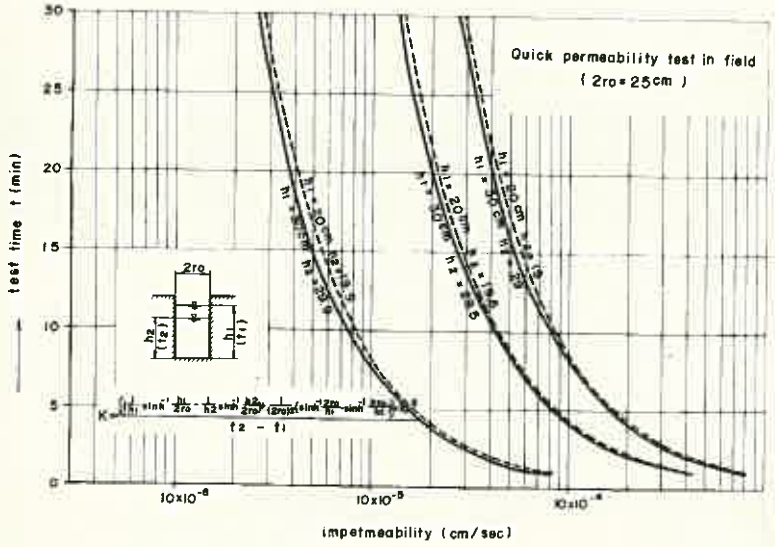

Fig-3 Time-impermeability curves used for quick permeability test in field

F. IN-SITU TESTING AND MEASUREMENT OF ROCK

USES OF ELECTRICAL PROSPECTING FOR TUNNEL GEOLOGICAL SURVEYING

Eizaburo YOSHIZUMI, Kyoto University
Chugoro SATO, Kajima Corporation

1. Introduction

During the recent past several years, tunnel engineering techniques have made rapid development and the plans of tunnel engineering works have grown very large. One of the problems of tunnel engineering works is to make tunnel geological conditions clear. Many tunnel engineers are turning to geophysical prospecting for an answer to some of these geological conditions. There are two major methods of geophysical prospecting. They are the earth resistivity prospecting method and the refraction seismic prospecting method. In tunnel geological surveying the latter is used mainly.

The cardinal aim of geophysical prospecting in geological surveying is to add a third dimension to surface geological maps. The primary job of the geophysicist is to analyze the data of geophysical constant which is used in prospecting and the secondary job is to translate these analyzed maps into the needed maps in geological surveying. This secondary job is called "interpretation", which seems to have indeterminate nature. First of all, the geophysicist has to make every effort to complete the primary job.

2. Earth resistivity prospecting

There are two kinds of measuring systems. They are so-called earthing resistance system and earth resistivity system as shown in Figs.1 and 2 respectively. The former is affected by the resistivity of material within a short

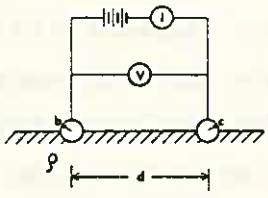

Fig.1 Earthing resistance system

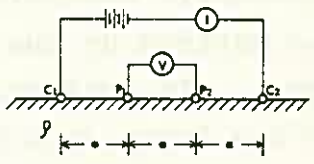

Fig.2 Earth resistivity system

distance of each electrode. For example, curves obtained by the earthing resistance measuring system in a borehole agree well with curves obtained by the cone penetration test qualitatively, because these curves are too much affected by a local earth structure. On the other hand, by using the latter the effect of the material near the electrode can be minimized.

There are many kinds of electrode configurations, one of which is shown in Fig.2. The so-called configuration or geometric factor of an electrode configuration is calculated by the distances of the four electrodes from each other and if the electrode configuration is altered so that the configuration factor becomes different. The so-called apparent resistivity is defined such a way that on homogeneous earth it remains the same value even if any kind of electrode configurations is employed. But on inhomogeneous earth it does not remain the same value and it shows the different value according to the different electrode configuration. Such physical interpretation of apparent resistivity makes this measuring method obscure.

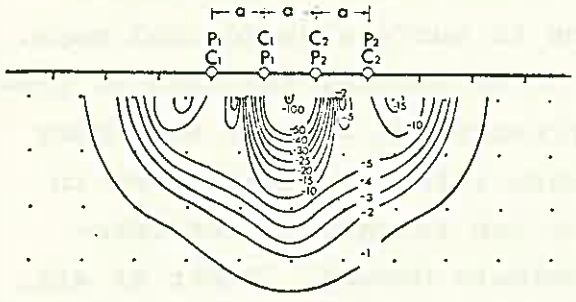

Fig.3 Sensitivity distribution

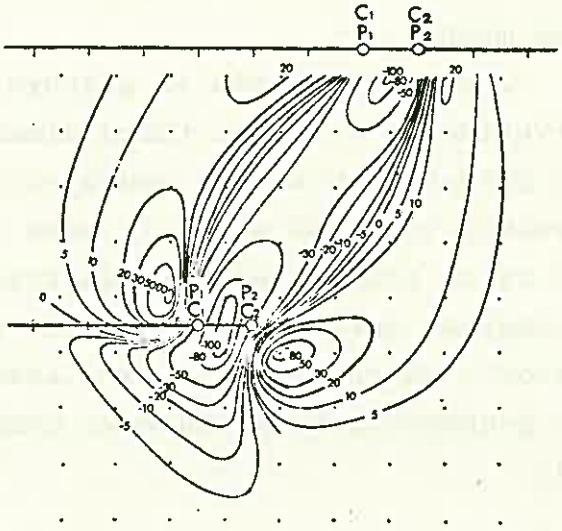

Fig.4 Sensitivity distribution

In order to make the feature of each electrode configuration distinctly characteristic, "sensitivity distribution" are proposed and defined by the authors and two examples are shown in Figs.3 and 4. In this report, the authors intend to explain the example of the Rokko Maya tunnel area by using the analog simulation analysis method and the sensitivity distribution analysis method.

3. Rokko Maya runnel area of New Sanyo Line

The aim of earth resistivity prospecting in this field is to prospect water-bearing fault zones. The subsurface cross-section of the Rokko Maya tunnel area is shown in Fig.5, depicting the topography, the tunnel and the proposed water-bearing fault zone which is analyzed by using the analog simulator which has been studied by the authors and their assistants since 1954. For example, resistivity profiles are shown in Fig.6 carried out at the earth surface of the field in Fig.5. Resistivity profiles at the corresponding earth surface of the analog simulator are shown in Fig.7 with homogeneous medium, namely with the topography only, by using the similar electrode configurations to the field procedure.

Broadly speaking, these resistivity profiles shown in Figs.6 and 7 are quite similar and it is clear that the anomaly in this case is keenly affected by the topography. The water-bearing zone in Fig.5 is analyzed by using the analog simulator and the solid electrode arrangement as well as the surface electrode arrangement, some sensitivity distributions of which are shown in Figs.6 and 7 respectively.

The authors wish to express thanks to members of the chair of geophysical prospecting, Kyoto Univ. and Kajima Corporation.

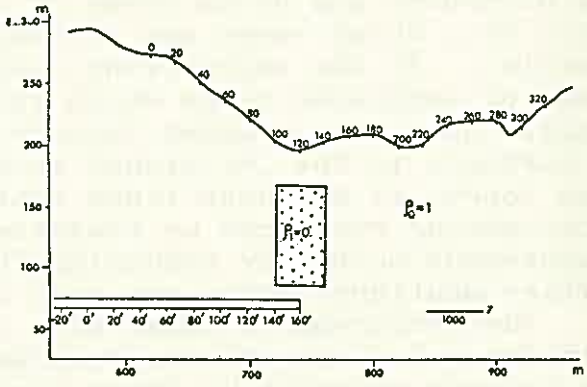

Fig.5 Subsurface cross section

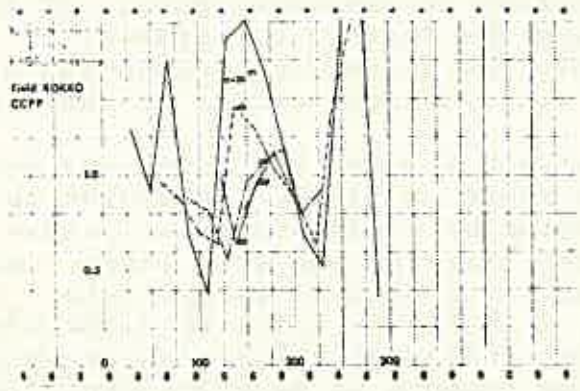

Fig.6 Profiles of field

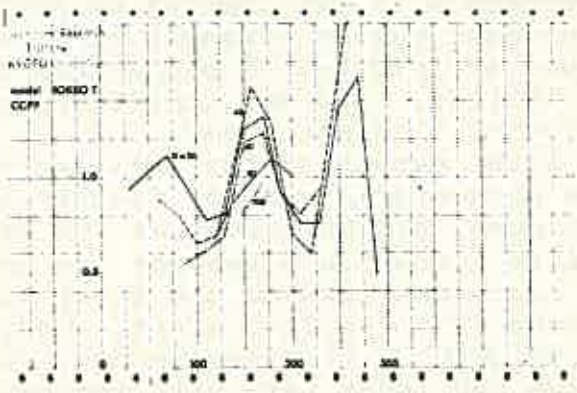

Fig.7 Profiles of simulator

GEOLOGICAL INVESTIGATION AND JUDGMENT OF ENGINEERING NATURE, UTILIZING BOREHOLE MEASUREMENTS

Kōzo TAKAHASHI, Honshu-Shikoku Bridge Authority
Kōji ISHIKAWA, Chuō Kaihatsu Corporation

1. Introduction

In investigating the engineering nature of foundation rocks for huge structures involving submarine rocks, such as the projected Honshu-Shikoku Liaison Bridges, there are restrictions which make it difficult to directly identify by the eye or inspect such rocks. Therefore, geological investigation method making use of borehole measurements has been applied, and attempts made to determine the engineering nature (particularly, deformation properties) using the various values obtained.

The rocks investigated are the weathered granites belonging to the Hiroshima and Ryoke types of the Cretaceous Period in the Mesozoic Era, which rocks are extensively distributed in the Inland Sea district. If the engineering nature, e.g., the deformation properties, of weathered rocks which intrin ically have fissures as the granite does, is governed largely by two factors, viz., the degree of hardness in the individual rocks and the degree of fissure in the base rocks, it has been found that the engineering nature of fissure-bearing rocks can be evaluated significantly with the borehole measurement method by combining those rocks in which the two properties mentioned above are easy to measure.

The measurements undertaken included judgement of the cores with the naked eye and the Rock Quality Designation Method (RQD), the primary velocity by Sonic Logging Method (Vps) and the formation resistivity by Electric Logging(Rt), the deformation modulus by Pressiometer(Esp), the uniaxial compressive strength(Qu) and the static elastic modulus(Esc) by coretesting

2. Index Properties of Measurement Values

The relationships shown between the various measurement values correspond with the degrees of weathering of the base rocks. If the measurement values strongly reflecting the factors of hardness or fissure are plotted as parameters into the dispersion tendencies of distribution, then the significance and index properties of the dispersion will become clear.

With respect to the relation between Esp and Vps, plotting Esp/Qu as parameter gives the results as shown in Fig.1. According to the figure, Esp/Qu which has the meaning of a modulus of a fissure tends to concentrate towards the upper limit of Esp with lower fissure rate, and towards the lower limit with higher fissure rate. In the case of a complete elastic body, E should be equal to $0.18\times10^{5}Vp^{2}$ (ρ=2.40, μ=0.3, V:km/sec)kg/cm^2, which indicates the degree to which modulus and index vary with increasing fissure as $Esp=100\sim50Vp^{3\sim4}$(kg/cm^2). When Esp and Vps are compared, meanwhile, the former is interpreted to reflect the two properties of hardness and fissure, the clearer if Qu showing the proper hardness of rock and Esp/Esc showing the degree of fissure are plotted as horizontal axis and parameter,

that Vps and RQD are evaluated as oppsite to each other, and that the softer rocks with less fissure lie closer towards the left side of the graph, or have Vps small and RQD large, while the harder rocks with more fissure lie closer towards the right side of the graph, or have Vps large and RQD small. Moreover, the tendency of the various parameters show by which of RQD and Vps they tend to be affected to a grater extent. Any change in this tendency seems to indicate that the degree of influence varies with the degree of hardness and fissure.

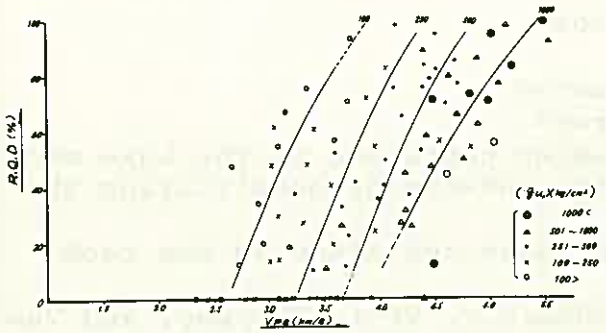

Fig-4 Relation Between R.Q.D and Primary Velocity (Vps)-(qu)

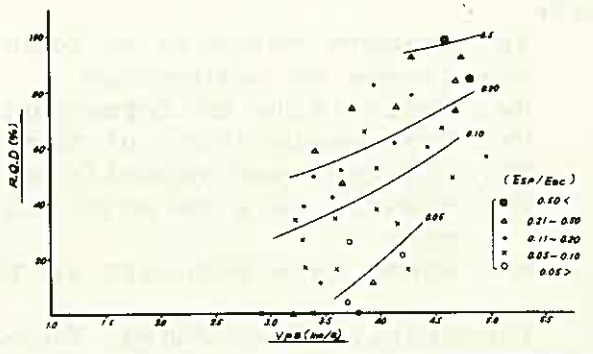

Fig-5 Relation Between R.Q.D and Primary Velocity (Vps) (Esp/Esc)

3. Judgment of Engineering Properties

If the engineering nature(deformation properties) of the base rock is governed largely by the two factors--the property of hardness inherent in the rock and the fissure of the rock as an aggregate--RQD which easily reflects the property of fissure relatively strongly, and Vps which easily reflects the property of hardness, among those which it is possible or easy to measure continuously, were combined and plotted with the measured values of Esp as parameters, to obtain the results as shown in Fig.6. According to this figure, it is judged that RQD and Vps are opposite to each other in their relationship with Esp. Moreover, this tendency is gentler (namely, greatly influenced by RQD) with the better-quality rocks, and steeper(namely, greatly influenced by Vps) with the worse-quality rocks.

From the foregoing studies, the engineering properties(deformation properties) of the base rocks can be judged. Fig.6 can be used as a judgment chart for engineering properties. Besides, it can be used as a judgment sub-chart in the Vp Rt or RQD Qu relation.

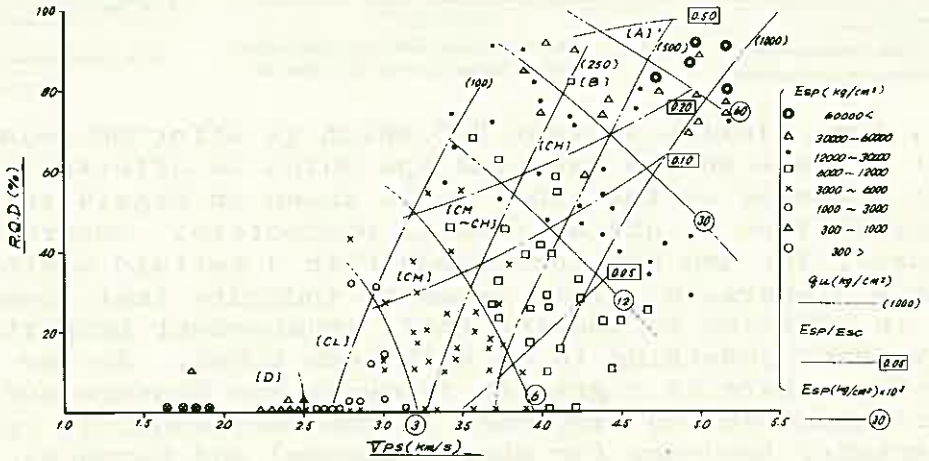

Fig-6 Engineering Judgement by R.Q.D. and Vps

respectively, to obtain the results shown in Fig.2.

Next, the relation between Vp and Rt is as shown in Fig.3, plotting 1/Vp as horizontal axis, $1/\sqrt{R}$ as vertical axis, and Ed as parameter. Generally Rt and Vps decrease with increasing degree of weathering, namely, with increasing porosity. When the degree of saturation, Sw, drops, Vps drops further, but Rt increases.

The empirical formulas of Wyllie (1956), Archie(1942), etc., can be rewritten and expressed, thus:

$$1/Vp=1/Sw\sqrt{Rw/Rt}(1/Vf-1/Vm)+1/Vm \quad \cdots\cdots(1)$$

$$1/Vp=(1-\phi)/Vm+\phi Sw/Vf+\phi(1-Sw)/Va \quad \cdots\cdots(2)$$

Where

Vp: primary velocity of base rock
Sw: degree of saturation
Rw: resistivity of formation water
Rt: true resistivity of base rock
Vf: elastic wave velocity of water contained in the base rock
Vm: elastic wave velocity in the substances constituting the rock
Va: sound wave velocity in the gases contained in the rock

Therefore, if Rw=20Ω-m, Vm=6.50km/sec, Vf=1.57km/sec, and Va=0.33km/sec, it can be shown by the graph of the figure.

From this it seems that Rt tends to be affected by both factors of fissure and hardness(viz., inherent fissure, and increased porosity following increased degree of weathering), and Vps tends to be greatly affected by hardness. By comparing these two factors, the degree of weathering in the base rock can be judged quantitatively irrespective of the degree of saturation.

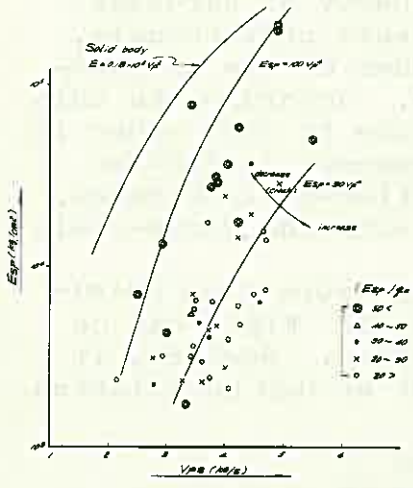

Fig-1. Relation Between Deformation Modulus (Esp) and Primary Velocity (Vp) (Esp/ρ)

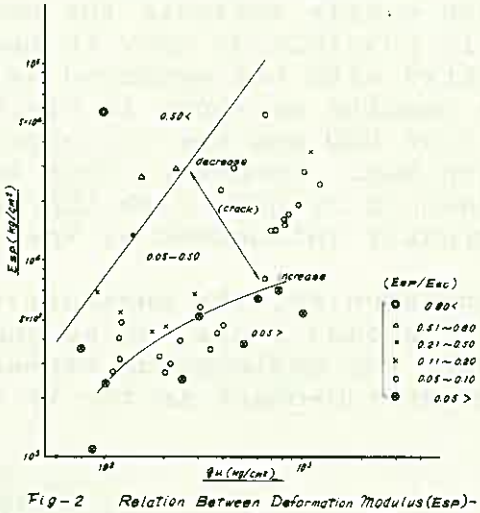

Fig-2 Relation Between Deformation Modulus (Esp)-Uniaxial Compressive Strength (qu) (Esp/Esc)

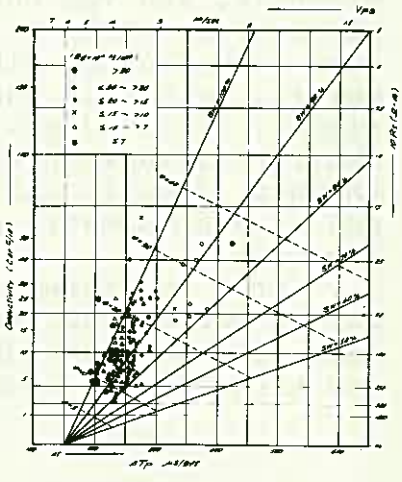

Fig-3. Relation Between Formation Resistivity (Rt) and Primary Velocity (Vps)-(Ed)

Next, the relation between RQD which is affected relatively greatly by fissure on one hand and Vps which is affected relatively greatly by hardness on the other is as shown in Figs.4 to 5, plotting classification Qu and Esp/Esc as parameters. According to these figures, Vps and RQD correspond with a certain width, but show considerable dispersion. This seems to indicate that fissure and hardness, in addition to showing their independent properties respectively, have something to do with each other. In the better-quality rocks, there is a greater tendency for fissure and hardness not to correspond but to disperse, in the worse-quality rocks, meanwhile, a greater tendency for shape(fissure) and hardness to correspond easily. This seems to mean that when weathering advances and the rock softens, brittleness is easily reflected in the shape of the core. As a result of the foregoing, the classification shows

ROCK PROPERTIES IN THE SEIKAN TUNNEL

Yutaka MOCHIDA
Japan Railway Construction Public Corporation

1) Introduction and Geology. The Seikan tunnel, conects Honshu and Hokkaido, is 53.85 km. long, including 23.3km. under sea part, and will be used for conventional railway and also for Sinkansen. Water depth on the tunnel is 140 m. maximum and its overlayer is 100 m. minimum. The geological surveys have been carried out by mean of dredging at sea bottom (2,109 points), seismic survey ("Sparker" 249 lines 2,027 km.)and drilling at the sea (4 sites) etc. This area is composed of sedimentary rocks, pyroclastic rocks and volcanic rocks, ranging over various ages of Neogene Tertiary. Volcanic rocks, andesite dolerite and rhyolite, are mainly exposed at southern part of the area. (Honshu side) All formations are disturbed by Neogene crustal deformations and as the result 10 big faults zone under the sea and basin structure at middle part of the straits were formed.

2) Rocks. In general rocks in the tunnel are soft rocks and semi-hard rocks, and these compressive strengthes are 50～1,000

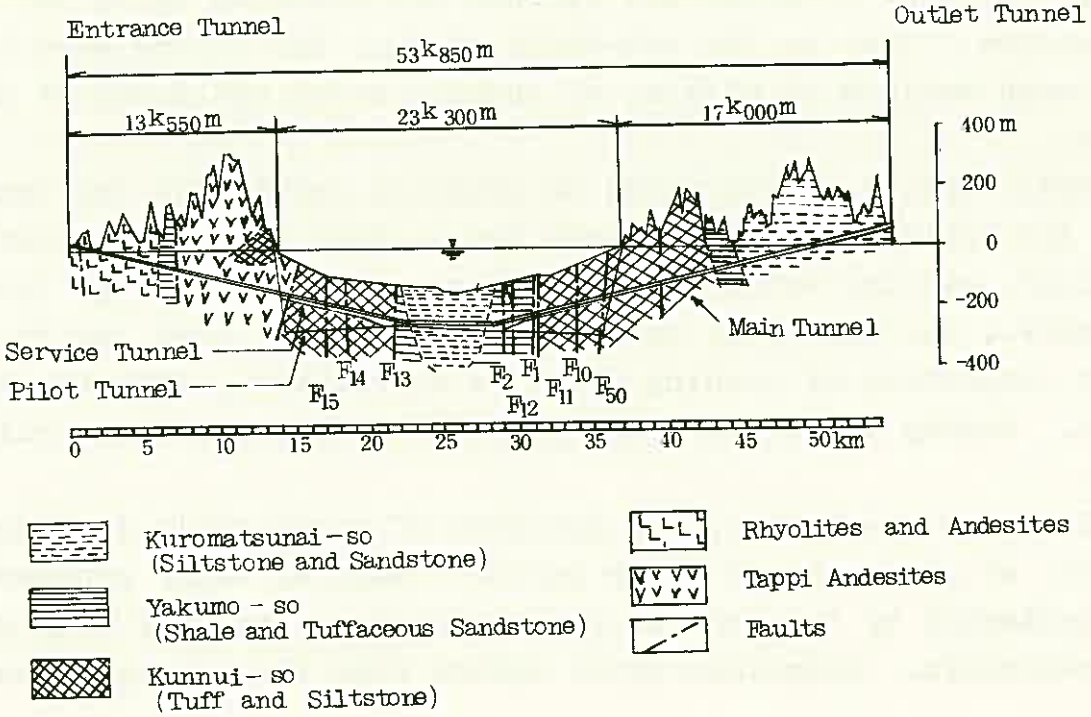

kg./cm². Volcanic rocks are comperative hard with many fissure and gushing water which usually should be cut off by grouting cement or the other materials pior to excuvation. 40,000 m³ grout have been carried out at Honshu side and 5,000 m³ at Hokkaido side (Northern part).

3) Faults. Some of big faults, F_{10} F_{15} F_{50} (see fig.) had been penetrated through. At F_{50} , a comperatively small fault, rocks were semi-hard rock with concentrated fructure and gushing water. Volume of grouted there materials was 1,3000 m³ F_{10} was one of bigger fault, and striking partially same direction of the tunnel. Rocks were tuff and siltstone with many montmorillonite. When swelling ground pressure exposed, gradually steel ring suports (ϕ5.0 m. 125 $^{m}/_{m}$ H-shape) had been deformed and collapsed. Reconstruction of this part was carried out with timbering 150 $^{m}/_{m}$ H-shape suport (ϕ5.0 m.) at out side and 125 $^{m}/_{m}$ H-shape suport (ϕ3.8 m.) at in side between them were sprayed 60 cm. thick shotcrete. F_{15} separated tafaceous part from andestic part at Honshu side and was intruded by thin dorelite dyke. From facing in F_{15} , water gushed out maximum 14 m³/min. with 300 m³ earth, and a length of 150 m. of inclined shaft was completely flooded. To excuvate though the F_{15} , exhautive grouting of colloid cement and chemical materials (2,500 m³) was carried out surrounding the tunnel to the thickness of 12 m. Prior to excavation 25 of drainge holes were drilled around the grouted zone to decreasing a water pressure for the tunnel. From them, 8 m³/min. of water was drained out assuring safty in excavation. Also in the sub-fault of F_{10} , the facing were broken down with maximum 10 m³/min. of gushing water and 1,000 m³ of earth.

4) Water inflow. Properties of grushing water into the tunnel (see the table) are mainly three types, that are fresh water near the land, captive water and sea water. Sea water change ions in the rocks, decreasing Mg and K, increasing Ca. Near the big fault properties of gushing water is approximatly same as sea water. Usualy these water was prospected by exploratry drillings.

5) In under sea tunnel, the pressure of water don't decrease inspite of great lot of water inflow. Most of water pressure are protected by the grounds consolidated as one body with grouting materials. Raimained water inflow from the grouted grounds

would be drained into the tunnel. On the basis of the above consideration water pressure would not press immediately against the tunnel lining except near the faults or the other soft ground at where linings would be pressed by ground pressure and some part of water pressure. Now quantities of water into the tunnel are 13.4 m^3/min at Honshu side excavated aproximately 3.3 km. long, and 5.2 m^3/min at Hokkaido side excavated aproximately 3.5 km. long in under the sea.

	Temp. (°C)	pH	Na^+ (ppm)	K^+ (〃)	Ca^{2+} (〃)	Mg^{2+} (〃)	Cl^- (〃)	So_4^{2-} (〃)
Sea water		8.4	11,000	430	390	1,272	19,560	2,520
Honshu side								
Pilot Tunnel	23	7.1	7,875	200	1,200	960	15,800	2,060
Service Tunnel		7.6	1,025	7	1,320	192	4,200	840
Hokkaido side								
Pilot Tunnel	30	7.3	1,800	8	846	69	2,772	2,080
Service Tunnel	21.5	7.6	3,300	6	1,624	163	6,700	2,420
F_{15}	24	7.3	9,300	265	880	1,536	18,815	1,980
F_{10}	19	8.4	10,000	250	1,000	1,056	18,500	2,360

Table Property of water

Rock	Density (wet)	Comp. strength kg/cm²	Tensile strength kg/cm²	Seismic velocity m/sec
Kunnui f.				
tuff	2.19	219	22	2,850
tuffbreccia	2.36	286	39	3,935
siltstone	2.18	474	33	3,050
Yakumo f.				
shale	1.82	629	107	2,650
siltstone	1.86	583	54	2,490
Kuromatsunai f.				
siltstone	1.11	49	9	1,320
sandstone	1.44	41	5	1,660
Andesite	2.72	964	111	5,495
Dorelite	2.66	571	84	5,030
Rhyolite	2.42	854	56	4,615

Mechanical properties of rocks

ROCK MASS INVESTIGATION —
AN ATTEMPT AT QUANTIFYING ITS MECHANICAL PROPERTIES

Tōru F. ONODERA, Ryūnoshin YOSHINAKA and Masanobu ODA,
Saitama University

Studies have been carried out to express the field data on the mechanical properties of rock mass quantitatively so as to furnish full boundary conditions for calculation.

1. Exposure survey on rock mass

1) Distribution of strength: Point load tensile strength tests on un-trimmed specimens were correlated to the uniaxial compressive strength and to the tensile strength by radial compression tests. An example of the distribution of rock strength on a proposed dam foundation of Miocene tuffaceous complex is shown in Fig. 1.

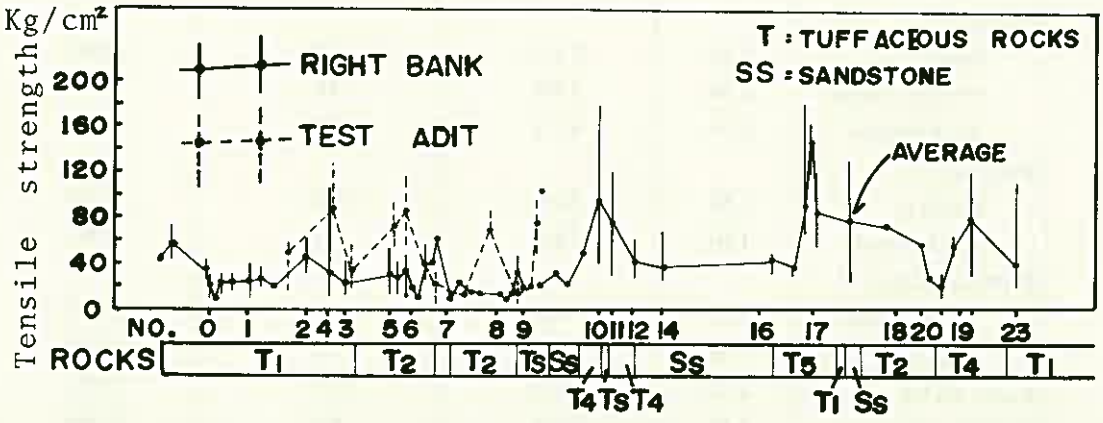

Fig. 1 Rock strength distribution

2) Friction test on joint surface by shearing device: Shearing device tests were applied to granite specimens of intact rock (simulating rock substance), split specimens by radial compression (simulating rough tension joint) and smooth cut specimens (simulating shear joint). Fig. 2 shows the relation of friction angles to porosity being a basic index property of the granite.

3) Application of Schmidt concrete test hammer: Rebound values by Schmidt test hammer were measured on rock masses of known geology. Statistical analyses on frequency distribution, mean values and variances of rebound values resulted that the

rebound value gives index to rock strength and loosening by joint frequency.

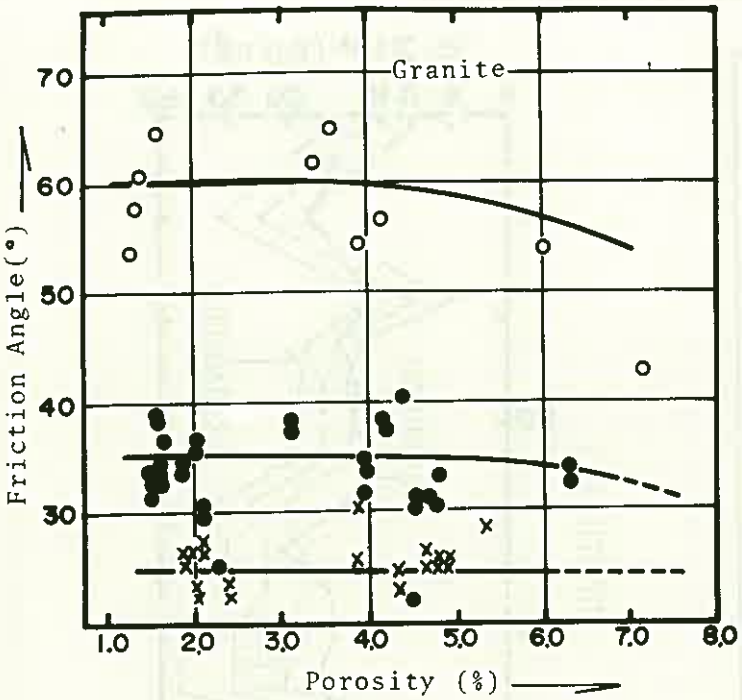

Fig.2

- o Internal friction angle of intact rock
- ● Angle of shearing resistance between rough serfaces at residual strength
- × Angle of shearing resistance between smooth (thawn) planes

2. Drilled core survey: Results of geological observations on the walls of test adits in granite were correlated to RQD (for each one meter) of pilot boring, physical and mechanical test values on the drilled core. Simple test values such as porosity n and Shore hardness compensate for observational discrimination. Fig. 3 summarizes some relations on a test adit.

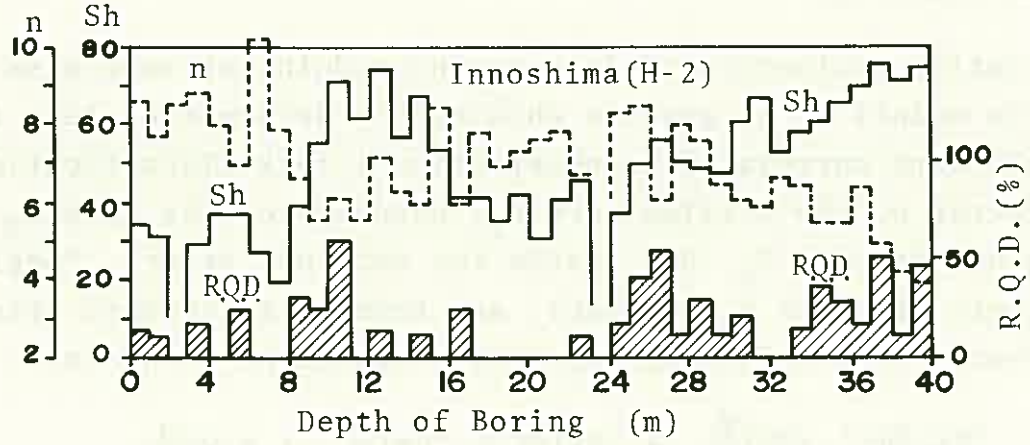

Fig. 3 Representation of test adit by boring core tests (n: porosity, Sh: Shore Hardness)

3. Tentative evaluation of shearing strength of rock mass: In-situ shear test results in test adits of granite mass of known geology were correlated to RQD, strength of drilled core, strength of rock specimens in the adits, basic physical properties and so

on. Fig. 4 shows an example in which shearing strength of the granite can be estimated by RQD for each adit at constant Shore hardness depending on internal friction angle.

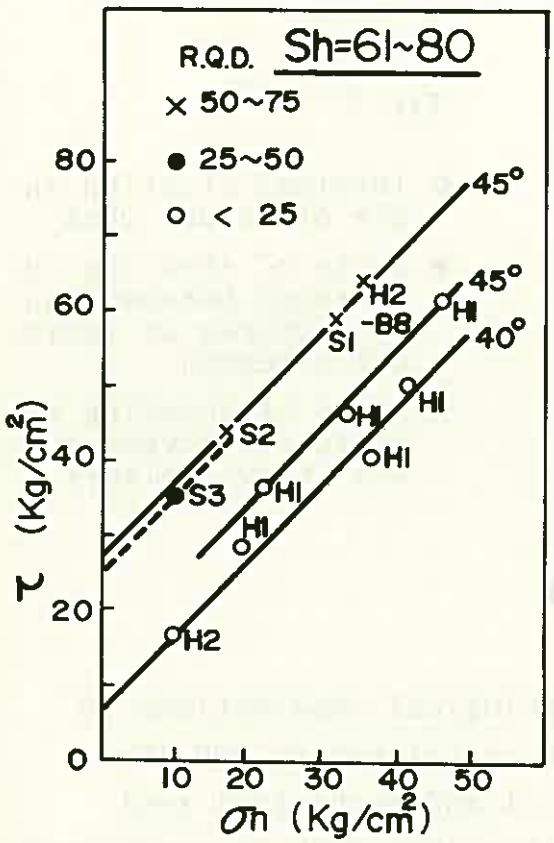

Fig. 4 Relation between shearing strength of rock mass and RQD at constant Sh.

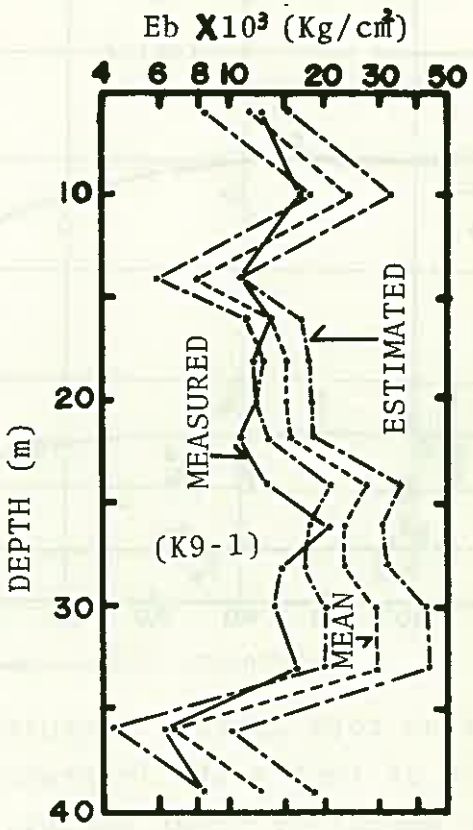

Fig. 5 Measured and estimated deformation modulus.

4. Tentative evaluation of deformation modulus of rock mass: Deformation moduli E_b on granite obtained by deformation test in the bore hole were correlated to observational rock classification C_1, shape factor of the drilled core C_2, hardness of the core C_3, weathering of the core C_4, RQD (ratio for each one meter), longitudinal seismic velocity V_p (km/sec), and transverse seismic velocity V_s (km/sec). The following regression equation is obtained;

$$\log_{10}Eb = 5.52\times10^{-2}C_1 - 4.76\times10^{-2}C_2 + 2.20\times10^{-1}C_3 - 1.92\times10^{-1}C_4 - 1.08\times10^{-3}RQD + 2.13\times10^{-1}V_p + 5.41\times10^{-2}V_s + CONST.$$

where const. equals 2.67. Fig. 5 shows the correlation in the sequence of depth of the drill hole. In the figure full line indicates measured values, dotted line indicates calculated values and chain lines show area of confidence coefficient 90%.

A NEW INVESTIGATIVE METHOD OF UNDERGROUND WATER
--Underground temperature survey in and around landslide areas--

Atsuo TAKEUCHI, Kyoto University

Some reports on landslide areas suggest strongly that the underground water relating with the landslide activity exists in vein stream form rather than in strata form. This conjecture may not be applied to all landslide areas, but in the case of interpreting the phenomena in landslide area, this seems to be reasonable. If a part of the underground vein stream in plugged by some causes, the confined water would be gathered behined that part and for this reason the pore water pressure would increase and the resistance against the sliding force of the landslide mass would decrease. It is considered sufficient to cause a partial landslide activity which spreads in all parts of this landslide area, which has been in the critical condition for sliding, resulting thus in a large scale landslide movement. Accordingly, if an abnormal fluctuation of water table is noticed, the water gathering in this section must be drained in a hurry, thus the partial landslide activity caused by abnormal ground water can be prevented and a large scale landslide movement can also be got rid of. For the purpose it is necessary that the position of the vein can be found out in advance in order to secure time for conducting proper measures for the drainage. However, the existing investigation method employing tracer, has many defects for the purpose to get information about the flowing channel of underground water.

Various kinds of investigation method of ground water are conducted at present for obtaining the information on the flowing channel of ground water , but in every methods, it is necessary to sample water directly from either bore holes, spring points, wells or ponds. This fact means that the applicability or reliability of interpretation on the basis of the above mentioned methods including the tracer method are limited by the available number of the sampling points. In practice it is difficult to get many sampling points as necessitated by economical or others reasons. Thus it would be dangerous to discuss the channels of vein stream in and around the landslide area on the basis of the results of the average tracer method utilizing a small number of sampling points. It is thus desirable to avoid carrying out landslide-preventive works related to underground water, until one has

collected accurate information about the channel of vein streams in order to improve the effect of the measures. The tracer method requires much time and expense and the information thus obtained are precious. The position of the channels of vein stream, therefore, should be presumed in advance by other methods and the effect of each stream on landslide activity is evaluated before conducting the tracer method. The method should be first conducted for the confirmation of the most important vein stream.

From the above mentioned considerations, the author discusses whether or not the underground temperature measurment, which is effective in a hot-spring survey, could be adopted as one of the methods to presume the position of vein streams in and around landslide areas.

For the purpose of trying the method, temperature measurment was conducted in the Kamioogi landslide area in Shiga Prefecture, which site is characterized by simple underground structure, simple configuration and the relatively uniform ground-surface condition. The geology of this area consists of the Namjo clay layer and the Kamioogi gravel layer overlying the former. The former is a sound impermeable layer and the latter is a sound permeable layer. Underground water exists mainly in the latter.

Measuring method of temperature is as follow: Making a hole in the ground of 1 m depth and 25 mm in diameter by piercing an iron bar into ground, and a thermistor is inserted into the hole. After ten minutes, the indication of thermistor is read, which may be regarded as the underground temperature at 1 m depth of the measuring point. Some results are shown in Fig.1. What is evident is that low temperature parts exist in each measuring line. These low temperature parts do not seem to be caused by the effects of geological and topographical difference, diurnal variation of underground temperature or difference of ground surface condition. In the results of the measurment, the total average of the temperature is 19.88°C and temperature of spring gushing out in this area 15.35°C. The temperature of water is very low compared with that of surounding underground. Accordingly if this cool water flows, taking heat away from the ground surface at the same time, the temperature around the cool

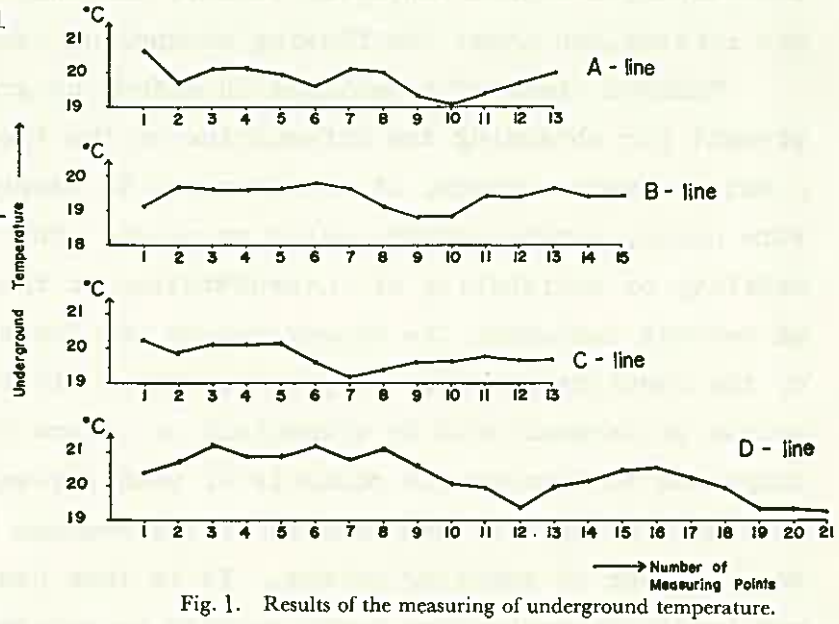

Fig. 1. Results of the measuring of underground temperature.

vein stream will become lower compared with that of other place. If the low temperature part is not the result of geological or other conditions, it may most reasonably be attributed to the effect of flowing cool vein stream. The vein stream line obtained by connecting the low temperature part with one another is shown in Fig.2. The dimension of the vein streams estimated by the YUHARA's method are shown in Fig.3. From the results it is suggested that there is a vein stream having the dimension of 5 m radius in 10 m depth. It is naturaly by no means insisted that the vein stream with a radius of 5 m exists in the presumed place and that water flows with a rush in the vein in reality. But at least it is suggested that the underground water having a higher velocity than those of the other flows is concentrated at the vein given by the calculation. Accordingly, if a water-collecting well is constructed at the place of the presumed vein, it is expected that a large quantity of water can be drained. On the basis of this result, a water-collecting well (III), which was 3 m in diameter and 15 m deep, was constructed at the position shown in Fig.2 and 3. A great amount of water gushed into the well in the depth between 3.5 m and 13 m. This quantity(51 l/min.) is greater than those at two other water-collecting wells (I and II) at the site (total quantity was 35 l/min.). A larger quantity of water was thus drained from one of three wells, nevertheless three wells were excavated in the same permeable layer. Therefore, it must be noted that there is a route where the underground water flows concentratedly even in an apparentry uniform permeable layer.

Above mentioned results indicate that measurment of underground temperature is one of the useful methods for vein-stream investigation.

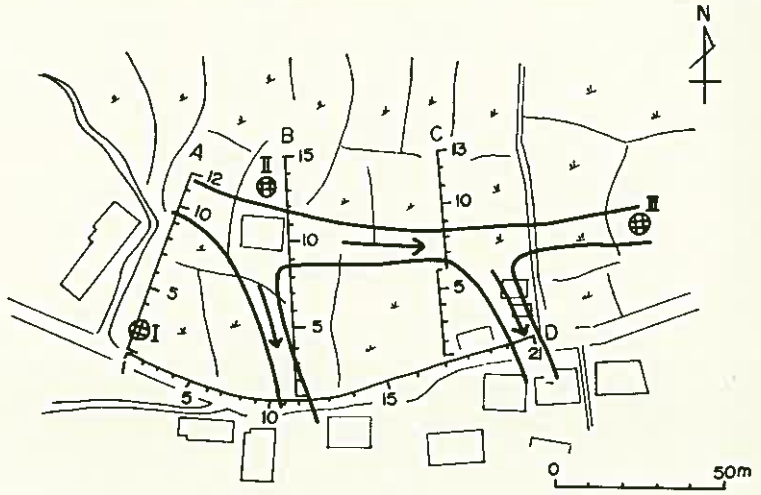

Fig. 2. Measuring lines of underground temperature survey and presumed channel of underground water vein-stream from its result.

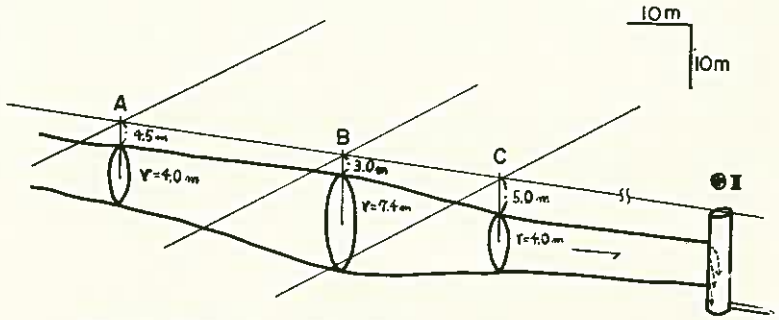

Fig. 3. Existent condition of the vein-stream by calculation.

G. PROBLEMS OF SEEPAGE FLOW

ON THE ANALYSIS OF STEADY STATE SEEPAGE THROUGH EMBANKMENT

Toshikazu KAWAMOTO, Depart. of Civil Eng. Nagoya University

Hiroya KOMADA, Central Research Institute of Electric Power Industry

Tomonobu MIYAGUCHI, Chubu Electric Power Co. Ltd.

Seepage problems have been solved by sketching flow nets or relaxation method. These methods are scarcely practical when the boundary of the region of seepage is not clearly defined and the soil media are non-homogeneous and nonuniformly anisotropic.

In this paper, the application of the finite element method to such problems is explained and the effective stress distribution due to seepage flow in a rock-fill dam is discussed.

A computing procedure of finite element analysis for estimating the seepage flow with unknown top flow surface in the embankment is shown in Fig. 1 and Fig. 2. In this analysis, the position of the top flow surface in the embankment is successively until the boundary conditions $H_s = y_s$, and $\partial H_s/\partial n = 0$ are satisfied on its surface. This procedure may be applied for any shape of embankment and non-homogeneous or anisotropic media. It is enough here to use only input data for the region of seepage which is primarily divided into an arbitrary system of triangular elements, since the successive steps of calculation are automatically performed in the computer. For an example of the calculated results, the top flow lines are illustrated in Fig. 3 for the embankment with slopes of 1 on 1.5. It has been found that the exit point obtained by the finite element method is about 5% higher than that drawn in the manner suggested by Casagrande at the upstream part within the embankment.

Then the quantities of seepage water through the section T_1, T_2, ... , T_5 in Fig. 3 are calculated using the velocity in the elements of both the uptream side and the downstream side of each section. The calculated values and the mean values between the both are presented in Table 1. On the other hand, the quantity calculated by Casagrande's method is 1.60. The accuracy of calculated seepage flow line and hydraulic potential distribution may be also estimated from the quantities of seepage flow. Maximum deviation of the quantity of flow is represented by the maximum value of $|\overline{q} - q_i|/\overline{q}$, in which q_i is the quantity of flow through earch section and $\overline{q}$ is its mean value. In this calculation, the maximum deviation is 0.006 using the quantities in Table 1. The top flow line in the embankment with anisotropic media ($k_y = 0.1\, k_x$) is simulta-

neously shown in Fig. 3. Besides the top flow line and the hydraulic potential distribution in the embankment with core media is presented in Fig. 4.

The equilibrium equations between the effective stress and the hydraulic potential due to seepage flow are obtained as follows from the relation as shown in Fig. 5.

$$\frac{\partial \sigma_x}{\partial x} + \frac{\partial \tau_{xy}}{\partial y} = \gamma_w \frac{\partial H}{\partial x} - X$$

$$\frac{\partial \sigma_y}{\partial y} + \frac{\partial \tau_{xy}}{\partial x} = \gamma_w \frac{\partial H}{\partial y} - Y$$

It is found from the above equations that the effective stress due to seepage flow may be estimated by treating the hydraulic gradient multiplied by γ_w for body forces.

For an example, the equivalent body forces to the seepage flow in the center core of rock fill dam are shown in Fig. 6. The effective stress distribution in core part and rock fill part of downstream side due to the equivalent nodel force given in Fig. 6 (b) is calculated in Fig. 7. It is found from the above that the effective stress due to seepage flow has much influence on the stability in core part and near downstream slope of rock fill dam.

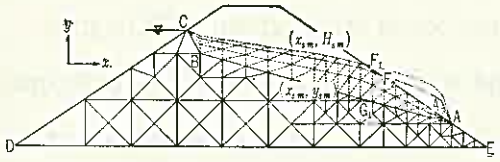

Fig. 1 Procedure of F. E. M. of steady state seepage through embankment

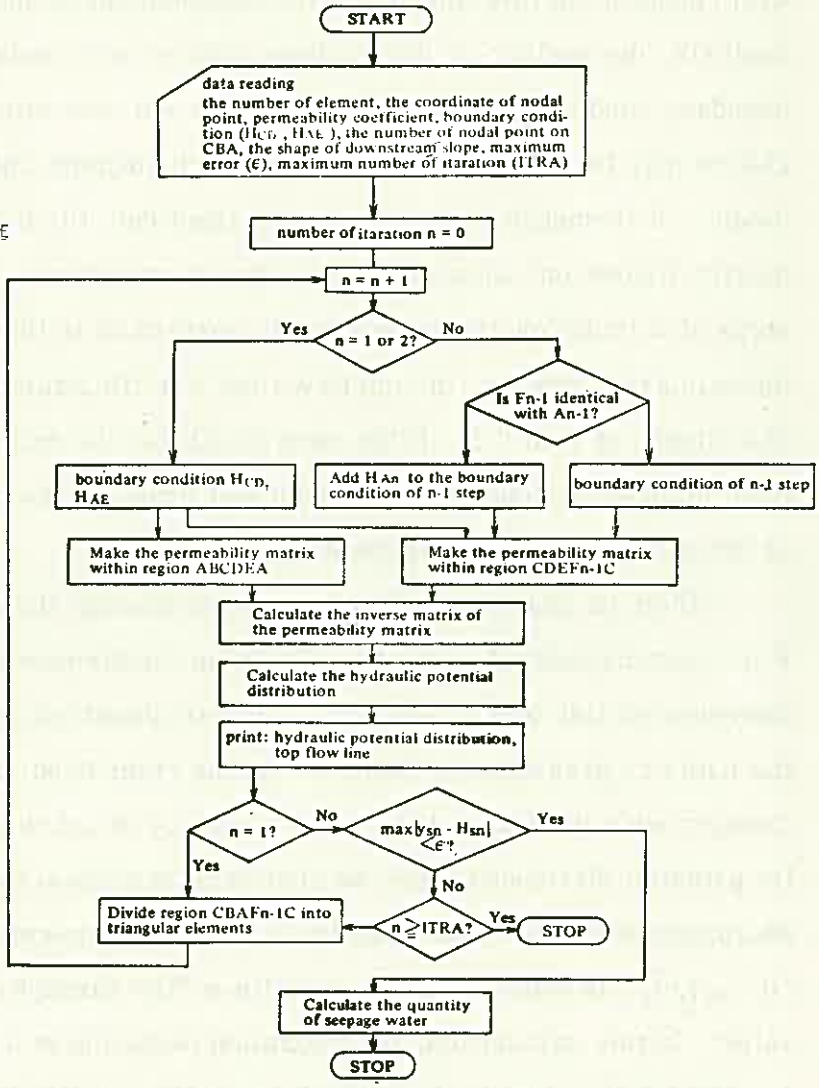

Fig. 2 Flow chart of seepage analysis in Fig. 1

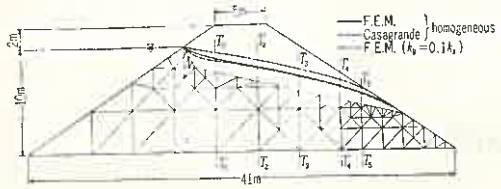

Fig. 3 Top flow line and section of calculated amount of flowing

Fig. 4 Seepage line and hydraulic potential distribution in embankment with core media

Table 1. Quantities of seepage water through each section in Fig. 3

section	upstream side $\Sigma Q_i{}^u/k$	downstream side $\Sigma Q_i{}^d/k$	mean Q/k
T_1	1.710	1.958	1.834
T_2	1.738	1.921	1.830
T_3	1.758	1.951	1.852
T_4	1.752	1.913	1.832
T_5	1.781	1.926	1.854

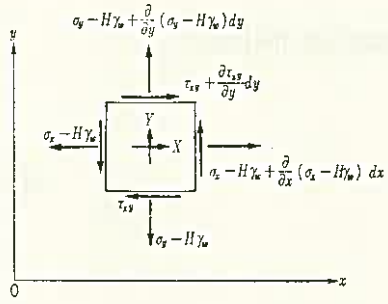

Fig. 5 Equilibrium of effective stress at two-dimensional state

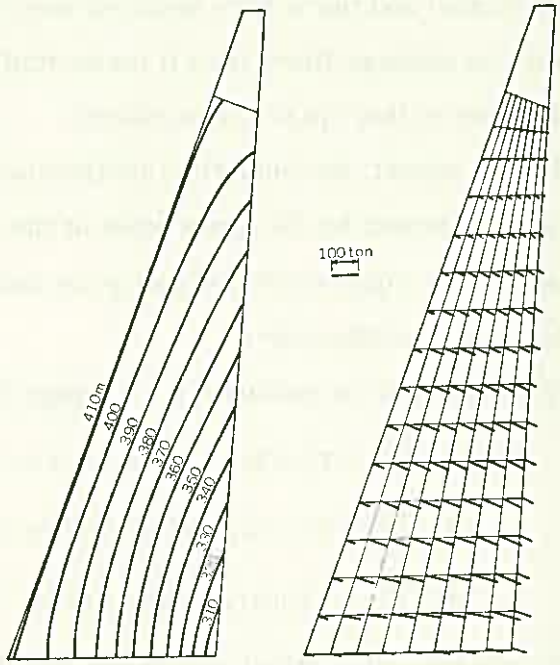

(a) Hydraulic potential distribution (b) Equivalent nodal force

Fig. 6 Hydraulic potential distribution and equivalent nodal force due to seepage flow in core part of rock fill dam

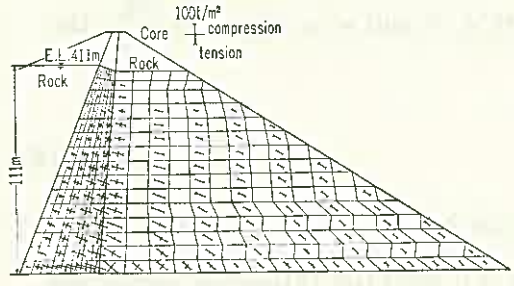

Fig. 7 Effective stress in rock fill dam due to seepage flow

ANALYSIS FOR NONSTEADY SEEPAGE FLOW[1)]

Ryuichi IIDA, Hajime ASAKURA
Public Works Research Institute, Ministry of Construction

Recently several studies on the analysis of seepage flows by finite element method are presented and there have been achieved some progresses in the field of numerical analysis on seepage flows but all these studies are restricted in steady flows or non-steady flows without phreatic surfaces.

In this report, the analytical method for nonsteady seepage flows with phreatic surface are presented by the application of the principle of variation to the equations of motion and the equation of continuity for seepage flow taking the equation of the phreatic surface into consideration.

The equations of motion for a seepage flow are represented as follows

$$\left.\begin{aligned} \beta_x \frac{\partial h}{\partial x} + \gamma (u/k_{11} + v/k_{12} + w/k_{13}) = 0 \\ \beta_y \frac{\partial h}{\partial y} + \gamma (u/k_{12} + v/k_{22} + w/k_{23}) = 0 \\ \beta_z \frac{\partial h}{\partial z} + \gamma (u/k_{13} + v/k_{23} + w/k_{33}) = 0 \end{aligned}\right\} \quad (1)$$

and the equation of continuity is represented as follows

$$\beta_x \frac{\partial u}{\partial x} + \beta_y \frac{\partial v}{\partial y} + \beta_z \frac{\partial w}{\partial z} = -\alpha \frac{\partial h}{\partial t} \quad (2)$$

If the equation of the phreatic surface is represented as follows

$$f(x, y, z, t) = 0 \quad (3)$$

and if the movement of the phreatic surface by velocity u, v and w is equal to $\frac{\partial h}{\partial t}$, the following equation must be held.

$$\beta_x u \frac{\partial f}{\partial x} + \beta_y v \frac{\partial f}{\partial y} + \beta_z w \frac{\partial f}{\partial z} = \gamma \frac{\partial f}{\partial z} \frac{\partial h}{\partial t} \quad (4)$$

If u, v, w and h satisfy the equation (1), (2) and if $u+\delta u$, $v+\delta v$, $w+\delta w$ and $h+\delta h$ satisfy the equation (1) and do not satisfy the equation (2), then the following equations must be held.

$$\beta_x \frac{\partial}{\partial x}(\delta h) + \gamma (\delta u/k_{11} + \delta v/k_{12} + \delta w/k_{13}) = 0$$

$$\beta_y \frac{\partial}{\partial y}(\delta h) + \gamma\,(\delta u/k_{12} + \delta v/k_{22} + \delta w/k_{23}) = 0$$

$$\beta_z \frac{\partial}{\partial z}(\delta h) + \gamma\,(\delta u/k_{13} + \delta v/k_{23} + \delta w/k_{33}) = 0$$

By these equations, we obtain

$$\iiint \Big[\Big\{ \beta_x \frac{\partial}{\partial x}(\delta h) + \gamma\,(\delta u/k_{11} + \delta v/k_{12} + \delta w/k_{13}) \Big\} u + \Big\{ \beta_y \frac{\partial}{\partial y}(\delta h) + \gamma\,(\delta u/k_{12} + \delta v/k_{22} + \delta w/k_{23}) \Big\} u + \Big\{ \beta_z \frac{\partial}{\partial z}(\delta h) + \gamma\,(\delta u/k_{13} + \delta v/k_{23} + \delta w/k_{33}) \Big\} w \Big] dx\,dy\,dz = 0$$

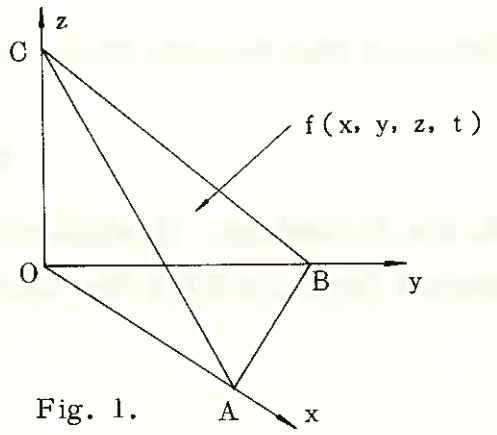

Fig. 1.

Now if the boundary surface on the phreatic surface denotes by F and the boundary surface in the permeable layer denotes by S, and if the equation (2) and (4) are substituted to this equation, we obtain the following equation.

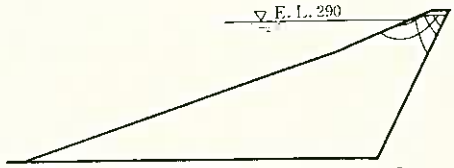

(a) $k=10^{-1}$ cm/sec, 2 hours after

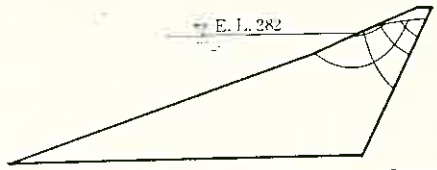

(b) $k=10^{-1}$ cm/sec, 4 hours after

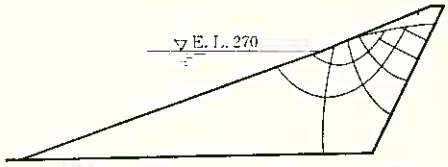

(c) $k=10^{-1}$ cm/sec, 6 hours after

Fig. 2.

$$\int \big[\beta_x u \cos(n, x) + \beta_y v \cos(n, y) + \beta_z w \cos(n, z)\big] \delta h\, ds + \int \gamma \frac{\partial h}{\partial t} \delta h \cos(n, z)\, ds + \iint \alpha \frac{\partial h}{\partial t} \delta h\, dx\,dy\,dz + \gamma \iiint \big[(u/k_{11} + v/k_{12} + w/k_{13}) + (u/k_{12} + v/k_{22} + w/k_{13}) \delta v + (u/k_{13} + v/k_{23} + w/k_{33}) \delta w \big] dx\,dy\,dz = 0 \qquad (5)$$

This is the variational equation for the seepage flow with a phreatic surface. By this equation analysis by finite element method for the seepage flow with phreatic surface become to be able. By this equation it becomes clear that the movement of the phreatic surface per unite time is proportional to the in-flow per unite time on the phreatic surface which is necessary to keep the phreatic surface on the same position.

Fig. 2 shows the results of calculation for the phreatic surfaces and the flow nets in

a rockfill dam when the water level draw down.

Reference

R. Iida, H. Asakura: "Analysis of Nonsteady Seepage Flows by Finite Element Method" Journal of Public Research Institute, Vol. 142, No. 1.

H. OTHERS

THE FLOW OF THE EARTH'S CRUST CONSIDERED FROM THE QUATERNARY CRUSTAL MOVEMENTS IN SOUTHWEST JAPAN

Hidebumi ITÔ, Kyoto Women's University
Kazuo HUZITA, Osaka City University

The mechanical behaviors of rocks during a long period of million years are considered on the scale of the earth's crust in this paper. Now, we are attending to the areas of Kinki and Chubu in the Inner Zone of Southwest Japan. Here, abundant active faults are distributed cutting the pre-Neogene basement

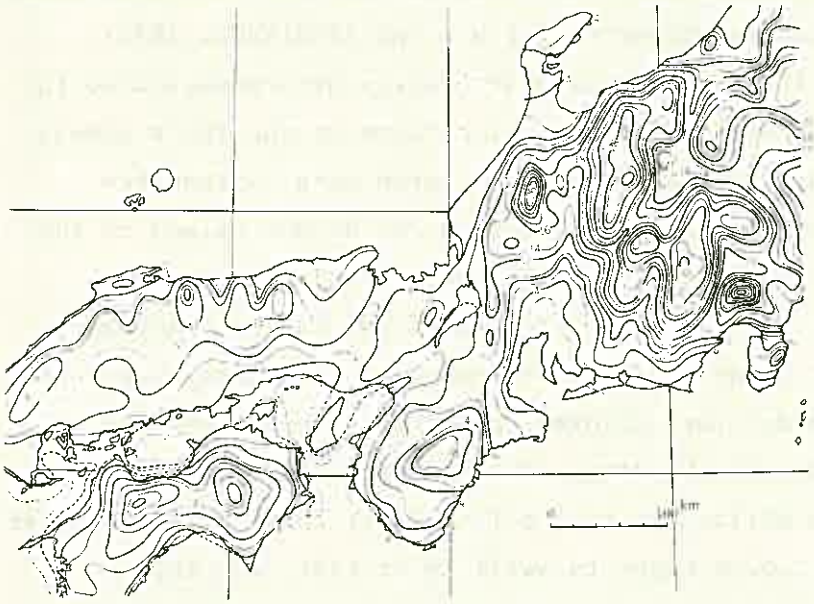

Fig.1 Summit level map of 200 m contours, drawn based on the highest points in 20 km quadrates using 1/200,000 topographic map of Japan (after M. TANAKA).

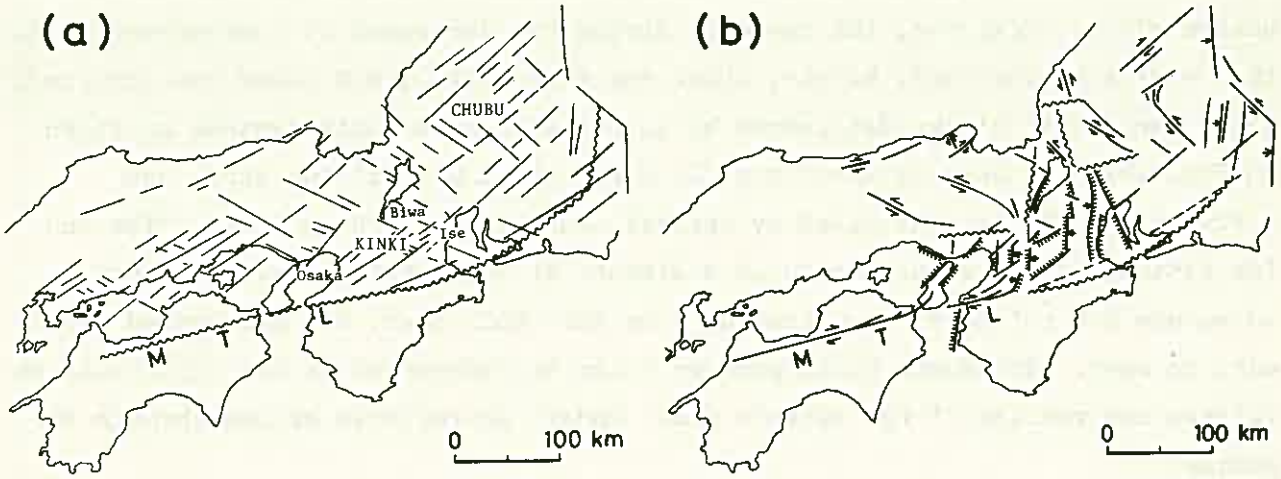

Fig.2 Process of developments of fault systems in the Inner Zone of Southwest Japan (HUZITA, 1974). (a) Older linearments recognized in the photographs of ERTS (Earth Resources Technology Satellite). These may represent strike-slip faults appeared 1.6 million years ago. (b) Active faults which have appeared since 0.3 million years ago.

rocks as shown in Fig.2(b), most of which coincide with the high-seismicity zones of microearthquake.

The Quaternary crustal movements of these areas have been revealed by the studies of HUZITA (1969, 1974) and his collaboratores from the view-points of neotectonics as follows. Before the Quaternary Period, the areas had been widely covered by the peneplain with low relief. The summit level map of Fig.1 showing the present topographic features reflects that the uplift and subsidence of the land during the Quaternary Period is due to the undulation (foundation folding of MAKIYAMA,1956) with axis of N-S trend. The strike-slip faults shown in Fig.2(b) consist of conjugate sets of NW-SE (left lateral) and NE-SW (right-lateral) trends. Whereas, the faults of N-S trend are thrust type. Such fold and fault systems suggest that the areas have been under the tectonic stress state of horizontal compression in E-W trend through the Quaternary Period. It has been also found that the earthquakes occurred in the crust of these areas have been generated by the tectonic pressure of E-W trend (ICHIKAWA, 1971). According to OIKE and others, the foci of microearthquakes are concentrated in the depths shallower than 15 km, which coincides with those of the fault planes estimated from the displacements of the faults associated with earthquakes. Therefore, we may conclude that the faults in these areas do not extend to the deeper part of the crust, but are limitted in the upper crust.

Thus, HUZITA has proposed the following process of the tectonic movements of the Inner Zone of Southwest Japan. At the beginning of the Quaternary Period (about 2 million years ago), undulatory deformations started under the E-W compression. Then, it entered into the stage of fracturing represented by strike-slip faulting about 1.6 million years ago (Fig.2(a)) to divide the upper crust into fault blocks. The blocks began to swell up or tilt, and then differentiation among the uplifted mountain lands and subsiding basins has become clear. Moreover, the tectonic stress has increased to concentrate it at the corners of the fault blocks, where the thrusting of N-S trend has occurred. Thus, many fault blocks determined by such complicated fault systems as shown in Fig.2(b) have been elevated rapidly since about 0.3 million years ago. A few tilted blocks controlled by special conditions, such as Osaka, Biwa and Ise basins, have accumulated thick sediments on the subsiding sides. Such movements did not go on simultaneously on the whole area, but propagated from east to west. The above whole processes can be understood as the expression of lateral contraction of the earth's crust under the tectonic stress through the period.

Although we can find out some places where the amount of the Quaternary uplift exceeds 1500 m, the average amount of it can be estimated to be 500 m from the 1/2,000,000 Quaternary tectonic map of Japan (1969). How much has the

crust been laterally contracted ? Considering that the Bouguer anomalies of gravity of these areas show almost keeping the state of isostacy, the crust has been deformed always in the state of isostacy. Assuming the mean density of the crust and that of the upper mantle to be 2.8 and 3.3 gm/cm^3 , the uplift of 500 m corresponds to the increment of 3,300 m of crust's thickness. Hence, the vertical expansion of the crust with about 40 km thickness is 8 % on the average. Since above mentioned conjugate strike-slip faults show that the minimum principal axis of stress is in the nearly N-S trend, the N-S horizontal expansion of the crust is above 8 %. Thus, the E-W horizontal contraction is estimated to be more than 16 %. Such a large contraction can not be explained only by the tilting or slipping movements of the rigid blocks of the upper crust, but each block itself has to be contracted as well as the crust does on the whole.

As the tectonic movement has been accelerated at the later stage, let us take the strain rate $\dot{e} = 0.16/1$ million years $= 1.6 \times 10^{-7}$ /year, provided the contraction $e = 0.16$. At the places where the uplift reaches 1500 m, $\dot{e} = 5 \times 10^{-7}$ /year. These strain rates equal the present strain rates gotten from geodetic data.

KUMAGAI and ITÔ have been continuing the experiments extending over 16 years on the creep of granite test-pieces, and they have concluded that 1) granite undergoes viscous flow and 2) its viscosity is $2 \sim 5 \times 10^{20}$ poises. Based on the conclusion 1), it seems to be proper to consider that all rocks in the crust make viscous flow. Assuming the viscous flow of the crust, we get the simple relation

$$p = 3\eta e,$$

where p is the tectonic stress and η is the viscosity of the crust. The value of p may be estimated by using the data of absolute rock stress measurements and those of stress release calculated by the analyses of earthquake faults.

Recently the initial rock stresses were measured by the stress relief technique using a borehole in the sites of Okutataragi (Kinki) and Shintakasegawa (Chubu) underground electric power stations. It was found that the rock stresses are connected closely with the tectonic stress in these areas (HIRAMATSU, OKA, ITÔ and TANAKA, 1973). We can deduce the tectonic stress $p = 40 \sim 120$ kg/cm^2, since the tectonic stress may be considered to be rock stress minus overburden pressure.

Thus we have been able to get the viscosity of the crust to be in the order of 10^{22} poises.

ON THE GEOLOGICAL CLASSIFICATION OF LANDSLIDES HORIZON

Takeshi ANDO, Geological Survey of Japan

Heavy rain, melting snow, earthquake, content of groundwater, soil pressure and sub-surface plane of discontinuity control the movement of landslides greatly. As well, geologic and geographic conditions are also primary cause of landslides. Especially, weathered terrain often causes landslides. Studies on elucidation of the mechanisms and the prediction of landslides require the consideration of geologic horizon.

Generally, the most essential geological factor related to the occurrence of landslides is the rock properties such as sedimentational and structural features, particle-size and composition of the rocks. Characteristics of structural geologic factors shown as fault, joint, fold, fracture and etc., and tectonic movement affect on it and thus make complicate the mechanism of landslide. Other factors such as properties of structure and facies change in sedimentary rocks are also control the occurrence, scale and movement of landslides to some extent.

The Japanese islands which locates on the circum-Pacific mobile belt is characterized by the complicated geological structure, in turn tremendous number of landslides and collapses. In the attached table, the classification of landslides in view of geologic horizon is shown. For understanding of landslides, rock mechanics, weathering, physical properties of sliding matter and the basic types of movement are necessary to study.

1. Landslides in Tertiary horizon

Neogene Tertiary region along the coast of the Sea of Japan (is called Inner Zone geologically) is most famous landslides area. In this area, originated from so-called "green tuff" volcanic activity, great deal of volcanic and pyroclastic rocks spout out and accumulated. The pre-Neogene basement, more over the petroliferous formation intercalates thin layers of tuff

very offen. The area in where black mudstone, hard shale, sandy mudstone and alternation of those are cropping out, is the potential landslides area.

In the Tertiary region which is overlain by younger volcanic rocks prevails "complex landslides" due to its geological condition. So-called "Hokusho type" landslide whose rock formation consisted of coal-bearing Tertiary formation and plateau basalts, and " "Hirane type" and "Oami type" landslides consisted of oil-bearing Tertiary sedimentary rock and younger volcanic products are very difficult to be elucidated.

2. Landslides in regional metamorphic zone

Landslides which occur in the area of crystalline schist are unique in Japan, and called "schist type". Also the landslides in the area the Sambagawa belt, which is consisted of crystalline schists, phyllites and accompanied by the Mikabu green-rocks are distributed is the most active landslide zone. This type of landslides is influenced by the characteristics of original rocks and their metamorphic grade, and develope widely on the black phyllite, green-schist and Mikabu green-rocks area. The development of joints, schistosities and cleavages is the major factor of the landslides causing fissility and breakable of rocks.

3. Landslides in igneous rocks, volcanic ash and altered volcanic areas

In the areas consists of serpentine, weathered granitic rocks and volcanic ash of "loam" and "Shiras", the landslides or collapes are easy to occur. Also in the area altered by volcanic fume, landslides occur remarkably.

Table 1. Geological classification of landslides horizon

Landslides		Geological classification	
		Type	Sub-type
Landslides in Tertiary region	Neogene system	Oil-Tertiary type (mainly middle-upper Miocene series)	Black mudstone type
			Hard shale type
			Sandy mudstone type
		Green-tuff type (mainly lower-middle Miocene series)	Mudstone and tuff type
			Tuffaceous rock type
			Propylite type
		Alternation type (mainly upper Miocene-Pliocene series)	
		Coal-Tertiary type	
		Paleogene system type	
		Complex type (in places of Tertiary formations and "cap rocks)	Hokusho type
			Hirane type, Oami type
			Shorinzan type
			Naniai type
Landslides in regional metamorphic zone		Schist type	Black phyllite type
			Green schist type
			Alternated schist type
			Mikabu green-rocks type
		Semi-schist type	
		Gness type	
Landslides in Mesozoic and Paleozoic areas		Mesozoic sediments type	
		Paleozoic sediments type	
Landslides in igneous rocks		Serpentine type	
		Granitic rocks type	
Landslides in volcanic ash		Loam type	
		Shirasu type	
Landslides in the volcanic altered areas		Volcanic fume type	
		Old volcanic altered type	
In Quaternary		Diluvium type	

[Excl. Sammarized remarks of Japanese text.]

THE STABILITY OF SLOPE DURING EXCAVATION
- THE METHOD OF ANALYSIS AND OBSERVATION -

Yoshihiro KITAHARA, Central Research Institute of Electric Power Industry
Yoshikazu FUJIWARA, Central Research Institute of Electric Power Industry
Masashi KAWAMURA, Chugoku Electric Power Co. Ltd.

SHIMANE Nuclear Power Plant had to be constructed on the narrow seashore which was surrounded by steep slope of hills. In order to obtain the flat area of about 120,000 square meters, a part of this slope must be cut out and the total volume of the excavation reached about 1,040,000 cubic meters.

The characteristics of this slope was the stratification of weathered shale in the surrounding hard tuff and the inclination of this stratification was downhill about 25 degrees from horizontal plane. (Fig. 1)

The cutting-out of the hills was to be conducted to the height of about 120 meters with an inclination of about 1.5 : 1.0. Then the problem occurred during the excavation whether the weathered stratification of shale was stable or not.

In this study, under the assumption of elastic non-homogeneous plane strain, (Table 1) safety factor for slide ($F_{25^\circ}^{*}$) along the stratification was analized by applying the Finite Element Method, and the observation of excavated slope was successfully made during excavation work by using a special instrument which was a version of Carlson type's joint meter.

As a result of both analytical and observatory approach, it is concluded as follows:

(1) Observed displacements were approximately from 60 to 80 percents of those calculated by F.E.M.. It was considered that the difference was due to the assumptions of plane strain, or to the assumed certain low values of Young's modulus. (Fig. 2)

(2) Stability of the slope was almost assured but the cautions must be taken to a few parts where the factor of safety was low and the observed displacement was large to a certain degree. (Fig. 3, 4, 5)

$$^{*}F_{25^\circ} = \frac{\tau r25^\circ}{\tau 25^\circ} = \frac{\tau 0 + \sigma n \tan\phi}{\tau 25^\circ}$$

where $\tau r25^\circ$; shearing resistance along the stratification
$\tau 0$; shearing strength along the stratification
$\tan\phi$; angle of internal friction along the stratification
$\tau 25^\circ$; calculated shearing stress along the stratification
σn; calculated stress normal to the stratification

Table 1 Fundamental Value of Mecanical Properties
(Natural Dry Condition)

quality of rock	High Class		Middle Class		Low Class	
kind of rock	Shale	Tuff	Shale	Tuff	Shale	Tuff
Elastic Modulus(Kg/cm²)	18,000	30,000	10,000	20,000	5,000	15,000
Poisson's Ratio	0.3	02	0.3	0.2	0.3	0.2
Shearing Strength(Kg/cm²)	2.0	4.0	1.5	3.0	1.0	2.0
Angle of Internal Friction(degree)	30°	40°	28°	35°	25°	30°
Specific Gravity	2.6	2.4	2.6	2.4	2.6	2.4

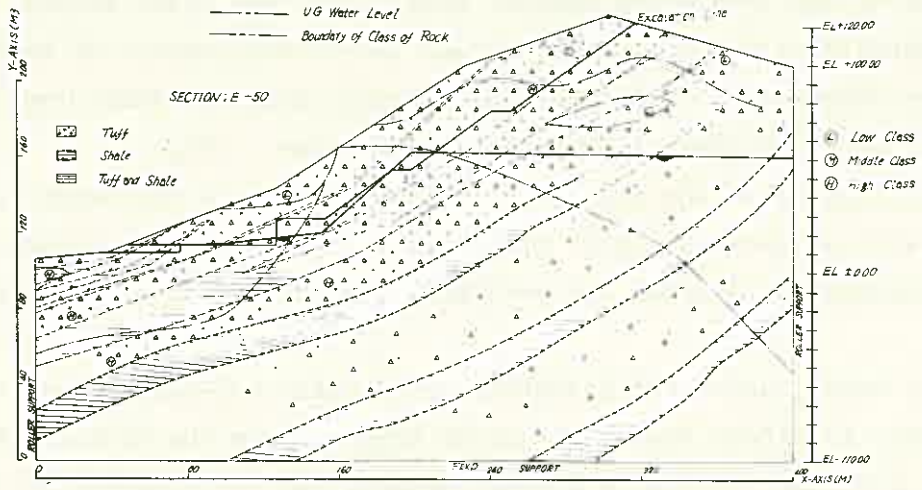

Fig.1 Analyzed Zone and Geological Map

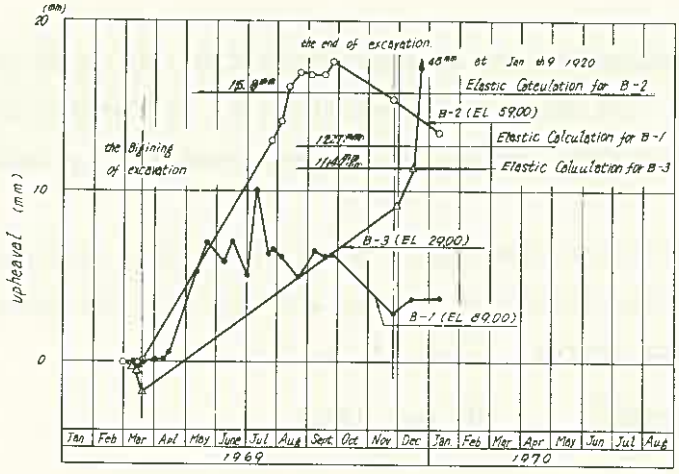

Fig.2 Ovserved Upheaval Displacement

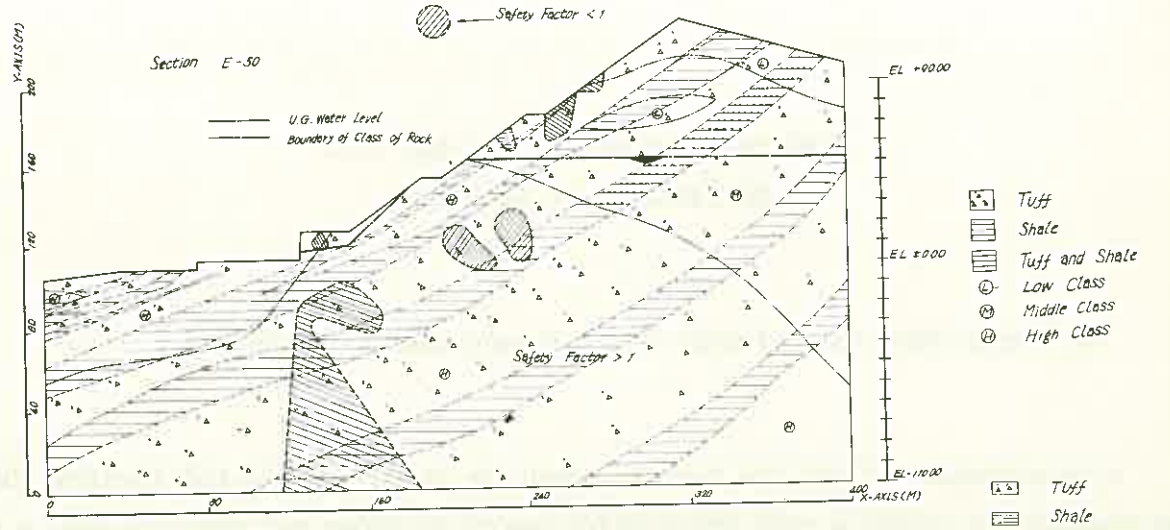

Fig.3 Unstable Zone Caused by Excavation

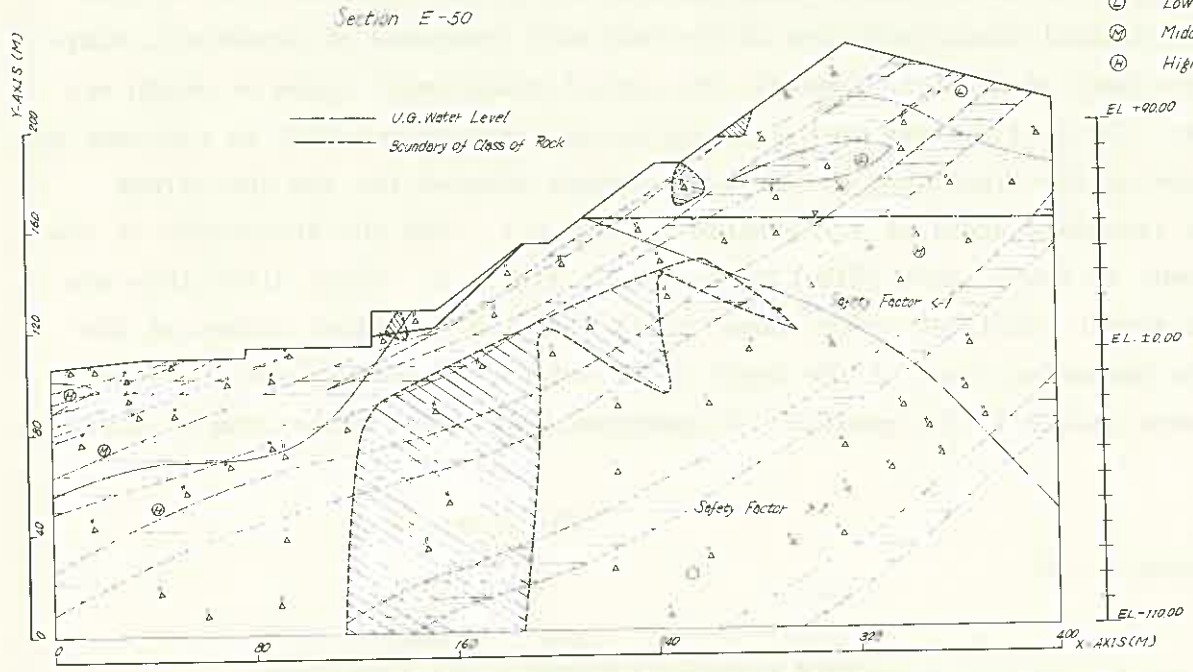

Fig.4 Unstable Zone caused by Horizontal Mass Force(0.2G)

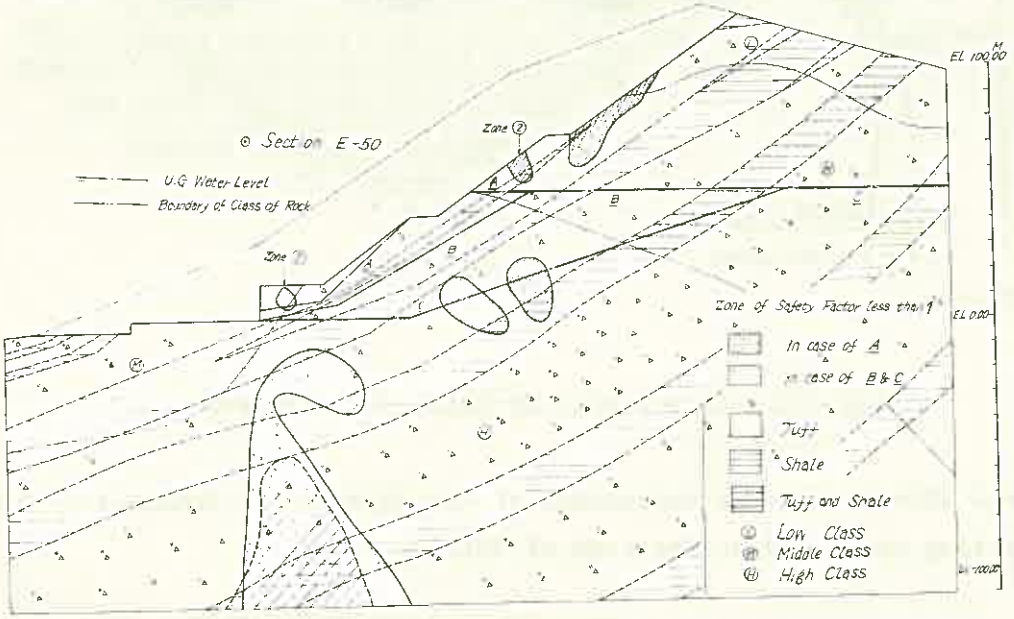

Fig.5 Effect of Underground Water Level on the Stability

LONG TERM MEASUREMENT OF BED ROCK DEFORMATION OF ARCH DAM

Dr. Kenzo AOKI and Joichiro TANO, Kyushu Electric Power Co., Inc.

A measurement of the bed rock movement in the Hitotsuse Dam (height 130 m), was carried out using a rock deformation meter in order not only to seek a guiding principle for safety maintenance and control of the dam, but also to find out the dynamical characteristics of the bed rock (composed of sandstone, clay-slate and their alternative layers), the actual measurement cases of which are very few. The Carlson-type rock deformation meters were embedded in the part of saddle and at the elevations of the arch element adopted for the dam stress analysis (analysis arch) as illustrated in Figure 1. And the directions of the measurement in their parts illustrates also in Figure 1. Their directions are arranged almost consistent with those of the computed principal stress of the dam. The measuring range of the depth is 20 meters as average and the stress meters were placed in the position of upstream, center and downstream of the dam.

Hitotsuse Dam

Section A - A

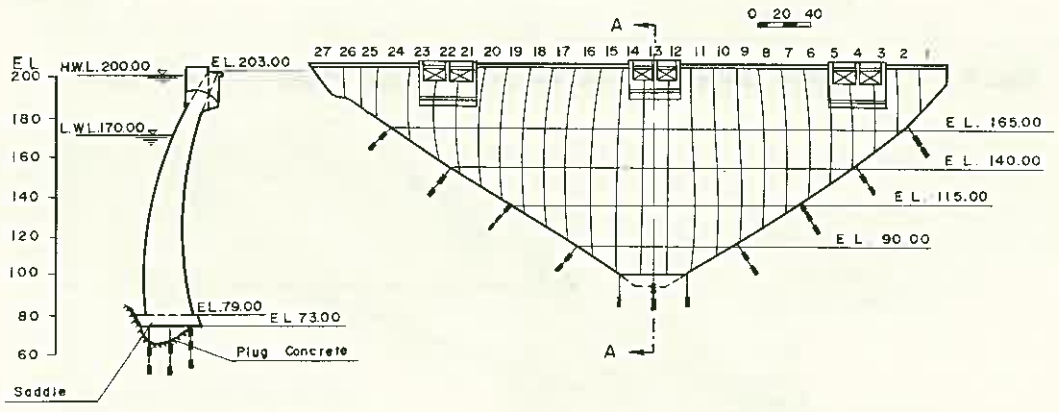

Figure 1. Arrangement of Deformation Meters

Figure 2 illustrates the comparison of the deformation immediately before start of filling water and at the time of full water.

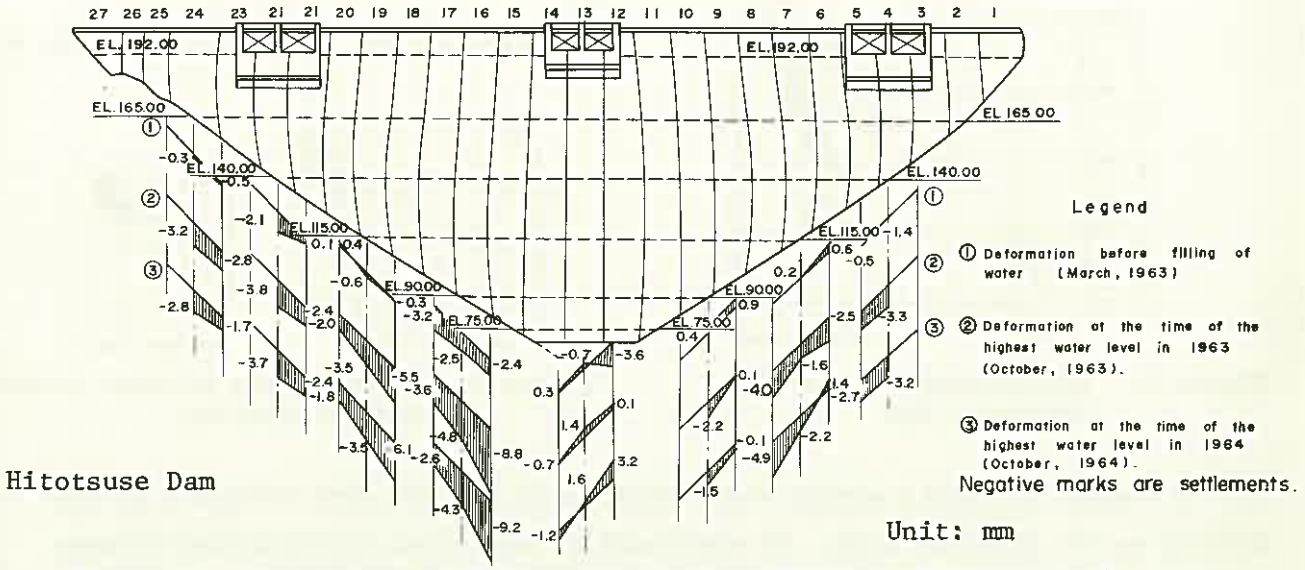

Figure 2. Comparison of Deformation before Filling of Water, and at the Time of Full Water

Figure 3 illustrates the historical record of the bed rock deformation at the elevations of the analysis arch after filling of water, developed over the extended period of seven years. The result of the measurement will be summarized as follows:

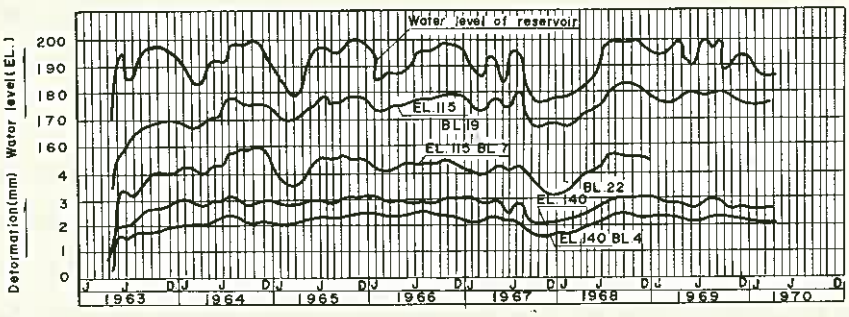

Figure 3. Measured Deformations at Elevations of Analysis Arch

(1) The development of deformation caused by filling of water is enormous during the first two months when the filling velocity is high (water level of reservoir is EL 90m. - EL 190m.), and it accounts for more than 80% of the largest deformation thereafter. The deformation of this early period is irreversible against change of the water level within the effective depth of water thereafter. Therefore, the deformation of the foundation against the change of the water level within the effective water depth develops making the deformation in the early period as minimum range. And the deformation of the foundation taking place periodically with the change of the water level thereafter is fairly elastic.

(2) By reviewing the deformation of the foundation at the time of the highest water level each year, we find that the deformation in the first year at filling of water is lesser and the degrees of the deformation later are almost the same. It is considered from this fact, that non-elastic deformation has come almost to end in two years after filling of water, and at the same time, it proves the stability of the foundation (Fig. 4).

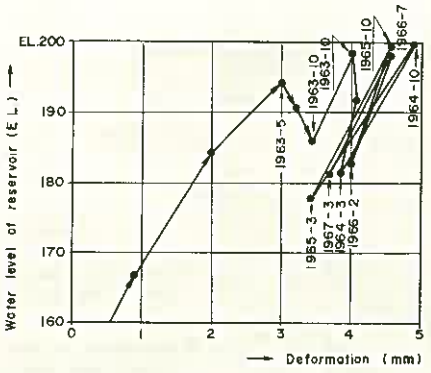

Figure 4. Deformation Pattern of Hitotsuse Dam

EL. 115, BL. 19 EL. 140, BL. 4

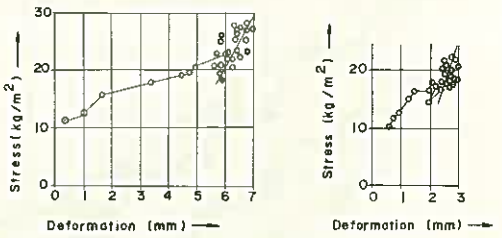

Figure 5. Correlations between Stress and Deformation

(3) A number of strain meters were embedded in the abutment concrete at the elevations of analysis arch. We succeeded in obtaining correlations between average principal stress and the deformation of bed rock with considerable accuracy. It is illustrated in Figure 5. The small circle marks connected by a line in this figure illustrates the values at the time of filling of water, and other scattered marks indicate the values after 1964. From this figure, we confirm that the gradients of the change of stress and deformation in the first year at filling of water is clearly different from those in later years, and the rigidity of the foundation after the converges of non-elastic deformation becomes considerably firm.

(4) With regard to the deformation of the foundation at EL 115m. and EL 140m., the modulus of deformability in the early period at filling of water and the modulus of elasticity at a later period are as Table 1. In this connection, the modulus of static elasticity of the foundation site prior to the dam construction by Jack test was 50 x 10^3kg. average, and ER = 50 x 10^3kg/cm^2 was employed for calculation for the dam construction plan.

Table 1. D_R and E_R of foundation rock (x 10^3kg/cm^2)

Elevation	year	left bank D_R	left bank E_R	right bank D_R	right bank E_R
EL 115	1963	35	—	24	—
	1965	—	52	—	75
	1968	—	65	—	60
EL 140	1963	30	—	44	—
	1965	—	163	—	118
	1968	—	93	—	119

Table 2. Comparison of E_C, E_R and E_C/E_R

	E_C	D_R or E_R	E_C/E_R
Stage of design	200,000 (assumed)	50,000	4
early stage after filling water	210,000	33,000	6.4
1965 - 1968	220,000	93,000	2.4

For the analysis of arch dam, the ratio of elasticity modulus of concrete EC to ER is considered as parameter to introduce the effect of deformation of the foundation. Their comparison of the values at the time of plan making and at a later period is illustrated in Table 2.

(5) We consider that the above measurement data will be useful for planning the arch dam construction and studying the actual measured stress of the arch dam in the future.

BEHAVIOR OF FRACTURED ROCKS AND ITS EFFECTS UPON STRUCTURES

Shigeru TANAKA, Kobe University

Deformation of the earth's crust caused by tectonic forces involves not only elastic strain but also plastic deformation and rigid body translations and rotations. Along fault zone, displacement may occur by slow, secular, differential slippage as well as by sudden rupture. Typical geologic section in fault zones shows a succession of crushed and sheared rock, gouge, breccia, and clays. Such materials would behave under pressure more as a viscous, plastic solid than as a brittle, elastic one. Faults and associated joints are preferred channelways for groundwater, whether of surface origin or of deep steated origin. Many faults are accompanied by extensive wall rock alteration,either by surface waters or by hydrothermal solutions derived from a hot source at depth. Breccia filling of local origin is found in some faults and consists of angular to rounded brittle rock fragments derived from adjacent competent rocks and rolled and abraded by movements of adjacent walls of the fault. Gouge deforms plastically, and under pressure it may squeeze slowly into underground openings. It may produce swelling pressures when it contacts with ground water, and also it is essentially impermeable to ground water movement. Water exists in rocks and associations with mineral grains and open spaces.

Fracture permeability is secondary permeability resulting from development of faults and joints in rocks of variable permeability. Open fractures may offer relatively slight frictional resistance to flow. Ground water flows may be classified as follows: (1) flows in fractures connecting with the earth's surface and fed by water from streams, standing bodies of water, or water-soaked surficial deposits, and (2) flows of stored or trapped water which is replenished slowly by water from the earth's surface.

Faults can destroy structures by shearing, compression, ex-

tension, and rotation caused by tilting or bending. And earthquakes may occur along them. Past faulting may have much affected the physical properties of foundation materials, by decreasing their strength, changing their permeability, or bringing together rock units having defferent physical properties. Fault rupture and the accompanying ground deformation can have serious consequences. At many places in Kansai area in Japan, the writer has investigated troubles occured at structures constructed in and in the vicinity of a main fault, and has been able to obtain a conclusion that there exists a close relationship between the said troubles and ground movements, either of fault zone or adjacent rocks. Structures in or across a fault zone that undergoes surface faulting had and may expect to have severe damage. Faults also have slippage, or creep, and progressively demolished and may destroy buildings and other structures on the faults. In the vicinity of a main fault, several closely-spaced fractured zones where embraced ground water shows independent head peculiar to each zone, have been found by the writers and others at some places in mountainous district in Kobe and its vicinity. An interesting phenomenon of ground motion, i.e. "Seasaw Motion" which is named by the writer, was discovered by the writer and engineers at Kobe City Office, at Tsurukabuto area in Kobe which was reclamated by cutting Mt. Tsurukabuto. At the location where many fractured zones are converging, narrow rock blocks devided by two adjacent fractures bordering each block, have been repeating continuous reciprocal motion, from the fracture with higher ground water head towards the opposite one with lower head, and furthermore, the head is alternatively changing. Water head in each fractured zone is not the same, but differs from zone to zone and in course of time, and shows its own behavior peculiar to the zone itself.

At the mountainous area in and near Kobe, where granite, alternation of sand stone, tuff, shale and conglomerate, and the same of loosely consolidated clay, sand, and gravel, are existing, the writer and his associates have been pursuing the researches on "the relationship between troubles occurred at structures and the behavior of fractured zones", and have obtained the following conclusion:

(1) When earthquakes may occur, not only faults themselves deform but also rock blocks devided by faults move very rapidly, the displacement of structure and that of the foundation may differ

very much, thus structures may be damaged.

(2) Along fault zone, slow, secular, differential slippage may occur, structures in or across the zone may be damaged.

(3) When fault zone containing ground water or the rock mass in front of the said zone may be cut, structures on the cut slope may be demolished, by the cause that the water pressure acting upon the rock block may often overcome the resistance to slide of the block, especially, in the case of heavy rain, and also that gouge emerged at the slope surface may rupture.

(4) When fractured granite zone near a main fault may be cut and thereafter structures may be constructed on it, embraced water in several fractures may increase its head, especially in the case of violent storm, and may cause slope rupture along a slide surface through extensively altered rock. Under such circumstances, the structures may receive serious damages.

(5) Structures constructed on an alternation of sand stone, tuff, shale, and conglomerate, where fractured zones densely exist, and also each rock layer is comparatively inclined, near a main fault, may often suffer from cracks or damages.

(6) An alternation of loosely consolidated clay, sand, and gravel, which is thickly accumulated on granite, having fractured zones, is also often affected by the said zones, especially in the clay layer. The layer often has fratured zone with some width, and underground water sometimes flows up through such openings to the upper sand or gravel layer, and the water head often shows a very good correspondence with heavy rain. Structures on or across this kind of fractured zone also may be damaged.

(7) The earthquake ground accelerations may differ from fractured zones to adjacent rock blocks, and they may induce complex inertia forces in a structure across the zones, sufficient to damage it. The earthquake may trigger landslides or similar local surficial movements that may destroy structures, especially at the site where base rocks are fractured.

DRUMMY ROCK DETECTION UNDER DISTURBANCE OF VARIOUS KINDS OF NOISES

Tomio HORIBE, Tohoku University
Minoru USHIDA, Tohoku University

Authors have developed a new method for the detection of drummy rocks by means of an acoustic analysis of an impact sound, measuring a ratio of the areas surrounded by the envelope of the form of the wave filtered by a one-third octave band pass filter and by that of the original wave of the impact sound of rocks in accordance with the arrangement of the block diagram shown in Fig.1.

Center frequencies of bands of the filter used in this study were 400, 500 and 630 Hz, because our preliminarly experiment showed that these frequency bands were most effective to distinguish drummy rocks from firm rocks[1) 2)].

There are many kinds of noises in underground that may disturb the detection of drummy rocks with the impact sound. Then over-all sound pressure level and the spectrum of each kind of noises were measured. These are shown in Figs. 2, 3 and 4.

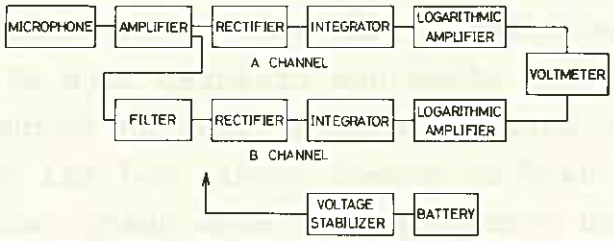

Fig. 1. Block diagram of drummy rock detector

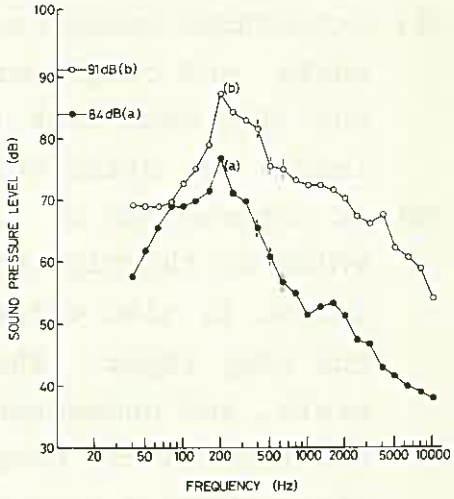

(a): racing of rock drill—distance 45m
(b): racing of rock drill—distance 35m
Fig. 2. Spectra of noises

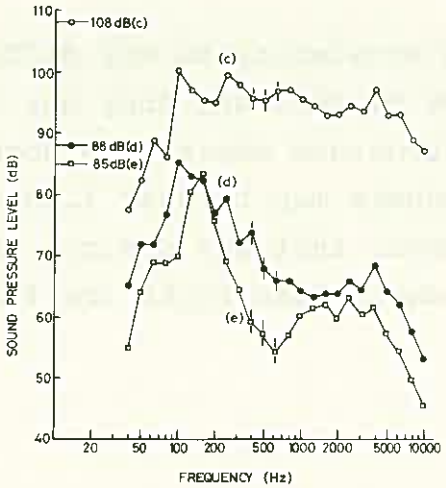

(c): drilling of rock drill—distance 5m
(d): drilling of rock drill—distance 40m
(e): operating of air-driven loader
Fig. 3. Spectra of noises

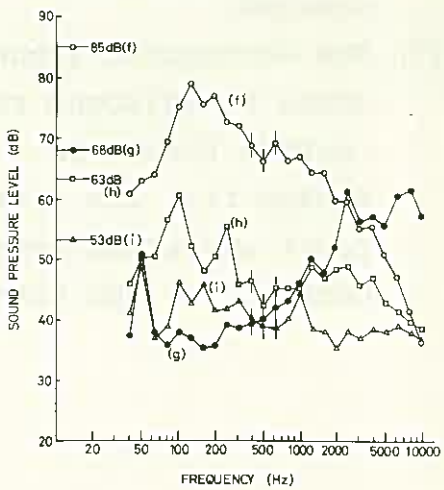

(f): passing of battery locomotive
(g): leakage of compressed air
(h): water flow
(i): drop of water
Fig. 4. Spectra of noises

Of these noises, the distance from the noise source to the microphone (A), the over-all sound pressure level at this distance (B), the

Table 1. Sound pressure level of noises

noise source	distance from noise source (m) (A)	over-all sound pressure level (dB) (B)	sound pressure level of each frequency band (dB) (C)			difference between (B) and (C) (dB) (D)		
			filter frequency			filter frequency		
			400Hz	500Hz	630Hz	400Hz	500Hz	630Hz
racing of rock drill (a)	45	84	66	61	57	18	23	27
racing of rock drill (b)	35	91	82	76	75	9	15	16
drilling of rock drill (c)	5	108	96	96	97	12	12	11
drilling of rock drill (d)	40	88	74	68	66	14	20	22
operating of air-driven loader (e)	40	85	59	57	55	26	28	30
passing of battery locomotive (f)	30	85	69	67	70	16	18	15
leakage of compressed air (g)	3	68	40	40	42	28	28	26
water flow (h)	1	63	46	42	45	17	21	18
drop of water (i)	1	53	40	39	39	13	14	14

sound pressure level of each frequency band (C) and the difference between over-all sound pressure level and the sound pressure level of each band (D) are given in Table 1.

However, there are two factors in the disturbance of noises for the detection of drummy rocks. One is (D) and the other is (B). The more is the value of (D), the smaller is the disturbance of noises for the detection of drummy rocks. Therefore, the degree of disturbance of noises from the air-driven loader and the leakage of compressed air should be small, while that of disturbance of noises from the battery locomotive, the water flow and the drop of water in underground should be great. And the degree of disturbance of noises from the rock drill would not be so great if it would be operated far from the detection place.

If the level of (B) becomes higher, even if (D) is great, the degree of disturbance of noises for the detection of drummy rocks would become greater, because the sensitivity of the microphone, even if the microphone is of the highly-directional type, could not be zero, although it should be set in the direction of its minimum sensitivity.

Thus, it was found that the degree of disturbance of noises from air-driven machines such as the rock drill and the loader, and that from the battery locomotive for the detection of drummy rocks were greater than that from the leakage of compressed air, the water flow and the drop of water.

Here, the distinction between the drummy rock and the firm rock was made by the auditory sense of a highly skilled technician.

When the experiment was carried out, impact sounds were made with the ball type hammer of 60 mm ϕ at these measuring points. Then the measurements of these sounds by a microphone were made at each five points of the drummy and firm rocks of a 3 m(w) x 2 m(h) drift of quartz-porphyry zone, located at 45 m and 35 m distances away from (a) and (b) noises, respectively. The microphone was set at the place of 50 cm distance apart from the impact point normal to the wall. The noise circumstances were given as follows ;

① silent state (about 36 dB level, at the measuring point)

② (a)－noise state, distance 45 m (about 84 dB level, the same above)

③ (b)－noise state, distance 35 m (about 91 dB level, the same above).

Consequently, in noise circumstance ① the drummy rock was able to be distinguished completely from the firm rock by using either the highly- or the uni-directional microphone and using any kind of above mentioned bands of filter.

In noise circumstance ②, shown in Fig.5(i), with the uni-directional microphone reading ranges of meter for the drummy rock and the firm rock were partially overlapped each other in any one of the frequency bands, so it was not easy to distinguish the drummy rock from the firm rock. But only by the use of the highly-directional microphone the drummy rock was able to be successfully distinguished.

In noise circumstance ③, shown in Fig.5(ii), with the uni-directional microphone the reading ranges were overlapped completely in any one of the frequency bands, so the distinction of drummy rock from the firm rock was almost impossible.

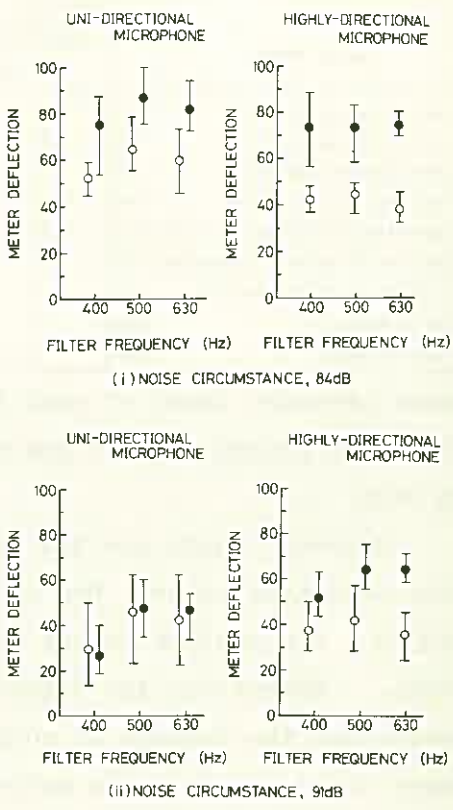

Fig. 5. Reading range of meter deflection vs. filter frequency

By the use of the highly-directional microphone the reading ranges were overlapped partially at frequency bands of 400 Hz and 500 Hz, but it was found that the drummy rock was able to be distinguished successfully by the selection of the frequency band of 630 Hz.

Incidentally, the acoustic characteristic of the underground drift was investigated with the standard sound of a pistol shot. Then it was shown that the frequency characteristic of the underground drift was generally flat and no resonance was recognized.

References

1) T. HORIBE, R. KOBAYASHI, M. USHIDA : Electroacoustic Study on Detecting Drummy Rock, J. Min. Met. Inst. Japan, Vol. 81 No. 928, Aug. 1965, P. 669-674

2) T. HORIBE, R. KOBAYASHI, M. USHIDA : Fundamental Investigation on Detecting Drummy Rock by Hammering (3rd Report), J. Tohoku Min. Soc., Vol. 12 No. 2, July 1966, P. 42-46

MICROSCOPIC STUDIES OF THE FISSURES IN COALS THROWN OUT BY OUTBURSTS AND ROCKBURSTS

Teizo YANO

1. Method of investigation.

Fine coals of 10 grams that were thrown out by outbursts were used commonly for investigation. The grain size of used samples were from -100 mesh to +200 mesh or sometimes small particle (several mm) and small lump coal. To make smooth the surface of them, alumina 1500-3000 and polisher (brand name "MAGOMET") were used. And those samples were photographed with POM polarized microscope by oil immersed reflection method. A photograph of one sample was composed of sixteen continuous photographs of surface of it.

2. The fissures in coal samples collected at site underground.

2-1 The fissures in coals thrown out by outbursts.

The produced fissures in coals thrown out by outbursts occurred at 8 coal mines that outbursts occurred frequently were investigated. Fig 1 shows a example of Naie coal mine (Hokkaido in Japan).

From results of general surveys, it was found that the fissures in coal samples had much the same apparent pattern, but micelic mechanics of coals, total length of the fissures were different from each other.

Fig 1 Coals thrown out by outbursts.

2-2 The fissures in coals from the vicinity of folds, faults and volcanic rocks underground.

In most samples of coals taken from the vicinity of folds and faults at coal mine, the fissures were not found. However, the above samples crushed by powerful air hummer mostly produced the fissures that were similar to them in coals thrown out by outbursts.

In natural cokes (thickness 20 cm) caused by intrusion of volcanic rocks (basalt) or in coals at the contact zones, the fissures produced also were of the same apparent pattern.

It may be those causes that some residual stress of orogenic movement or stress caused by excavation have remained. Fig 2 and 3 show the examples of Utashinai coal mine (Hokkaido).

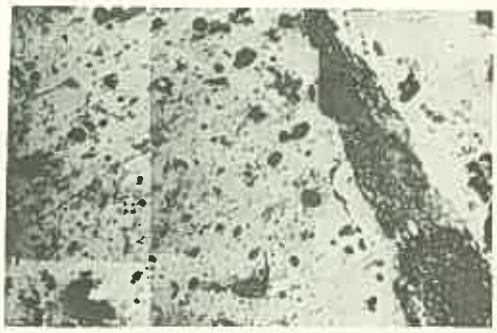

Fig 2 Natural cokes.

Fig 3 Natural cokes crushed by air hummer.

2-3 The fissures of drillings produced by boring at coal face.

In case of the standard volume (calculated volume) of drillings were produced by boring in coal face, the fissures were not found in them. However, in case of the drillings volume were produced several times that of the standard, the fissures were apparently found.

These fissures indicated the dangerous degree of outbursts corresponding with the author's assumptive rank "A" or "B".

Fig 4 shows a typical example at Oyubari coal mine.

Fig 4 Drillings.

3. The fissures in case of adding an external force on the coal sample.

The fissures produced by changing moderately the sort and force of stress were surveyed. The used samples were hard coals (friability 15-20) and compressive tests for them were carried out with 10 tons amsler or 400 tons press. The fissures in fractured samples were not produced in each case of tension, shearing and bending test, but after the above tested samples were crushed by powerful air hummer, the fissures similar to them in coals thrown out by outbursts were produced in the samples. Fig 5 shows a typical example.

Fig 5 Coal crushed by air hummer after carried out bending test.

4. The fissures of coals having artificial thermal strain.

The coals were heated for several hours in N_2 atmosphere and were cooled in water immediately. By this way, static strain-stress should be generated and remained in the coals. After that, those coals were crushed by powerful air hummer, then the fissures were remarkably similar to them in coals thrown out by outbursts were produced in the coals.

Heat temperature was rised from 50 degree C to 200 degree C, holding constant temperature for 2 hours at every 50 degree. Fig 6 shows a example in case of coals heated at 200 degree C.

5. Conclusion

(1) The state of the fissures in coals thrown out by outbursts occurred at 8 coal mines were photographed with polarized microscope. Those photographs were remarkably similar to each other. So it would be fact that the apparent pattern are common to outbursts occurred in coal mines of Ishikari coal field in Hokkaido.

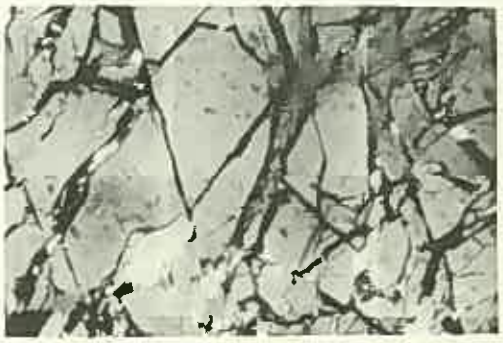

Fig 6 Samples crushed by air hummer with coals having thermal strain.

(2) In coals at faults zones, fold zones and natural coke zones caused by intrusion of volcanic rocks underground or contact zones of them, the fissures were not found, but in the above coals crushed by powerful air hummer, the fissures similar to them in coals thrown out by outbursts were found. As this reason, those fissures may be produced on account of remained stress caused in coals by orogenic movement or excavation.

(3) The drillings volume produced by pilot boring may be possible to predict dangerous rank of outbursts.

(4) When forces being contrary to each others (bending stress, shearing stress, etc.) act at the same time in coal seam, outbursts of gas and coal will be subject to occur.

(5) It is important that in proportion to heat volume of coals having thermal strain, total length of the fissures per unit area (cm^2), and interval of the branching fissures are different from each other.

III LIST OF LITERATURE

III LIST OF LITERATURE

1. Soil Mechanics and Foundation Engineering (Journal of the Japanese Society of Soil Mechanics and Foundation Engineering)
   1) Kunio SUYAMA, Takeshi OHKUBO, Hiroshi TSUTIYA: Elastic Wave Velocity as a Factor to Determine Feasibility of Slope Cut, Vol.18, No.1 (Jan. 1970) p.23-32 (F)
   2) Isao NODA, Juro KODERA, Noriyuki TAKADA, Takeshi OHMACHI: Experimental Study on Fixation of Pier to the Base Rock, Vol.18, No.2 (Feb. 1970) p.11-26 (H)
   3) Eiichi ODA, Takuo YAMAGAMI: On the Distribution of Stresses of the Plastic Region around a Circular Tunnel without Lining Driven in the Ground of Clay, Vol.19, No.3 (Mar. 1971) p.39-46 (B)
   4) Takeshi OHKUBO, Akira TERASAKI: Physical Property of Rock and Elastic Wave Velocity, Vol.19, No.7 (July 1971) p.31-37 (A, F)
   5) Hiroshi NIINO: Problems Relating to Investigation of Sea Bottom Strata, Vol.20, No.9 (Sep. 1972) p.3 (F)
   6) Kozo TAKAHASHI, Gaku SUGITA: Investigation of Sea Bottom Strata in Akashi Strait, Carried out for Construction of Honshu-Shikoku Bridge Construction, Vol.20, No.9 (Feb. 1972) p.21 (F)
   7) Ryozo NIIYA, Gaku SUGITA: Investigation of Sea Bottom Strata Formation by Sonic Wave, Vol.20, No.9 (Sep. 1972) p.27 (F)
   8) Yoshiharu UMEGAKI: General Description of Geology in Chugoku District, Vol.20, No.10 (Oct. 1972) p.61 (H)
   9) Toru ONODERA: Development of Rock Formation Engineerings and Formulation of Investigation System of Same, Vol.21, No.3 (Mar. 1973) p.1-4 (H)
   10) Masao HAYASHI: Corelations Among Dynamic Properties, Behaviour Analysis and Measurement Results, of Rock Formations and Rocks Comprising of Coarse Grain Particles, Vol.21, No.3 (Mar. 1973) p.5-14 (A)
   11) Kozo TAKAHASHI, Shiro TAKADA, Koji ISHIKAWA, Tadao HRYU: Investigation of Rock Formation (Weathered Granite) Using Bore Hole Measurement, Vol.21, No.3 (Mar. 1973) p.15-24 (F)
   12) Takayasu YAMANO: Use of Soft Rocks as Fill Materials of Rock Fill Dam, Vol.21, No.3 (Mar. 1973) p.25-32 (E, G)
   13) Kazuhiko IKEDA: Application of Results of Rock Formation Investigation on Design and Construction of Tunnel, Vol.21, No.3 (Mar. 1973) p.33-42 (F)
   14) Kunitaro MATSUOKA: Investigation of Rock Formation in Connection with Road Construction, Vol.21, No.3 (Mar. 1973) p.43-50 (F)
   15) Akimitsu OHHASHI, Mituru KIMOTO: Investigation and Design of Base Rock Strata Where Piers of Kanmon Bridge Were Constructed, Vol.21, No.3 (Mar. 1973) p.51-58 (F)
   16) Keiji ADACHI: Rock Excavation, Vol.21, No.3 (Mar. 1973) p.59-65 (D)
   17) Ryunoshin YOSHINAKA: Classification of Rock Masses and the Representation, Vol.21, No.3 (Mar. 1973) p.67-74 (H)
   18) Shoichi NISHIDA, Mitsuharu MINAMOTO: Characteristics of Tertiary Land Slide in Niigata Prefecture and the Treatment, Vol.21, No.7 (July 1973) p.5-21 (E, H)
   19) Motohisa HARUYAMA, Etsuro SHIMOKAWA: Report of the State on Slope Failures in Kagoshima Prefecture Occurred in June and July of 1972, Vol.21, No.7 (July 1973) p.13-16 (E, H)

20) Masayasu INOUE: Land Slides in Amakusa and Shinko, Vol.21, No.7 (July 1973) p.17-20 (E, H)
21) Hiroo YAMAMOTO, Morito HOSOKAWA, Hirotaka SOKOBIKI, Kunitake HASHIKAWA: Slope Failures in Hiroshima Prefecture, Vol.21, No.7 (July 1973) p.21-28 (E, H)
22) Kno UESHITA, Tadashi KUWAYAMA: Land Slides Occurred in the Western Mikawa Area by Heavy Rain-Fall in July, 1972, Vol.21, No.7 (July 1973) p.29-32 (E, H)
23) Bungo TAMADA: Mechanisms of Occurrence of Landslides in The Tertiary Period Strata, Vol.21, No.7 (July 1973) p.33-40 (C)
24) Kojiro NAKASEKO: Landslides Observed in The Group of Osaka Strata, Vol.21, No.7 (July 1973) p.45-48 (H)
25) Goji YAMADA: Landslides Phenomena with The Excavation of Limestone, Vol.21, No.7 (July 1973) p.49-54 (C, H)
26) Sumiji KOBASHI, Masami OGURA: Methods of Investigation to Establish Stability of Slopes at Open Cuts, Vol.21, No.7 (July 1973) p.55-62 (F, H)
27) Harumi ARAKI: Investigation of Slope Destruction by Appraisal of Aerophotography, Vol.21, No.7 (July 1973) p.63-68 (H)
28) Makoto NAKAMURA: Engineering Method to Prevent Slope Destruction, Vol.21, No.7 (July 1973) p.69-74 (E)

2. Soils and Foundations (in English)
1) Motohisa HARUYAMA: Effect of Surface Roughness on the Shear Characteristics of Granular Materials, Vol.IX, No.4 (1969) p.48-67 (A)
2) Shin-ichiro MATSUO, Kazuhiko NISHIDA: The Properties of Decomposed Granite Soils and Their Influence on Permeability, Vol.X, No.1 (1970) p.93-105 (A)
3) Yoshiaki YOSHIMI: An Outline of Damage during the Tokachioki Earthquake, Vol.X, No.2 (1970) p.1-14 (H)
4) PUBLIC WORKS RESEARCH INSTITUTE, MINISTRY OF CONSTRUCTION: Damage to Roads, Dikes and Highway Bridges during the Tokachioki Earthquake, Vol.X, No.2 (1970) p.15-38 (H)
5) Shiro MISHIMA, Hideo KIMURA: Characteristics of Landslides and Embankment Failures during the Tokachioki Earthquake, Vol.X, No.2 (1970) p.39-51 (H)
6) Takeichiro IKEHARA: Damage to Railway Embankments due to the Tokachioki Earthquake, Vol.X, No.2 (1970) p.52-71 (H)
7) Masahiro MORIYA, Noritada KAWAGUCHI: Damage to Small Earthfill Irrigation Dams in Aomori Prefecture during the Tokachioki Earthquake, Vol.X, No.2 (1970) p.72-82 (H)
8) Toyotoshi YAMANOUCHI, Sadakatsu TANEDA, Taizo KIMURA: Damage Features in 1968 Ebino Earthquakes from the Viewpoint of Soil Engineering, Vol.X, No.2 (1970) p.129-144 (H)
9) N. RADHAKRISHNAN, Lymon C. REESE: A Review of Applications of the Finite Element Method of Analysis to Froblems in Soil and Rock Mechanics, Vol.X, No.3 (1970) p.95-112 (C)
10) Shin-ichiro MATSUO, Mamoru FUKUTA, Kazuhiko NISHIDA: Consistency of Decomposed Granite Soils and Its Relation to Engineering Properties, Vol.X, No.4 (1970) p.1-9 (C)
11) Ichiro UCHIDA: The Properties of Decomposed Granite Soils and Their Influence on Permeability, Vol.X, No.4 (1970) p.65-66 (A, F)
12) Masanobu ODA: Initial Fabrics and Their Relations to Mechanical Properties of Granular Material, Vol.XII, No.1 (1972) p.17-36 (A)
13) Shin-ichiro MATSUO, Kazuhiko NISHIDA: The Properties of Decomposed Granite Soils and Their Influence on Permeability, Vol.XII, No.1 (1972) p.45-46 (A, F)

14) —: Seikan Undersea Tunnel, Vol.XII, No.1 (1972) p.53-58 (F, H)
15) Tadahiro ODA: The Mechanism of Fabric Changes during Compressional Deformation of Sand, Vol.XII, No.2 (1972) p.1-18 (A)
16) Yasumasa FUKUMOTO: Study on the Behaviour of Stabilization Piles for Land-slides, Vol.XII, No.2 (1972) p.61-73 (E)
17) Takeaki FUKUMOTO: Effect of Particle Breakage on Compaction Density of Decomposed Granite Soils, Vol.XII, No.3 (1972) p.55-63 (A)
18) Tadahiro ODA: Deformation Mechanism of Sand in Triaxial Compression Tests, Vol.XII, No.4 (1972) p.45-63 (A)
19) Shin-ichiro MATSUO, Kohei SAWA: The Indentification of Weathering Patterns and their Representation Methods Based on Observations of Broken Surface on Decomposed Granites, Vol.XII, No.4 (1972) p.105-112 (H)
20) Shin-ichiro MATSUO, Kohei SAWA: Identification of Quantities of Coloured Minerals and Degrees of Weathering Using Representation Method of MASA (Decomposed Granite Soils) Colour, Vol.XIII, No.1 (1973) p.113-122 (H)

3. Proceedings of the Symposium of the Japanese Society of Soil Mechanics and Foundation Engineering.
1) Eizaburo YOSHIZUMI, Tsuyoshi SUGAMO, Chugoro SATO, Harushige TANIMOTO: The Electrical Survey for the Landslide, 6th Conf. (1970) p.1-5 (E)
2) Michitaka SAITO: Precaution against Unstable Slope and Forecasting the Time of Its Failure, 6th Conf. (1970) p.6-10 (E)
3) Kenzo AOKI, Jyoichiro TANO: Long-term Deformation Characteristics of Foundation Rock about a High Arch Dam, 6th Conf. (1970) p.16-20 (B)
4) Takao NAKADE: Bed Rock Excavation and Stability of Cut Slope under Roadway Construction, 6th Conf. (1970) p.11-15 (C, D)
5) Shinsaku HORIGUCHI: Foundation Treatment at Takane No.1 Dam, 6th Conf. (1970) p.21-25 (D)
6) Hiroya KOMADA, Toshikazu KAWAMOTO: On the Analysis of Seepage in Foundation and Embankment, 6th Conf. (1970) p.26-30 (B)
7) Ryuichi IIDA, Shigetoshi KOBAYASHI: A Mechanical Analysis about Nonelastic-behaviour in Rock-masses, 6th Conf. (1970) p.31-37 (B)
8) Ken-ichiro HORII, Mututo KAWAHARA: A Numerical Analysis on Visco-elastic Structures by the Finite Element Method, 6th Conf. (1970) p.38-42 (B)
9) Kazumasa TOMITA, Masatsugu AKIMOTO, Toshikazu KAWAMOTO: On the Characteristics of Deformation of Rock-like Materials, 6th Conf. (1970) p.43-47 (A)
10) Ken ZAKO, Mitsuo TONISHI, Masao NISHI: Measurement of Dynamic Characteristics of Rock with Specially Designed Pick-up Set in Boreholes in the Dense Traffic Area, 6th Conf. (1970) p.48-52 (B, F)
11) Kazuhiko IKEDA: A Classification of Rock Conditions for Tunneling, 6th Conf. (1970) p.53-57 (H)
12) Rock Engineering Laboratory, Saitama University: Field Survey Methods for Estimating Engineering Properties of Rock-mass.
(1) Case for Distribution of Joint and Strength in Sedimentary Rock Field, 6th Conf. (1970) p.58-62 (H)
13) Masao HAYASHI, Yoshihiro KITAHARA, Katsuko NAKAARAI, Satoshi HIBENO: Behaviour of Rock Foundation-Expectation and Observation, 6th Conf. (1970) p.63-69 (A)
14) Seisuke MISAWA, Akinori TAKAHASHI: Anchor Mechanism Rock Bolts, 6th Conf. (1970) p.70-74 (E)
15) Akira YOKOYAMA, Toshio INOUE: Water Seal Grouting in Seikan Tunnel, 6th Conf. (1970) p.75-79 (G)

16) Takao SIMADA: The Subsidence of the Ground by Tunnel Excavation, 6th Conf. (1970) p.80-84 (D)
17) Takemi SHIBUYA, Hakaru TAMURA, Nobuyuki OKABAYASHI: Tunnel Excavation and Rock Behaviours in A Former Landslide Area, 6th Conf. (1970) p.85-89 (D)
18) Masao HAYASHI, Satoshi HIBINO, Tadashi KANAGAWA: On the Effect of Inclination of Ground Pressures on Relaxed Zones Formed by Excavation of Underground Power Station, 7th Conf. (1972) p.1-5 (B)
19) Ryuichi IIDA, Hajime ASAKURA, Jǫji HARADA: Analysis of Time Dependent Seepage Blow by Finite Element Method, 7th Conf. (1972) p.6-10 (B)
20) Yoshihiro KITAHARA, Yoshikazu FUJIWARA, Masashi KAWAMURA: The Stability of Slope during Excavation-The Method of Analysis and Observation, 7th Conf. (1972) p.11-15 (B)
21) Shunsuke SAKURAI, Shozo MORITA, Yoshiteru YOSHIMURA, Taro KAJI: Estimation of Initial Stress in Viscoelastic Underground, 7th Conf. (1972) p.16-20 (B)
22) Ken-ichi HIRASHIMA, Yosiji NIWA: Stresses and Deformation around Two or More Pressure Tunnels in Isotropic and Anisotropic Elastic Rock Masses, 7th Conf. (1972) p.21-25 (B)
23) Shoichi KOBAYASHI, Sunao MORITAKE: Effects of Couple Stresses on Stress Distributions around a Lind Circular Tunnel, 7th Conf. (1972) p.26-30 (B)
24) Seisuke MISAWA, Takashi SAKURAI, Akinori TAKAHASHI: Method of Test and Survey for Estimating the Mechineability of Rocks for Rock Tunnelling Machine, 7th Conf. (1972) p.31-35 (D, E)
25) Eizaburo YOSHIZUMI: On the Electrical Prospecting in Tunnel Geological Surveyings, 7th Conf. (1972) p.36-40 (E)
26) Toru ONODERA, Masanobu ODA, Toshiaki ISHII: Strength and Deformation Characteristics of Gypsum Plaster Specimen Jointed at Random, 7th Conf. (1972) p.41-45 (A)
27) Masao SATAKE, Hisataka TANO: A Note on the Final Strength of Brittle Materials with Single Slit, 7th Conf. (1972) p.46-50 (A)
28) Ryunoshin YOSHINAKA, Yukio HAGINO, Kazuyoshi ARAI: Strength of Continuous Joint with Regular Teeth, 7th Conf. (1972) p.51-55 (A)
29) Eizaburo YOSHIZUMI, Soji YOSHIKAWA, Chugoro SATOH, Takemi SHIBUYA: Measurement of Physical Constants of Shirasu (Whitish Grey Welded Tuff) Ground, 7th Conf. (1972) p.56-60 (E)
30) Akiyoshi ISHIZAKI, Nobuo IWATA: Grouting Practice in the Seikan Undersea Tunnel, 7th Conf. (1972) p.61-65 (D)
31) Eizaburo YOSHIZUMI, Soji YOSHIKAWA, Tsuyoshi SUGANO, Chugoro SATOH, Takemi SHIBUYA: Determination of Grouting Effectiveness in the Rock Foundation of A Dam, 7th Conf. (1972) p.66-70 (D)
32) Ryoji KOBAYASHI: On Crack Distribution Measured by Borehole Crack-Detector Using Ultrasonic Pulse Method, 7th Conf. (1972) p.71-75 (E)
33) Masao HAYASHI, Yoshikazu FUZIWARA, Hiroya KOMADA: Static and Dynamic Properties of Rock Fill Material, and Relation between Numerical Analysis and Observation, 7th Conf. (1972) p.76-81 (B)
34) Motoo OTUKA, Masataka UENO: Design of Rock Bolts, 7th Conf. (1972) p.82-85 (D)
35) Hiroshi KIMBARA: The Rock-Bolting System in Japan, 7th Conf. (1972) p.86-90 (D)
36) Motoo OTSUKA, Masataka UENO: Stress Distribution Near Cylindrical Tunnel, 8th Conf. (1973) p.1-5 (B)
37) Masao HAYASHI, Yoshihiro KITAHARA, Yoshikazu FUJIWARA, Hiroya KOMADA: In-Situ Repeated Loading Test of Dynamic Elasticity and Viscosity of Rock Masses, 8th Conf. (1973) p.6-10 (B)

38) Shunsuke SAKURAI, Taro KAJI: Dynamic Behaviour of Underground Pipe under Excitation of Rayleigh Waves, 8th Conf. (1973) p.11-15 (B)
39) Masao SATAKE, Hisataka TANO: On the Fracture Modes and Strength of Rocks under Uniaxial Compression Test, 8th Conf. (1973) p.16-20 (A)
40) Toshiaki SAITO, Toshikazu KAWAMOTO: Stress Analysis of Underground Structures Based on Fracture Mechanics, 8th Conf. (1973) p.21-25 (B)
41) Ken-ichi HIRASHIMA, Masayasu HISATAKA: Stress Distributions Around Two Adjoining Circular Tunnels Under Three-Dimensional Stress State, 8th Conf. (1973) p.26-30 (B)
42) Kazuhiko IKEDA, Yoshimasa KOBAYASHI, Takeshi SAKURAI: Effects of Flaws on the Strength of Rocks, 8th Conf. (1973) p.31-35 (A)
43) Ryuichi IIDA, Shigetoshi KOBAYASHI: Relation between the Looseness of Rockmasses and the Mechanical Characteristics of Rockmasses Observed from in Situ Loading Tests, 8th Conf. (1973) p.36-41 (B)
44) Masaji SAGARA, Kozo TAKAHASHI, Keiji MIYAJIMA, Toshiaki TAKEUCHI: Development of a High Pressure Load Tester in a Borehole and Application to Rock Materials, 8th Conf. (1973) p.42-46 (E)
45) Eizaburo YOSHIZUMI, Tuyoshi SUGANO, Chugoro SATOH, Takemi SHIBUYA, Katuki NISHIURA: The Electrical Prospecting at the Ohirayama Tunnel of the New Sanyo Line, 8th Conf. (1973) p.47-51 (E)
46) Soji YOSHIKAWA, Chugoro SATOH, Takemi SHIBUYA, Hakaru TAMURA: Geological Survey by Borehole Geophones in Kokedani of Ohira Tunnel, 8th Conf. (1973) p.52-56 (E)
47) Sadahiko ADACHI, Osamu SHIGEMATSU, Takefumi TANI: Measuring of Earth Pressure in Expansive Layer of Tunnel at the Momijiyama Railway Line, 8th Conf. (1973) p.57-61 (B)
48) Ryoki NAKANO: On the Mechanism of Squeezing and Swelling Rock Pressure of Mudstone on Tunnel Support in Relation with the Case History of Nohiro Tunnel, 8th Conf. (1973) p.62-66 (B)
49) Youichi MIMAKI: Results of Measurement the Initial In Situ Stresses in the Underground at the Shintakasegawa Underground Powerhouse, 8th Conf. (1973) p.67-71 (B)
50) Tatsuo NISHIGORI: The Method of Deformation-Measurement and the Results for Underground Power Station, 8th Conf. (1973) p.72-76 (E)
51) Isao SHIBATA, Masakiyo TAHARA, Saburo MIURA: Test Grouting for Layers of Pumice Flow and Scoria in Aso Lava, 8th Conf. (1973) p.77-81 (D)
52) Toru SAITO, Risaburo MAGARIO: Engineering Results and Consideration of Rock Bolting, 8th Conf. (1973) p.81-86 (D)

4. Proceedings of the Conference of the Japanese Society of Soil Mechanics and Foundation Engineering.

1) Takeaki FUKUMOTO: Failure Characteristics of Compacted Decomposed Granite Soil (Masa), 18th Conf. (1973) (A)
2) Shin-ichiro MATSUO, Kohei SAWA: Differential Fracturing of the Soil Particle of Decomposed Granite Soil (Masa), 18th Conf. (1973) (A)
3) Kiichi TANIMOTO: Engineering Properties of Weathered Granite Soil (Masa) Dynamic Properties, 18th Conf. (1973) (A)
4) Shigeru TANAKA: Practical Treatment of Decomposed Granite Soil (Masa), Failure of the Slope, 18th Conf. (1973) (E)
5) Ichiro UCHIDA, Katsutada ONIZUKA, Tokio HIRATA: Experimental Studies on the Failure of Embankment Slope of Decomposed Granite Soil (Masa), 18th Conf. (1973) (C)
6) Shin-ichiro MATSUO: Slope Stability of Decomposed Granite Soil by Lime Treatment Method, 18th Conf. (1973) (E)
7) Izumo HOSHINO: Slope Stability by Soil Cement, 18th Conf. (1973) (E)

5. Journal of the Japan Society of Civil Engineers
   1) Rock Mechanics Committee of JSCE: Shearing Strength of Rock Mass, Vol.55, No.6 (June 1970) p.53-63 (B)
   2) Seiichi KITAHARA: Pilot Tunnelling of the Seikan Tunnel, Vol.56, No.4 (Apr. 1971) p.2-8 (D)
   3) Committee for Rock Mechanics of JSCE: On the Manual of Foundation Grouting of Concrete Dams, Vol.57, No.8 (Aug. 1972) p.59-60 (D)
   4) Rock Mechanics Committee of JSCE: Shearing Strength and Deformation of Rock Mass, Vol.57, No.9 (Sep. 1972) p.51-58 (B)
   5) Y. IWATA, Y. IIDA, T. TANI: Construction of the Oni-Toge Tunnel in the Momijiyama Line, Vol.58, No.7 (July 1973) p.30-37 (D)

6. Proceedings of Japan Society of Civil Engineers
   1) Yoshiji NIWA, Syoichi KOBAYASHI, Ken-ichi HIRASHIMA: Stress and Deformation Around a Circular Tunnel Excavated in Orthotropic Elastic Ground Under a Three-Dimensional Stress State, No.173 (Jan. 1970) p.7-18 (B)
   2) Takeo KAJITA, Toshikazu KAWAMOTO: Finite Element Analysis on Uniaxial Compressive Strength of Cylindrical Brittle Specimen, No.177 (May 1970) p.71-76 (A)
   3) Zenjiro HOKAO: Studies on Boring and Cutting of Rocks by Supersonic Jet Flames, No.180 (Aug. 1970) p.71-82 (C)
   4) Shunsuke SAKURAI: Lining of Circular Tunnel in Viscoelastic-Plastic Medium, No.181 (Sep. 1970) p.77-90 (D)
   5) Yoshiji NIWA, Ken-ichi HIRASHIMA: Gravitational Stress Distribution on Deep Tunnel in Anisotropic Elastic Ground with Constant Inclined Surface, No.182 (Oct. 1970) p.31-40 (B)
   6) Yoshiji NIWA, Syoichi KOBAYASHI, Kazuo YOKOTA: Application of Integral Equation Method to the Determination of Static and Steady Slate Dynamic Stress Around Many Cavities on Arbitrary Shape, No.195 (Nov.1971) p.27-36 (B)
   7) Sakuro MURAYAMA, Toru FUJIMOTO: Earth Pressure on Circular Tunnel Lining Due to Stress-Relaxation in Visco-Elastic Ground, No.205 (Sep. 1972) p.93-186 (B)

7. Journal of the Mining and Metallurgical Institute of Japan.
   1) Masatsugu AKIMOTO, Toshikazu KAWAMOTO: On the States of Stress and Deformation Around the Bottom of a Circular Vertical Shaft (report 2) - Non-linear stress analysis - Vol.86, No.981 (Jan.1970) p.1-7 (B)
   2) Ko SUZUKI, Yuichi NISHIMATSU, Masao AKIYAMA: The Torsion Test and the Modulus of Rigidity of the Rock, Vol.86, No.981(Jan. 1970) p.8-12 (A)
   3) Ko SUZUKI, Yoji ISHIJIMA: Simulation of Progressive Failure in Rock Around Mining Excavations, Vol.86, No.982 (Feb. 1970) p.69-74 (B)
   4) Umetaro YAMAGUCHI, Makoto OKUMURA, Syozo KOIZUMI: Development of a Modified Sonic System for Probing the Rock Around Mining Openings and Result of the Field Trial — Seismic Field Study for the State of Stresses or Cracks of Rock Around Mining Openings (1st Report), Vol.86, No.982 (Feb. 1970) p.75-80 (A)
   5) Taizo YANO: Microscopic Studies of the Fissures in Coal Thrown Out by Outbursts and Rockburst, Vol.86, No.982 (Feb. 1970) p.81-86 (A)
   6) Ko SUZUKI, Yoji ISHIJIMA: Theoretical Consideration on Some Fundamental Problems Concerning in Situ Measurements of Stresses in Rock by Relief Techniques, Vol.86, No.983 (Mar. 1970) p.151-156 (B)
   7) Kunihisa KATSUYAMA, Koichi SASSA, Ichiro ITO: Effect of the Guide Hole on the Breakage of Rock by Smooth Blasting, Vol.86, No.984 (Apr. 1970) p.195-200 (C)

8) Umetaro YAMAGUCHI, Michio MIYAZAKI: A Study of the Strength or Failure of Rocks Heated to High Temperatures, Vol.86, No.986 (May 1970) p.346-351 (A)
9) Ko SUZUKI, Yuichi NISHIMATSU, R. HEROESEWOJO: The Statistical Distribution of Fatigue Life and the S-N Curve of Rocks — The Study on the Fatigue Failure of the Rock (1st Report) — Vol.86, No.986 (May 1970) p.353-358 (A)
10) Ko SUZUKI, Yuichi NISHIMATSU, R. HEROESEWOJO: The Rheological Properties of Rocks Under the Pulsating Compressive Load (1st Report) Vol.86, No.987 (June 1970) p.413-418 (A)
11) Ko SUZUKI, Yuichi NISHIMATSU, R. HEROESEWOJO: The Rheological Properties of Rocks Under the Pulsating Compressive Load (2nd Report) Vol.86, No.988 (July 1970) p.477-482 (A)
12) Ryoji KOBAYASHI: Mechanical Properties of Rocks Under High Rates of Loading (2nd Report), Vol.86, No.989 (Aug. 1970) p.525-529 (A)
13) Giichi MORI, Kiyoshi HORI: Studies on Conditions of Surface Subsidence Caused by Underground Mining, Vol.86, No.989 (Aug. 1970) p.531-536 (D)
14) Tadashi NISHIDA, Ken GOTO: Damage to Irrigation Pond Due to Mining Subsidence, Vol.86, No.990 (Sep. 1970) p.571-574 (D)
15) Shigeru YAMASHITA, Shigenori KINOSHITA: Estimation of Cutting Forces on Rake Surface and Clearance Surface of the Tools — Experimental Investigations on the Cutting of Brittle Material (1st Report)— Vol.86, No.992 (Nov. 1970) p.835-840 (A)
16) Yoshiteru KANDA, Saburo YASHIMA, Jyunzo SHIMOIIZAKA: Size Effects and Energy Laws of Single Particle Crushing of Irregular Shaped Particle, Vol.86, No.992 (Nov. 1970) p.847-852 (A)
17) Yoji ISHIJIMA, Jin KOIDE, Ko SUZUKI: Theoretical Consideration on the Rock Stress Measurement by the Complete Stress Relief Technique Using a Borehole Deformation Method, Vol.86, No.993 (Dec. 1970) p.901-906 (B)
18) Umetaro YAMAGUCHI, Makoto OKUMURA, Michiaki MORI: A Field Measurement of Sound Velocity on the Mine Pillar and the Fundamental Laboratory Tests for the Study of Sound Velocity Changes in Rocks — Seismic Field Study for the State of Stresses or Cracks of Rock round Mining Openings (2nd Report) — Vol.87, No.994 (Jan. 1971) p.7-10 (A)
19) Yuichi NISHIMATSU: On the Effects of Tool Velocity in the Rock Cutting, Vol.87, No.995 (Feb. 1971) p.65-74 (C)
20) Ryoji KOBAYASHI, Kiyohiko OKUMURA: Study on Shear Strength of Rocks, Vol.87, No.999 (May 1971) p.407-412 (A)
21) Kunihisa KATSUYAMA, Koichi SASSA, Ichiro ITO: Growth Mechanism and Properties of Crack Caused by an Intense Stress Wave, Vol.87, No.1000 (June 1971) p.471-476 (C)
22) R. HEROESEWOJO, Yuichi NISHIMATSU, Ko SUZUKI: The Effects of Repeated Compressive or Tensile Load on the Mechanical Properties of Rock, Vol.87, No.1001 (July 1971) p.515-520 (A)
23) Yusaku TOMINAGA, Shigenori KINOSHITA: A theoretical Analysis of the Stress Distribution Around Multiple Holes in an Elastic Infinite Plate, Vol.87, No.1004 (Oct. 1971) p.739-743 (B)
24) Umetaro YAMAGUCHI: Measurement of Amplitude Attenuation of Sound Waves on Cement Mortar Blocks, Vol.87, No.1004 (Oct. 1971) p.745-748 (A)
25) Ichiro ITO, Koichi SASSA, Kunihisa KATSUYAMA, Masafumi HAMAZAKI, Noriaki NAKAJIMA: How to Control the Direction of Radial Crack Caused by an Explosion, Vol.87, No.1006 (Dec. 1971) p.1035-1040 (C)
26) Kiyoshi HASHIMOTO, Hisao HONMA: Study of Rock Breakage by Blasting, Vol.88, No.1007 (Jan. 1972) p.11-16 (C)

27) Yoshiteru KANDA, Saburo YASHIMA, Shoichi MOROHASHI, Fumio SAITO, Takatoshi SAGAWA: Experimental Study on the Relationships between Specific Fracture Energy and Specific Surface Area of Fractured Product in Single Particle Crushing, Vol.88, No.1007 (Jan. 1972) p.29-34 (A)
28) Yoshinori INADA, Makoto TERADA, Ichiro ITO: A Fundamental Study on Rock Excavation Using the Mechanical Cutting Method Combined with Thermal Action by Flame (1st Report), Vol.88, No.1008 (Feb. 1972) p.79-84 (C)
29) Masayasu INOUE, Michito OHMI, Jun-ichi MORITA: Study on the Relationship of Water Content to Velocities of Elastic Waves and Compressive Strength of Sedimentary Rocks, Vol.88, No.1009 (Mar. 1972) p.143-148 (A)
30) Yoshiaki MIZUTA, Yoshio HIRAMATSU, Yukitoshi OKA: Studies on the Stress in Rib Pillars (2nd Report) —Influence of the Original Stress State and Geometrical Conditions on the Stress in Pillars- Vol.88, No.1010 (Apr. 1972) p.191-196 (B)
31) Yuichi NISHIMATSU: A Preliminary Study on the Cutting Force of Toothed Roller Cutter, Vol.88, No.1010 (Apr. 1972) p.197-201 (C)
32) Yoshinori INADA, Makoto TERADA, Ichiro ITO: A Fundamental Study on Rock Excavation Using the Mechanical Cutting Method Combined with Thermal Action by Flame (2nd Report), Vol.88, No.1013 (July 1972) p.423-428 (C)
33) Kunihisa KATSUYAMA, Koichi SASSA, Ichiro ITO: Formation of Cracks and Crater Caused by a Blasting with One Free Face, Vol.88, No.1014 (Aug. 1972) p.465-470 (C)
34) Shigemasa KIMURA: Geological Study in Miike Coal Field by Sonic Exploration (1st Report), Vol.88, No.1015 (Sep. 1972) p.515-520 (E)
35) Iwao NAKAJIMA, Shigenori KINOSHITA: The Cutting Force of Rock in the Formation of Small Chips, Vol.88, No.1015 (Sep. 1972) p.521-526 (A)
36) Zenjiro HOKAO: Development of Thermodrills for Under Water Boring, Vol.88, No.1015 (Sep. 1972) p.533-538 (C)
37) Shigemasa KIMURA: Geological Study in Miike Coal Field by Sonic Exploration (2nd Report), Vol.88, No.1017 (Nov. 1972) p.769-774 (E)
38) Yusaku TOMINAGA, Shigenori KINOSHITA: Stress Concentration Around the Multiple Circular Openings in the Elastic Rock, Vol.88, No.1017 (Nov. 1972) p.775-780 (B)
39) R. HEROESEWOJO, Yuichi NISHIMATSU, Ko SUZUKI: The Rheological Properties of Rocks Under the Pulsating Tensile Loads, Vol.88, No.1017 (Nov. 1972) p.781-786 (A)
40) Tadashi NISHIDA, Nobuhiro KAMEDA: On the Mechanism of Caving-in due to Mining at a Shallow Depth, Vol.88, No.1018 (Dec. 1972) p.863-868 (D)
41) Tadashi NISHIDA, Kazuo AOKI, Osamu SAKAI: Fundamental Studies on the Mechanism of Failure of Jointed Rock, Vol.89, No.1019 (Jan. 1973) p.2-6 (B)
42) Kunihisa KATSUYAMA, Koichi SASSA, Ichiro ITO: Computer Calculations for the Processes of Crack Development Caused by a Smooth Blasting, Vol.89, No.1019 (Jan. 1973) p.7-12 (C)
43) Yoshiaki MIZUTA, Yoshio HIRAMATSU, Yukitoshi OKA: Deformation Characteristics of Pillars Subjected to an Axial and a Shear Force together with a Bending Moment Induced, Vol.89, No.1020 (Feb. 1973) p.79-83 (B)
44) Zenjiro HOKAO, Teijiro SHIBATA, Shoji OHMURA: Construction and Technical Characteristics of the Thermodrill for Under Water Operation — Piercing Holes in Sea-bed Rocks (1st Report) — Vol.89, No.1020 (Feb. 1973) p.89-93 (C)

45) Zenjiro HOKAO, Teijiro SHIBATA, Shoji OHMURA: Piercing Tests in Seto Inland Sea — Piercing Holes in Sea-bed Rocks by a Thermodrill (2nd Report) — Vol.89, No.1021 (Mar. 1973) p.155-160 (C)
46) Iwao NAKAJIMA, Shigenori KINOSHITA: The Fracture Mechanism of Rock in Rotary Cutting, Vol.89, No.1023 (May 1973) p.291-295 (C)
47) Nobuhiro TAKAHASHI: Application of the Third Theory to the Grindability Test, Vol.89, No.1023 (May 1973) p.301-305 (A)
48) Kunihisa KATSUYAMA, Koichi SASSA, Ichiro ITO: Computer Calculations of the Effects of the Pre-split on the Blasting Close Proximity to It, Vol.89, No.1024 (June 1973) p.357-362 (C)
49) Kiyoshi HASHIMOTO, Masuyuki UJIHIRA: Some Causes of an Outbreak of Gas-outburst, Vol.89, No.1024 (June 1973) p.369-372 (B)
50) Kazuo KURIHARA, Shigeo ABE, Miyoshi ISHIGAKI, Shoji NAKAMURA, Akira KIKUCHI, Chiyota INABA: Outbursts of Coal and Gas at Longwall Faces, Vol.89, No.1024 (June 1973) p.373-380 (B)
51) Teizo YANO: Microscopic Studies of the Fissures in Coal Thrown Out by Outbursts and Rockbursts, Vol.89, No.1024 (June 1973) p.381-386 (A)
52) Yusaku TOMINAGA, Shigenori KINOSHITA: Measurement of Ground Stress by Multiple Circular Holes Method, Vol.89, No.1025 (July 1973) p.449-454 (B)
53) Takakoto SHIMOTANI, Umetaro YAMAGUCHI, Yataro SHIMOMURA: A Consideration on the Mechanical Behaviour of Schistose Rocks, Vol.89, No.1026 (Aug. 1973) p.515-520 (A)
54) Zenjiro HOKAO, Teijiro SHIBATA: On Fire Jet Piercing Tests at Depths of 10 to 30 meters under Water, Vol.89, No.1026 (Aug. 1973) p.521-525 (C)
55) R. HEROESEWOJO, Yuichi NISHIMATSU, Ko SUZUKI: The Effects of Repeated Concressive or Tensile Load on the Mechanical Properties of Rock (2nd Report), Vol.89, No.1027 (Sep. 1973) p.588-592 (A)
56) Yoshio HIRAMATSU, Yukitoshi OKA, Yoshiaki MIZUTA: Determination of the Width Ratio of Rib Pillars to Openings, Vol.89, No.1027 (Sep. 1973) p.593-598 (B)
57) Hirohide HAYAMIZU, Saburo TAKAOKA, Shigeo MISAWA: A Study of Determination of the Hardness and Viscousness of Rock for Percussive Drilling, Vol.89, No.1028 (Oct. 1973) p.639-644 (C)
58) Takeichi YANAGIMOTO, Ken-ichi UCHINO: Measurement of Thermal Conductivities of Coals and Rocks in Coal Measure, Vol.89, No.1028 (Oct. 1973) p.645-650 (A)
59) Zenjiro HOKAO, Shohei SHIMADA, Keiichi KOMAI: — On Temperature of Fire Jet Stream — Study on Parametes of Fire Jet Stream on Thermal Fracturing of Rock (1st Report), Vol.89, No.1028 (Oct. 1973) p.651-656 (C)
60) Tomio HORIBE, Minoru USHIDA: On Influence of Various Noises in Underground to Detection of Drummy Rock, Vol.89, No.1029 (Nov. 1973) p.711-716 (A)
61) Zenjiro HOKAO, Shohei SHIMADA, Ken-ichi KOMADA: — On Heat Transfer Coefficient of Fire Jet Stream — Study on Parameters of Fire Jet Stream on Thermal Fracturing of Rock (2nd Report), Vol.89, No.1029 (Nov. 1973) p.727-732 (C)

8. Journal of the Society of Materials Science, Japan
1) Kazuo YAMAMOTO, Masaki ARIOKA: Materials Properties of Anisotropic-Brittle with Joints Respecting Fracture, Vol.19, No.197 (Feb. 1970) p.130-137 (A)
2) Yoshiji NIWA, Syoichi KOBAYASHI, Ken-ichi HIRASHIMA: Stresses Around a Tunnel with an Arbitrary Cross Section Excavated in Anisotropic Elastic Ground, Vol.19, No.197 (Feb. 1970) p.138-144 (B)

3) Yuichi NISHIMATSU: A New Element of the Mechanical Model of Rock Substance, Vol.20, No.209 (Feb. 1971) p.129-135 (A)
4) Shunsuke SAKURAI: Rheological Equation of Anisotropic Viscoelastic Material and Its Application to Problems Pertinent to Rock Mechanics, Vol.20, No.209 (Feb. 1971) p.136-142 (A)
5) Kiyoo MOGI: Failure Criteria of Rocks (Study by a New Triaxial Compression Technique), Vol.20, No.209 (Feb. 1971) p.143-150 (A)
6) Norihisa ADACHI, Akimasa SERATA: Viscoplasticity and Direct Shear Test of Rock-Type Materials, Vol.20, No.209 (Feb. 1971) p.151-155 (A)
7) Toshikazu KAWAMOTO, Kazumasa TOMITA: Variation in Characteristics of Deformation of Marble and Mortar Due to Transition of Stress from Isotropic State to Anisotropic State, Vol.20, No.209 (Feb. 1971) p.156-163 (A)
8) Shoichi KOBAYASHI: Initiation and Propagation of Brittle Fracture in Rock-Like Materials under Compression, Vol.20, No.209 (Feb. 1971) p.164-173 (A)
9) Yuichi NISHIMATSU, R. HEROESEWOJO: The Effects of the Mean Stress and of the Stress Amplitude on the Rate Constants of Fatigue Failure of the Rock, Vol.20, No.209 (Feb. 1971) p.174-178 (A)
10) Kumikoto IIDA, Hiroaki TSUKAHARA, Yoji KOBAYASHI, Isao SUZUKI, Jyunzo KASAHARA, Mineo KUMAZAWA: Deformation of Dunite at Slow Strain Rates under High Temperature and Pressure, Vol.20, No.209 (Feb. 1971) p.179-184 (A)
11) Naoichi KUMAGAI, Hidebumi ITO: The Experimental Study of Secular Bending of Big Granite Beams for a Period of 13 Years with Correction for Change in Humidity, Vol.20, No.209 (Feb. 1971) p.185-189 (A)
12) Hidefumi ITO, Kazuo FUJITA: The Flow of the Earth's Crust Considered from the Quarternary Crustal Movements in Southwest Japan, Vol.20, No.209 (Feb. 1971) p.190-196 (B)
13) Yoshiaki MIZUTA, Yoshio HIRAMATSU, Yukitoshi OKA, Yoshihiko TANAHASHI: The Stress in and Near the Pillars, Vol.20, No.209 (Feb. 1971) p.199-202 (B)
14) Ichiro ITO, Koichi SASSA, Chikaosa TANIMOTO: Mechanism of Rock Breakage under Pressure of Gas Explosion, Vol.20, No.209 (Feb. 1971) p.203-208 (C)
15) Koichi SASSA, Ichiro ITO: The Breakage and Stress Waves Caused by Detonative Loading, Vol.21, No.221 (Feb. 1972) p.123-129 (C)
16) Koichi HANASAKI, Ichiro ITO: Stresses around One Hole or Two Holes Subjected to Internal Pressures in Semi-Infinite or Infinite Medium, Vol.21, No.226 (July 1972) p.652-659 (C)
17) Kunihisa KATSUYAMA, Koichi SASSA, Ichiro ITO: Numerical Analysis of Dynamic Stress in a Material with a Cavity under Impulsive Loading, Vol.21, No.228 (Sep. 1972) p.839-845 (C)
18) Makoto OKUMURA, Umetaro YAMAGUCHI: Measurement of the Attenuation Constant of Sound Waves in Rock (Measurement by the Free Vibration Method), Vol.21, No.228 (Sep. 1972) p.869-875 (A)
19) Yuichi NISHIMATSU, R. HEROESEWOJO: The Fatigue Failure of Rock as a Stochastic Process under the Pulsating Tensile Stress, Vol.21, No.230 (Nov. 1972) p.1024-1029 (A)
20) Yuichi NISHIMATSU, R. HEROESEWOJO: The Failure Process and Statistical Distribution of Fatigue Lives of the Rock Sample, Vol.22, No.233 (Feb. 1972) p.153-158 (A)

9. Proceedings of the National Symposium on Rock Mechanics, Japan
1) Masayasu INOUE, Michito OHMI: Relations among Longitudinal Velocity, Apparent Density and Compressive Strength of Common Sedimentary and Igneous Rocks, 3rd Symposium (Nov. 1970) p.1-6 (A)

2) Umetaro YAMAGUCHI: Proposed Method to Determine the Degree of Weathering of Rock, 3rd Symposium (Nov. 1970) p.7-12 (A)
3) Akio DAICHO, Yukichi MORITA, Isao NISHII: Relation between Specimen Size and Maximum Grain Size of Granular Material in Consolidation Test, 3rd Symposium (Nov. 1970) p.13-16 (A)
4) Yuichi NISHIMATSU, R. HEROESEWOJO: The Effects of the Mean Stress and Stress Amplitude on the Rate Constants of Fatigue Failure of the Rock, 3rd Symposium (Nov. 1970) p.17-22 (A)
5) R. HEROESEWOJO, Yuichi NISHIMATSU: The Influence of Repeated Loading on the Mechanical Properties of Rock, 3rd Symposium (Nov. 1970) p.23-28 (A)
6) Tomio HORIBE, Ryoji KOBAYASHI, Yasuhiro IKEMI: Fatigue Test of Rocks, 3rd Symposium (Nov. 1970) p.29-34 (A)
7) Tsuneo KIZAWA: A Comparative Study on Mechanical Characteristics of Rock in Green Shist Zone Through Test In-situ and in Laboratory, 3rd Symposium (Nov. 1970) p.35-40 (B)
8) Kumikoto IIDA, Kiyoo MOGI: Deformation and Fracture of Rocks, 3rd Symposium (Nov. 1970) p.41-46 (B)
9) Ryunoshin YOSHINAKA, Toru ONODERA: Stereographic Projection Method for the Analysis of Mechanical Features of Rock Mass, 3rd Symposium (Nov. 1970) p.47-52 (B)
10) Hitoshi KOIDE: Condition for Formation of Microfractures in Rocks, 3rd Symposium (Nov. 1970) p.53-58 (A)
11) Takeshi MITANI, Keiji ADACHI, Takeo KAWAI: On the Size of Cylindrical Specimen in Rock Strength Test, 3rd Symposium (Nov. 1970) p.59-62 (A)
12) Koichi AKAI: Failure Surface of Isotropic and Anisotropic Rocks under Multiaxial Stresses, 3rd Symposium (Nov. 1970) p.63-68 (A)
13) Syuichi MURATA, Toyosato YAMAUCHI: On Brittle Failure of the Sample of Undisturbed Shirasu with Tensile Strength (Collapsible Deposit Layer of Volcanic Product), 3rd Symposium (Nov. 1970) p.69-74 (A)
14) Toshiaki TAKEUCHI, Kazuhiko KAJIMA: Consideration on the Results of Rock Shear Test in-situ (Relationship between the Weathering Classification and the Shearing Behaviour of Rocks.), 3rd Symposium (Nov. 1970) p.75-80 (B)
15) Norihisa ADACHI: Viscoplasticity and Direct Shear Test of Rock-Type Materials, 3rd Symposium (Nov. 1970) p.81-86 (B)
16) Bungo TAMADA: The Process of Formation of the Landslide Plane in the Sedimentary Layer of Tertiary Formation, 3rd Symposium (Nov. 1970) p.113-118 (B)
17) Syunsuke SAKURAI: Deformable Behaviour of Circular Tunnel in Orthotropic Viscoelastic Medium, 3rd Symposium (Nov. 1970) p.119-124 (B)
18) Ryuichi IIDA, Shigetoshi KOBAYASHI: A Mechanical Study on the Characteristics of the Rock-masses Behaviours Obtained from Shear Tests, 3rd Symposium (Nov. 1970) p.125-130 (B)
19) Yoji ISHIJIMA, Ko SUZUKI: Some Fundamental Problems on the Stress Measurements in Rock by the Borehole Deformation Methods, 3rd Symposium (Nov. 1970) p.131-136 (B)
20) Toshio TANAKA, Akira IIZUKA: A Geophysical Interpretation of the Subsidence of Ground above a Tunnel due to Excavation, 3rd Symposium (Nov. 1970) p.137-142 (B)
21) Yoshiji NIWA, Ken-ichi HIRASHIMA: Stress Distribution Around Two Circular Tunnels in Anisotropic Elastic Body, 3rd Symposium (Nov. 1970) p.143-148 (B)
22) Masao HAYASHI, Satoshi HIBINO, Tadashi KANEGAWA: Visco-plastic Analysis on Progressive Relaxation of Under-ground Power Station, 3rd Symposium (Nov. 1970) p.149-154 (B)

23) Yoshio HIRAMATSU, Yukitoshi OKA, Yoshiaki MIZUTA, Yoshihiko TANAHASHI: The Stress in and Near Pillars, 3rd Symposium (Nov. 1970) p.155-160 (B)
24) Cyugoro SATO, Osami SHIBUYA, Ken ZAKO, Hakaru TAMURA, Nobuyuki OKABAYASHI, Harushige TANIMOTO: Tunnel Excavation in a Landslide Area, 3rd Symposium (Nov. 1970) p.161-166 (B)
25) Ken-ichi OTOFUJI, Akimitsu OHHASHI: Foundations, Kanmon Suspension Bridge, on the Weathered Rock, 3rd Symposium (Nov. 1970) p.167-172 (D)
26) Ichiro ITO, Koichi SASSA, Chikaosa TANIMOTO: Mechanism of Rock Breakage by the Pressure of Explosion Gas, 3rd Symposium (Nov. 1970) p.173-178 (C)
27) Eizaburo YOSHIZUMI, Tsuyoshi SUGANO, Syojiro SUZUKI, Cyugoro SATO: Electrical Measurement for Long Term Variation of Earth Structure in Ono Dam, 3rd Symposium (Nov. 1970) p.179-184 (D)
28) Eizaburo YOSHIZUMI, Soichi TANAKA, Syoji MATSUI: Electrical Measurement for Grouting Effect in Tail Race Tunnel of Kisenyama Underground Power Plant, 3rd Symposium (Nov. 1970) p.185-190 (D)
29) Jun YOKOTA: On the Behaviour of Rock Foundation Supporting Kurobe Dam, 3rd Symposium (Nov. 1970) p.191-194 (D)
30) Cyugoro SATO, Osami SHIBUYA, Ken ZAKO, Nobuyuki OKABAYASHI, Masahiro NOGUCHI: Mechanical Properties of Foundation Rock at Nuclear Power Station Construction Sites, 3rd Symposium (Nov. 1970) p.195-200 (D)
31) Chugoro SATO, Ken ZAKO, Masakuni MATSUI, Tatsuo NISHIFUJI, Harushige TANIMOTO, Kanji TANAKA: Prediction of Somadani Fractured Zone in the Maya Section of Rokko Tunnel on New Sanyo Railroad Line, 3rd Symposium (Nov. 1970) p.201-206 (D)
32) Toshiro ISOBE: Causes and Preventive Measures on Rock-burst, 3rd Symposium (Nov. 1970) p.207-212 (B)
33) Hidehumi ITO, Kazuo FUJITA: The Flow of the Earth's Crust Considered from the Quarternary Crustal Movements in Southwest Japan, 3rd Symposium (Nov. 1970) p.213-218 (B)
34) Keiji KOJIMA, Syoichi TANAKA, Mitsuo SATO, Yasusuke SAITO: Undisturbed Core Sampling and Testing Techniques of Soft Rocks and Weak Zones in Hard Rocks, 4th Symposium (Nov. 1973) p.1-6 (E)
35) Yoshihiro OGATA, Akira TAKATA: A Measuring Method of Bar-Velocity for Rock Specimens, 4th Symposium (Nov. 1973) p.7-12 (A)
36) Ken-ichi HIRASHIMA, Akira KOGA: Theory of Determination of Stresses in an Anisotropic Elastic Medium, 4th Symposium (Nov. 1973) p.13-18 (B)
37) Takazo TAKAHASHI, Shiro TAKADA, Koji ISHIKAWA, Tadao HARYU: Approach to Rock Classification System by the Borehole Measurements in Granites, 4th Symposium (Nov. 1973) p.19-24 (B)
38) Hiroto OCHI, Tsukasa NOTO, Hisashi FUKUZAWA: A Proposed Method about Evaluation of Rock Quality, 3rd Symposium (Nov. 1973) p.25-30 (E)
39) Umetaro YAMAGUCHI, Takakoto SHIMOTANI, Jiro YAMATOMI: Compression Test for Soft Clayey Rock, 4th Symposium (Nov. 1973) p.31-36 (A)
40) Tsuneo KIZAWA: An Attempt on Rock Classification for Excavation Purposes, 4th Symposium (Nov. 1973) p.37-42 (E)
41) Koichi AKAI, Toshihisa ADACHI, Nobuo TABUSHI: Mechanical Properties of Soft Rock in Terms of Effective Stress, 4th Symposium (Nov. 1973) p.43-48 (A)
42) Masao SATAKE, Hisakata TANO: Consideration on the Fracture Modes and Strength of Rocks under Compression Test, 4th Symposium (Nov. 1973) p.49-54 (A)
43) Jyun-ichi SEKI, Koichi SASSA, Ichiro ITO: Experimental Studies on the Effects of the Existence of Cracks on the Elastic Wave Propagation, 4th Symposium (Nov. 1973) p.55-60 (A)

44) Masanobu ODA, Toru ONODERA: An Approach from Granular Mechanics to Rock Mechanics on Mechanical Properties of Clastic Materials, 4th Symposium (Nov. 1973) p.61-66 (B)
45) Yoshiji NIWA, Syoichi KOBAYASHI, Takuo FUKUI: Analysis of Seepage Problems by the Integral Equation Method, 4th Symposium (Nov. 1973) p.67-72 (E)
46) Isao OHURA: Machine Tunneling of Soft Rock, 4th Symposium (Nov. 1973) p.73-78 (C)
47) Yutaka MOCHIDA, Kenji NODA, Jyunko KUSHIDA: Vertical Shaft Sinking in Volcanic Sediments — Nakayama Tunnel at Joetsu New Trunk Line — 4th Symposium (Nov. 1973) p.79-84 (D)
48) Tomoyuki AKAGI: Loss of Pretension in Rock Bolt due to Creep of Rock Mass, 4th Symposium (Nov. 1973) p.85-90 (B)
49) Michito OHMI, Masayasu INOUE, Keizo SUZUKI: Relationship of Water Saturation to Velocities of Elastic Waves and Elastic Module of Rocks, 4th Symposium (Nov. 1973) p.91-96 (A)
50) Masao HAYASHI, Yoshihiro FUJIWARA, Hiroya KOMADA: Dynamic Deformability and Viscosity of Rock Foundation and Rock Granular Material, 4th Symposium (Nov. 1973) p.97-102 (A)
51) Masamitsu NEGISHI, Makoto HOSHINO: Studies on the Strength of Rock — Especially on the Relationship between the Compressive, Tensile, Shearing Strength and Ultrasonic Velocity of Propagation — 4th Symposium (Nov. 1973) p.103-108 (A)
52) Ryuichi OKAMOTO, Hayashi SUGAHARA: On Change of Strength Properties of "Soft Rocks" under the Long-Term Loading, 4th Symposium (Nov. 1973) p.109-114 (A)
53) Toru ONODERA, Ryunoshin YOSHINAKA, Masanobu ODA: On the Characters of Void and Their Relations to the Mechanical Properties of Weathered Granite, 4th Symposium (Nov. 1973) p.121-126 (A)
54) Yuichi NISHIMATSU, Koji MATSUKI, Syozo KOIZUMI: Failure Process of Rock in Compression, 4th Symposium (Nov. 1973) p.127-132 (A)
55) Takeshi MITANI, Takeo KAWAI: Investigation for the Relationships between the Engineering Property of Rocks and the Drillability of Mechanical Bits, 4th Symposium (Nov. 1973) p.133-138 (C)
56) Akira TAKATA, Yoshihiro OGATA: Some Experiments on Rock Fracturing by Electric Spark Discharge, 4th Symposium (Nov. 1973) p.139-144 (C)
57) Hikoji TAKAHASHI: Tunnel Collapse and Earth Pressure Theory — Phenomenal Earth Pressure Theory —, 4th Symposium (Nov. 1973) p.145-150 (B)
58) Syunsuke SAKURAI: Theoretical Considerations of Pressure Acting on Tunnel Support Structure in Viscoelastic Medium, 4th Symposium (Nov. 1973) p.151-156 (B)
59) Yoshio HIRAMATSU, Yukitoshi OKA, Hidebumi ITO, Yutaka TANAKA: The Correlation of the Rock Stress Measured in Situ and the Tectonic Stress Inferred from Geophysical and Geological Studies, 4th Symposium (Nov. 1973) p.157-162 (B)
60) Yoshiji NIWA, Syoichi KOBAYASHI, Tadaaki MATSUMOTO: Transient Stresses Produced around Tunnels by Travelling Waves, 4th Symposium (Nov. 1973) p.163-168 (B)
61) Takeshi YANAGIBA, Mitsuyoshi SHIUSA, Mitsuho WADA, Ryoichi SAKANO, Masashi NAKANO: Tunnel Excavation-Effect against the Adjacent Tunnel and Their Preventive Measures — Report on the Chuo Expressway's Sasago Tunnel Work —, 4th Symposium (Nov. 1973) p.169-174 (B)

10. Large Dams
1) Takeo MOGAMI: Embankment Materials, Especially in Respect of Shear Resistance of Materials, No.54 (1970) p.149-164 (A)

2) Eishiro MIKUNI: Rockfill Dams, Compaction of Materials and Behaviour of Dam, No.54 (1970) p.165-179 (A, D)
3) Toshio FUJII: Behaviour of Surrounding Rock in the Treatment of Fault at Nagawado Dam, No.56 (1971) p.31-40 (B, D)
4) Masayoshi NOSE: Observation and Measurement of Dynamic Behaviour of the Kurobe Dam, No.57 (1971) p.26-34 (B)
5) Toshio FUJII: Foundation Grouting at Nagawado Dam, No.57 (1971) p.55-64 (D)

11. ZISHIN, Journal of the Seismological Society of Japan
1) Mamoru ABE: Measurement of the Attenuation of Elastic Waves in Rocks, Vol.25, No.3 (1972) p.265-266 (A)
2) Yoshio YAMAZAKI: Electrical Resistivity of Strained Rocks (Construction of a Resistivity Variometer), Vol.26, No.1 (1973) p.55-66 (A)

12. ZISUBERI
1) Masayoshi MATSUBAYASHI, Koichi MOCHIZUKI: Ground Water of the Landslide Zone, Chausuyama, Vol.6, No.3 (Feb. 1970) p.1-10 (E)
2) Kyoji TAJIME, others: Preliminary Surveys of Resistivity Near the Reservoir of Takadomari in Hokkaido, Vol.6, No.3 (Feb. 1970) p.11 (E)
3) Hiroyuki NAKAMURA: Shear Strength at the Clay-film of Slip Surface, Vol.6, No.4 (May 1970) p.1-5 (B)
4) Hiroshi FUSE: On the Mechanism of Landslide, Vol.6, No.4 (May 1970) p.6-9 (E)
5) Kyoji TAJIME, Tsutomu MURASE: On the Under-ground Survey by the Specific Resistance Method at Pirikauta, Akkeshi Town, Vol.6, No.4 (May 1970) p.10-13 (E)
6) Yasumasa FUKUMOTO: On the Property of the Pile Strength for Landslide Prevention and Control, Vol.6, No.4 (May 1970) p.15-25 (D)
7) Dai UMEZAKI, Koko MISAWA: Study on the Quality of Ground Water in Landslide Areas, Vol.6, No.4 (May 1970) p.26-32 (E)
8) Hiroyuki NAKAMURA, Masashi KONDO, Kazuo SHIRAISHI: On Measurement of Underground Water Level and Pore Water Pressure at the Landslide with Cohesive Soil as the Principal Constituent, Vol.7, No.1 (Aug. 1970) p.1-7 (E)
9) Seiji TAKAYA: The Study of Landslide Topography Used Aerical Photographs, Vol.7, No.1 (Aug. 1970) p.9-12 (E)
10) Bungo TAMADA: Studies on the Mechanism of Landslide at Hokusho in Nagasaki Prefecture, Vol.7, No.1 (Aug. 1970) p.13-23 (E)
11) Hiroshi FUSE: On the Definition of Landslide and Debris-flow, Vol.7, No.1 (Aug. 1970) p.24-28 (E)
12) Keisuke KUBOMURA: Appearances of Landslide at the 7th Shiboro Kabetsu River Bridge Near Shimizuzawa along Yubari Line, J.N.R., Vol.7, No.2 (Dec. 1970) p.1-7 (E)
13) Hiroyuki NAKAMURA: Earth Pressure Acting on Piles for the Treatment of Landslides and their Design, Vol.7, No.2 (Dec. 1970) p.8-12 (D)
14) Seiji TAKAYA: The Study of Landslide Topography Used Areal Photographs, Vol.7, No.2 (Dec. 1970) p.13-18 (E)
15) Atsuo TAKEUCHI: On the Fractured Zone Type Landslide in Kochi Prefecture by the Electrical Resistivity Survey, Vol.7, No.2 (Dec. 1970) p.19 (E)
16) Hung Teh Lin, Shin-ichi YAMAGUCHI: The Decision of Moving Cycle of Landslides in Past Time by the Age Measurement of Bogwood Obtained from Landslide Area, Vol.7, No.3 (Apr. 1971) p.1-6 (E)
17) Koichi MOCHIZUKI: On Landslides in the Mountainous Area along Sai River and Hime River in the Northern Part of Nagano Prefecture (1), Vol.7, No.3 (Apr. 1971) p.7-14 (E)

18) Makoto HOSHINO, Tamotsu YOSHIDA: The Distribution of Landslides in Mushinai Area,Hokkaido, Vol.7, No.3 (Apr. 1971) p.15-20 (E)
19) Seiji TAKAYA: The Study of Landslide Topography Used Aerial Photographs, Vol.7, No.3 (Apr. 1971) p.21-25 (E)
20) Shin-ichi YAMAGUCHI: The Distribution of Landslides in Formosa, Vol.7, No.3 (Apr. 1971) p.26-27 (E)
21) Bungo TAMADA: On the Process of Formation of the Slide Planes at Kuchinotsu Landslide Area (I), Vol.7, No.4 (June 1971) p.1-8 (E)
22) Tomomitsu YASUE: A Standard Classification for the Failures of Steep Slopes, Vol.7, No.4 (June 1971) p.9-12 (E)
23) Hiroyuki NAKAMURA: On the Displacement of the Clayey Landslide Gliding Over the Base-Rock, Vol.7, No.4 (June 1971) p.13-20 (E)
24) Masami FUKUOKA: Report of Landslides Caused by San Fernando Earthquake, Vol.7, No.4 (June 1971) p.21-26 (E)
25) Masasuke WATARI: On Types of Landslide and their Control Methods, Vol.8, No.1 (Aug. 1971) p.1-5 (E)
26) Bungo TAMADA: On the Process of Formation of the Landslide Planes at Kuchinotsu Landslide Area (II), Vol.8, No.1 (Aug. 1971) p.6-10 (E)
27) Goji YAMADA, Sumiji KOBASHI, Kunishige KUSANO: Collapse of Takabayama Tunnel Caused by Landslide, Vol.8, No.1 (Aug. 1971) p.11-24 (E)
28) Koichi MOCHIZUKI: On Landslides in the Mountanous Area along Sai River and Hime River in the Northern Part of Nagano Prefecture (2), Vol.8, No.1 (Aug. 1971) p.25-31 (E)
29) Akitoshi FUJIWARA: Some Examples of the Landslide Prediction in Indonesia, Vol.8, No.1 (Aug. 1971) p.32-40 (E)
30) Takeshi ANDO: On Weathering Mechanism in Landslides, Vol.8, No.2 (Oct. 1971) p.1-10 (E)
31) Akitoshi FUJIWARA: Geological Judgment for Analysis of Sliding Mechanism, Vol.8, No.2 (Oct. 1971) p.11-15 (E)
32) Hisaya MATSUNO, Kashiro NISHIMURA: On the Pattern of the Surface Movements of the Landslide Mass, Vol.8, No.2 (Oct. 1971) p.16-20 (E)
33) Syojiro NAKAYA, others: On the Tokiwadai-Kitaichinosawa Landslide (1), Vol.8, No.2 (Oct. 1971) p.21-28 (E)
34) Koichi MOCHIZUKI: On Landslides in the Mountanous Area along Sai River and Hime River in the Northern Part of Nagano Prefecture (3), Vol.8, No.2 (Oct. 1971) p.29-38 (E)
35) Bungo TAMADA: On the Process of Formation of the Slide Planes at Kuchinotsu Landslide Area (III), Vol.8, No.2 (Oct. 1971) p.39-43 (E)
36) Atsuo TAKEUCHI: Investigation Methods of Underground Water in Landslide Areas, Vol.8, No.3 (Feb. 1972) p.3-12 (E)
37) Seiji TAKAYA, Toru YAMAMOTO: On Micro-Topographic Features and X-ray Analysis of Clay at Nishinokawa Landslide Area, Vol.8, No.3 (Feb. 1972) p.13-18 (E)
38) Atsuyuki SAKAI: On London Clay, Vol.8, No.3 (Feb. 1972) p.19-22 (A)
39) Takeshi ANDO: On the Geological Classification of Landslides Horizon, Vol.8, No.4 (April 1972) p.1-7 (E)
40) Shin-ichi YAMAGUCHI: On the New Method that Estimate Style of Landslide Mass by Pipe Strain Gauge, Vol.8, No.4 (Apr. 1972) p.8-11 (E)
41) Ryoji ISHII, others: The Landslide at the Site of Takinosawa on Sapporo-Otaru Highway Projected, Hokkaido, Vol.8, No.4 (Apr. 1972) p.12-20 (E)
42) Syun OKUBO, Toshiaki UESAKA, Masatsugu FUNASAKA: The Investigation Method of Surface Layer on the Slope Using Handy Dynamic Cove Penetrometer, Vol.8, No.4 (Apr. 1972) p.20-29 (E)
43) Atsuo TAKEUCHI: Underground Temperature Survey in and around the Landslide Area (2), Vol.8, No.4 (Apr. 1972) p.29 (E)

44) Hiroyuki NAKAMURA: On Characteristic of Movement of the Sarukuyoji-Landslide Obtained from the Measurements Using Extensometers, Vol.9, No.1 (July 1972) p.1-8 (E)
45) Bungo TAMADA: Studies on the Stability Calculation of the Landslide Planes with Contained Water Film Faces, Vol.9, No.1 (July 1972) p.9-19 (E)
46) Kozo YUHARA: On the Yasu Landslide in Tochio City, Niigata Prefecture, Vol.9, No.1 (July 1972) p.20-31 (E)
47) Atsuo TAKEUCHI: Underground Temperature Survey in and around the Landslide Area (3), Vol.9, No.1 (July 1972) p.32-38 (E)
48) Makoto HOSHINO, Tamotsu YOSHIDA, Shigeyoshi ISHIMAKI: Investigation on the Mechanism of Toyohama Landslide, Otobe, Hiyama Province, Hokkaido, Vol.9, No.2 (Oct. 1972) p.3-19 (E)
49) Masayoshi MATSUBAYASHI: On the Groundwater Cut-off Work with Chemical Groutings and its Effectiveness in Landslide Area, Vol.9, No.2 (Oct. 1972) p.21-32 (D)
50) Hiroyuki NAKAMURA: Geotechnical Properties of the Landslides, Especially Sarukuyoji Landslide, Observed in the Areas Composed of Black Mudstone, Vol.9, No.2 (Oct. 1972) p.33-43 (E)
51) Kazuo KURODA: On the Classification of Landslides, with some Reconsiderations to Koide's Geologic Classification, Vol.9, No.3 (Jan. 1973) p.1-6 (E)
52) Takashi FUJITA: A Review of Geological Studies in the Kamenose Landslide Area, Vol.9, No.3 (Jan. 1973) p.7-12 (E)
53) Atsuo TAKEUCHI: Underground Temperature Survey in and around the Landslide Area (4), Vol.9, No.3 (Jan. 1973) p.13-22 (E)
54) Hiroshi YAMASHITA: Talking of Spectacle of Landslide Occurrence at Mt. Myoko by a Mountaineer, Vol.9, No.3 (Jan. 1973) p.22-26 (E)
55) Hiromu SHIMA: Micro-tremor and an Attempted Application to Exploration of Landslide Areas, Vol.9, No.4 (May 1973) p.1-8 (E)
56) Atsuo TAKEUCHI: Underground Temperature Survey in and around the Landslide Area (5), Vol.9, No.4 (May 1973) p.9-16 (E)
57) Saburo NAKAMURA: A Consideration on the Landslide Terrain, Vol.10, No.1 (Aug. 1973) p.1-5 (E)
58) Hiroyuki NAKAMURA, Yoshinobu SHIRAISHI: On Influence of Snow upon Landslides, Vol.10, No.1 (Aug. 1973) p.6-16 (E)
59) Atsuo TAKEUCHI: Underground Temperature Survey in and around the Landslide Area (6), Vol.10, No.1 (Aug. 1973) p.17-34 (E)

13. Engineering Geology
1) Yoshinori TANAKA: On the Measurement of the Crack Quantity in Rocks by the Elastic Wave Velocity, Vol.11, No.1 (1970) p.1-7 (E)
2) Kiyoshi MIURA, Akinori HATA: The Collapse Related to Rock Joints and Joints Clay of Weathered Granites, Vol.11, No.2 (1970) p.40-72 (A)
3) Keiji MIYAJIMA: Tunnel Construction and its Geology in Shikoku, Vol.11, No.2 (1970) p.73-83 (E)
4) Makoto HOSHINO, Masamitsu NEGISHI: An Experimental Study on Mechanical Properties of Rocks, Vol.11, No.3 (1970), p.91-96 (A)
5) Yoshiro HAYASHIDA: Mechanical Properties of Izumi Sandstone (No.2), Vol.11, No.4 (1970) p.127-131 (A)
6) Masayasu INOUE, Mitito OHMI, Takeshi YOSHIDA: Relations among the Propagation Velocities of Elastic Waves, the Elastic Modulus and the Saturation of Rock Specimens (No.1), Vol.11, No.4 (1970) p.132-138 (E)
7) Yotaro SEKI: A Profile of Landslide Observed in Northern Tanzawa Mountains, Vol.11, No.4 (1970) p.149-151 (E)

8) Taro KASAMA, Michiji TSURUMAKI: Occurrence and Quality of Groundwater in the Tunnels of the Rokko Mountain Area, Kinki District, Japan, Vol.12, No.1 (1971) p.16-28 (E)
9) Akira ABE, Hirotake IWATA, Masao ISHIKAWA, Makoto NISHIKAWA: On the Calamity by the Heavy Rain Fall in the Southern Chiba Prefecture in July, 1970, Vol.12, No.1 (1971) p.29-50 (E)
10) Toshio IKEDA: Active Fault and Foundation Design for Shin-Kobe Railway Station Structures, Vol.12, No.2 (1971) p.77-82 (D)
11) Seiji TAKAYA: Considerations About "Slickenside" on Landslide Area, Vol.12, No.3 (1971) p.129-135 (E)
12) Masayasu INOUE, Michito OHMI: Relations Among Compressional Wave Velocity, Apparent Density and Uniaxial Compressive Strength of Common Sedimentary and Igneous Rocks, Vol.12, No.3 (1971) p.136-141 (A)
13) Kazuhiko IKEDA: On the Stability of Detritus-Slope, Vol.12, No.3 (1971) p.142-149 (E)
14) Yoshiro HAYASHIDA: Strengths, Young's Moduli and Elastic Wave Velocities of Rock, Vol.12, No.3 (1971) p.150-156 (A)
15) Masaya INOUE, Michito OHMI, Masao NOMURA: Relation Among the Propagation Velocities of Elastic Waves, the Elastic Modulus and the Saturation of Rock Specimens (No.2), Vol.12, No.4 (1971) p.184-192 (A)
16) Masao NAKAGAWA, Yoshio NAKAYAMA, Katsuo YASUE, Syoji UENO: On the Calamity by the Heavy Rain Fall in the Southwestern Hyogo Prefecture on July 18, 1971, Vol.12, No.4 (1971) p.199-211 (E)
17) Seiken OGATA: Quantitative Analysis of Landslides in Respect to Terrestrial Features, Vol.13, No.1 (1972) p.62-74 (E)
18) Makoto HOSHINO, Yuichi KOBAYASHI, Tamotsu YOSHIDA: Swelling of Rock and Geotechnical Significance, Vol.13, No.2 (1972) p.62-74 (A)
19) Kazukuni KIMIYA: A Simple Method of Study to Predict Mountainslide, Vol.13, No.2 (1972) p.75-90 (E)
20) Keizo TSUDA: Effects of the Active Faults on the Constructions in the Rokko Area, Vol.13, No.3 (1972) p.101-111 (D)
21) Kei TAKAMOTO, Ken KODAMA, Takashi KAJIYA: The Mechanical Properties of Weathered Granite at the Foundation Locations of Hayase Ohashi, Vol.13, No.3 (1972) p.112-121 (A)
22) Yoshiaki TANAKA: On the Relation Between the Recession of the Cut-Slope and the Mechanical Properties of Rocks in the Chichibu Basin, Vol.13, No.4 (1972) p.151-160 (E)

14. Geophysical Exploration
1) Masayasu INOUE, Michito OHMI: On the Variation of Propagation Velocity of Elastic Waves in Water Saturated Porous Rocks, Vol.23, No.4 (1970) p.193-201 (A)
2) Syoichi KUNORI, Tsukasa ABE, Tokumi SAITO: Study on Weathering of Granite Rocks (I), Vol.24, No.1 (1971) p.6-17 (A)
3) Tokumi SAITO, Tsukasa ABE, Syoichi KUNORI: Study on Weathering of Granitic Rocks (II), Vol.24, No.5 (1971) p.222-227 (A)
4) Masayasu INOUE, Michito OHMI: On the Variation of Poisson's Ratio of Rocks Related to Saturation of Water, Vol.25, No.1 (1972) p.1-10 (A)
5) Kazuhiko IKEDA, Yoshimasa KOBAYASHI, Takashi SAKURAI: Effect of Flaws on the Strength of Rocks, Vol.25, No.5 (1972) p.217-226 (A)
6) Tsuneo IMAI, Masayoshi YOSHIMURA: The Relation of Mechanical Properties of Soils to P- and S-Wave Velocities, Vol.25, No.6 (1972) p.283-292 (A)

7) Syozo KOMAKI, Minami ICHIKAWA: Application of Seismic-Wave Velocity to Estimation on Difficulty of Excavation at Gravel Layers, Vol.25, No.6 (1972) p.293-301 (E)
8) Tokumi SAITO, Tsukasa ABE: Study on the Physical Properties of Weathered Igneous Rocks by Schmidt Test Hammer, Vol.26, No.1 (1973) p.19-31 (E)

15. Hydro Electric Power
1) Tsugio HARADA: An Investigation on Design of Fundamental Profile of Rockfill Dam, No.106 (May 1970) p.59-71 (D)
2) Toshio FUJII, others: Instrumental Measurement of Nakawado Dam, No.112 (May 1971) p.28-62 (B)
3) Syuichi YAGASAKI, Tsugio HARADA: Design and Construction of Shimokotori Rockfill Dam (Part I), No.120 (Sep. 1972) p.32-62 (A, B, D)
4) Syuichi YAGASAKI, Tsugio HARADA: Design and Construction of Shimokotori Rockfill Dam (Part II), No.121 (Nov. 1972) p.26-49 (A, B, D)
5) Seizaburo NISHIKAWA, Etsuo SOEDA: Pressure Tunnel, Its Diameter and Thickness of Concrete Lining, No.121 (Nov. 1972) p.69-74 (B)
6) Ken-ichi SAKAI, Yukihiro AKATSU, Yasuo ASO: Drift Chamber Blasting at Stone Quarry of Niikapu Dam, No.122 (Jan. 1973) (C)
7) Syuichi YAGASAKI, Tsugio HARADA: Design and Construction of Shimokotori Rockfill Dam (Part III), No.122 (Jan. 1973)(A, B, D)
8) Ietaka MATSUI, Ken-ichi SAKAI: Observation of Inside Behaviour of Niikapu Rockfill Dam During Construction and Its Numerical Analytic Investigation, No.123 (Mar. 1973) p.30-39 (B, D)
9) Jyun YOKOTA, Akio DAICHO: Design and Construction of Tataragi Dam, No.125 (July 1973) p.53-71 (A, B, D)

16. Preprint of the Fall Symposium, MMIJ
1) Kumikoto IIDA: Effects of Porosity and Anisotropy of Rock on The Elastic Wave Velocity, (1970) A9 (A)
2) Kazuo INAMI: Physical Property of Rock Under Compression and Resultant Changes in Elastic Wave Velocity, (1970) A10 (A)
3) Koichi SASSA: An Interpretation of Finite Element Method, (1970) B1 (B)
4) Ko SUZUKI, Yoji ISHIJIMA: Analysis of Rock Stress Phenomena by Finite Element Techniques, (1970) B2 (B)
5) Yoshio HIRAMATSU, Yukitoshi OKA, Yoshiaki MIZUTA, Haruhiko KURITA: Stresses in Pillars Influenced by Topographical Conditions, (1970) B3 (B)
6) Masao HAYASHI, Satoshi HIBINO: Problems Relating to Elastic and Plastic Behaviour of Rock Formation in Particular at The Start of Underground Excavation, (1970) B4 (B)
7) Umetaro YAMAGUCHI, Yataro SHIMOMURA: Some Practical Problems in Application of Smooth Blasting, (1970) D3 (C)
8) Ichiro ITO, Koichi SASSA: Controlled Blasting Adjacent to Existing Structures, (1970) D4 (C)
9) Ichiro ITO, Koichi SASSA, Koichi HANASAKI, Chikaoki TANIMOTO: Application of Finite Element Techniques to The Analysis of Destruction Phenomena by Explosion, (1970) B5 (C)
10) Takeshi ISHIMOTO, Masabumi HAMAZAKI, Noriaki NAKAJIMA: Rock Blasting by C.C.R. Explosives, (1970) D6 (C)
11) Takehisa SAKURAI, Hiroshi SAKAI, Michiaki SAKAGUCHI, Takeo UEDA, Koichi SASSA: Some Experiments in Controlled Blasting, (1970) D7 (C)
12) Yukitoshi OKA, Yoshio HIRAMATSU, Toshiaki SAITO, Katsuhiko SUGAWARA: Mechanism of Static Destruction of Rocks, (1970) K1 (A)

13) Ichiro ITO, Makoto TERADA, Koichi SASSA, Kunihisa KATSUYAMA: Dynamic Destruction of Rocks, (1970) K2 (A)
14) Yuichi NISHIMATSU: Effects of Cutting Speed on The Mechanical Fracture of Rock, (1970) K3 (C)
15) Saburo TAKAOKA, Hirohide HAYAMIZU, Shigeo MISAWA, Michio KURIYAGAWA: Mechanical and Thermal Fracture of Rocks, (1970) K4 (C)
16) Zenjiro HOKAO: Drilling and Cutting of Rock by Rocket Jet, (1970) K5 (C)
17) Shigeru MUKAI, Minoru ICHIDATE: Theories of Fracture and Particle Sizes Distribution of The Products, (1970) K6 (E)
18) Shigeru YAMASHITA, Shigenori KINOSHITA: Distribution of Stresses in Portion of Object Adjacent to Cutter Blade, (1971) A1-1 (A)
19) Yukitoshi OKA, Katsuhiko SUGAWARA, Yoshio HIRAMATSU: Analysis of Stresses Created in Circumference of Bored Holes, (1971) A1-2 (B)
20) Yoshiaki MIZUTA, Yukitoshi OKA, Yoshio HIRAMATSU, Hiroshi OGASAWARA: Studies on Pillars in The Mining of Vein Type Deposits, (1971) A1-3 (B)
21) Yoji ISHIJIMA, Ko SUZUKI: Application of FEM on Destruction of Rock Formation Around The Underground Open Cavities, (1971) A1-4 (B)
22) Toshikazu KAWAMOTO, Toshiaki SAITO, Masatsugu AKIMOTO: Development of Stresses and Deformation of Rock Formation Adjacent to Pillar, (1971) A1-5 (B)
23) Eiichi YAMAMOTO, Tateki SATO, Kunihisa YOSHIDA: An Experimental Research on The Progress of Destruction of Rocks, (1971) A2-1 (A)
24) Gensuke ENDO, Seiji TANAKA, Ichiro KUSUDATE: Basic Research for Establishment of Excavation Criteria at Ohoyaishi Green-tuff Mining, (1971) A2-2 (A)
25) Yuichi NISHIMATSU: Probability Theory Applied to Rock Strength, (1971) A2-3 (A)
26) Yukitoshi OKA, Katsuhiko SUGAWARA, Yoshio HIRAMATSU, Yoichi MIZUOCHI: Theories of Rock Destruction Derived from Probability Theory, (1971) A2-4 (A)
27) Iwao MORI, Yusaku TOMINAGA: Stress Concentration at Fragile Points in Rocks, (1971) A2-5 (A)
28) Ryoji KOBAYASHI: Studies on Behaviour of Rock Upto Destruction, (1971) A2-6 (A)
29) Yuichi NISHIMATSU: Correlation Between Cutting Resistance of Rocks and Cutting Depth of Blade, (1971) A3-2 (C)
30) Shigeru YAMASHITA, Shigenori KINOSHITA: Mechanism of Rock Cutting-- Analysis of Single Cutting Mechanism by Symmetric Wedge Shaped Cutter Blade, (1971) A3-3 (C)
31) Iwao NAKAJIMA, Shigenori KINOSHITA: Theories and Measurement on The Resistance of Rocks Against Rotary Cutting, (1971) A3-4 (C)
32) Saburo TAKAOKA, Hirohide HAYAMIZU, Shigeo MISAWA, Michio KURIYAGAWA: Research on Mechanical Excavation of Vertical Shaft in Underground, (1971) A3-5 (C)
33) Ichiro ITO, Koichi SASSA: An Approach to Develop Blasting Techniques on a Basis of Rock Mechanics, (1971) A3-6 (C)
34) Ichiro ITO, Makoto TERADA, Yoshinori INADA: Rock Excavation Using Mechanical Cutting Method Combined with Thermal Action by Flame, (1971) A3-7 (C)
35) Seisuke MISAWA, Akinori TAKAHASHI: Possibility of Rock Fracture by Means of Electromagnetic Waves, (1971) A3-8 (C)
36) Yoshihisa MAENO, Yoshiro KAGAWA: Effects of Percussive Energy Transmitted Through Drill Steel, (1971) A3-9 (C)
37) Umetaro YAMAGUCHI: Explanation on Rock Burst Mechanism, (1971) H3 (B)

38) Ko SUZUKI: Cause of Rock Burst, Its Prediction and Possibility of Prevention, (1971) H4 (B)
39) Yoshio HIRAMATSU, Yukitoshi OKA: Explanation on Rock Burst, (1971) H5
40) Toshiro ISOBE: Explanation on Rock Burst and Gas Out-burst, (1971) H7 (B)
41) Masayasu INOUE, Michito OHMI: Presumptive Methods to Determine Strength of Rock and Rock Formation, (1972) B1 (A)
42) Tomio HORIBE, Ryoji KOBAYASHI, Takashi MURAKAMI: Various Methods of Measuring Mechanical Properties of Rock and Formation, (1972) B-2 (A, B)
43) Umetaro YAMAGUCHI, Takakoto SHIMOTANI: Measurements of Thermal Property of Rocks, (1972) B3 (A)
44) Takeichi YANAGIMOTO, Ken-ichi UCHINO: Measurement of Heat Conductivity of The Rocks in Coal Bearing Seam, (1972) B4 (A)
45) Kazuhiko SATO, Shigenori KINOSHITA: Measurements of Deformation Behaviour of Rocks Subject to High Velocity Loads, (1972) B5 (A)
46) Akira TAKATA, Yoshihiro OGATA: Instrument Measurement of Vibrations in Underground Mining, Its Purpose and Practice, (1972) B6 (B)
47) Ichiro ITO, Koichi SASSA: Measurements of Vibration Upon Blasting, (1972) B7 (C)
48) Yoshio HIRAMATSU, Yukitoshi OKA: Interpretation of Measurement Results of Stresses in Rock by Means of Stress Release Analysis, (1972) B8 (B)
49) Shigeru OGASAWARA, Kaoru ISHIHARA, Kusuo SAKAI: Observation of Rock Noises in Besshi Mine, (1972) B9 (B)
50) Yusaku TOMINAGA, Shigenori KINOSHITA: A New Method for Measuring Rock Pressures, (1972) B10 (B)
51) Toshikazu KAWAMOTO, Toshiaki SAITO: Measurements of Deformation and Application of The Results to Stress Analysis, (1972) B11 (B)
52) Ichiro ITO, Makoto TERADA, Yoshinori INADA: Mechanism of Fragmentation of Rock Which is Subject to Mechanical Cutting Combined with Thermal Action by Flame, (1972) L1 (C)
53) Zenjiro HOKAO: Rock Drilling by Means of Flame Jet Stream, (1972) L2 (C)
54) Keiji TANEDA, Yoshiaki KANEKO: Experiments on Super Sonic Vibration Excavation, (1972) L3 (C)
55) Umetaro YAMAGUCHI: Current Rock Blasting Technology, (1972) L4 (C)
56) Yuichi NISHIMATSU: Evaluation of Various Methods of Rock Excavation, (1972) L5 (C)
57) Minoru SAKURADA: Current Raise Boring Techniques, (1972) L6 (C, D)
58) Saburo TAKAOKA, Hirohide HAYAMIZU, Shigeo MISAWA, Michio KURIYAGAWA: Research and Manufacture of Proto Type Ring Shape Shaft Excavator, (1972) L7 (C, D)
59) Norio OKUBO: Experiences with a Tunnel Boring Machine, Model Kawasaki-Jerva, (1972) L8 (D)
60) Masao ISHIKAWA: Tunnel Boring Machine, Model IHI-Atlas Copco--Operating Results at Seikan Tunnel, (1972) L9 (D)
61) Keiji TAKAHASHI: Methods to Prevent Propagation of Vibration from Blasting, (1972) Q11 (C)
62) Jyunji HASHIMOTO: Vibration Caused from Blasting, (1972) A12 (C)
63) Yukitoshi OKA, Katsuhiko SUGAWARA, Hiroyuki KOHAMA: Investigation of Fracture Phenomena in View of Rock Mechanics, (1972) S1 (E)
64) Saburo YASHIMA, Yoshiteru KANDA: Single Fracture--Dimensional Effect on The Strength,(1972) S2 (E)
65) Toshio INOUE: Fracture of Solids and Distribution of Sizes of Particles, (1972) S4 (E)
66) Kunio MATSUI: Definition of Grinding Work and Grindability, (1972) S5 (E)

67) Inosuke MIYAWAKI, Kazuhiro FUJISAKI: Theory of Grinding Velocity, (1972) S6 (E)
68) Yukitoshi OKA, Yoshiaki MIZUTA, Yoshio HIRAMATSU: Subsidence of Cavity Roof in Underground, (1973) C1 (B)
69) Yukitoshi OKA, Katsuhiko SUGAWARA, Yoshio HIRAMATSU: Behaviour of Rock Formation Around Circular Drift and Its Relation to Composition Equation of Rock Formation, (1973) J1 (B)
70) Shigenori KINOSHITA, Atsushi FUKUSHIMA: Dilatancy of Rock in Uni-axial Compression, (1973) J2 (A)
71) Ryoji KOBAYASHI: Deformation and Breakage of Rock and Rock Formation, (1973) J3 (A, B)
72) Akira TAKATA, Yoshihiro OGATA: Instruments in Practice for Measurements of Deformation and Breakage of Rock Formation, (1973) J4 (B)
73) Umetaro YAMAGUCHI, Takakoto SHIMOTANI: Practical Application of Rock Mechanics at Site, (1973) J5 (B)
74) Ryuichi IIDA: Rock Mechanics with Reference to Civil Engineerings, (1973) J6 (B)
75) Katsuo CHONAN: Changes of Rock Pressure at Stopes, Observed on The Artificial Roofings, (1973) J7 (B)
77) Nobukazu NANKO: Design and Control of Pillars, (1973) J9 (B)